NUREG/CR-2526
PNL-4164

LOCA Simulation in NRU Program

Data Report for Thermal-Hydraulic Experiment 2 (TH-2)

Prepared by C. L. Mohr, G. M. Hesson, L. L. King, R. K. Marshall, L. J. Parchen, J. P. Pilger, G. E. Russcher, B. J. Webb, N. J. Wildung, C. L. Wilson, M. C. Wismer

Pacific Northwest Laboratory
Operated by
Battelle Memorial Institute

Prepared for
U.S. Nuclear Regulatory Commission

GPO Printed copy price: $6.50

NUREG/CR-2526
PNL-4164
R3

LOCA Simulation in NRU Program

Data Report for Thermal-Hydraulic Experiment 2 (TH-2)

Manuscript Completed: October 1982
Date Published: November 1982

Prepared by
C. L. Mohr, G. M. Hesson, L. L. King, R. K. Marshall,
L. J. Parchen, J. P. Pilger, G. E. Russcher, B. J. Webb,
N. J. Wildung, C. L. Wilson, M. C. Wismer

Pacific Northwest Laboratory
Richland, WA 99352

Prepared for
Division of Accident Evaluation
Office of Nuclear Regulatory Research
U.S. Nuclear Regulatory Commission
Washington, D.C. 20555
NRC FIN B2277

ACKNOWLEDGMENTS

The authors would like to thank Chalk River Nuclear Laboratories (CRNL) for their assistance in performing this test. A special acknowledgment is due to CRNL staff members B. De Abreu, J. P. Inglis, P. E. Kelly, J. W. Logie, D. T. Nishimura, and I. D. Ross, who made major contributions in keeping this test on schedule. The test staff would also like to thank CRNL staff members D. J. Axford, I. C. Martin, and S. J. McAuley for ensuring a safe test. R. Van Houten, NRC/RSR/FB program manager, provided helpful directives to the program.

The technical assistance of L. D. Hochreiter of Westinghouse Electric Corporation and T. Healey, I. Gibson, J. Gittus, and other members of the United Kingdom Atomic Energy Authority team that participated in this test is greatly appreciated. The authors would also like to thank the technical editor, S. K. Edler.

ABSTRACT

A series of thermal-hydraulic and cladding material experiments are being conducted using light-water reactor fuel bundles as part of the Pacific Northwest Laboratory Loss-of-Coolant Accident (LOCA) Simulation Program. Experimental data and initial results from the fourth experiment in the program--thermal-hydraulic experiment 2 (TH-2)--are presented in this report. The program is being conducted in the National Research Universal (NRU) reactor, Chalk River, Ontario, Canada. A full-length test bundle containing nonpressurized water reactor fuel rods was used to develop reflood control parameters and procedures that will produce a reduced heatup rate or a "flat top" transient for extended periods of time. Variable reflood rates were used, and experimentally determined control system logic parameters were developed. Using these concepts, fuel cladding temperatures from 1033 to 1274K (1400 to 1834°F) were produced for 283 s.

SUMMARY

The Loss-of-Coolant Accident (LOCA) Simulation Program is being conducted by Pacific Northwest Laboratory (PNL) to evaluate the thermal-hydraulic and mechanical deformation behavior of a full-length light-water reactor (LWR) fuel bundle under LOCA conditions. The test conditions are designed to simulate the heatup, reflood, and quench phases of a large-break LOCA and are performed in the National Research Universal (NRU) reactor using nuclear fission to simulate low-level decay power typical of these conditions.

Data and initial results from the fourth experiment in the program—thermal-hydraulic experiment 2 (TH-2)--are presented in this report. TH-2 included 14 tests and had the following major objectives:

- to develop operating conditions for the loop control system (LCS) that could be used for a subsequent materials experiment (MT-3)
- to evaluate the possibility of using a combination of preset reflood flow rates to produce a peak fuel cladding temperature in the range of 1033 to 1089K (1400 to 1500°F) for up to 200 s
- to demonstrate the capability of the data acquisition and control system (DACS) using measured temperature in a feedback control loop to provide a peak fuel cladding temperature in the range of 1033 to 1089K (1400 to 1500°F) for up to 200 s.

The results of the experiment showed that the DACS controlled peak fuel cladding temperatures better than a combination of preset reflood flow rates. The delay time and automatic control system used to control the variable reflood rate demonstrated the capability of holding temperatures above 1033K (1400°F) for periods of up to 280 s. The experimental conditions approach a steady-state boil-off condition in which the quench front is in an equilibrium position with the reflood rate. Test repeatability was also demonstrated by precise control of peak cladding temperature.

Graphical data are presented from 4 of the 14 TH-2 tests: TH-2.02, TH-2.12, TH-2.13, and TH-2.14. The data demonstrate fuel cladding temperature control using both preset reflood flow and temperature feedback. Test repeatability is demonstrated using temperature feedback control, and local fuel power temperature effects are shown. Preliminary graphical data on test assembly temperatures, cooling flow, and the neutronics environment are presented in the appendices.

CONTENTS

FIGURES

TABLES

INTRODUCTION

The Loss-of-Coolant Accident (LOCA) Simulation Program is being conducted in the National Research Universal (NRU) reactor at Chalk River Nuclear Laboratories (CRNL),[a] Chalk River, Ontario, Canada, by Pacific Northwest Laboratory (PNL).[b] The program is sponsored by the U.S. Nuclear Regulatory Commission (NRC) to evaluate the thermal-hydraulic and mechanical deformation behavior of a full-length, 3% enriched light-water reactor (LWR) fuel rod bundle during the heatup, reflood, and quench phases of a LOCA. Low-level nuclear fission heat simulates the decay heat in the fuel and cladding that is typical of a LOCA.[1]

The program is composed of thermal-hydraulic experiments using nonpressurized test fuel rods and cladding material experiments using pressurized test assemblies that balloon and rupture. The initial thermal-hydraulic experiment (PTH-1), which was performed in October 1980, provided a data base for predicting the quenching characteristics of Zircaloy-clad fuel rods under various reflood conditions.[2] The first materials experiment (MT-1) was performed in April 1981 and used a pressurized cruciform of 11 test rods with 1 water tube and 20 unpressurized guard rods. The test rods were pressurized to 3.1 MPa (450 psig). The delay time and the reflood rate were selected to duplicate the TH-1.10 experiment, which reached a peak fuel cladding[c] temperature of 1144K (1600°F). These conditions were achieved, and 6 of the 11 rods ruptured.[3]

The second materials experiment (MT-2), which was performed in July 1981, used the same guard rod and shroud assembly as MT-1; it was reconstituted in the rod bay underwater using a new cruciform test bundle. One test objective was to perform a low-temperature--1089K (1500°F)--test using variable reflood rates. A malfunction of the test loop occurred and resulted in an adiabatic heat transfer condition as well as higher temperatures than desired. Eight of the 11 rods ruptured during the MT-2 experiment.[4]

This report presents data and initial results from the second thermal-hydraulic experiment (TH-2), which was performed in September 1981. The experiment was jointly funded by the NRC and the United Kingdom Atomic Energy Authority (UKAEA) to evaluate the thermal-hydraulic test conditions for "flat top" or extended transient LOCA conditions. A new unpressurized 12-rod test bundle was inserted into the guard rod and shroud assembly previously used for MT-1 and MT-2. The results from the previous MT-2 experiment had made it apparent that in-reactor flat top transient test conditions are difficult to obtain and that significant modifications to the test procedure were needed. These flat top transient conditions require that Zircaloy cladding temperatures be maintained in the high alpha range of 1033 to 1103K (1400 to 1525°F) for

---

(a) Operated by Atomic Energy of Canada Ltd. (AECL).
(b) Operated for the U.S. Department of Energy (DOE) by Battelle Memorial Institute.
(c) Fuel cladding is subsequently referred to as cladding.

more than 200 s. To obtain these conditions, a variable reflood rate was needed; and, due to the variability in the control parameters, it was shown that preprogrammed or manual over-ride control concepts would provide the accuracy required.

During TH-2, the variable reflood feedback control logic concepts demonstrated that it was possible to maintain the temperature in the ballooning window for up to 280 s. Thermal-hydraulic calculational techniques adequately predicted the Zircaloy cladding thermal behavior in the peak-power region for the initial part of the transient but were not able to account for steam cooling conditions caused by prolonged low reflood flow rates or for the behavior of the fuel rod out of the peak-power region.

TH-2 was a calibration experiment that was performed to develop reflood control parameters and procedures for the subsequent materials experiment (MT-3). TH-2 consisted of 14 tests that developed the capability of the data acquisition and control system (DACS) and the loop control system (LCS) to control the variable reflood flow rate, thus producing an elevated peak cladding temperature for an extended time. TH-2 fuel rods were pressurized with helium at 0.101 MPa (14.7 psia), which was low enough that many LOCA transients could be simulated without causing fuel rod deformation or rupture.

The primary objective of TH-2 was to develop reliable cladding temperature control of a simulated LOCA. Peak cladding temperatures were to range from 1033 to 1089K (1400 to 1500°F) for at least 150 s, using variable rate reflood water coolant.

A secondary objective was to develop experiment protection controls that would trip the NRU reactor and establish emergency coolant flow if 1) the peak cladding temperature exceeded a trip set point or 2) the cladding heatup rate was not maintained or did not meet preselected requirements of magnitude and time. In addition, each test in TH-2 provided thermal-hydraulic test data for low reflood rates and variable reflood conditions that were not previously available.

The results from TH-2 provide full-length nuclear-heated cladding thermal-hydraulic response data in the high alpha temperature range for variable reflood conditions. These conditions extend the existing data base on thermal-hydraulic response to LOCA operating conditions not previously investigated by FLECHT[5] or other out-of-reactor test programs. These tests provided valuable information on the control of quench fronts and two-phase cooling that will be used for subsequent thermal-hydraulic and materials experiments. They also provided information on the quenching characteristics of nondeformed rods as compared with deformed rods.

Data from TH-2 will be used in conjunction with previous test results to assess various calculational models for reactor safety analyses and conclusions derived from the large series of electrically heated tests and smaller scale in-reactor tests being conducted elsewhere. The experimental results of the program address 17 specific items outlined in the Code of Federal Regulations 10 CFR 50.46 and 10 CFR 50, Appendix K. These results will be used to

provide additional data for model calibration and to help define the primary heat transfer mechanisms for new analytical models. The major contribution of these tests to LWR technology is to reduce the uncertainty on licensing criteria and offer the potential for raising the operating limits on some commercial LWRs.

The data presented in this report form the basic understanding of how to control peak elevated temperatures in a test assembly using reflood rate. The concepts developed are the building blocks for future severe fuel damage testing and give some insight into the thermal-hydraulic response that can be expected.

EXPERIMENT DESCRIPTION

This section describes the components of the test train assembly that was used for TH-2 and details the instrumentation that was provided. The test operation consisted of a preconditioning phase with 3 rises to power, 2 adiabatic transient tests, and 12 reflood transient tests.

TEST TRAIN ASSEMBLY

A schematic of the test train used for the LOCA test program is depicted in Figure 1. The total length of the test train (including the head closure, hanger tube, and test assembly) was ~9 m (~30 ft). The closure region provided the primary pressure boundary and included penetrations for 183 instrumentation leads. The hanger tube was used to suspend the test bundle and shroud from the head closure plug, and instrument leads were attached to the hanger to protect them during transport and testing. The shroud, which supported the fuel bundle and served as a protective liner during the experiment and transfer operations, also provided proper coolant flow distribution during various stages of the experiment. The stainless steel (SS) shroud consisted of two halves clamped together at 17.78-cm (7-in.) intervals and attached at the end fittings. The split shroud design makes it possible to disassemble, examine, and reassemble the test train underwater after its irradiation. The highly instrumented shroud and test assembly was approximately 4.27 m (14.17 ft) long.

The test assembly consisted of a 6 x 6 segment of a 17 x 17 PWR fuel assembly with the four corner rods removed (see Figure 1). Of the 32-rod fuel array, the 20 rods in the outer row were guard rods and the 12 inner rods were test rods arranged in a cruciform pattern (see Table 1). All 32 unpressurized fuel rods were filled with helium.

The test train instrumentation included: 24 self-powered neutron detectors (SPNDs), 115 fuel rod thermocouples (TCs), 18 steam probe TCs, and 4 closure head TCs. The instrumentation was located at 21 elevations or levels along the test train assembly. Each of these levels is defined in Figure 2, and Figures 3 through 6 detail the instrumentation at each level. Four TCs were located at an additional level to measure the closure temperature. Additional detail and nomenclature can be found on the blueprints referenced in Figure 3.

Turbine flowmeters and TCs provided the main source of thermal-hydraulic data. Local coolant temperatures were measured with steam probe TCs that protruded into the coolant channel and with TCs attached to the shroud. TCs were also located at the fuel centerline and attached to the inside of the cladding surface to measure azimuthal temperature variations. These cladding TCs were spot welded to the interior cladding surface and monitored the cladding temperature without interference from fuel pellet chips or unintentional TC relocation.

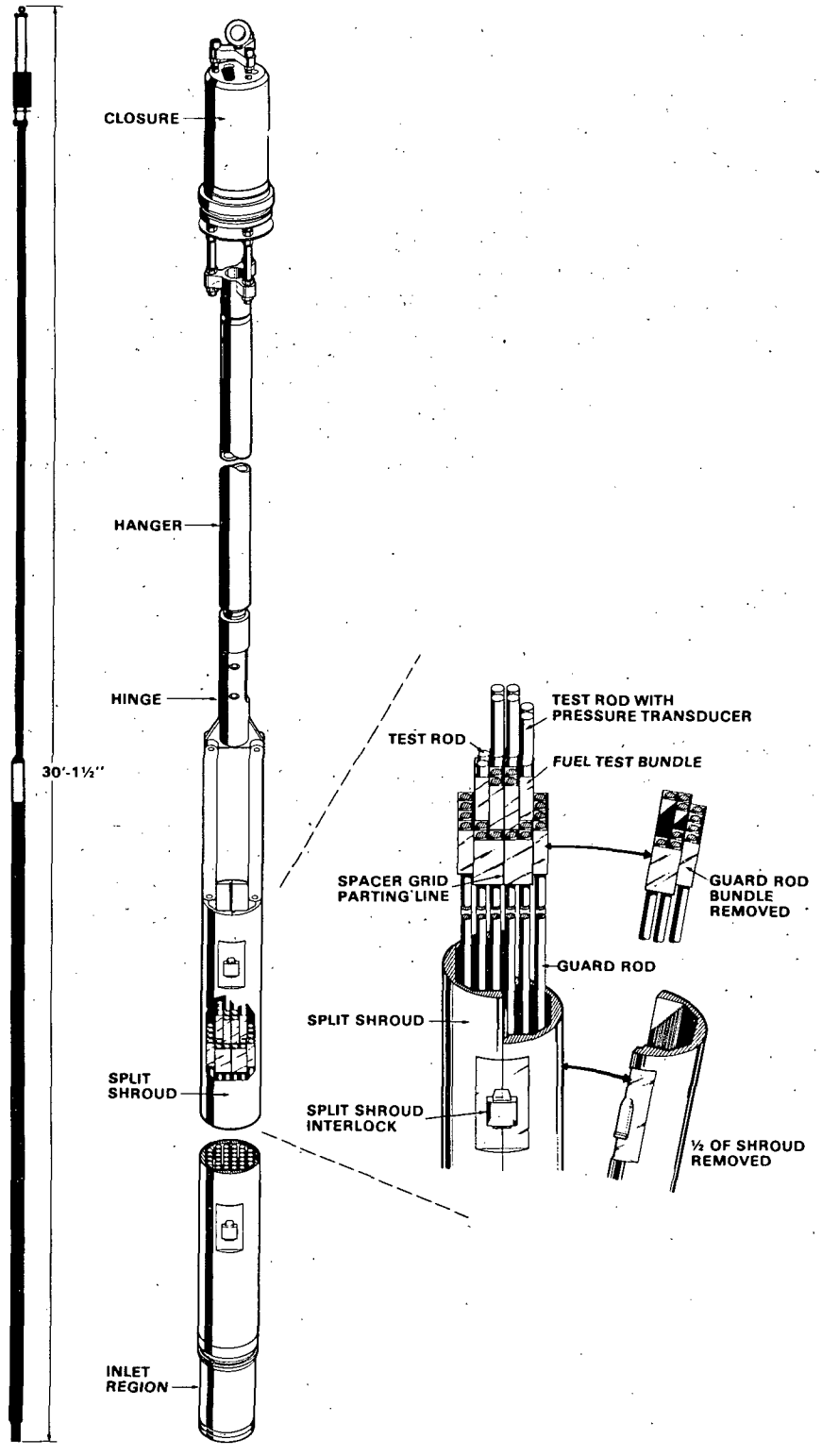

FIGURE 1. Schematic of NRU Loss-of-Coolant Accident Test Train

TABLE 1. Test Fuel Rod Design Variables

Cladding material	Zircaloy-4
Cladding outside diameter (OD)	0.963 cm (0.379 in.)
Cladding inside diameter (ID)	0.841 cm (0.331 in.)
Pitch (rod to rod)	1.275 cm (0.502 in.)
Fuel pellet OD	0.826 cm (0.325 in.)
Fuel pellet length	0.953 cm (0.375 in.)
Active fueled length	365.76 cm (144 in.)
Total shroud length	423.1 cm (170.125 in.)
Helium pressurization	unpressurized(a)
Fuel enrichment	2.93% ^{235}U

(a) 0.101 MPa (14.7 psia).

SPNDs provided neutron flux measurements within the fuel bundle. They could also detect coolant density variations (through flux changes) associated with the quench front that passed each SPND during the reflood phase of the transient. SPND data with regard to coolant density are currently being evaluated.

The instrument signals were monitored on a real-time basis with the DACS. The recorded data characterized the coolant flow rates, temperature, neutron flux, and operating history.

EXPERIMENT OPERATION

The TH-2 experiment included a preconditioning phase and 14 successive tests, each having a pretransient and transient phase. All of the tests were conducted in position L-24 of the NRU reactor (see Figure 7). The TH-2 assembly was oriented in the reactor with side F facing north (fuel rods 2F, 3F, 4F, and 5F faced north).

Preconditioning was conducted at an average test assembly fuel rod power of about 18.7 kW/m (5.7 kW/ft) with the U-2 loop providing water cooling. Three short runs to full power permitted the fuel to crack and relocate within the cladding in a prototypic manner. System loop pressure was held at 8.62 MPa (1250 psia). Test assembly power was determined by calorimetric methods.

The pretransient phases of the tests were conducted with steam cooling provided by the U-1 loop at a mass flow rate of about 0.378 kg/s (3000 lbm/n) and a reactor power of about 7.4 MW. NRU reactor power was increased or decreased as required to maintain the same steam temperature increase across the test assembly. Even though the peak cladding temperatures varied from test to test, the total assembly power remained about the same since the cooling steam flow rate was maintained as consistently as possible at 0.378 kg/s (3000 lbm/h). During the TH-2.10 pretransient, it was discovered that the temperature reading of one of the four TCs in the test assembly outlet temperature pseudo sensor had been drifting downward over the test period, which meant

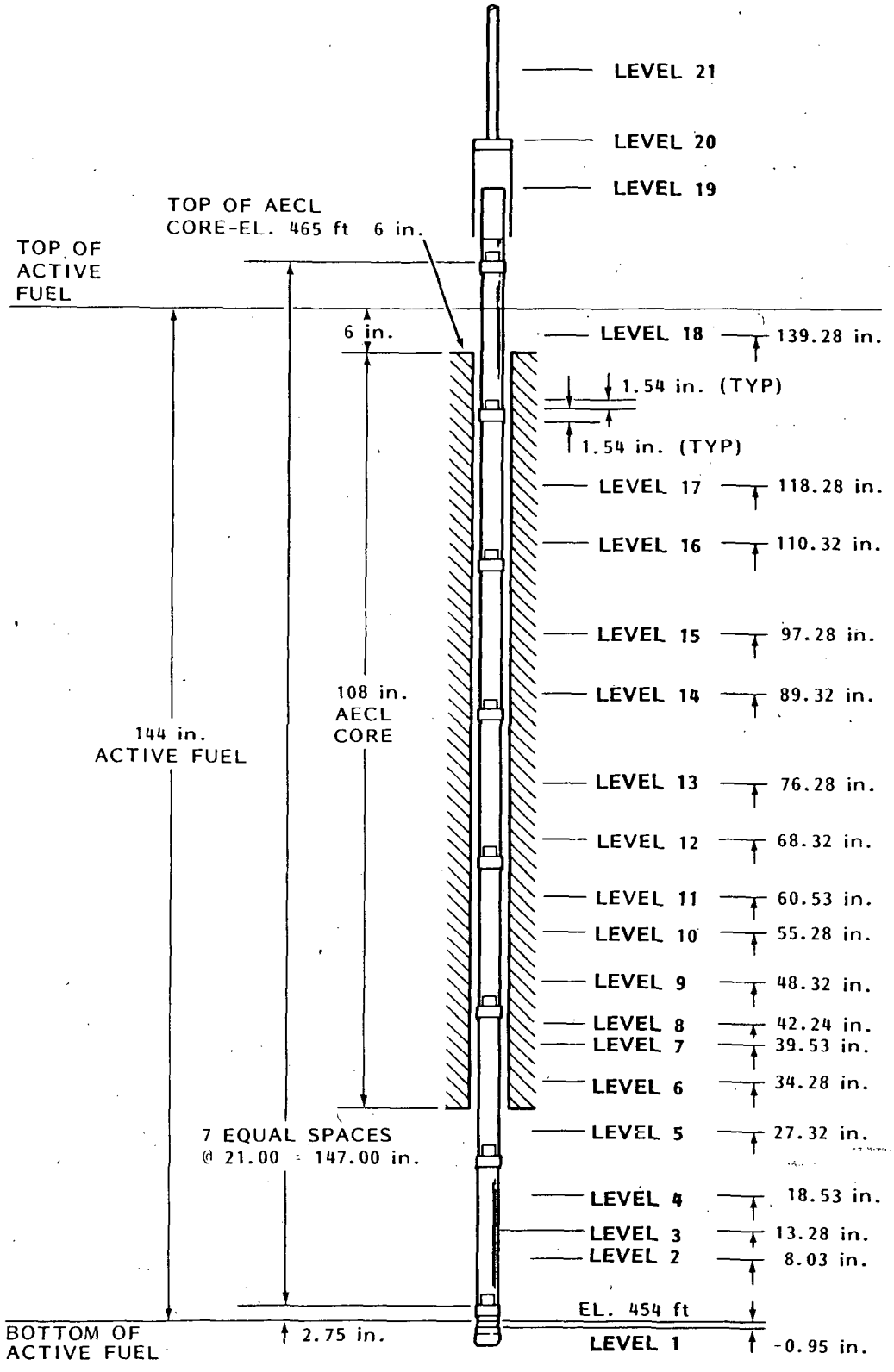

FIGURE 2. Instrumentation Levels in the TH-2 Test Assembly

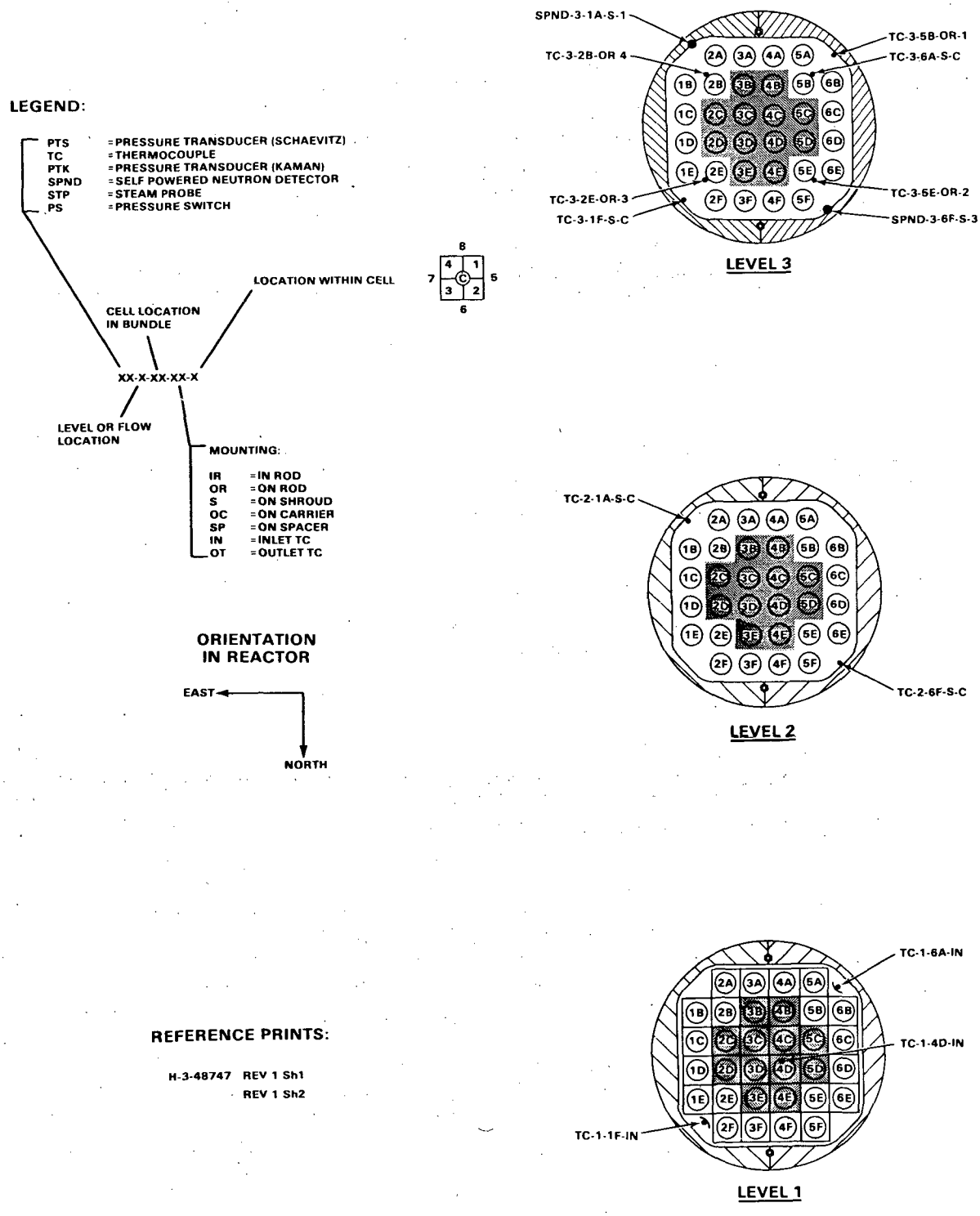

FIGURE 3. Instrumentation at Levels 1 Through 3 in the TH-2 Test Assembly

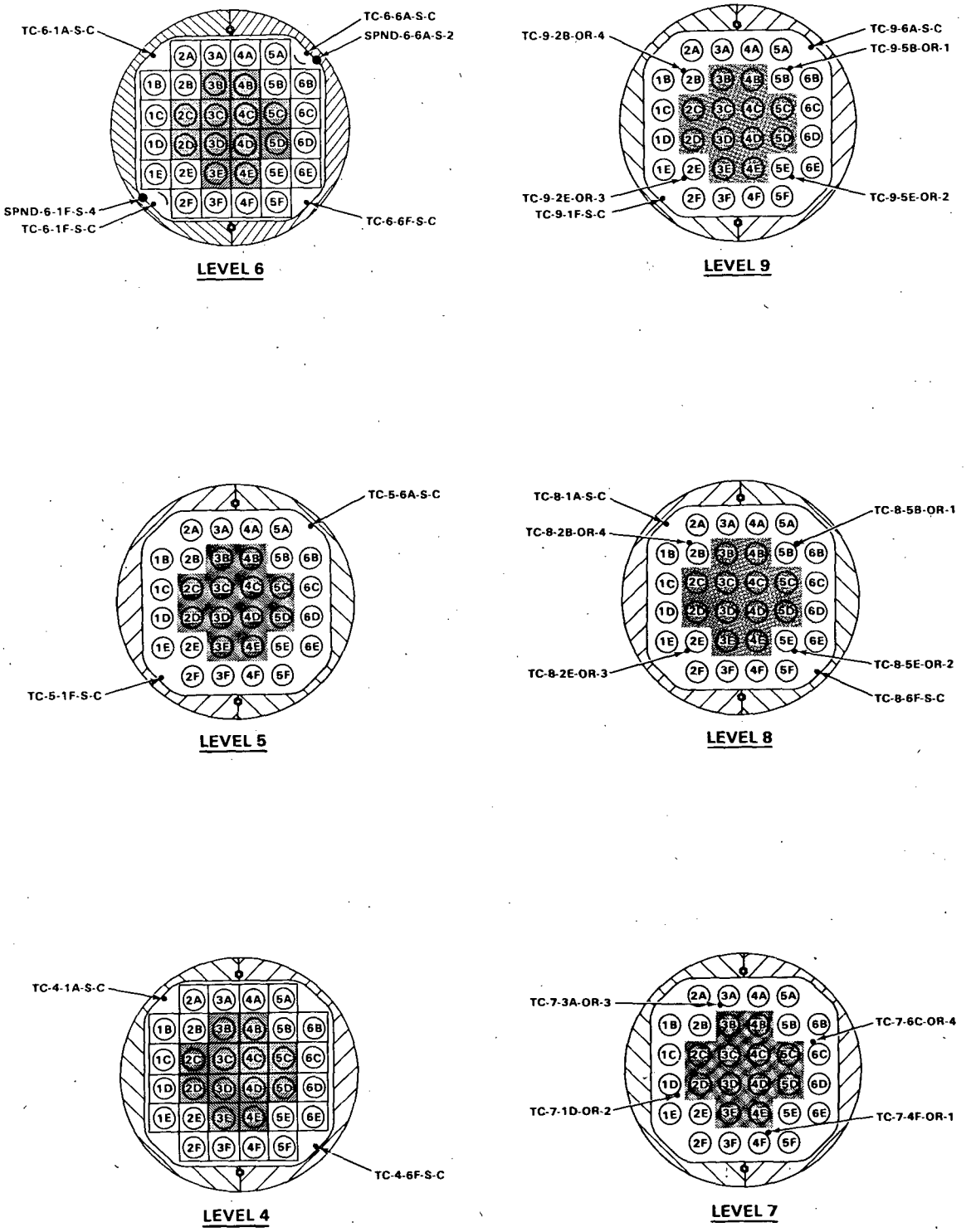

FIGURE 4. Instrumentation at Levels 4 Through 9 in the TH-2 Test Assembly

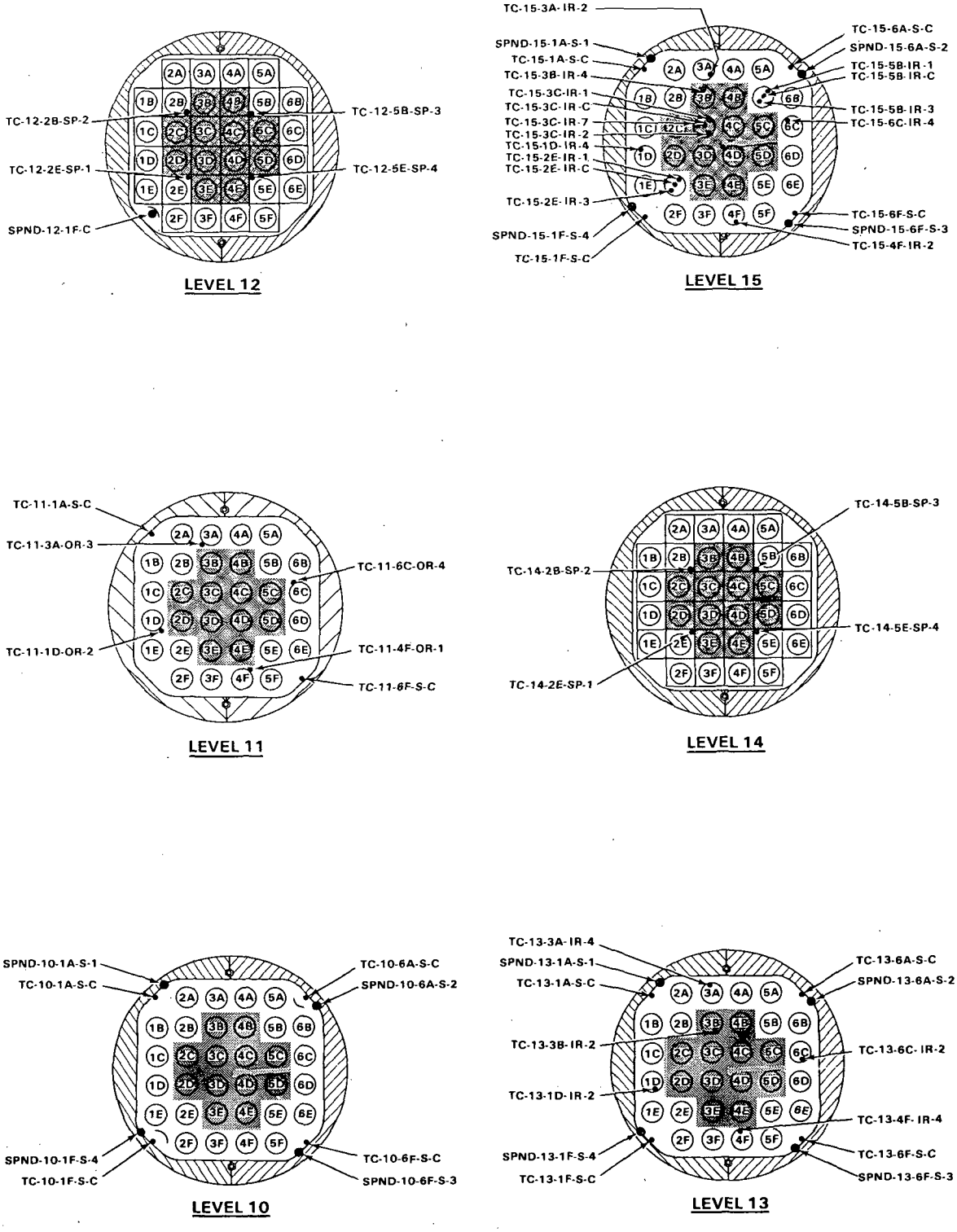

FIGURE 5. Instrumentation at Levels 10 Through 15 in the TH-2 Test Assembly

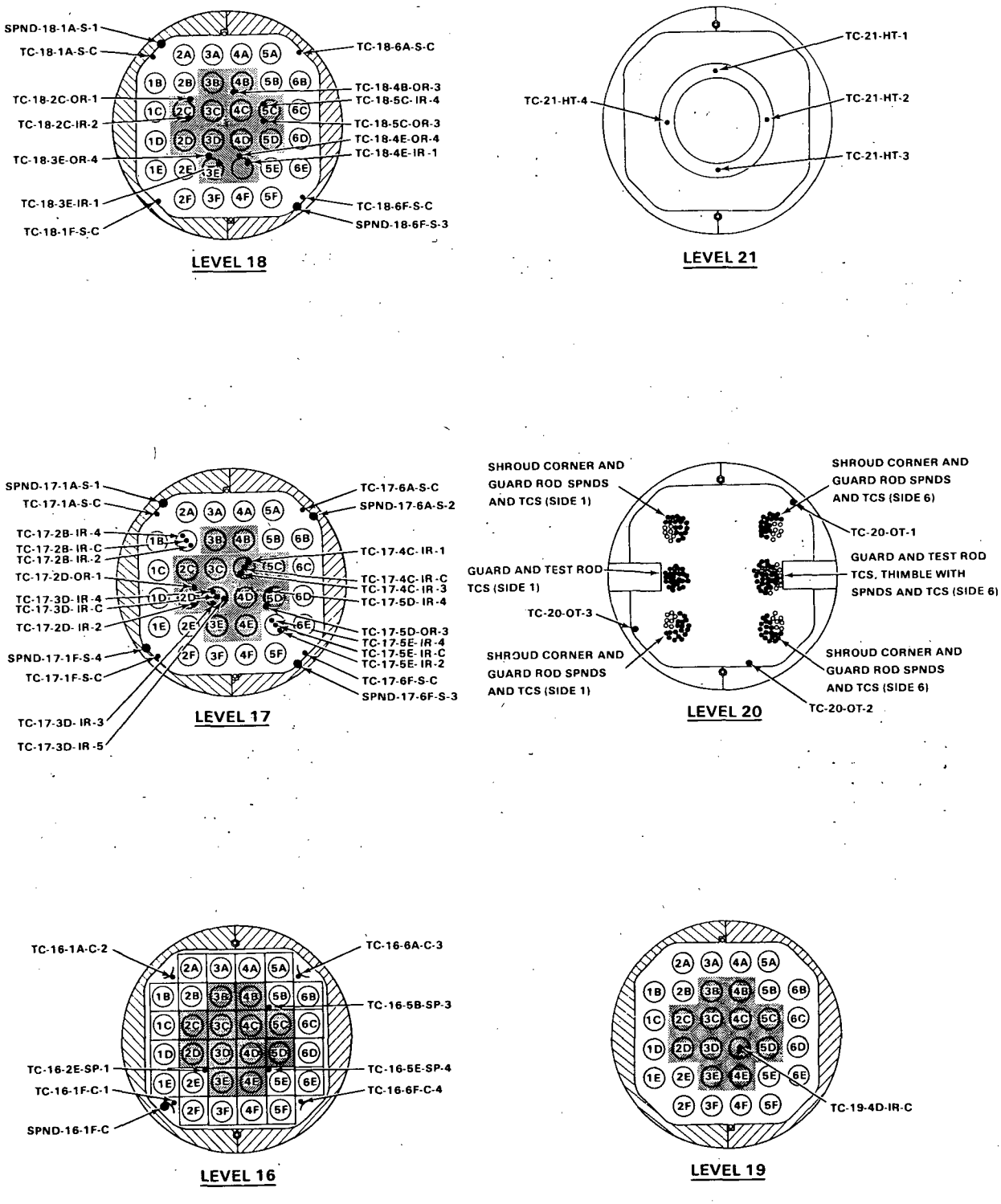

FIGURE 6. Instrumentation at Levels 16 Through 21 in the TH-2 Test Assembly

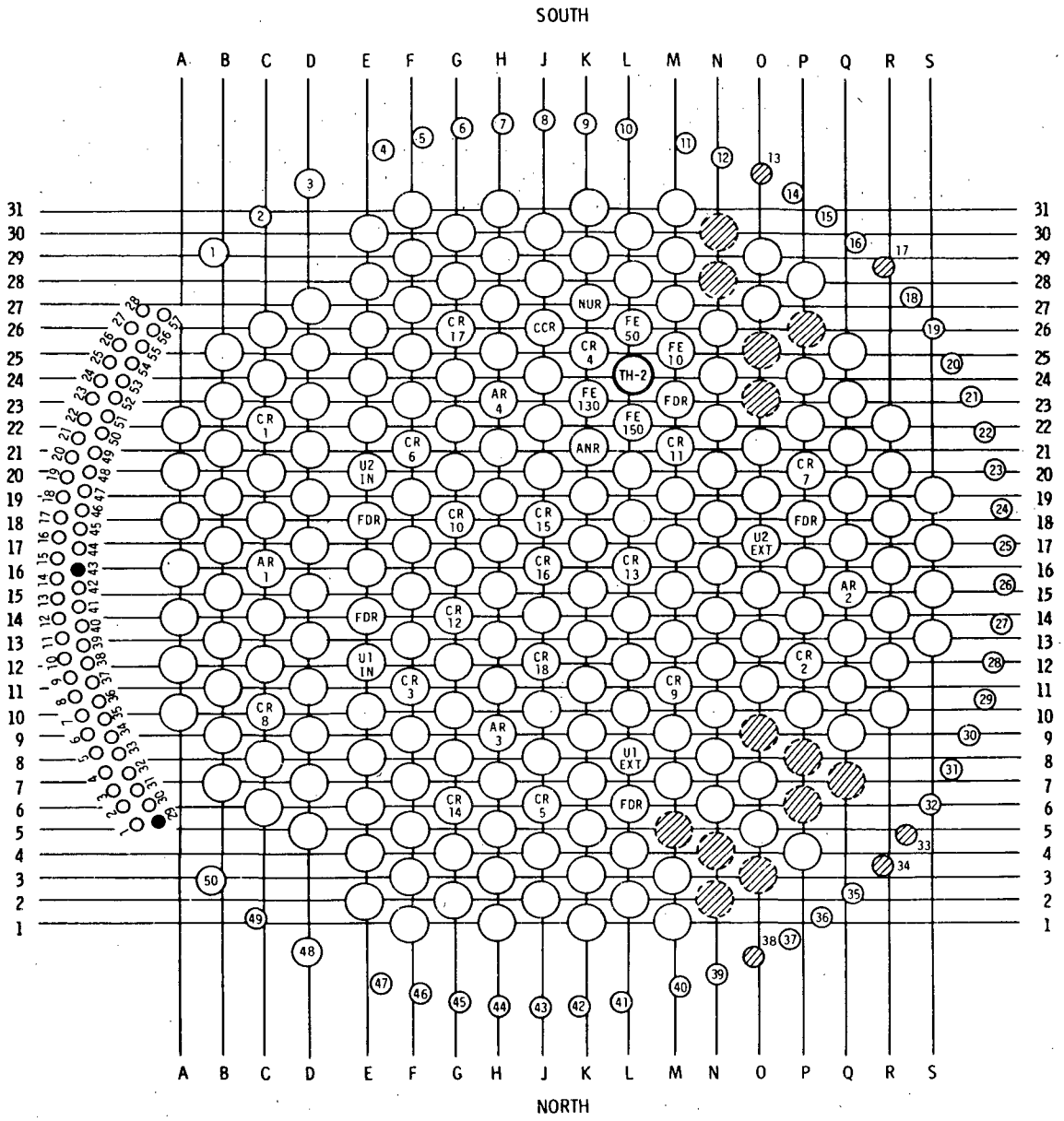

CR CONTROL ROD

AR ADJUSTER ROD

FDR FLUX DETECTOR ROD

U-1 IN, U-2 IN — DOWN FLOW CHANNEL - DUMMY FUEL

U-1 EXT, U-2 EXT — UP FLOW CHANNEL - DUMMY FUEL

○ STANDARD LATTICE POSITION

▨ BLOCKED CHANNEL - NOT FUELED

CCR COBALT CARRIER ROD

NUR NATURAL URANIUM ROD

ANR ALUMINUM NITRIDE ROD

FE 50 FUEL ELEMENT - 50 MWd BURNUP

FE 10 FUEL ELEMENT - 10 MWd BURNUP

FE 130 FUEL ELEMENT - 130 MWd BURNUP

FE 150 FUEL ELEMENT - 150 MWd BURNUP

FIGURE 7. NRU Reactor Core Configuration

meant that test assembly power and coolant temperature had gradually increased. For the remaining tests (10 through 14), this TC was removed from the outlet temperature pseudo sensor. Test TH-2.13 was an adiabatic test that used no reflood water; it was conducted to determine the fuel rod axial power distribution using a temperature ramp rate technique. The average assembly power for TH-2.13 was 1.228 or 1.310 kW/m (0.3744 or 0.3993 kW/ft) as determined by calorimetric and adiabatic power calculation techniques, respectively.

The transient phase for each TH-2 test began when the steam coolant flow was reduced from 0.378 kg/s (3000 lbm/h) to 0 (as indicated by a sharp drop in temperature of the Level 1 TCs); reactor power was maintained at about 7.4 MW. Test TH-2.02 was the only test to use a preprogrammed reflood delay and reflood coolant flow controlled by the LCS with no temperature feedback control; all remaining tests used feedback control concepts. Tests TH-2.03 through TH-2.05 used LCS preprogrammed control for 85 s and DACS temperature feedback after 85 s. Tests TH-2.06 through TH-2.14 (excluding adiabatic test TH-2.13) used LCS preprogrammed control for 95 s and DACS temperature feedback after 95 s. The DACS with temperature feedback monitored selected temperatures (hot spot sensors) at Levels 13, 15, and 17 and used the hottest average for control. After test TH-2.03, the hot spot sensors at Level 13 were removed from the control system. The DACS used a combination of proportional, integral, and differential control. Weighting parameters for the first and second derivative of temperature with respect to time were changed with successive tests to optimize performance.

EXPERIMENT CONDITIONS AND RESULTS

The test conditions measured during the experiment are described in Table 2. The table also includes the reactor trip criteria, the type of test (adiabatic, reflood, or transient), and the type of reflood control (LCS preprogrammed reflood flow or DACS with temperature feedback).

Test TH-2.02 used a preprogrammed reflood delay and reflood coolant flow controlled by the LCS. One of the major problems with preprogrammed control is obtaining the precise reflood delay time. A slightly different delay time can affect the time at temperature and the test repeatability. The average test rod temperatures at Levels 13, 15, and 17 for TH-2.02 are presented in Figure 8.

With the exception of adiabatic test TH-2.13, tests TH-2.03 through TH-2.14 used LCS preprogrammed flow for the first 85 to 95 s and DACS cladding temperature feedback control for the remainder of the test. These tests developed the DACS parameters until the desired control and repeatability were obtained in tests TH-2.12 and TH-2.14. Figures 9 through 19 demonstrate the evolution of the DACS using temperature feedback where selected hot spot sensors were used.

Adiabatic heatup tests determined local fuel power for the first test (TH-2.01) and for test TH-2.13. These adiabatic tests are compared in Figures 20 through 22.

Test repeatability using the DACS for companion tests TH-2.12 and TH-2.14 is shown in Figures 23 through 25. Average test rod inside cladding temperatures at Levels 13, 15, and 17 and reflood rates are indicated.

Appendices A through F summarize the preliminary data resulting from tests TH-2.02, TH-2.12, TH-2.13, and TH-2.14. The data are arranged as follows:

Appendix A - Preconditioning Test Assembly Temperatures
Appendix B - Pretransient Test Assembly Temperatures
Appendix C - Transient Fuel and Cladding Temperatures
Appendix D - Test Coolant and Shroud Temperatures
Appendix E - Neutron Flux
Appendix F - Reflood Flow Measurements.

TABLE 2. Measured Experimental Operating Conditions[a]

Parameter	Preconditioning	Reflood Calibration	Transient, TH-2.01	Transient, TH-2.02	Transient, TH-2.03	Transient, TH-2.04	Transient, TH-2.05	Transient, TH-2.06
Reactor power, MW	127	0	~7.4	~7.4	~7.4	~7.4	~7.4	~7.4
Test assembly power, kW								
Coolant	U-2 water	U-1 steam/ reflooding	U-1 steam/ reflooding	U-1 steam/ reflooding	U-1 steam/ reflooding	U-1 steam/ reflooding	U-1 steam/ reflooding	U-1 steam/ reflooding
Coolant flow, kg/s (lbm/h)	0 to 16.30 (0 to 129,400)	0.378 (3000)	0.380 (3016)	0.383 (3040)	0.382 (3030)	0.382 (3030)	0.382 (3030)	0.381 (3023)
Reflood delay, s	NA[b]	0	NA					
Reflood rates, m/s (in./s)		0.0508, 0.0254, 0.0508 (2.0, 1.0, 2.0)	0					
Transient initiation time[c]	NA	NA	9/30/81 ~21:25:44	9/30/81 ~23:07:43	10/1/81 ~1:29:40	10/1/81 ~14:20:04	10/1/81 ~16:46:10	10/1/81 ~18:13:45
Pretransient cladding temperature, K (°F)	NA	NA	707 (813)					
Peak cladding temperature (PCT), K (°F)	700 (800)	433 (320)	1005 (1350)					
Reactor conditional trip criteria (PCT), K (°F)		NA	978 (1300)	1103 (1525)	1103 (1525)	1144 (1600)	1144 (1600)	1144 (1600)
PCT turnaround time,[d] s			~30 s ~9/30/81 21:27:48					
Bundle quench time,[d] s			NA					
Type of test	NA	Reflood	Adiabatic	Transient	Transient	Transient	Transient	Transient
Type of reflood control			NA	LCS[e]	DACS[f] after 85 s	DACS after 85 s	DACS after 85 s	DACS after 95 s

TABLE 2. (contd)

Parameter	Transient, TH-2.07	Transient, TH-2.08	Transient, TH-2.09	Transient, TH-2.10	Transient, TH-2.11	Transient, TH-2.12	Transient, TH-2.13	Transient, TH-2.14
Reactor power, MW	~7.4	~7.4	~7.4	~7.4	~7.4	~7.4	~7.4	~7.4
Test assembly power, kW						138.7	143.8	142.8
Coolant	U-1 steam/ reflooding	U-1 steam/ reflooding	U-1 steam/ reflooding	U-1 steam/ reflooding	U-1 steam/ reflooding	U-1 steam/ reflooding	U-1 steam/ reflooding	U-1 steam/ reflooding
Coolant flow, kg/s (lbm/h)	0.383 (3040)	0.378 (3000)	0.379 (3010)	0.378 (3000)	0.378 (3000)	0.378 (3000)	0.378 (3000)	0.378 (3000)
Reflood delay, s						/	NA	/
Reflood rates, m/s (in./s)						0.572 (2.25) for 52 s; 0.0361 (1.42) for 16 s; 0.029 (0.90) for 20 s; 0.032 (1.19) for 26 s; 0.0137 (0.54) for 172 s	0	0.055 (2.18) for 54 s; 0.0361 (1.42) for 15 s; 0.0226 (0.89) for 24 s; 0.0345 (1.36) for 16 s; 0.0137 (0.54) for 136 s; 0.0188 (0.74) for 14 s; 0.0130 (0.51) for 72 s
Transient initiation time	10/1/81 ~19:30:49	10/2/81 ~9:46:09	10/2/18 ~11:22:25	10/2/81 ~12:53:52	10/2/81 ~14:37:11	10/2/81 ~15:59:07	10/2/81 ~16:39:31	10/2/81 ~17:20:21
Pretransient cladding temperature, K (°F)						743 (877)	783 (869)	737 (867)
Peak cladding temperature (PCT), K (°F)						1174 (1653)	1013 (1364)	1274 (1634)
Reactor conditional trip criteria (PCT), K (°F)	1144 (1600)	1144 (1600)	1144 (1600)	1144 (1600)	1144 (1600)	1144 (1600)	1144 (1600)	1144 (1600)
PCT turnaround time, s						273	33	244
Bundle quench time, s						306	NA	338
Type of test	Transient	Transient	Transient	Transient	Transient	Transient	Adiabatic	Transient
Type of reflood control	DACS after 95 s	DACS after 95 s	DACS after 95 s	DACS after 95 s	DACS after 95 s	DACS after 95 s	NA	DACS after 95 s

(a) TH-2.12 and TH-2.14 were the principal TH-2; tests data not reported for the other tests may be reported in a subsequent report.
(b) Not applicable.
(c) Transient initiated by termination of steam flow.
(d) Time after initiation of transient.
(e) LCS = loop control system.
(f) DACS = data acquisition and control system.

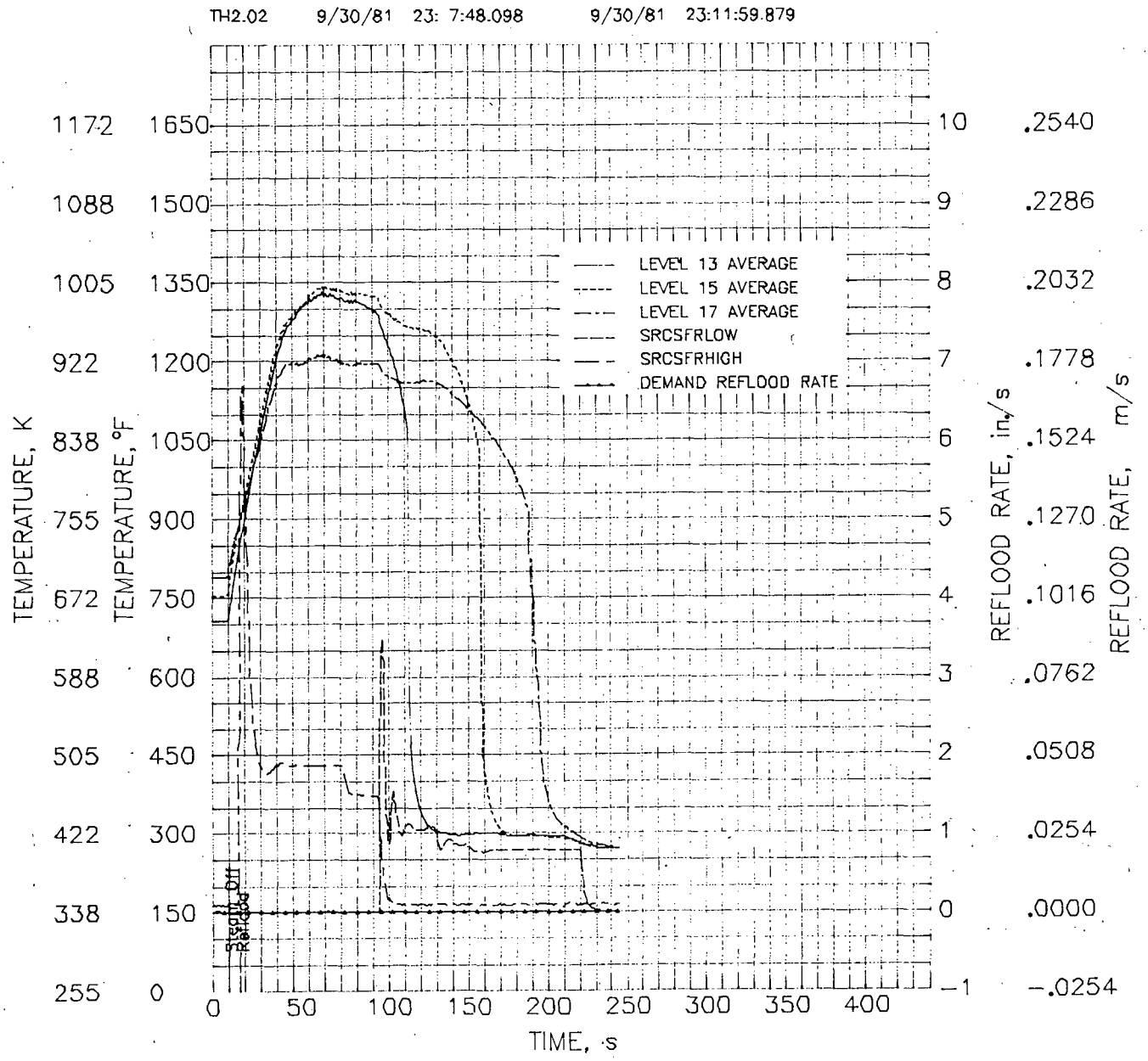

FIGURE 8. Average Test Rod Temperatures at Levels 13, 15, and 17 and Demand and Actual Reflood Flow Rates for TH-2.02 Using LCS Preprogrammed Reflood Control

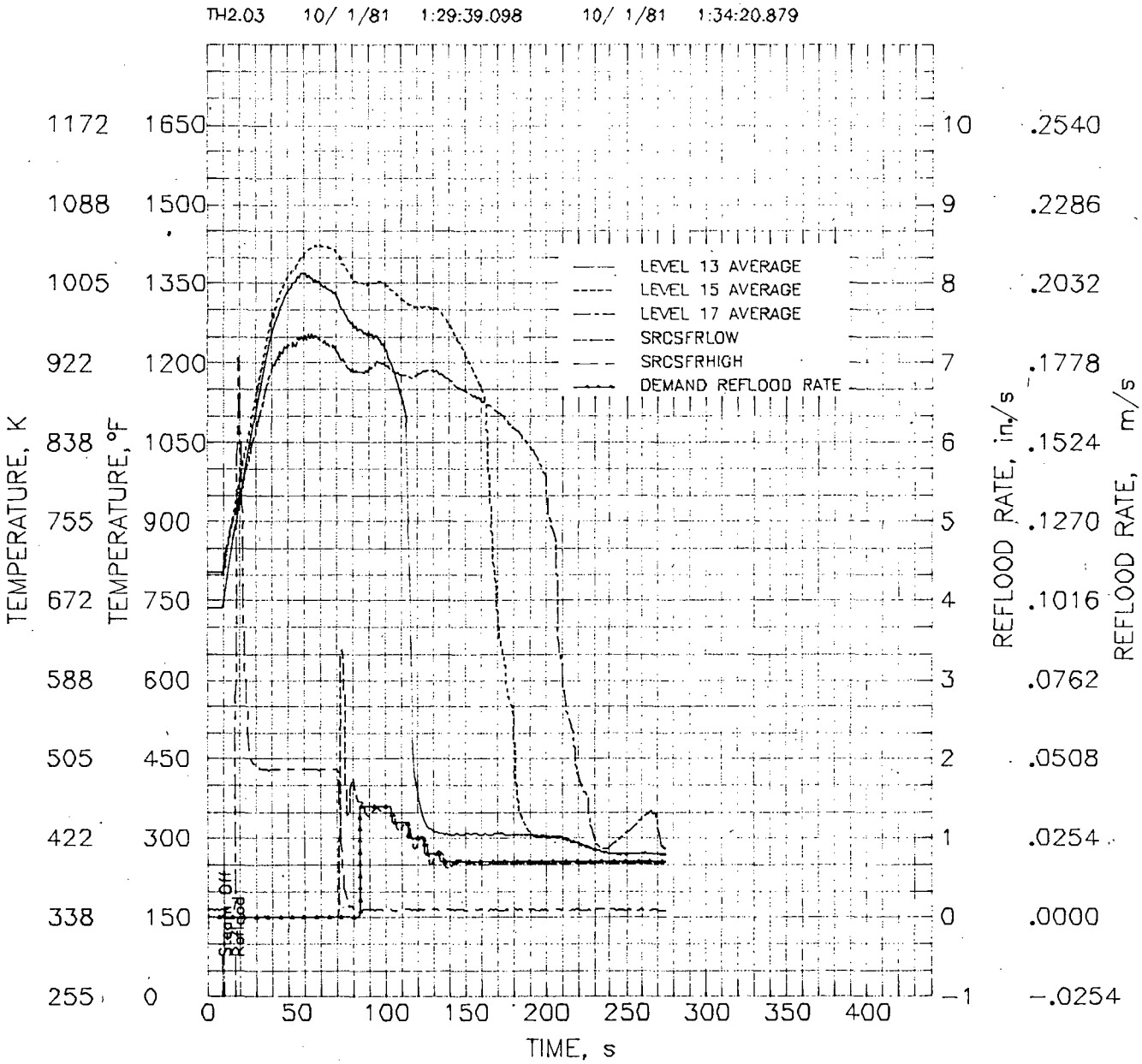

FIGURE 9. Hot Spot Sensor Averages at Levels 13, 15, and 17 (85 s after steam off) and Demand and Actual Reflood Flow Rates for TH-2.03 Using DACS Control

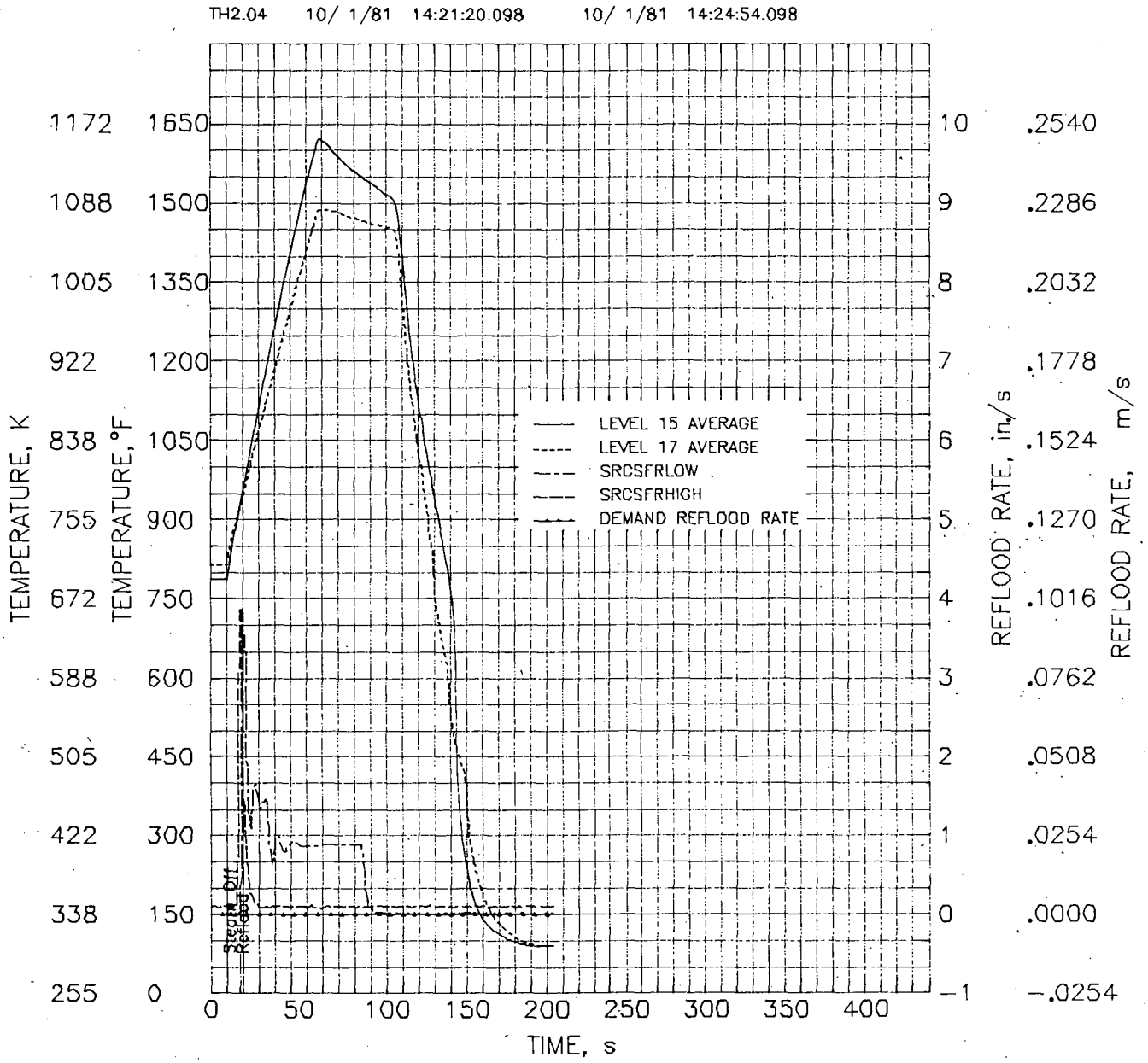

FIGURE 10. Hot Spot Sensor Averages at Levels 15 and 17 (85 s after steam off) and Demand and Actual Reflood Flow Rates for TH-2.04 Using DACS Control

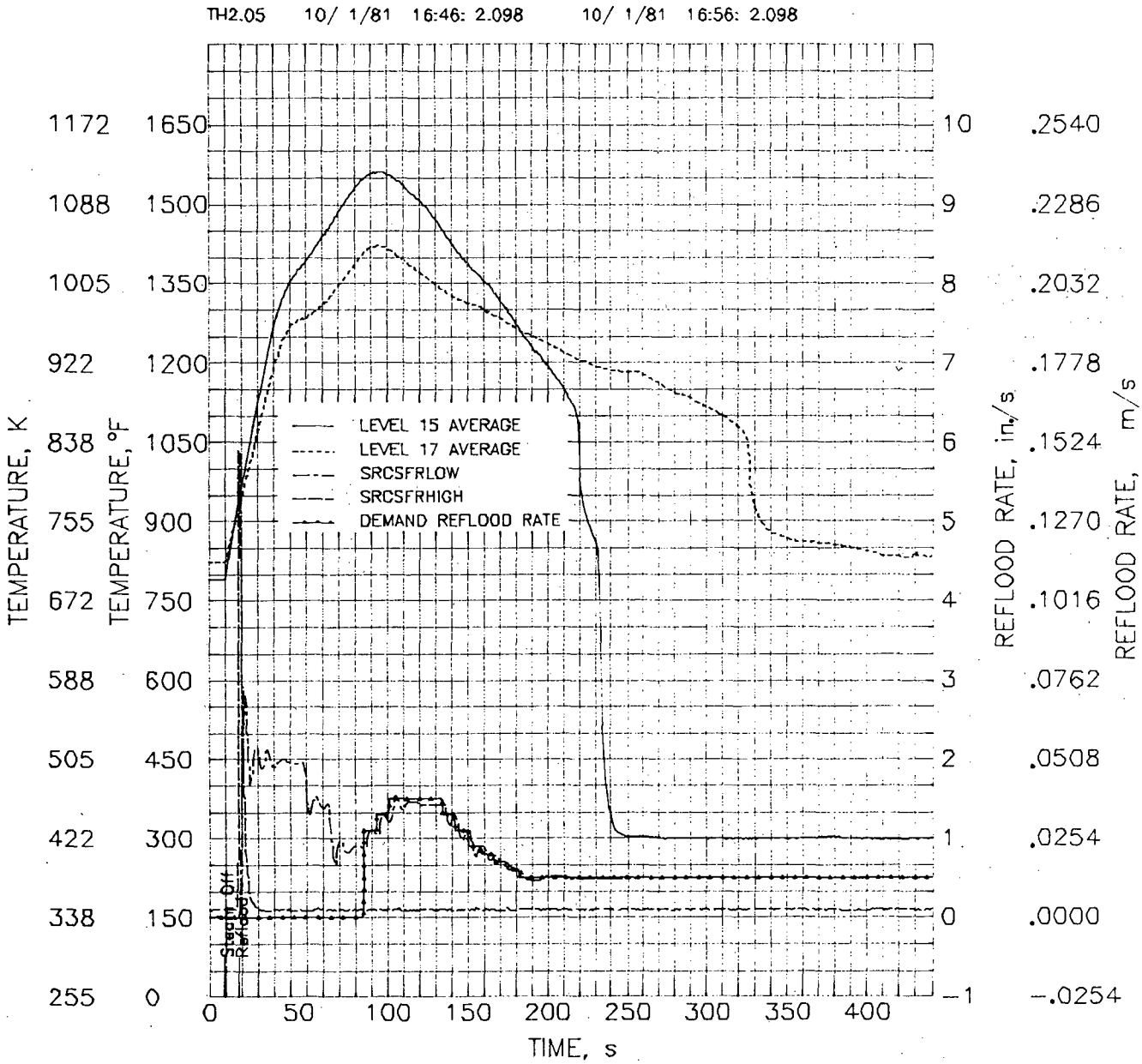

FIGURE 11. Hot Spot Sensor Averages at Levels 15 and 17 (85 s after steam off) and Demand and Actual Reflood Flow Rates for TH-2.05 Using DACS Control

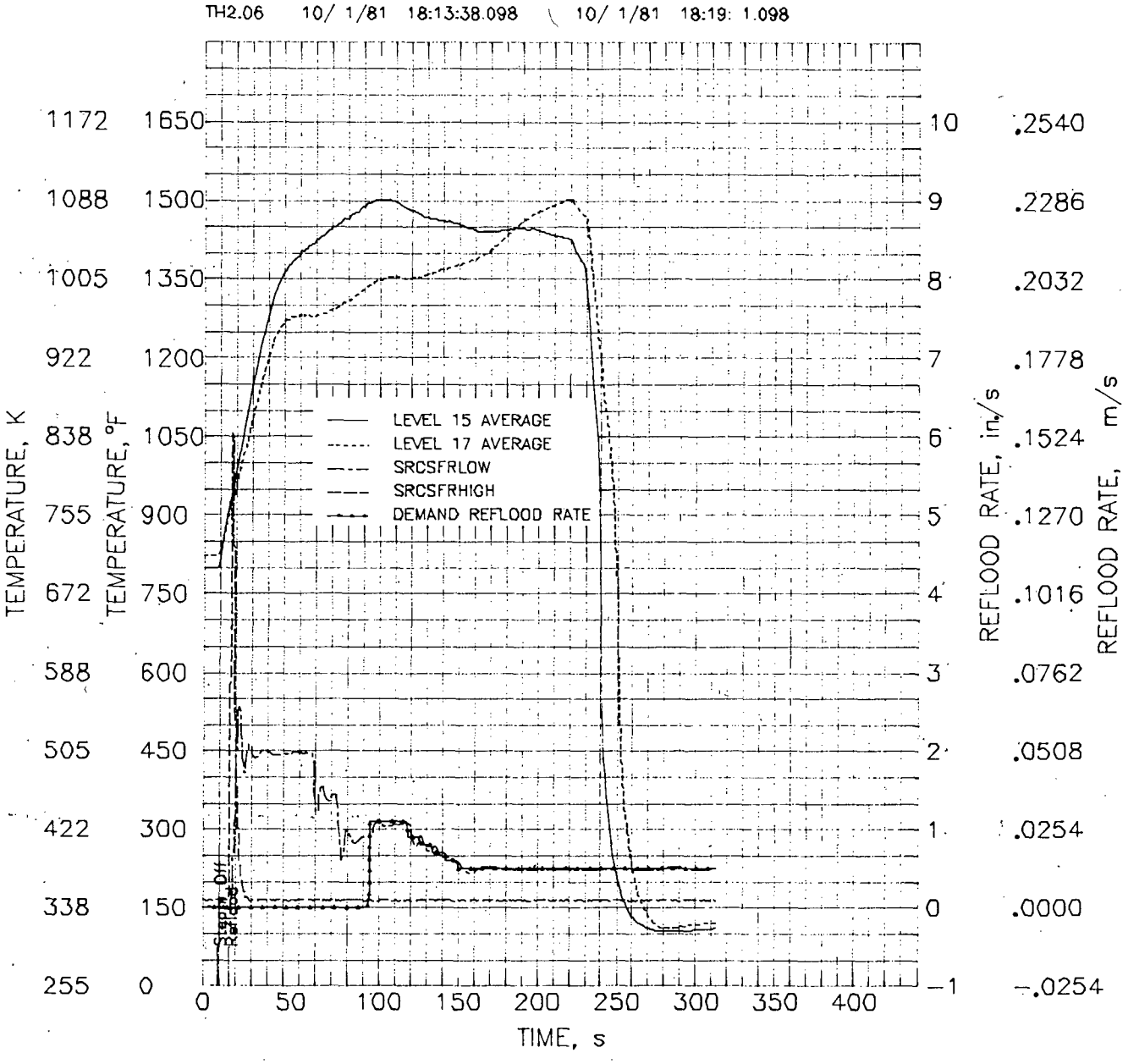

FIGURE 12. Hot Spot Sensor Averages at Levels 15 and 17 (95 s after steam off) and Demand and Actual Reflood Flow Rates for TH-2.06 Using DACS Control

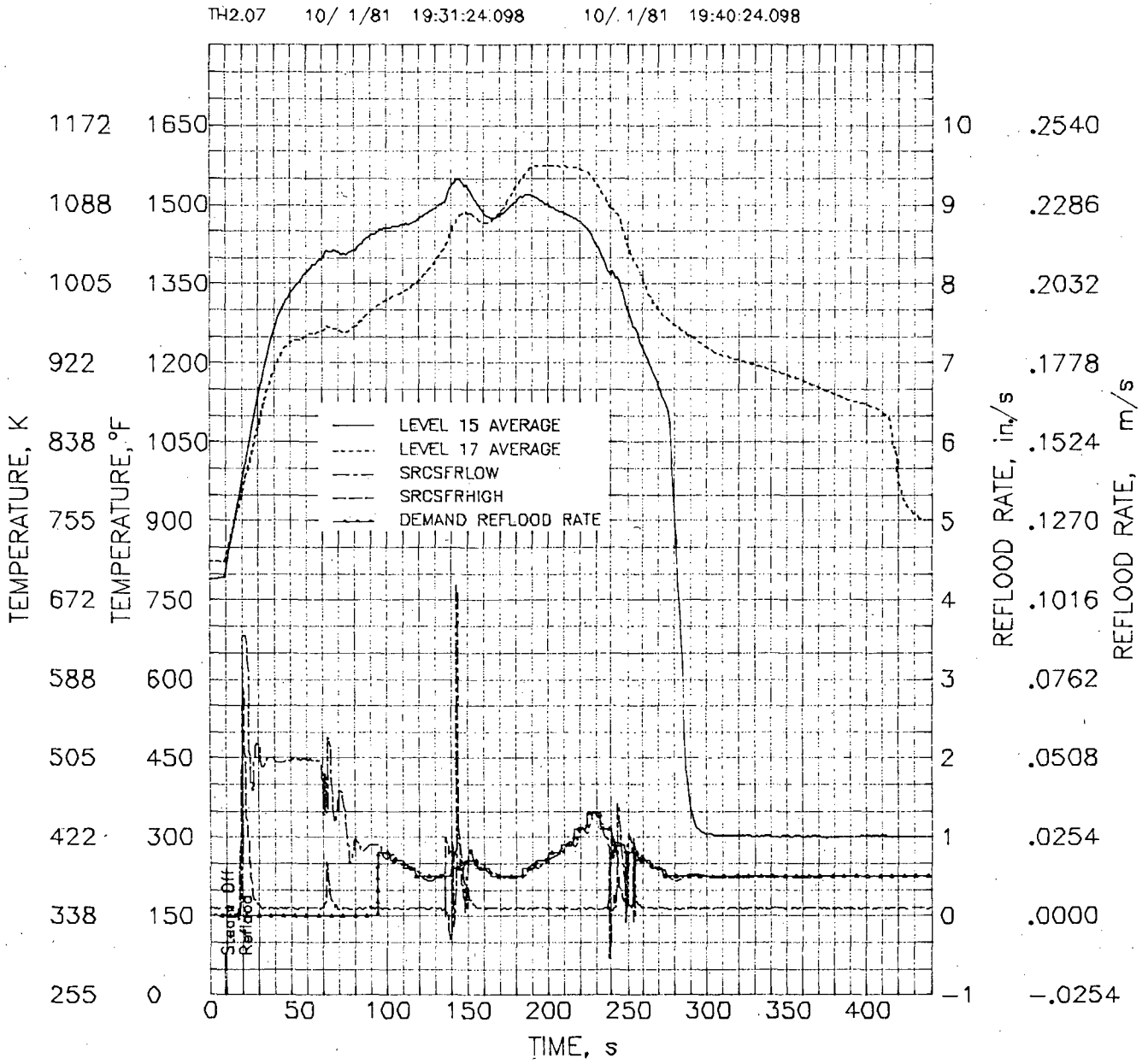

FIGURE 13. Hot Spot Sensor Averages at Levels 15 and 17 (95 s after steam off) and Demand and Actual Reflood Flow Rates for TH-2.07 Using DACS Control

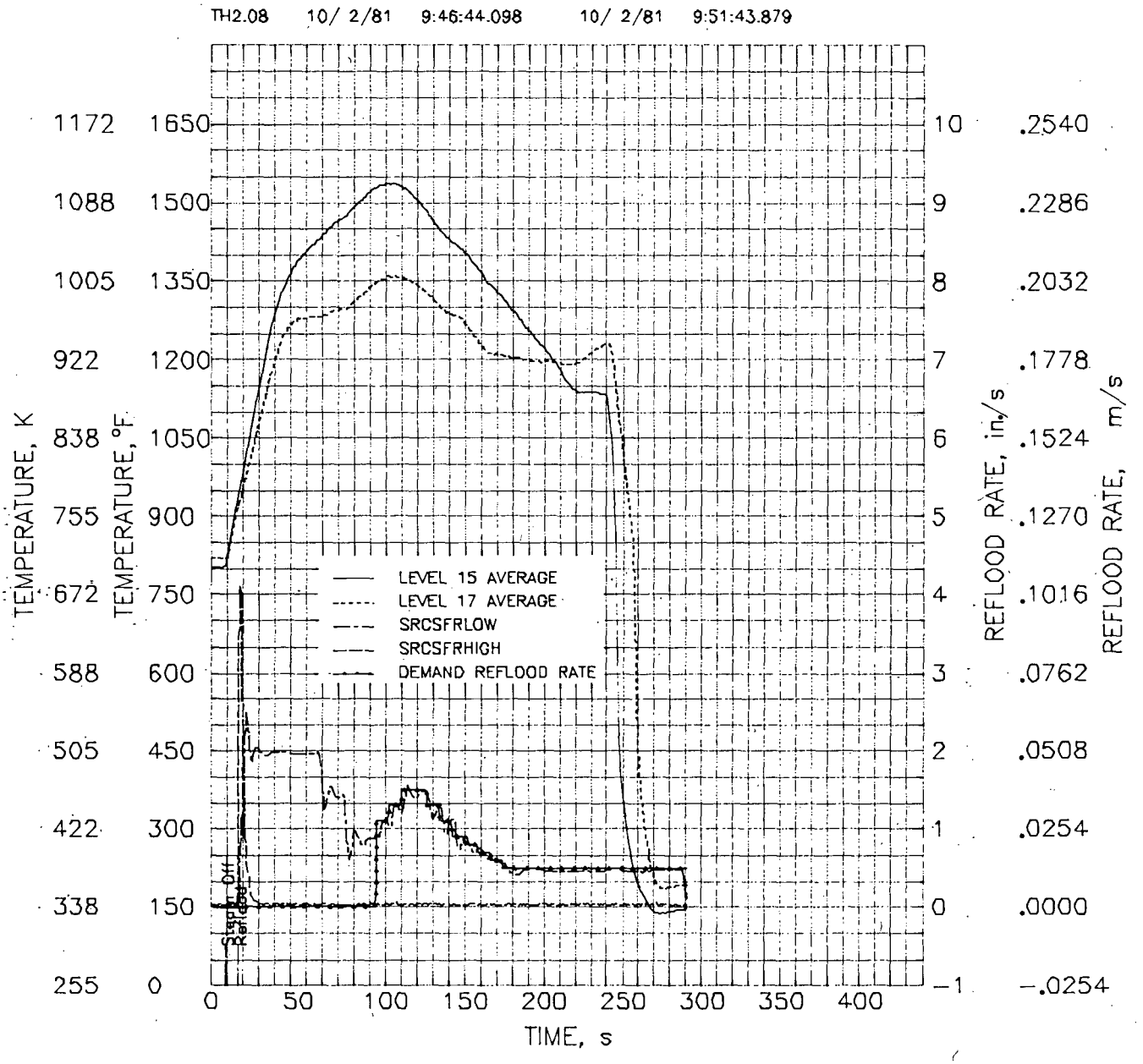

FIGURE 14. Hot Spot Sensor Averages at Levels 15 and 17 (95 s after steam off) and Demand and Actual Reflood Flow Rates for TH-2.08 Using DACS Control

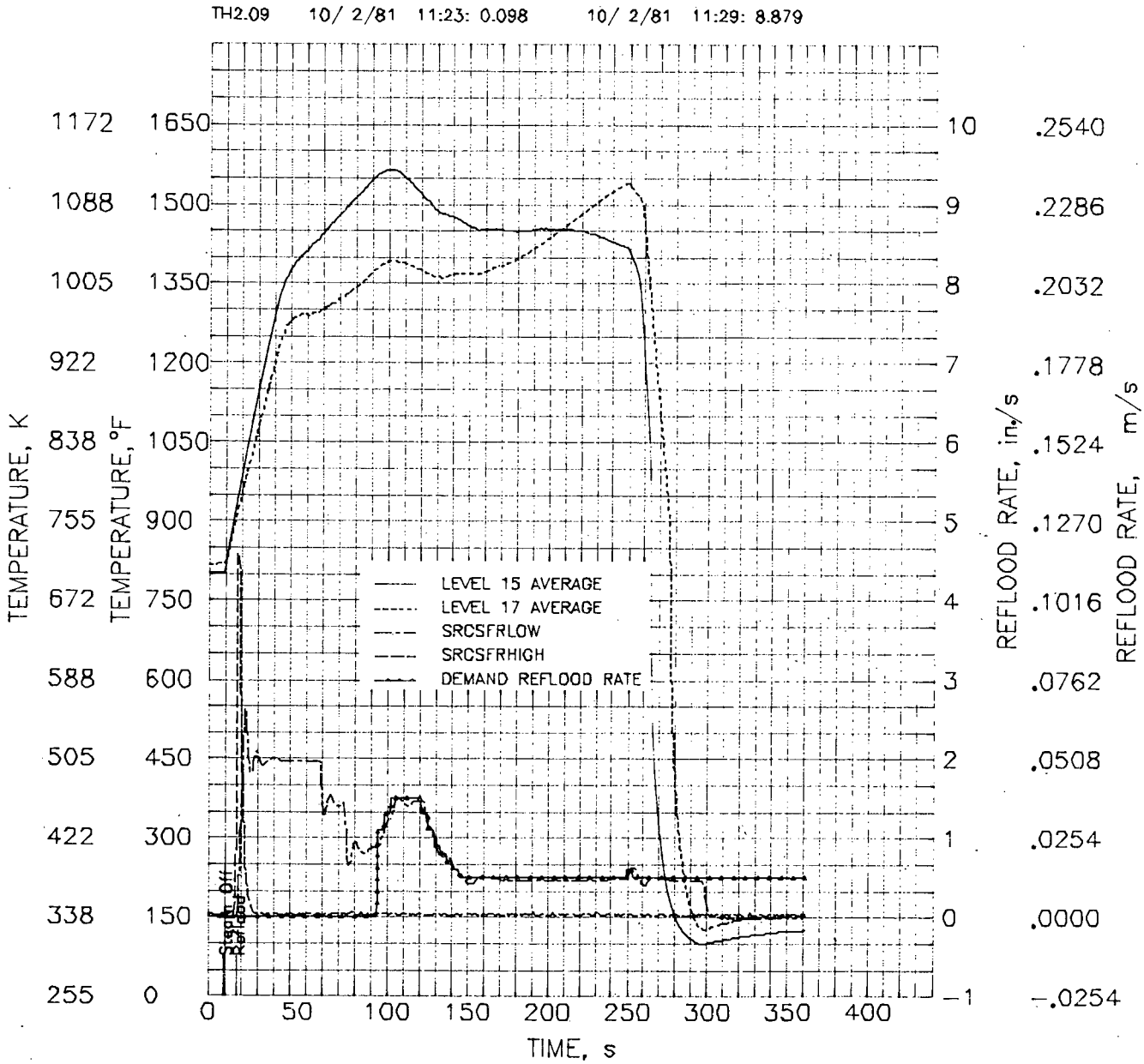

FIGURE 15. Hot Spot Sensor Averages at Levels 15 and 17 (95 s after steam off) and Demand and Actual Reflood Flow Rates for TH-2.09 Using DACS Control

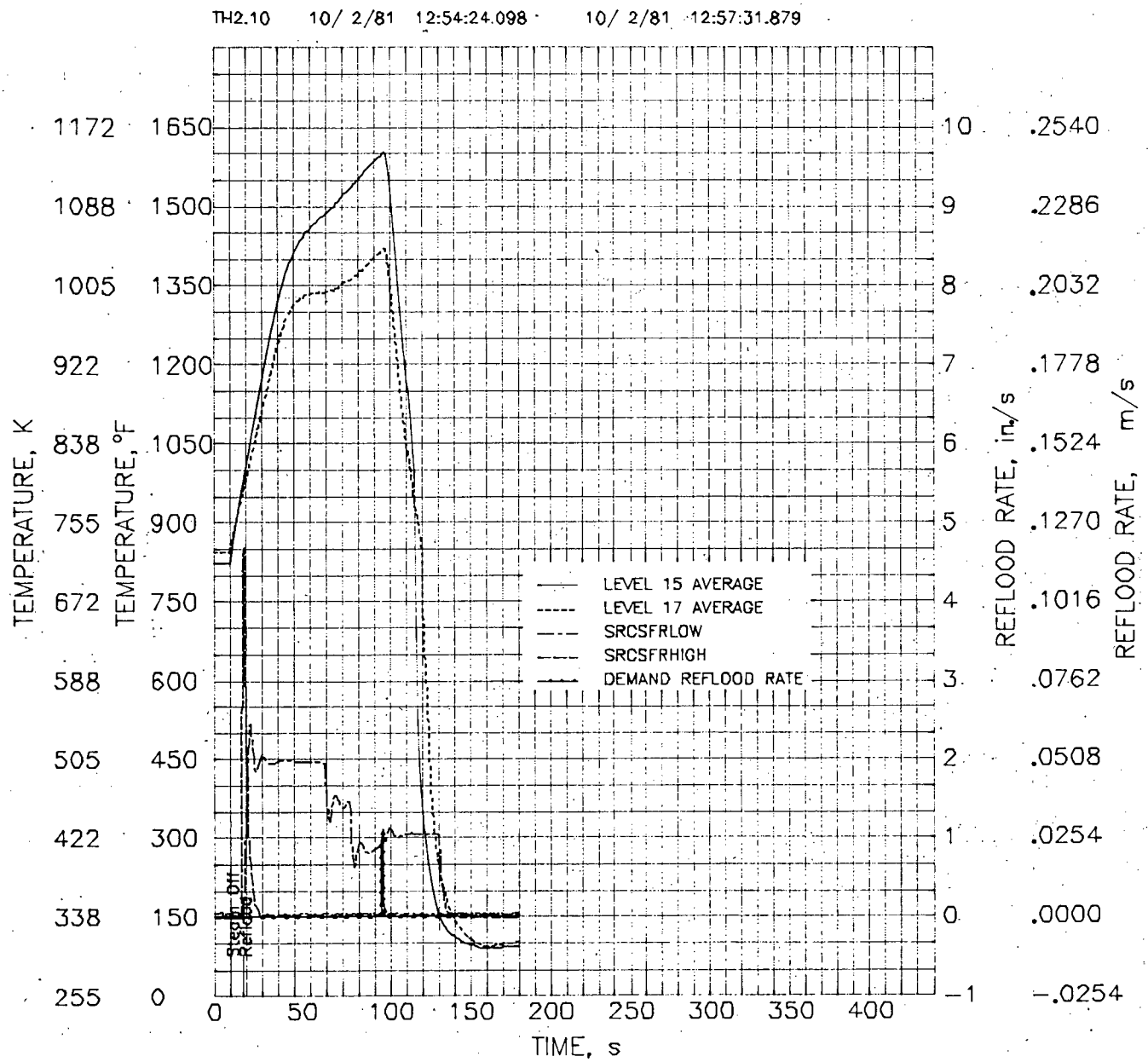

FIGURE 16. Hot Spot Sensor Averages at Levels 15 and 17 (95 s after steam off) and Demand and Actual Reflood Flow Rate for TH-2.10 Using DACS Control

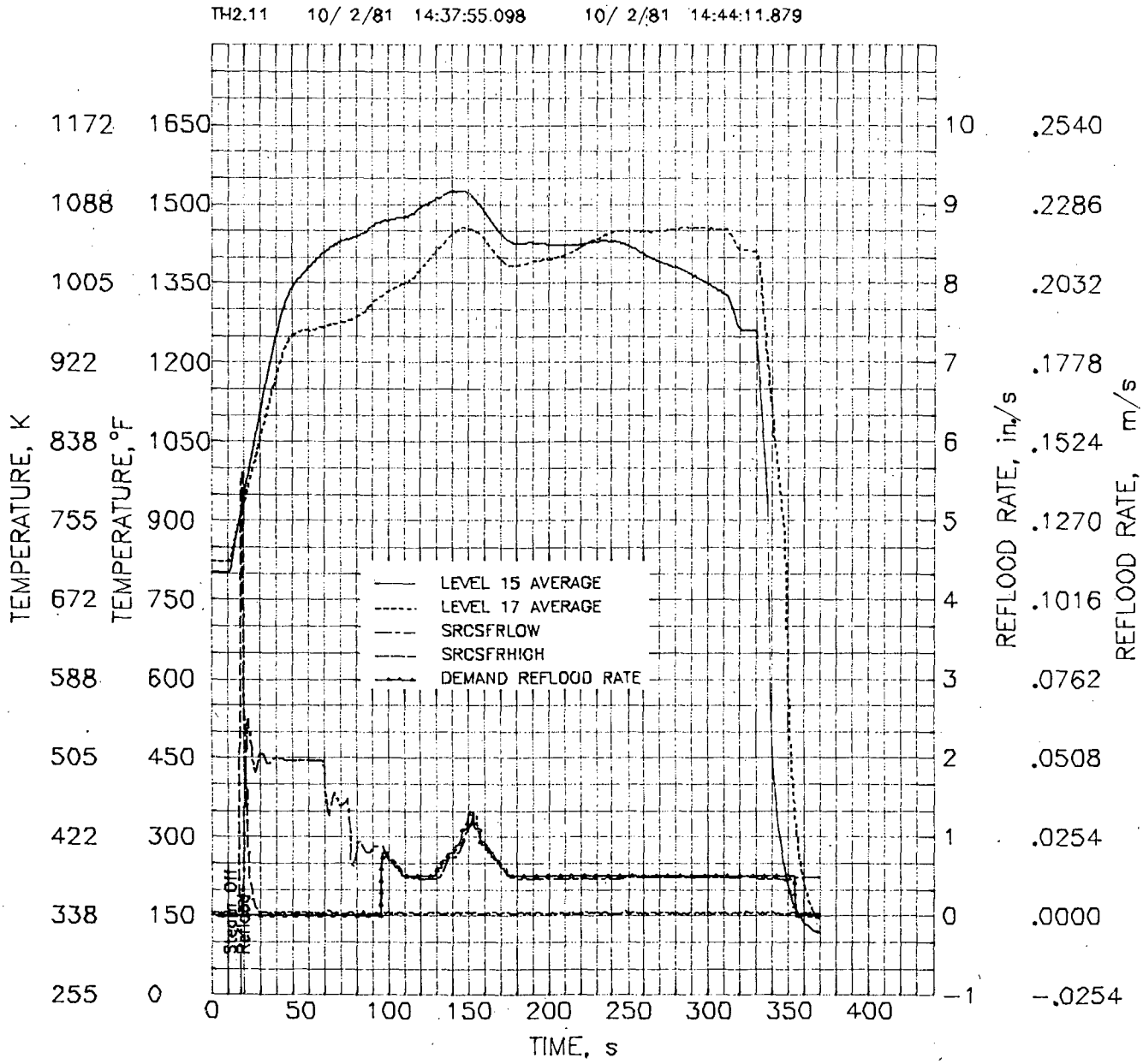

FIGURE 17. Hot Spot Sensor Averages at Levels 15 and 17 (95 s after steam off) and Demand and Actual Reflood Flow Rates for TH-2.11 Using DACS Control

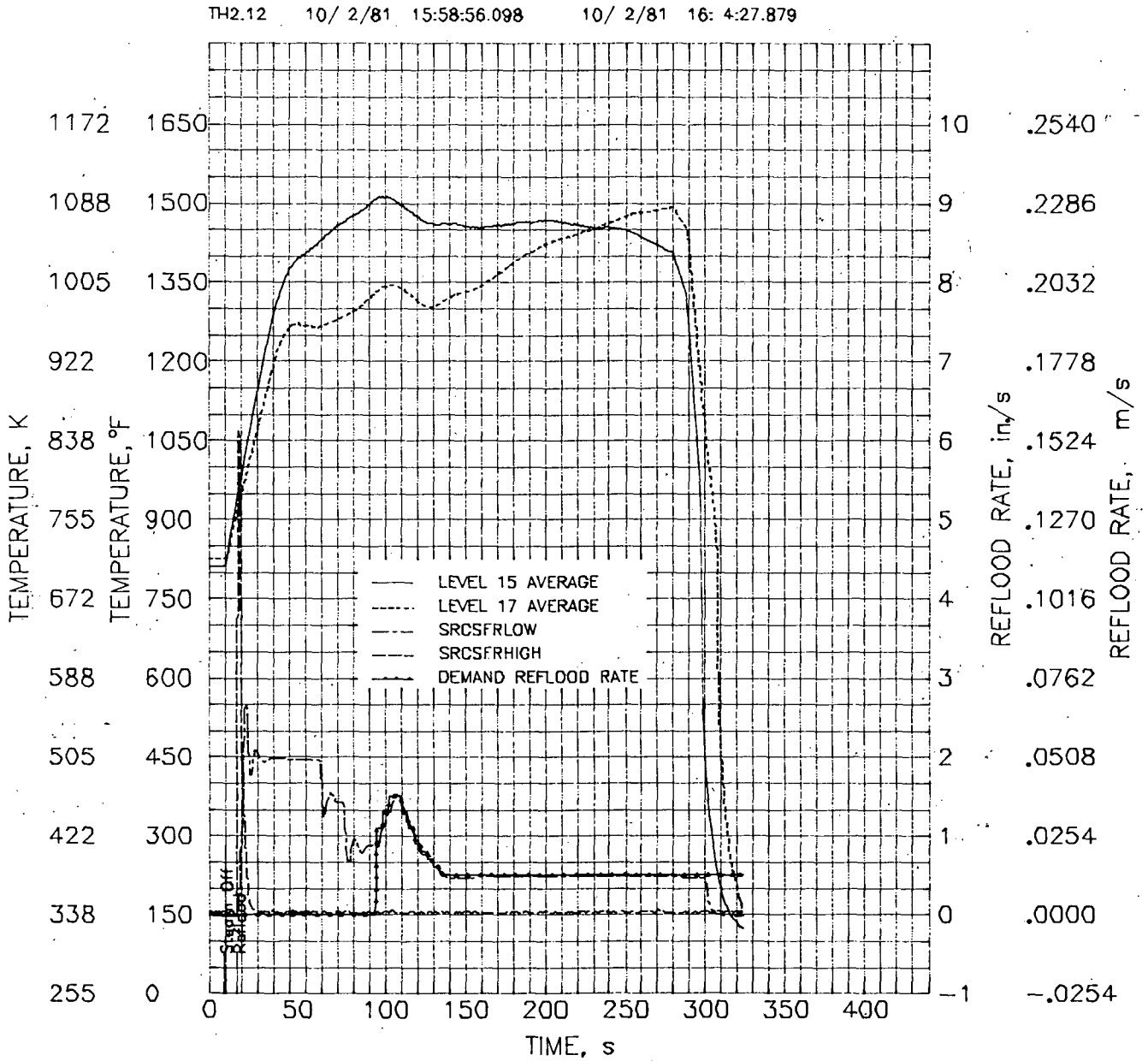

FIGURE 18. Hot Spot Sensor Averages at Levels 15 and 17 (95 s after steam off) and Demand and Actual Reflood Flow Rates for TH-2.12 Using DACS Control

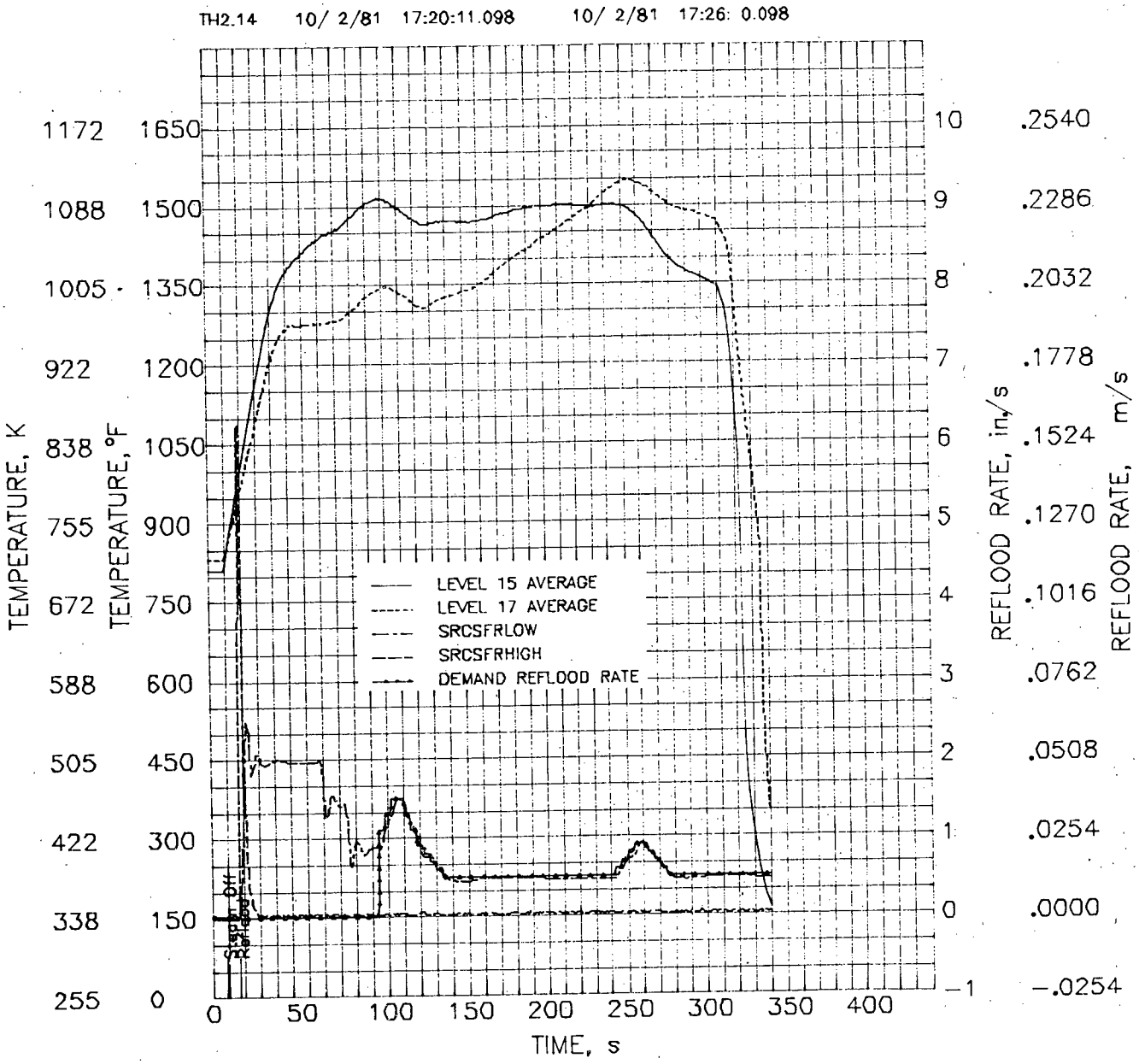

FIGURE 19. Hot Spot Sensor Averages at Levels 15 and 17 (95 s after steam off) and Demand and Actual Reflood Flow Rates for TH-2.14 Using DACS Control

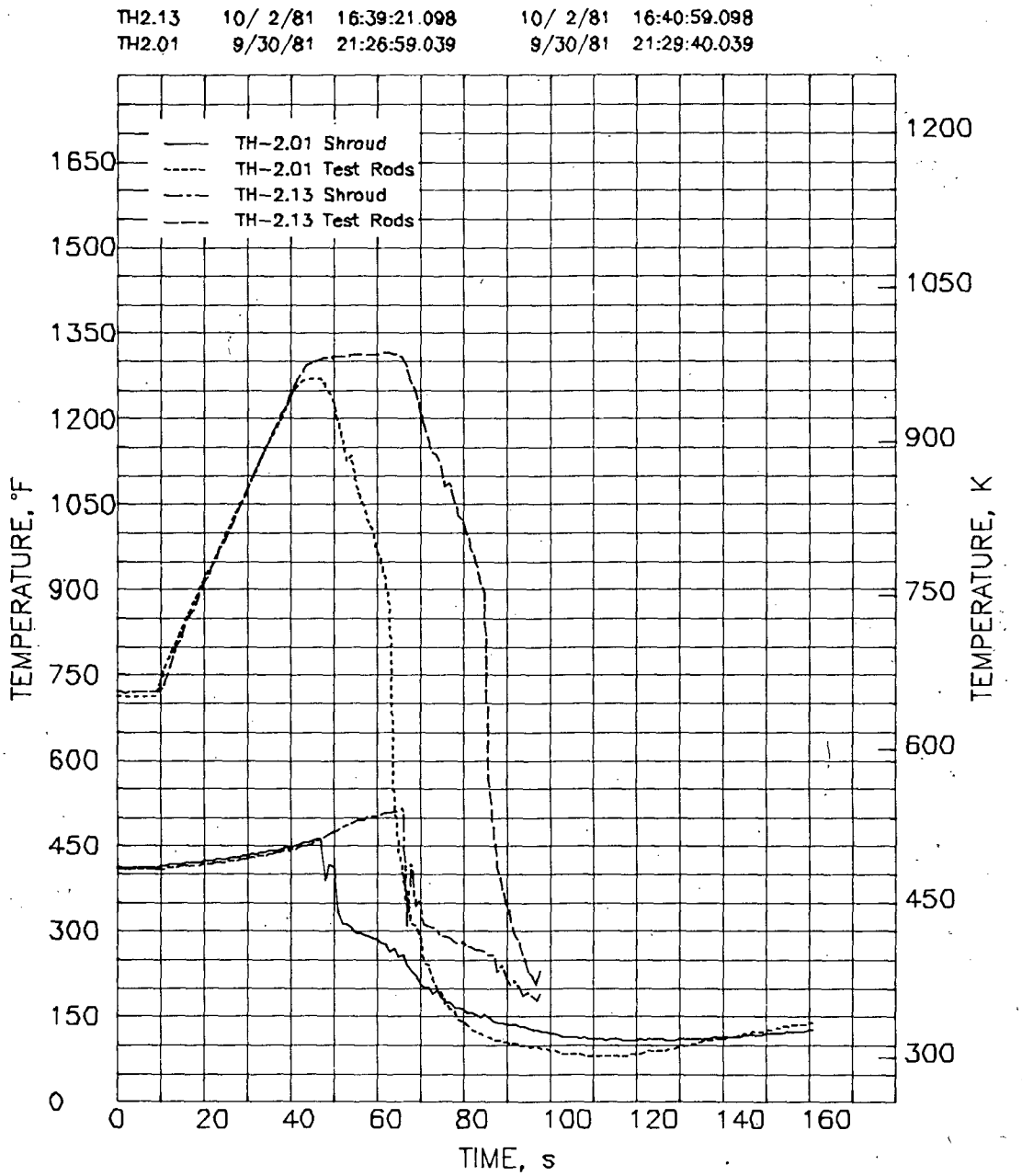

FIGURE 20. Comparison of Adiabatic Tests TH-2.01 and TH-2.13 Showing Average Test Rod and Shroud Temperatures at Level 13

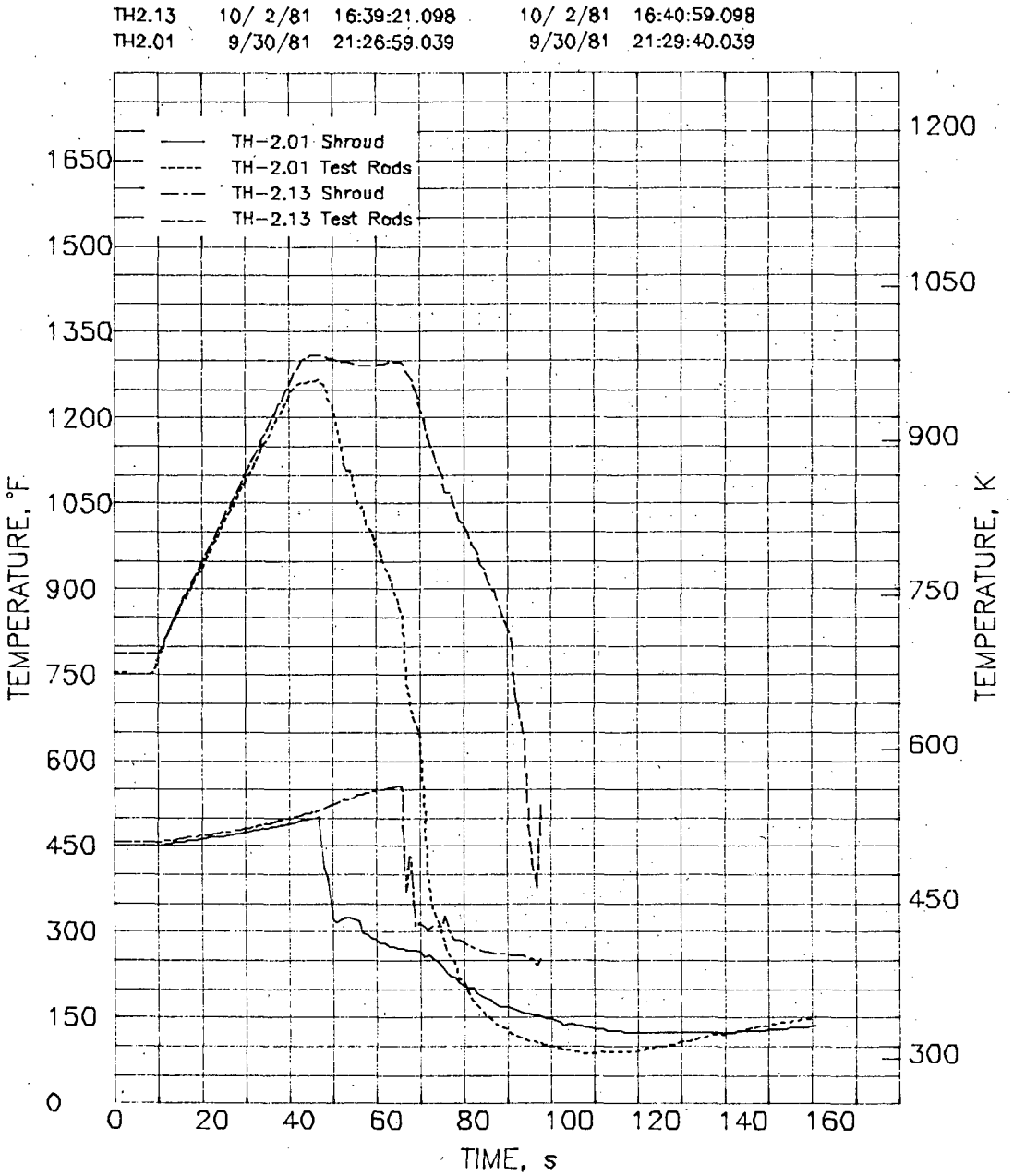

FIGURE 21. Comparison of Adiabatic Tests TH-2.01 and TH-2.13 Showing Average Test Rod and Shroud Temperatures at Level 14

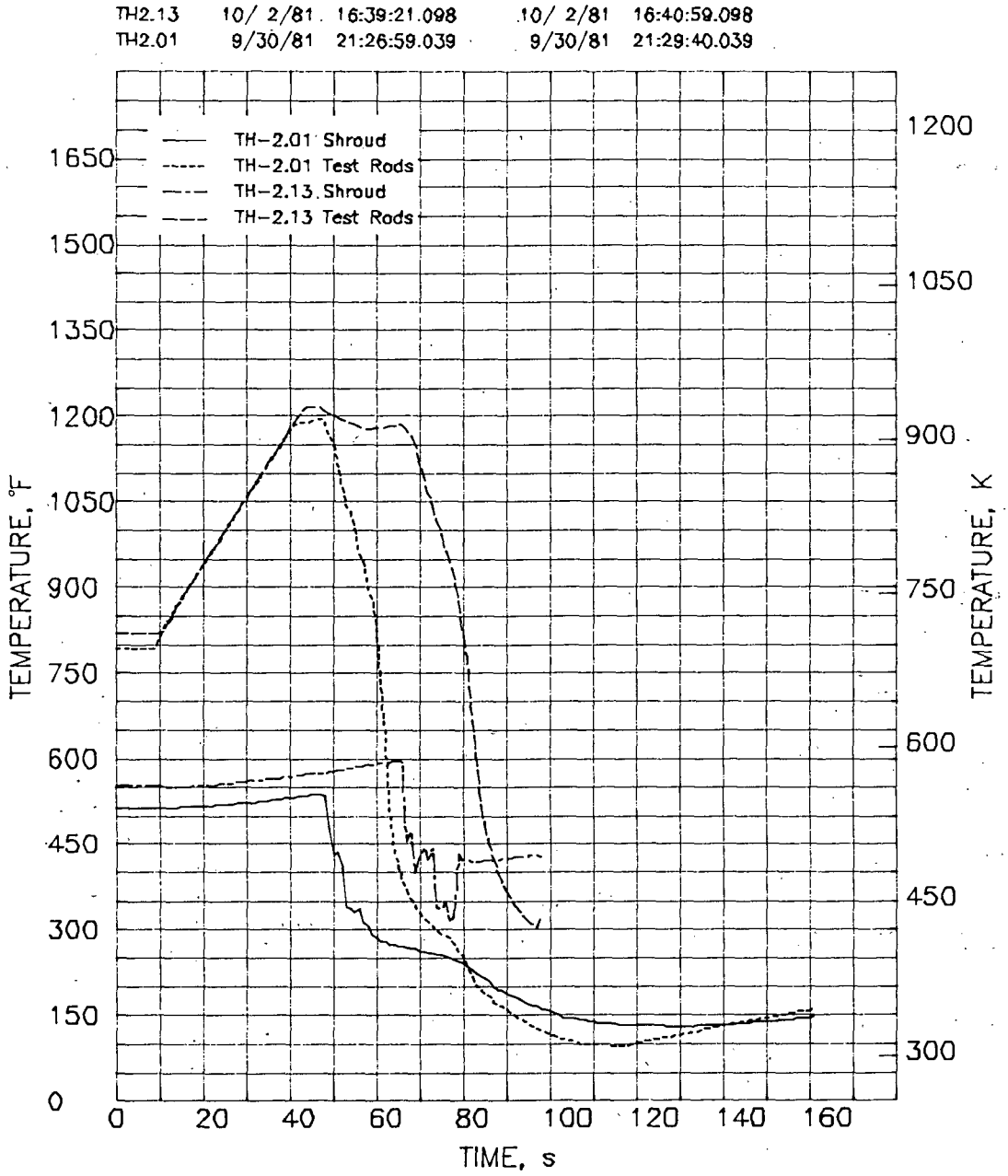

FIGURE 22. Comparison of Adiabatic Tests TH-2.01 and TH-2.13 Showing Average Test Rod and Shroud Temperatures at Level 17

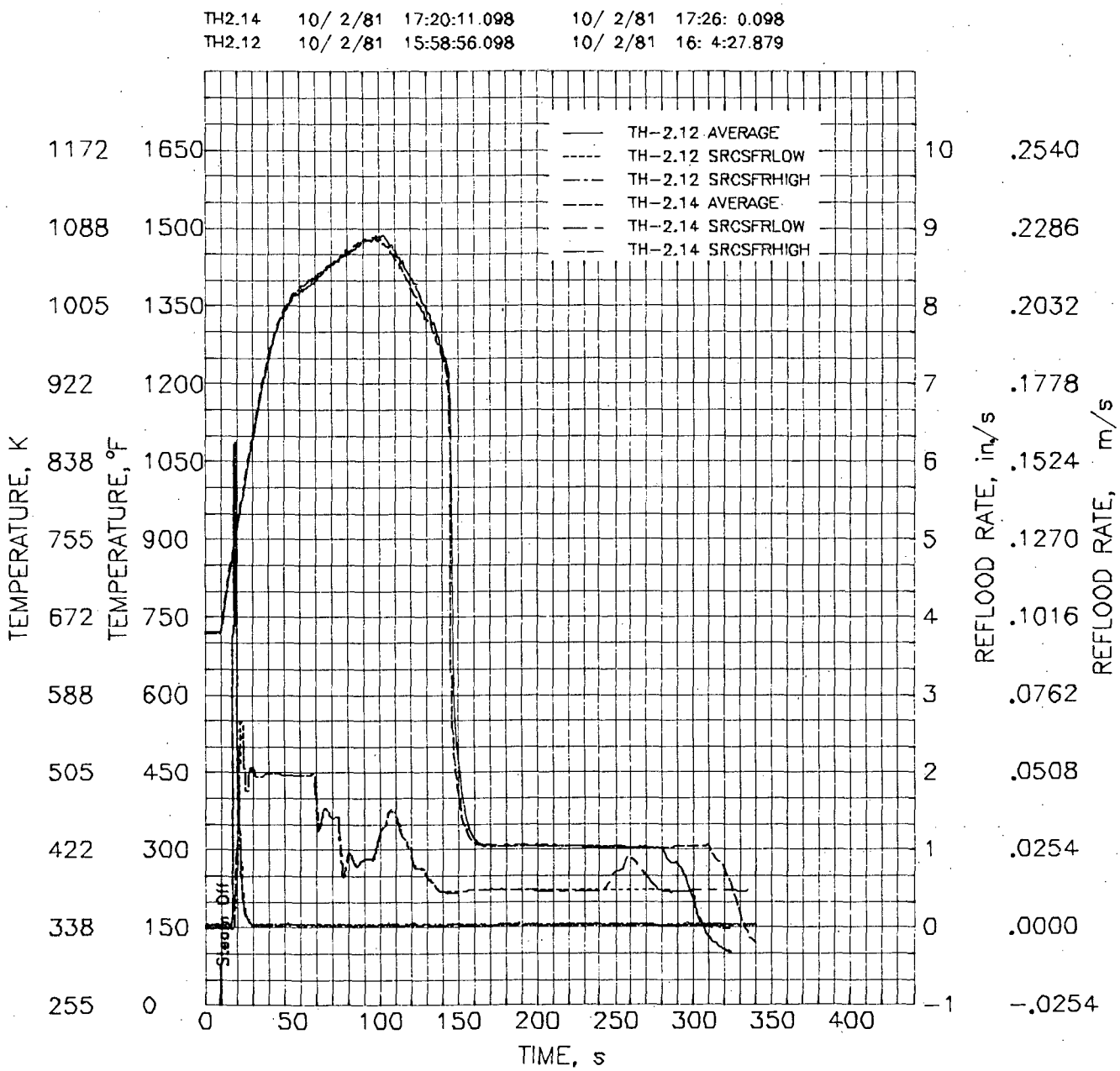

FIGURE 23. Comparison of Tests TH-2.12 and TH-2.14 Showing Average Test Test Rod Temperatures and Reflood Flow Rates at Level 13

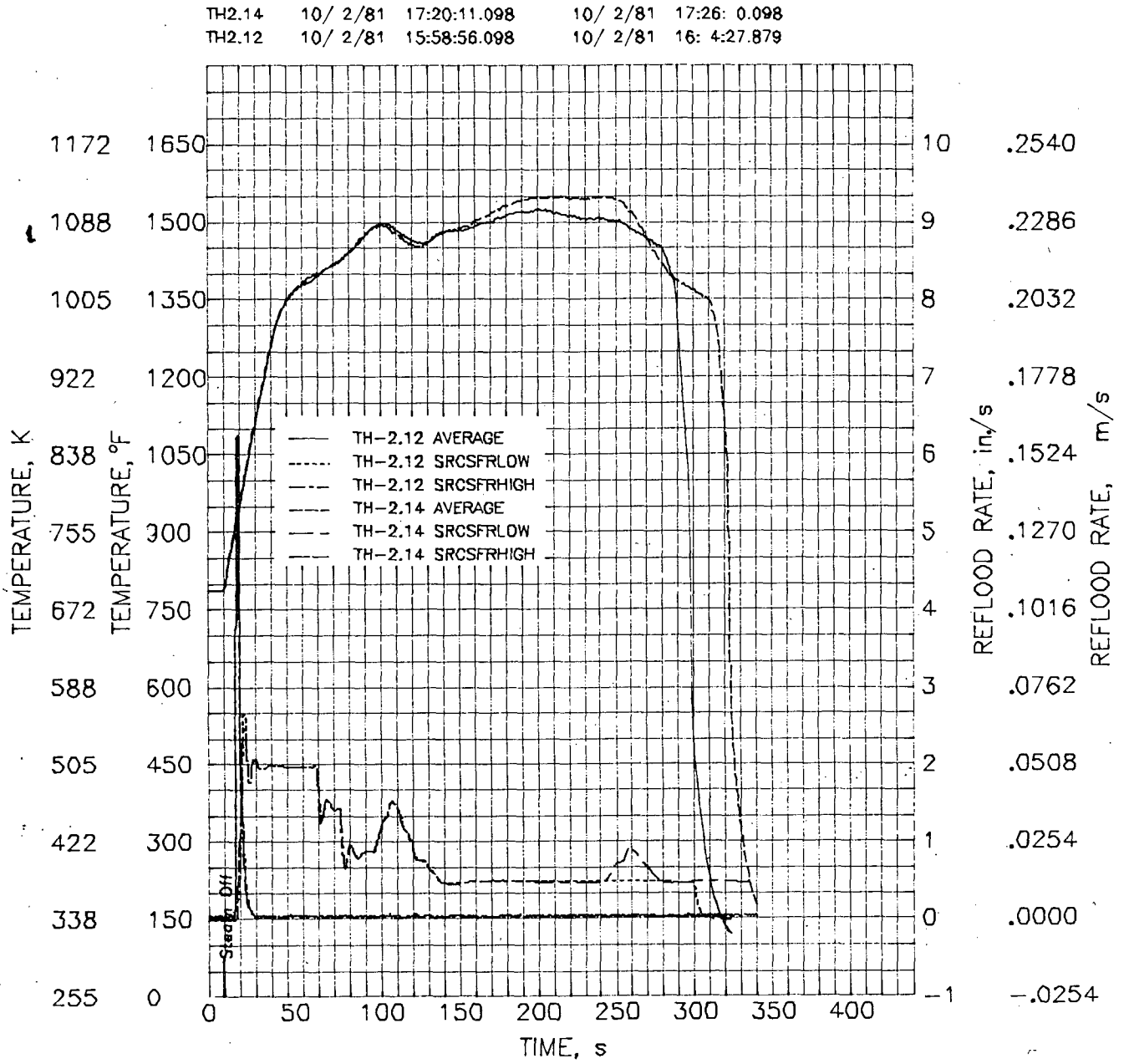

FIGURE 24. Comparison of Tests TH-2.12 and TH-2.14 Showing Average Test Rod Temperatures and Reflood Flow Rates at Level 15

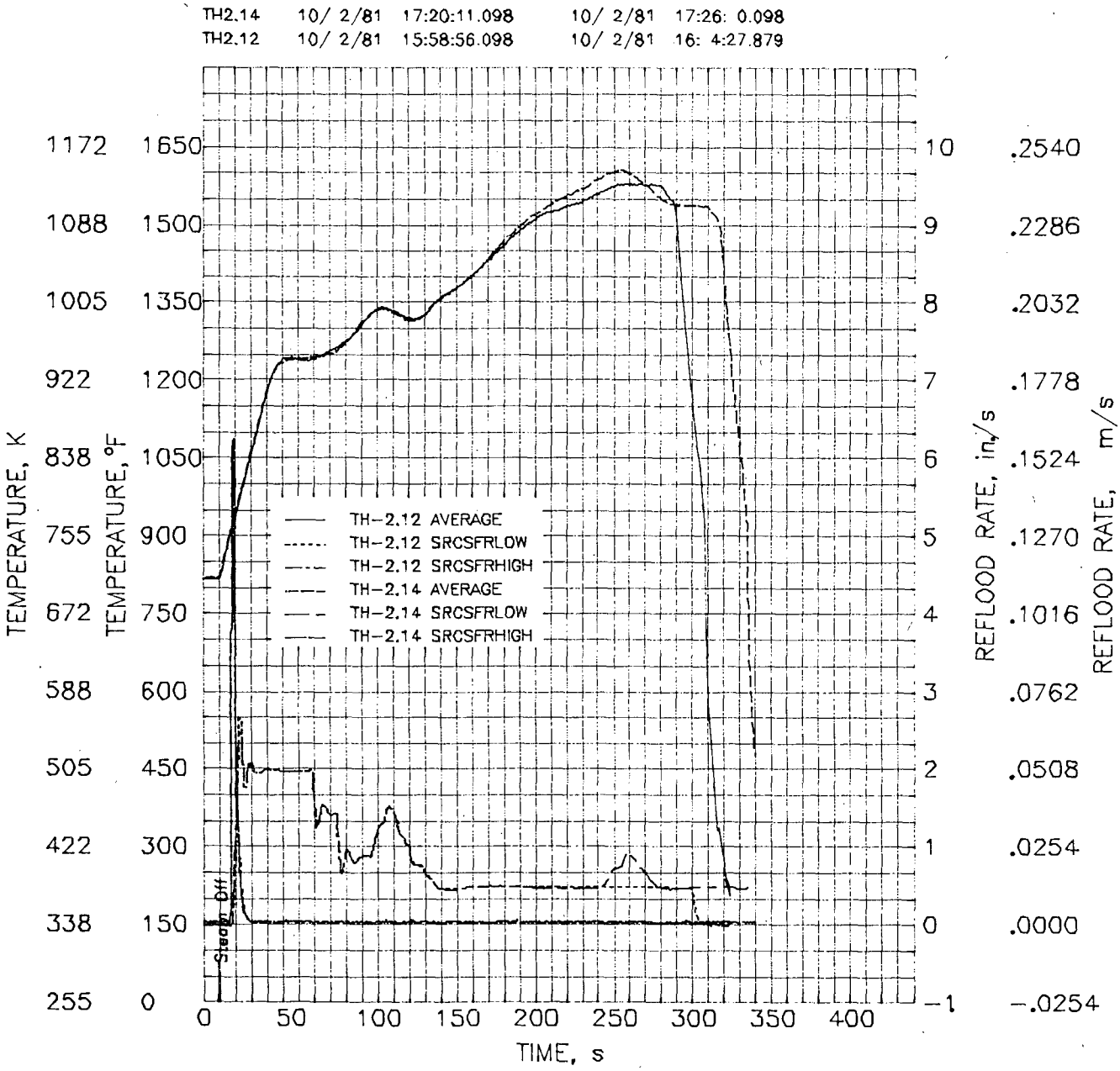

FIGURE 25. Comparison of Tests TH-2.12 and TH-2.14 Showing Average Test Rod Temperatures and Reflood Flow Rates at Level 17

INSTRUMENTATION FAILURES

The assembly used in this series of tests consisted of a new test rod fuel bundle with the guard rod bundle and shroud that had been used in the MT-1 and MT-2 experiments. Table 3 lists the test assembly instrumentation that failed and indicates when failure occurred.

TABLE 3. TH-2 Test Assembly Instrumentation Failure Status

Instrument	Time of Failure
TC-3-6A-S-C	before TH-2.01 transient
TC-4-6F-S-C	during TH-2.04 transient
TC-6-6A-S-C	before TH-2.01 preconditioning
TC-7-6C-OR-4	before TH-2.01 preconditioning
TC-7-4F-OR-1	before TH-2.01 preconditioning
TC-7-1D-OR-2	before TH-2.01 preconditioning
TC-7-3A-OR-3	during TH-2.01 transient
TC-8-5B-OR-1	before TH-2.01 preconditioning
TC-8-6F-S-C	before TH-2.01 preconditioning
TC-8-5E-OR-2	during TH-2.04 transient
TC-10-1A-S-C	before TH-2.01 preconditioning
TC-11-6C-OR-4	before TH-2.01 preconditioning
TC-11-4F-OR-1	during TH-2.05 transient
TC-12-2B-SP-2	before TH-2.01 preconditioning
TC-14-5B-SP-3	before TH-2.01 preconditioning
TC-14-2B-SP-2	before TH-2.01 preconditioning
TC-15-3C-IR-2	before TH-2.01 preconditioning
TC-15-1F-S-C	before TH-2.01 preconditioning
TC-16-2E-SP-1	before TH-2.01 preconditioning
TC-16-2B-SP-2	removed at reconstitution of TH-2
TC-16-5E-SP-4	before TH-2.01 preconditioning
TC-17-3D-IR-3	before TH-2.01 preconditioning
TC-17-5E-IR-4	between TH-2.07 and TH-2.08
TC-17-5D-OR-3	during TH-2.11 transient
TC-21-HT-1	before TH-2.01 preconditioning
TC-21-HT-2	not connected to DACS
TC-21-HT-3	not connected to DACS
TC-21-HT-4	not connected to DACS
SPND-3-6F-S-3	before TH-2.01 preconditioning
SPND-6-1F-S-4	before TH-2.01 preconditioning
SPND-10-6A-S-2	before TH-2.01 preconditioning
SPND-13-1F-S-4	before TH-2.01 preconditioning
SPND-13-1A-S-1	before TH-2.01 preconditioning
SPND-13-6A-S-2	before TH-2.01 preconditioning
SPND-15-1A-S-1	before TH-2.01 preconditioning
SPND-16-1F-C	before TH-2.01 preconditioning
SPND-17-6A-S-2	before TH-2.01 preconditioning
SPND-17-1F-S-4	before TH-2.01 preconditioning
SPND-18-6F-S-3	between TH-2.13 and TH-2.14
SPND-18-1A-S-1	before TH-2.01 preconditioning

THERMAL-HYDRAULIC ANALYSIS AND COMPARISON OF TEST DATA

A thermal-hydraulic analysis was conducted prior to TH-2 using the TRUMP code to determine the test parameters required for a flat top temperature test. For this test, the peak cladding temperature rose from about 728 to 1033K (850 to 1400°F) and was maintained between 1033 and 1103K (1400 and 1525°F). Post-test analyses were also performed using improved test parameters obtained from the TH-2 test data. The TRUMP code analysis, the test assembly power calculations, a comparison of TH-2.12 and TH-2.14 test data, and quench-front behavior are discussed in this section.

TRUMP CODE ANALYSIS

Pretest calculations for TH-2 were made using heat transfer coefficients determined from the FLECHT correlation[5] as input to the TRUMP[6] heat conduction code. The calculations were performed to determine the best combination of parameters (for example, average rod power, delay time, and reflood rates) to obtain a rapid cladding heatup to between 1033 and 1103K (1400 to 1525°F) and then reduce the heatup rate to <1K/s (1.8°F/s). Once the cladding temperature reached this range, the accuracy of the prediction for the slower heatup rate was less important for running the test. Feedback control using the DACS was designed to account for small changes in the heatup rate.

For these calculations, the control period of preprogrammed parameters was limited to 90 s--at which time the peak cladding temperature was expected to be between 1033 and 1103K (1400 and 1525°F). The average cladding temperatures for tests TH-2.12 and TH-2.14 at level 15 are compared with a TRUMP-FLECHT prediction in Figures 26 and 27, respectively.

TH-2.12 and TH-2.14 post-test calculations involved evaluating the test data to improve the ability of TRUMP to calculate cladding temperatures for a given set of test parameters for up to 90 s, which would also provide improved pretest calculations for following tests. The test data evaluation included determining specific delay times, reflood rates and their durations, and the local axial rod power (used to modify the FLECHT convection heat transfer input to TRUMP). Measured cladding temperature data are compared with the TRUMP-FLECHT post-test calculation for the temperature ramp values of the fuel rod linear power in Figures 28 through 33, which illustrate temperature histories at Levels 13, 15, and 17.[a] These figures demonstrate 1) the ability of the improved TRUMP model to determine peak cladding temperatures for the first 90 s and 2) the limitations of TRUMP to model cladding temperatures later in the test. The FLECHT heat transfer coefficients were obtained from tests

(a) Levels 13, 15, and 17 are 1.94, 2.47, and 3.00 m (76.3, 97.3, and 118.3 in.), respectively, from the bottom of the fuel.

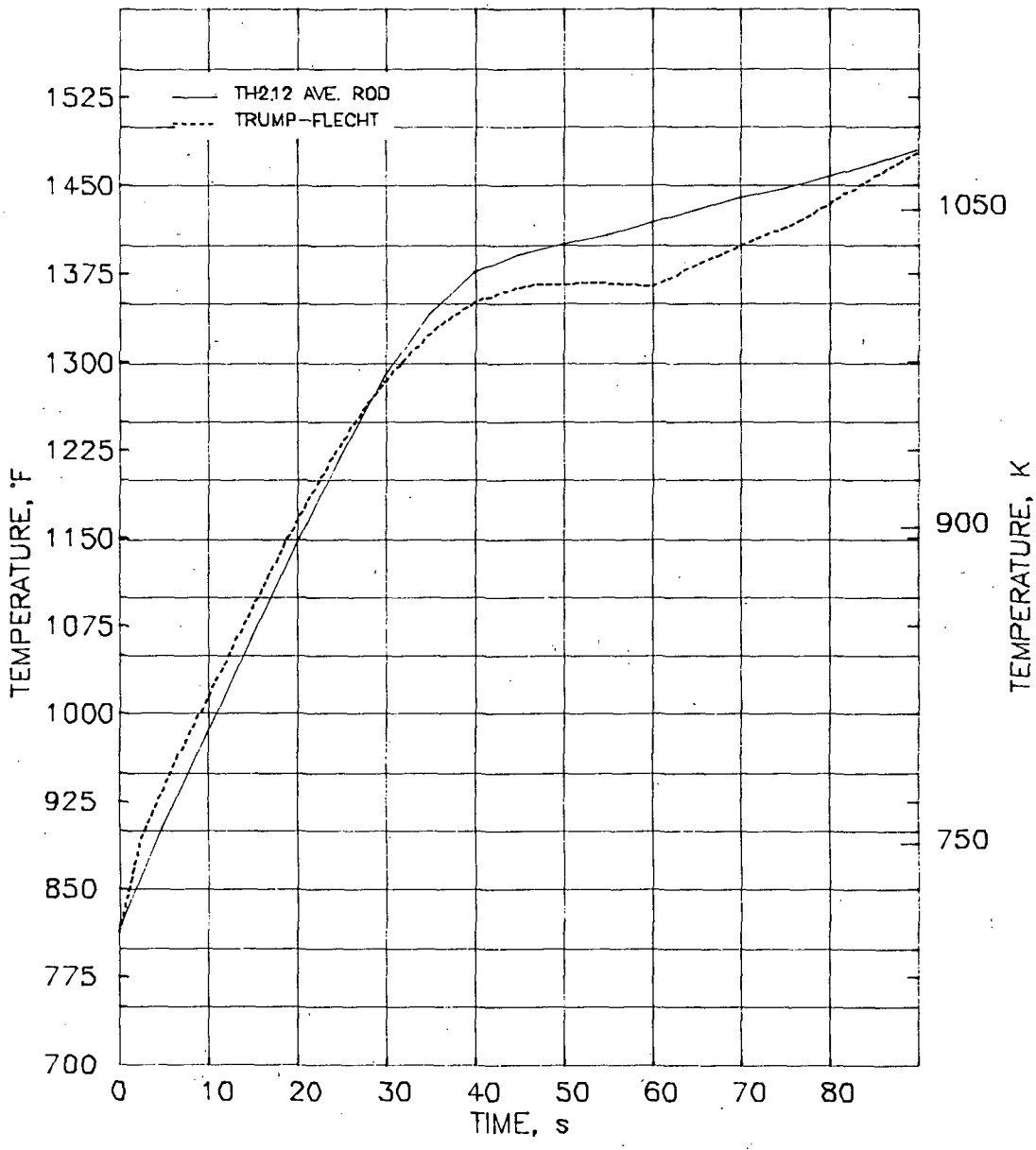

FIGURE 26. Comparison of Average Cladding Temperature and TRUMP-FLECHT Prediction for Level 15 During TH-2.12

that had reflood rates ranging from 0.010 to 0.254 m/s (0.4 to 10 in./s). At reflood rates below ~0.010 m/s and for pseudo steady-state test conditions with a large two-phase region, TRUMP using FLECHT was less accurate. Additional limitations of the TRUMP model are that it used 1 rod instead of 32 rods and did not consider heat losses to the shroud.

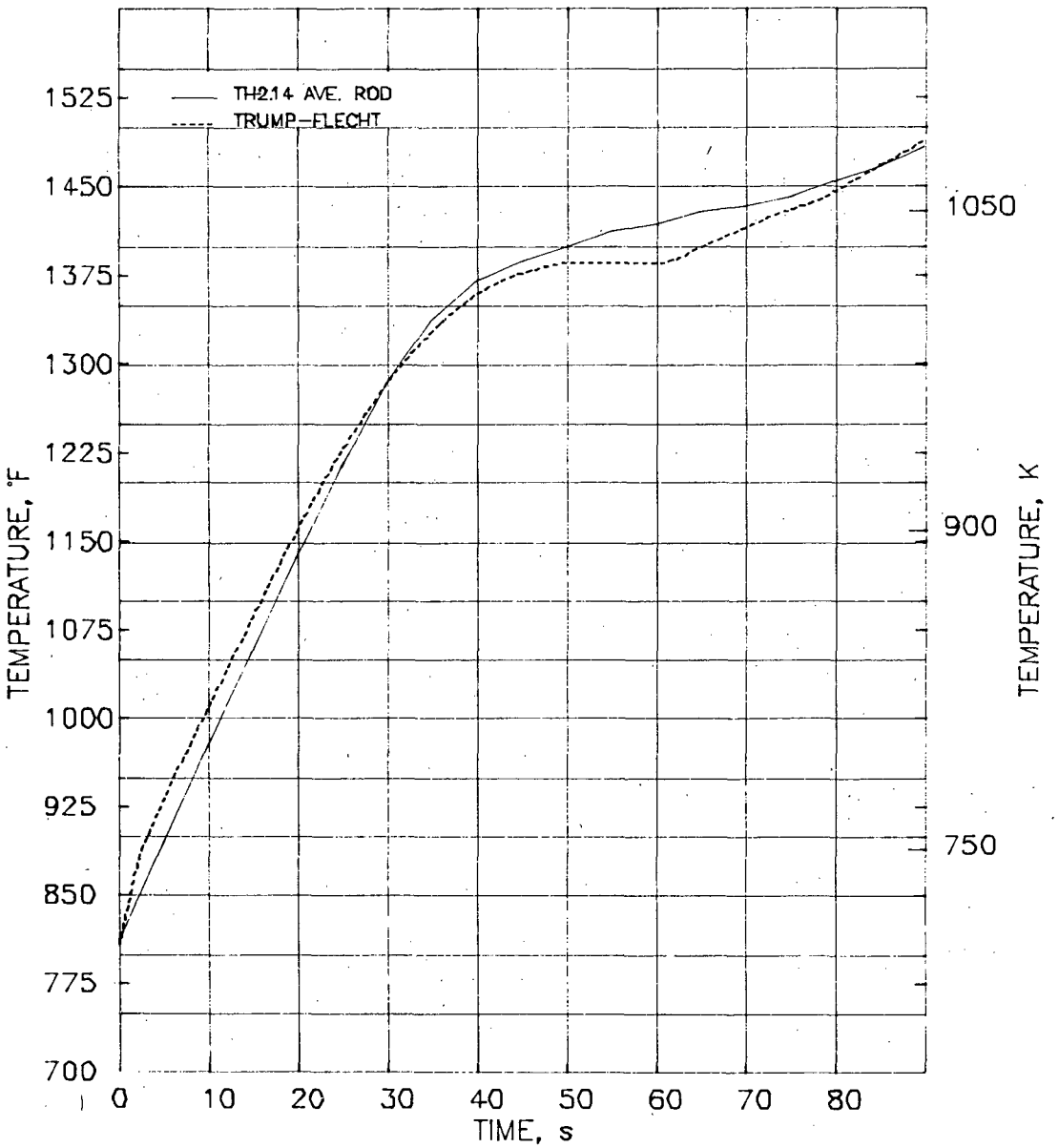

FIGURE 27. Comparison of Average Cladding Temperature and TRUMP-FLECHT Prediction for Level 15 During TH-2.14

TEST ASSEMBLY POWER CALCULATIONS

Test assembly powers for the TH-2.12, TH-2.13, and TH-2.14 pretransients were calculated by a calorimetric and a heat conduction method. The calorimetric powers were obtained using the flow rates measured by the U-2 loop instrumentation, the inlet test assembly (Level 1) TC readings, and the outlet

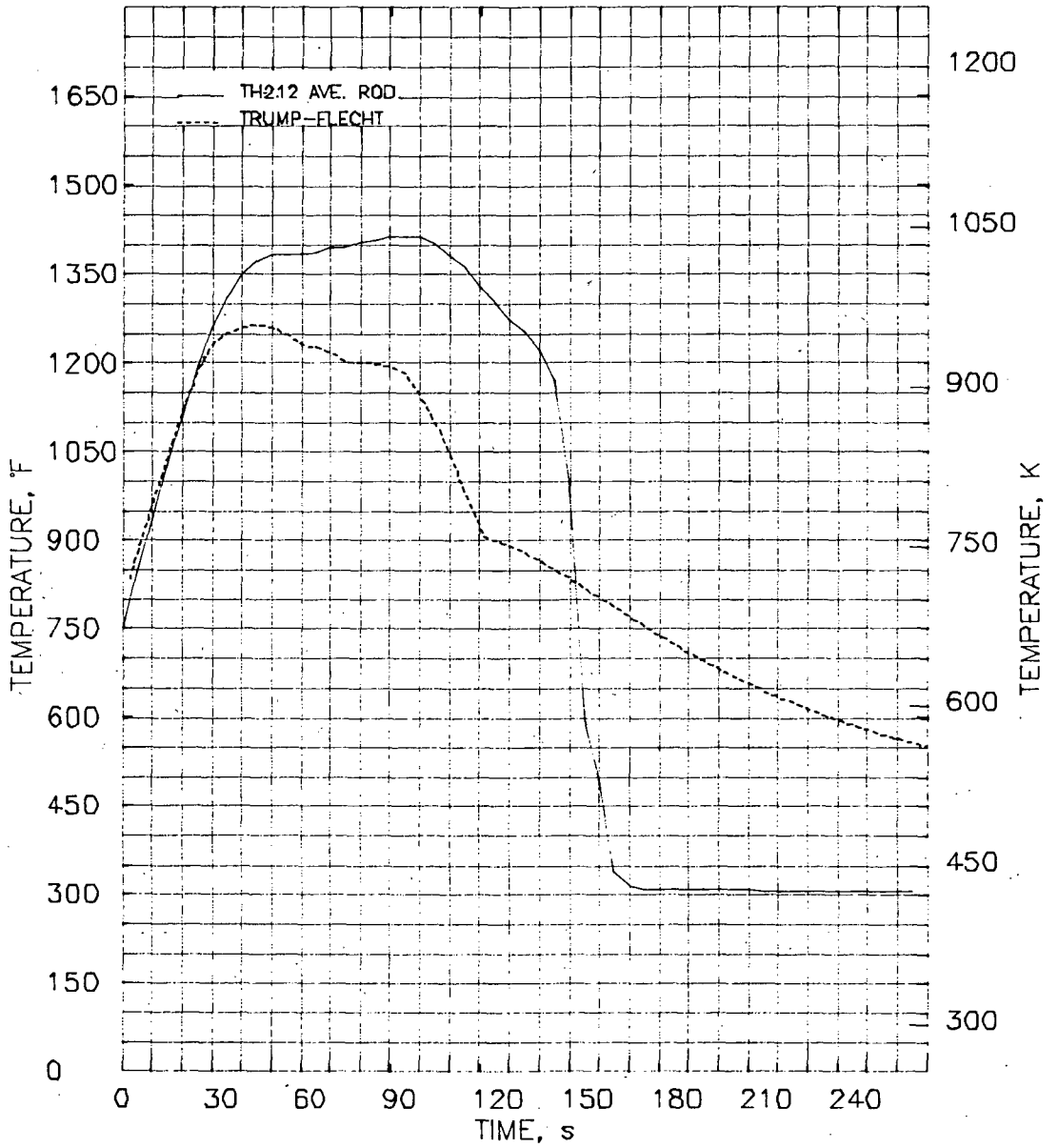

FIGURE 28. Comparison of Measured Average Cladding Temperature and Post-Test TRUMP-FLECHT Calculation for Level 13 During TH-2.12

(Level 20) TC readings. Using this method, average rod powers were calculated as 1.185, 1.228, and 1.220 kW/m (0.361, 0.374, and 0.372 kW/ft) for TH-2.12, TH-2.13, and TH-2.14, respectively.

Local fuel rod powers were also calculated by using a heat conduction calculation based on the cladding temperature heatup rates during the nominally adiabatic heatup period between the times when the steam cooling was turned off

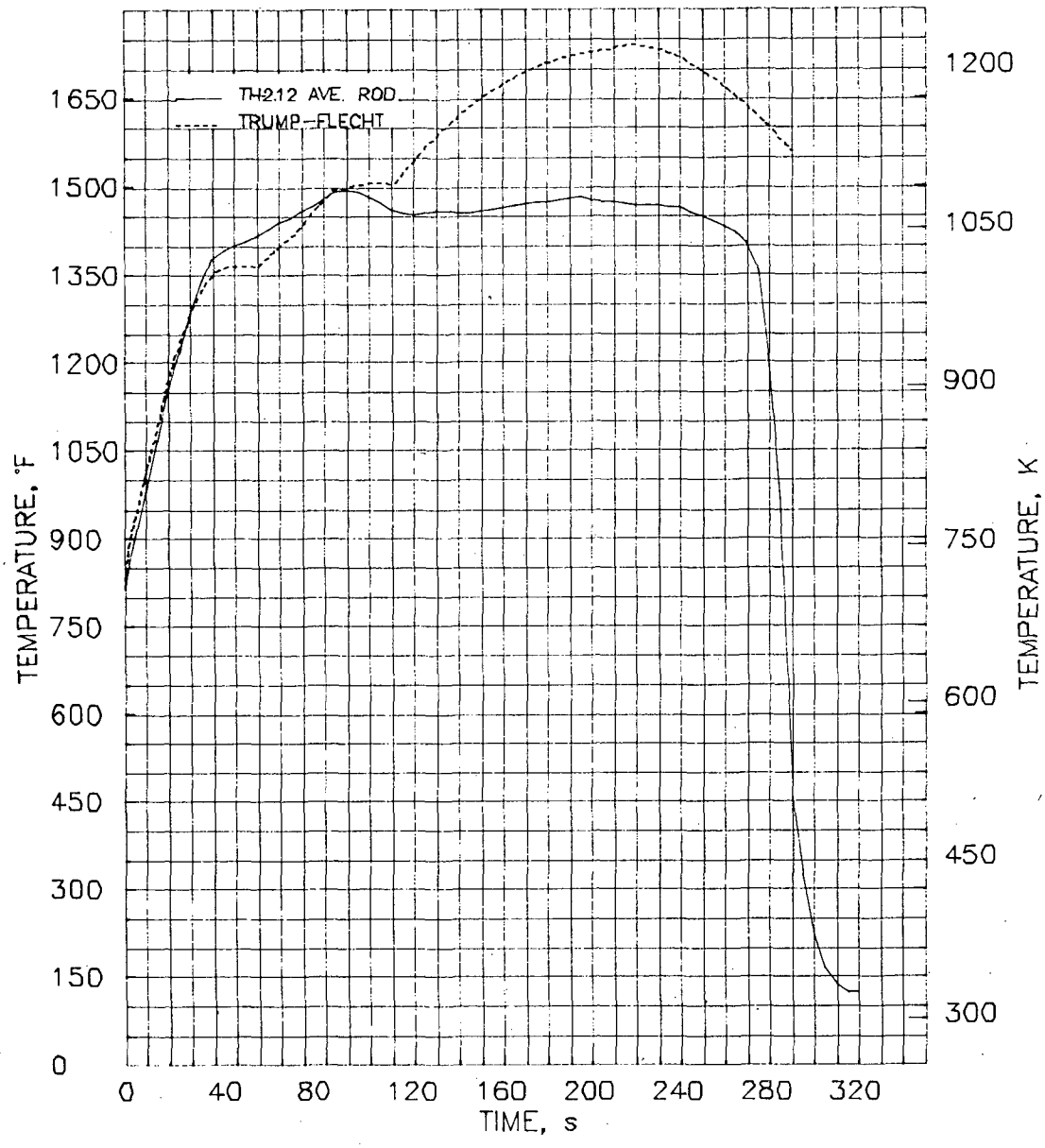

FIGURE 29. Comparison of Measured Average Cladding Temperature and Post-Test TRUMP-FLECHT Calculation for Level 15 During TH-2.12

and the reflood cooling was turned on. Total assembly powers are calculated by adding local fuel rod powers to those of the shroud. Test TH-2.13 was performed between tests TH-2.12 and TH-2.14 to obtain heatup rate data. Integration of the axial power distribution so obtained gave an average fuel rod power of 1.309 kW/m (0.399 kW/ft)--a difference of 6.7% greater for the heatup rate than for the calorimetric calculation. The heatup rate method of determining local fuel power was used for post-test TRUMP code calculations as described in the previous section.

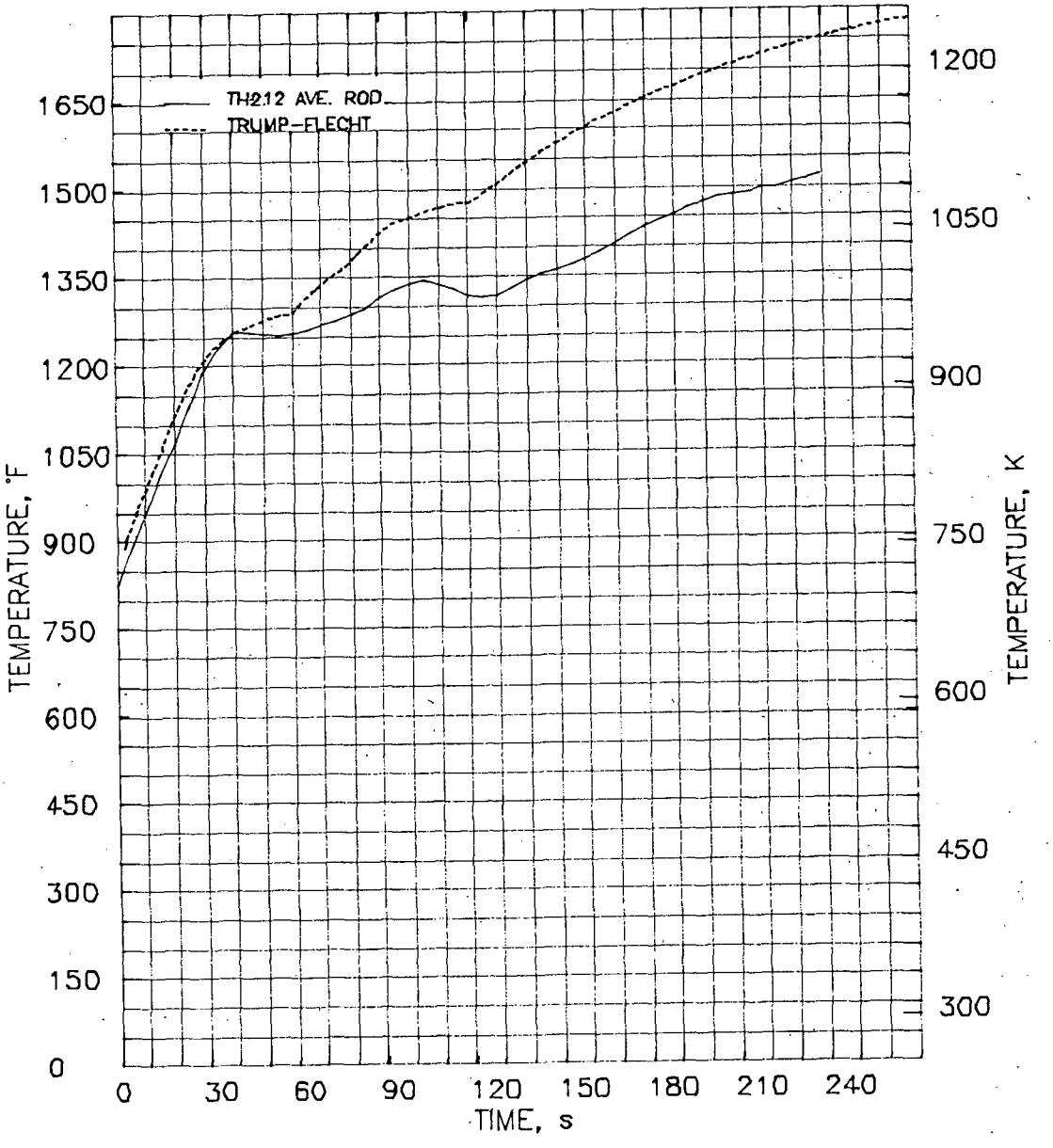

FIGURE 30. Comparison of Measured Average Cladding Temperature and Post-Test TRUMP-FLECHT Calculation for Level 17 During TH-2.12

TH-2.12 AND TH-2.14 CONVECTIVE HEAT TRANSFER COEFFICIENTS

The heat transfer coefficients for TH-2.12 and TH-2.14 were calculated based on local assembly powers and the difference between the average fuel rod temperature and an artificial coolant temperature, which was assumed to be at saturated conditions for 40 psia (267°F). Local heat transfer coefficients for TH-2.12 and TH-2.14 at Levels 13, 15, and 17 were used as input to predictive

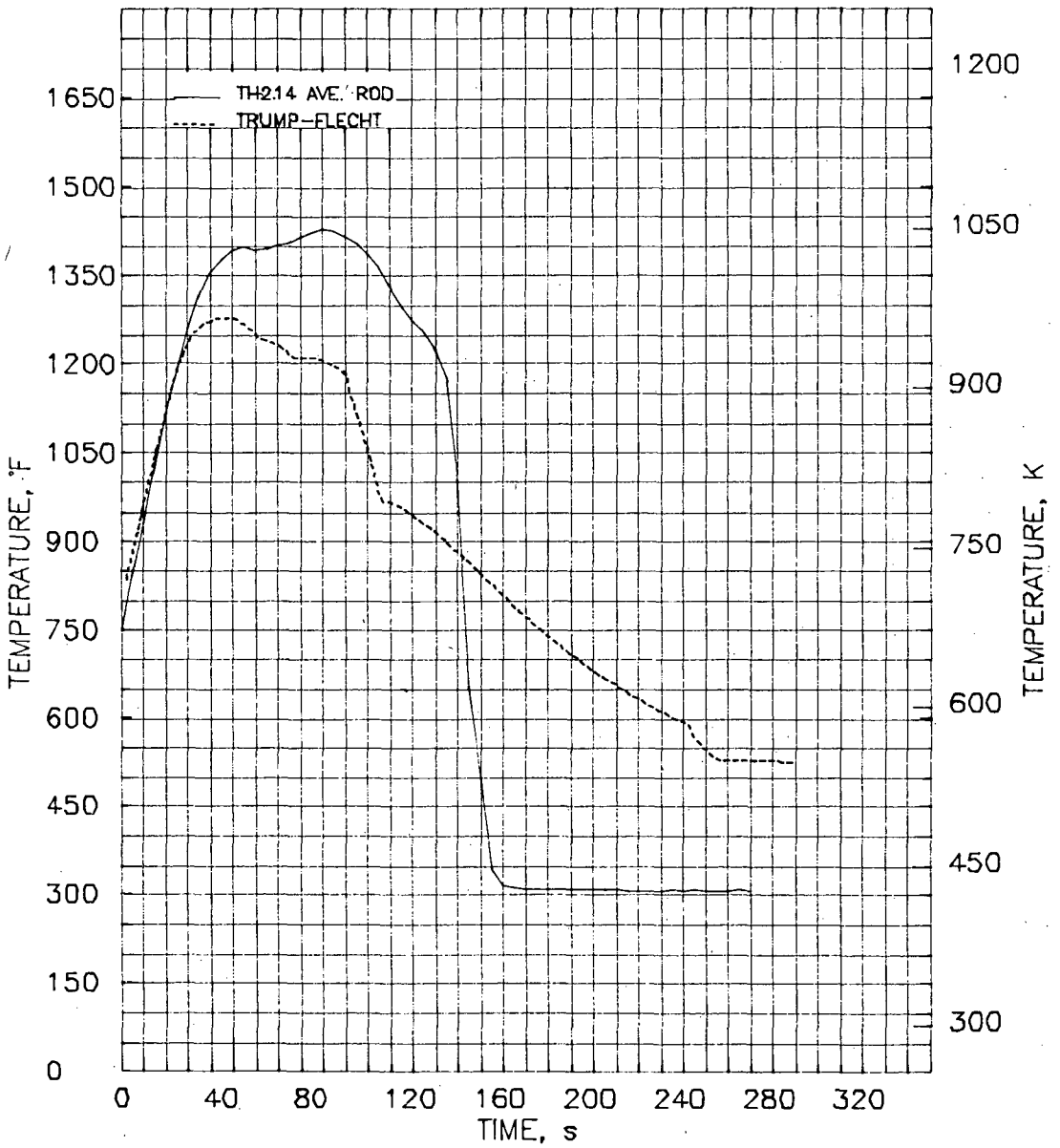

FIGURE 31. Comparison of Measured Average Cladding Temperature and Post-Test TRUMP-FLECHT Calculation for Level 13 During TH-2.14

codes to provide information on test rod ballooning and deformation (see Figures 34 through 36). These heat transfer coefficients were also input to TRUMP to improve cladding temperature predictions.

QUENCH-FRONT ANALYSIS

A look at the quench front helps demonstrate what is happening in the test assembly. During the TH-2.14 transient, the quench front for the cladding

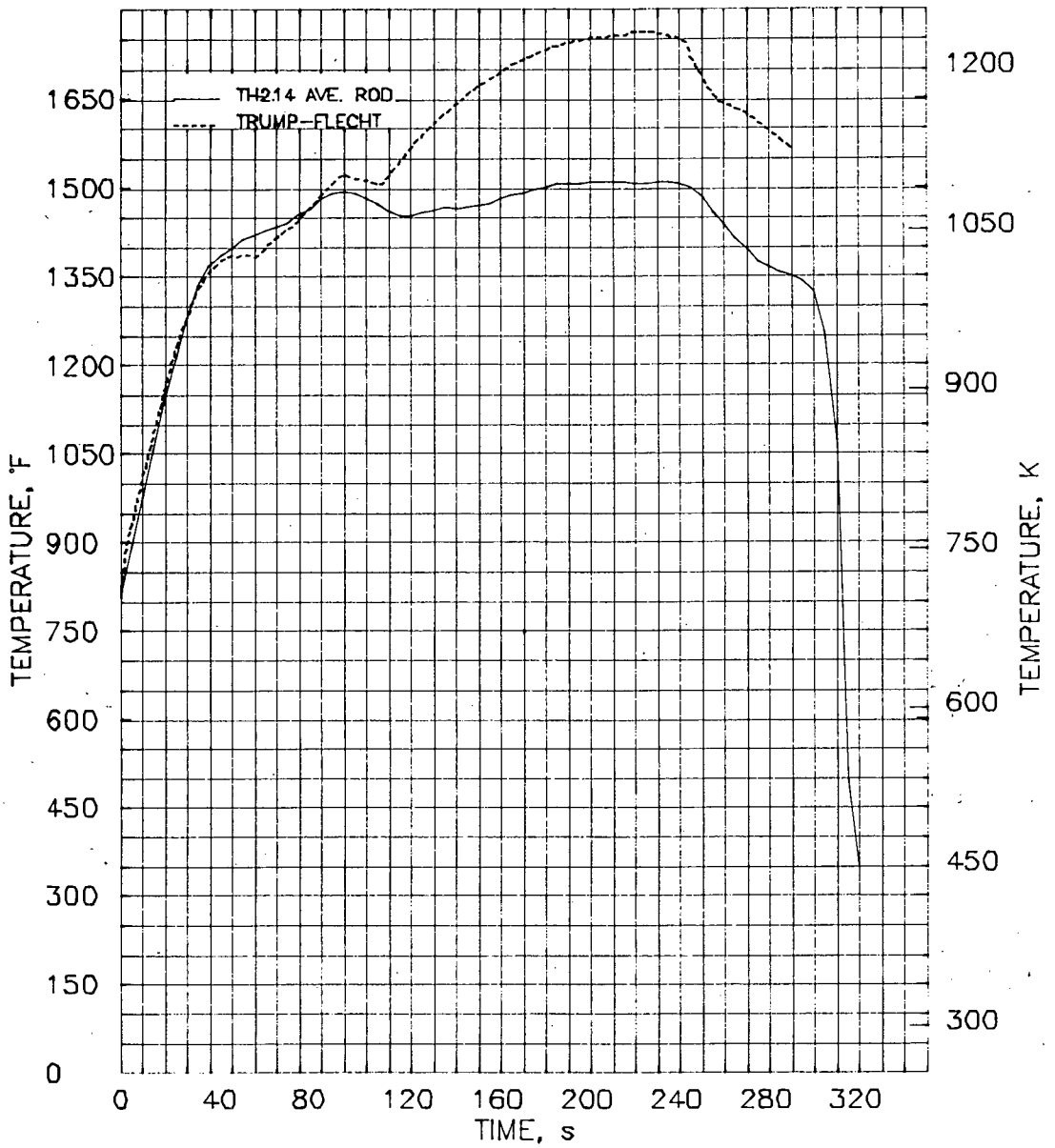

FIGURE 32. Comparison of Measured Average Cladding Temperature and Post-Test TRUMP-FLECHT Calculation for Level 15 During TH-2.14

started at the bottom of the test assembly and moved upward as the reflood water started to flood the test assembly from the bottom (see Figure 37). The test conditions between 150 and 300 s were such that a near steady-state boil-off condition was achieved as shown by the low slope in Figure 37. The circles represent the first and last rod cladding that quenched at a given elevation, and the line represents the average quench time. As the test progressed, the quench front moved upward; and finally the reactor tripped.

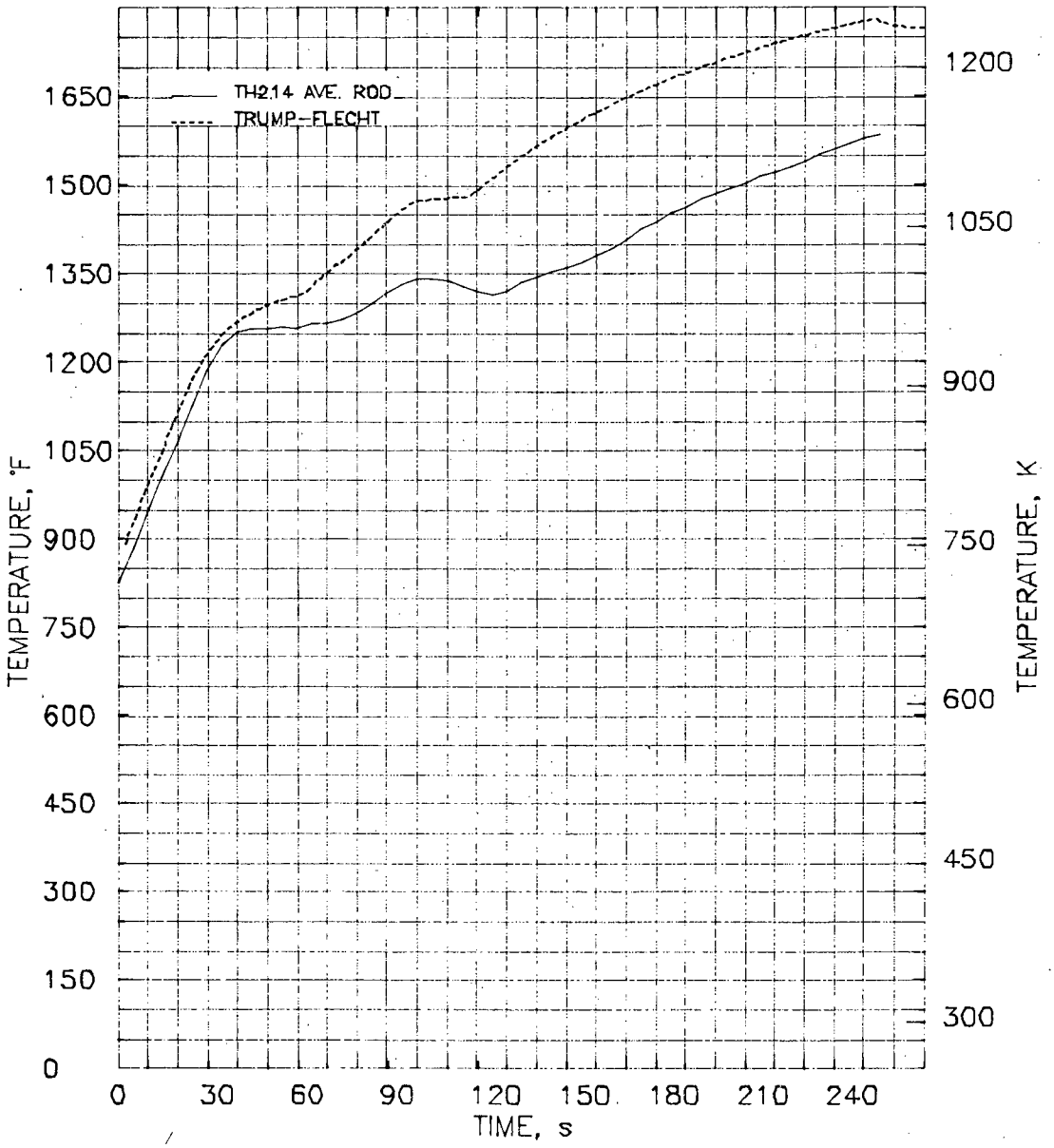

FIGURE 33. Comparison of Measured Average Cladding Temperature and Post-Test TRUMP-FLECHT Calculation for Level 17 During TH-2.14

Figure 38 shows the quench-front elevation data for the shroud during the TH-2.14 test. The shroud quenched before the cladding because it was cooler.

Figures 39 through 41 present the test and guard rod cladding temperatures within ±1 standard deviation of the average temperature. The fuel rods were hotter than the shroud, which is consistent with the shroud quenching before the rods. There was a tendency for the test rods to become hotter than the guard rods, showing that heat was transferred radially outward and

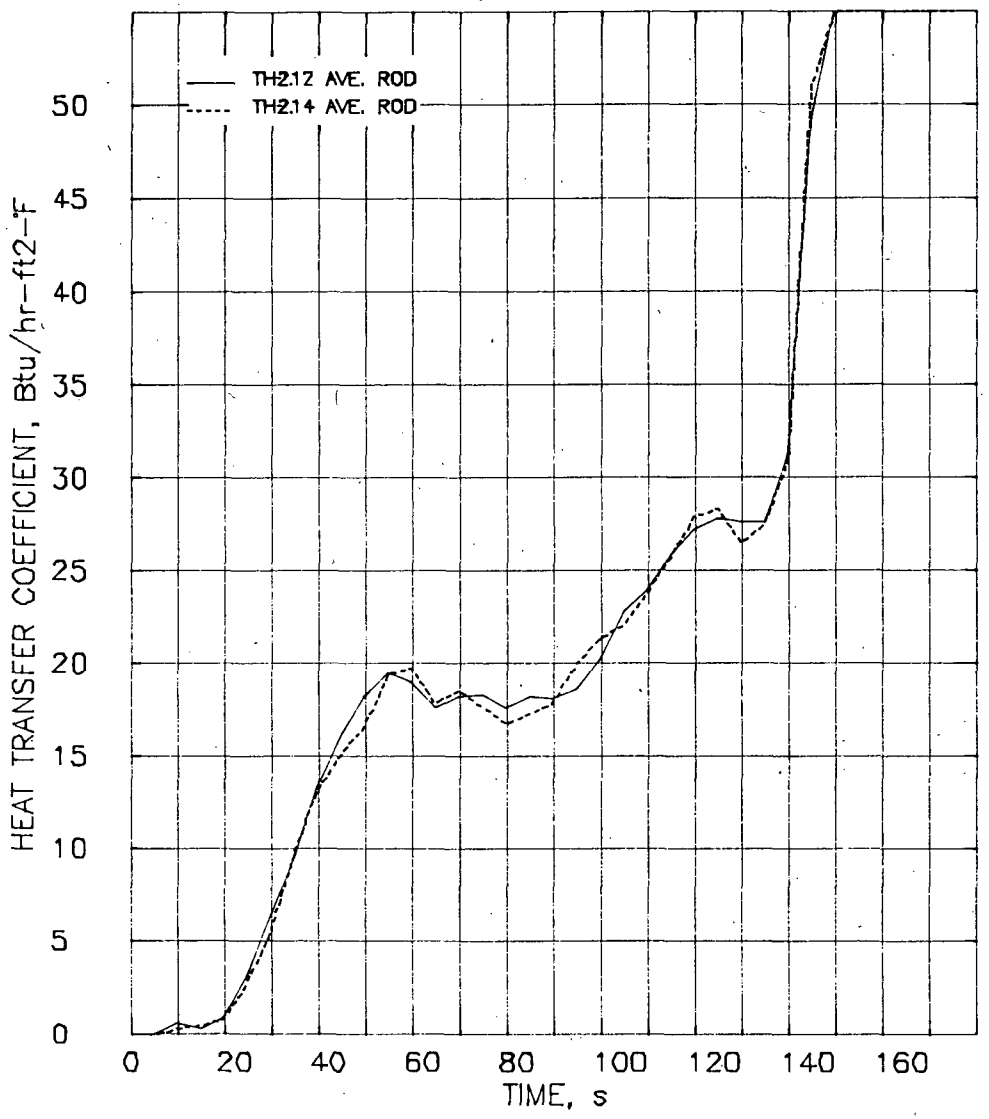

FIGURE 34. Comparison of Heat Transfer Coefficients for Level 13 During TH-2.12 and TH-2.14

demonstrating the need for the guard rods. Adiabatic tests have demonstrated that the guard rods heat up faster than the test rods, which tends to indicate that the NRU fuel is driving the test assembly. The fact that the guard rods are at a higher power and lower temperature than the test rods further establishes that heat is transferred radially outward from the test rods.

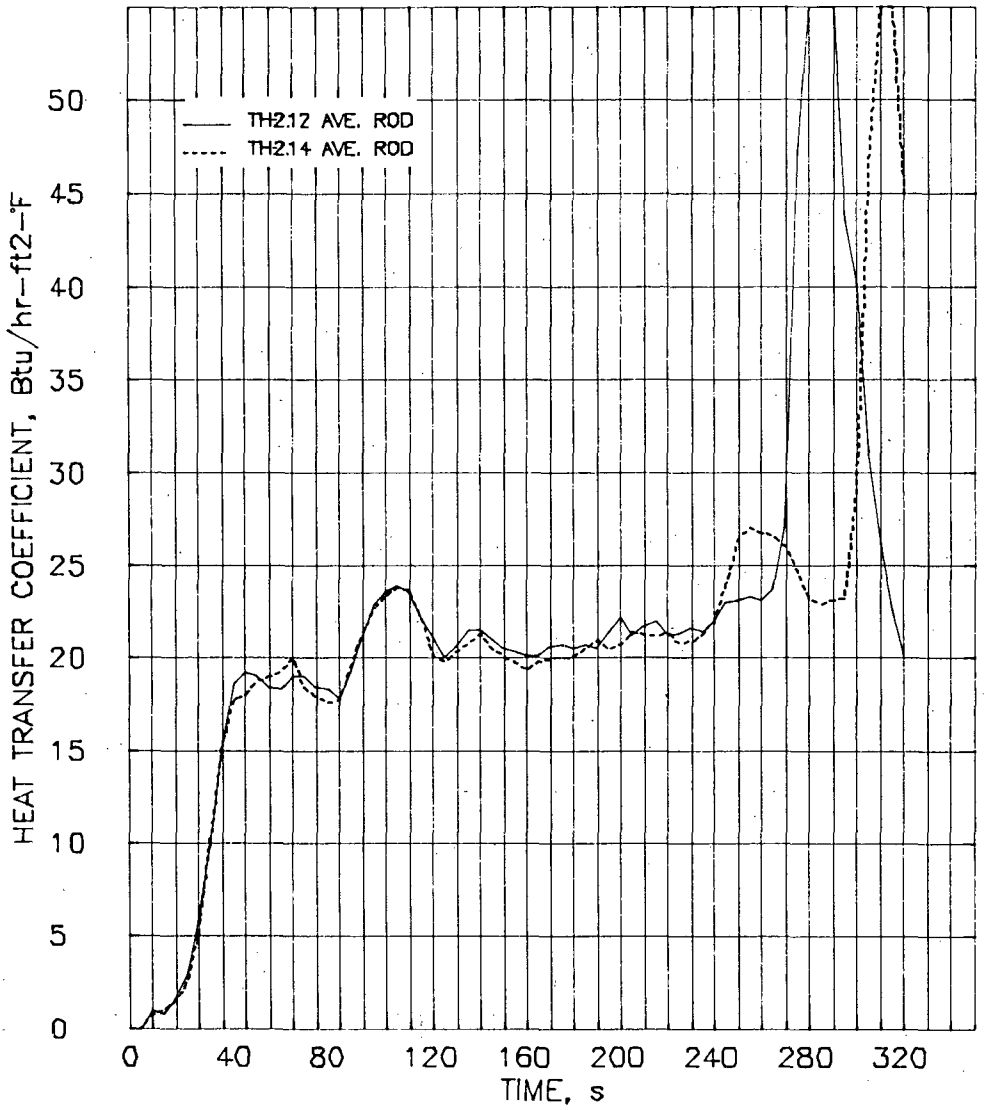

FIGURE 35. Comparison of Heat Transfer Coefficients for Level 15 During TH-2.12 and TH-2.14

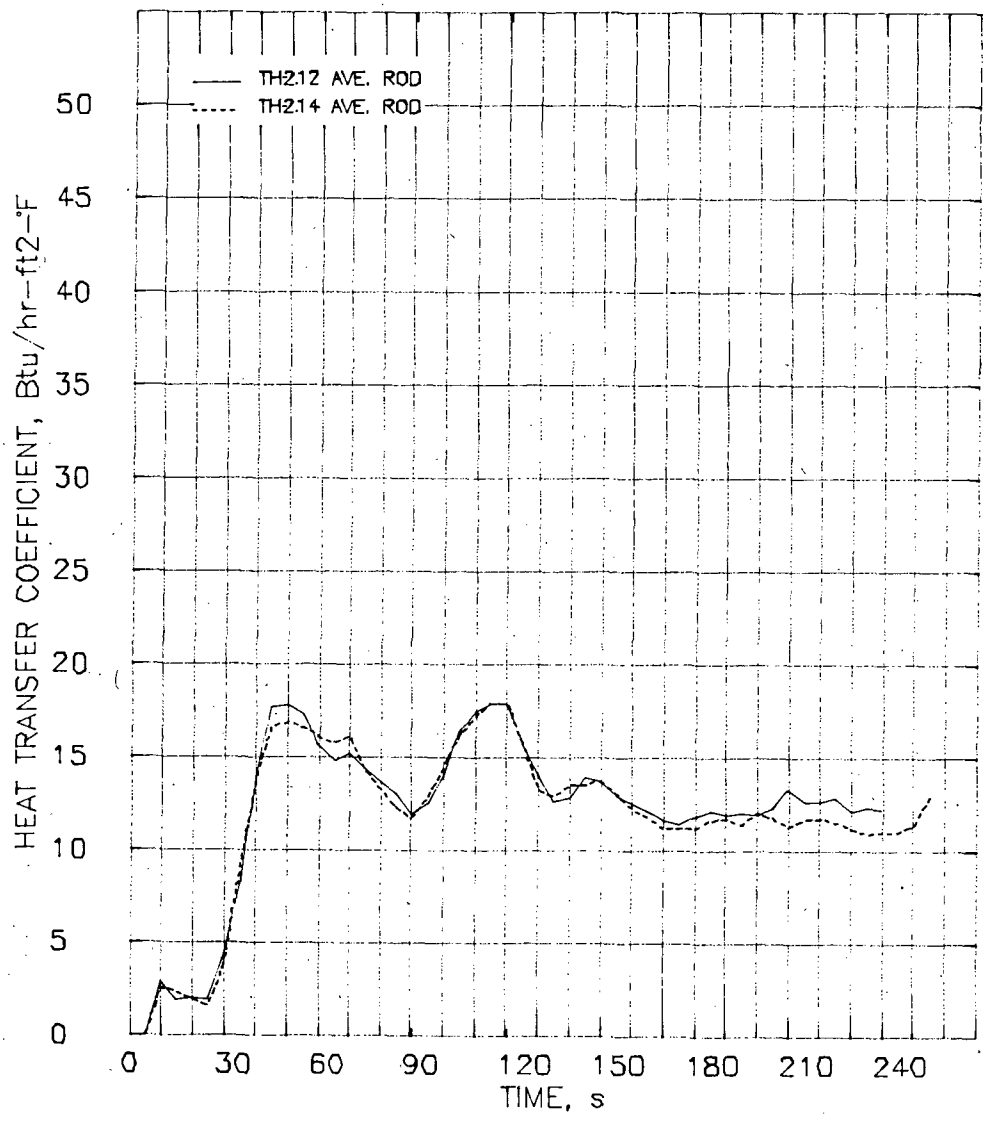

FIGURE 36. Comparison of Heat Transfer Coefficients for Level 17 During TH-2.12 and TH-2.14

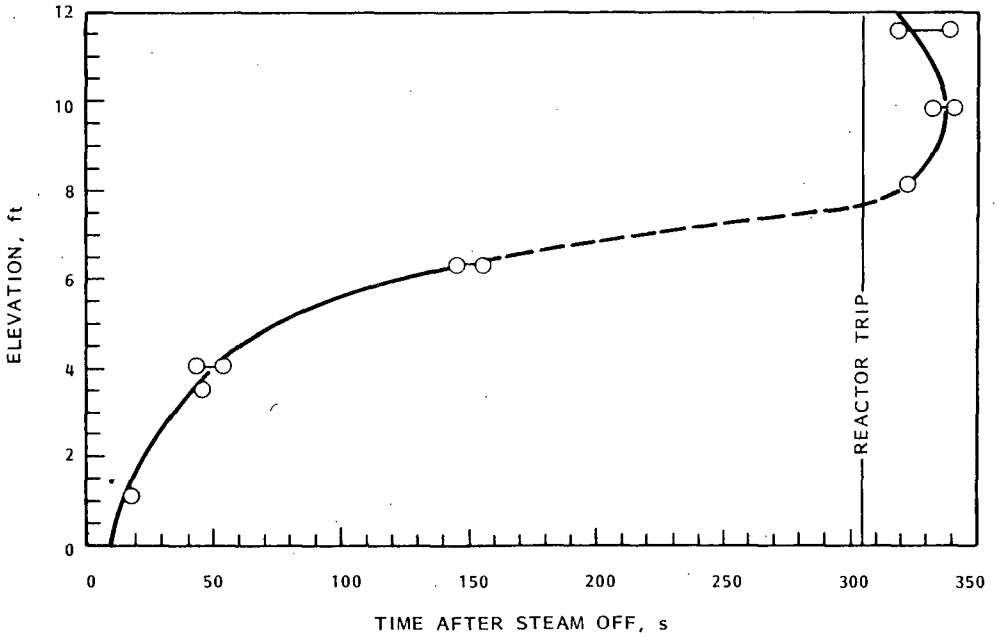

FIGURE 37. Quench-Front Elevation Data for the Rods in TH-2.14

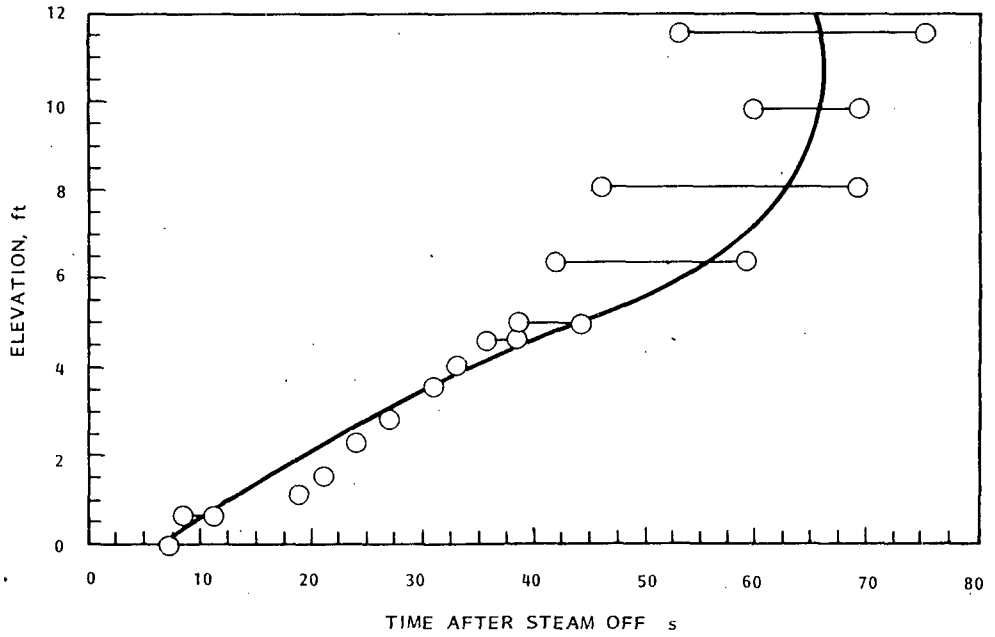

FIGURE 38. Quench-Front Elevation Data for the Shroud in TH-2.14

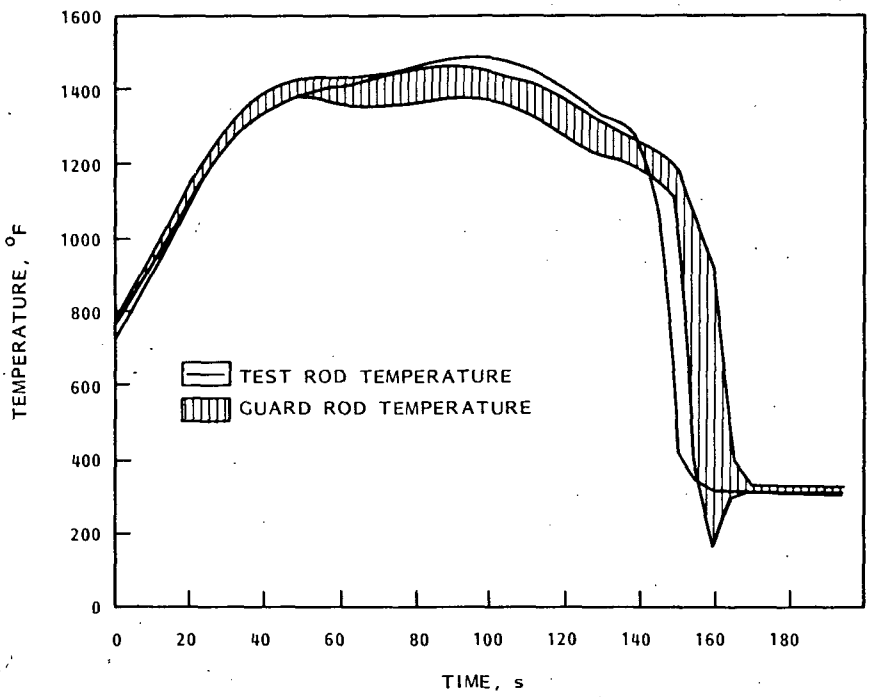

FIGURE 39. Comparison of Test Rod and Guard Rod Average Temperatures (±1 standard deviation) for Level 13 During TH-2.14

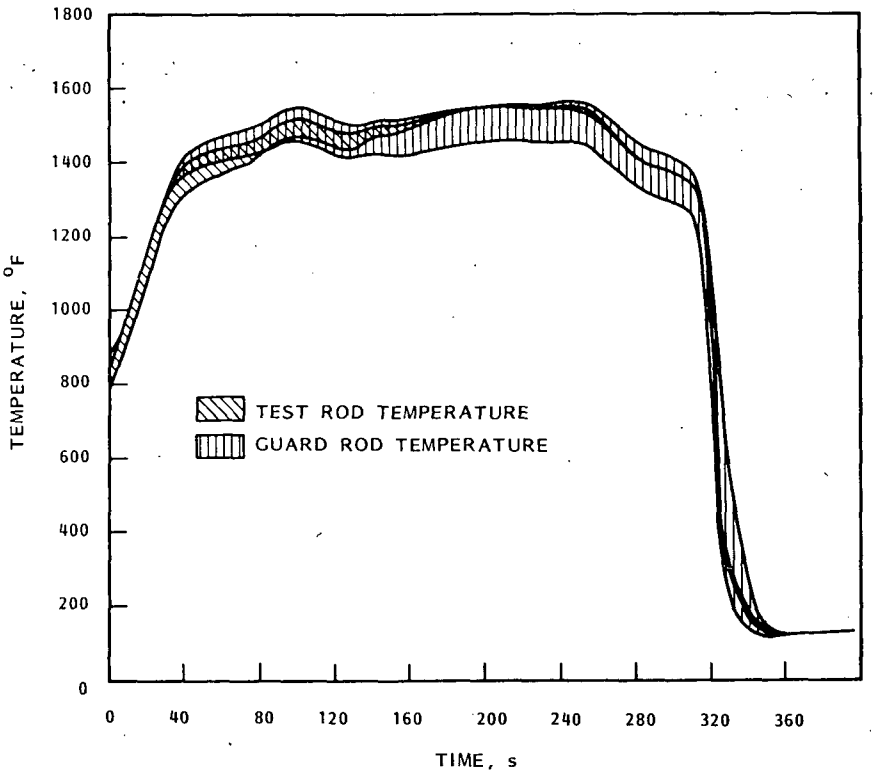

FIGURE 40. Comparison of Test Rod and Guard Rod Average Temperatures (±1 standard deviation) for Level 15 During TH-2.14

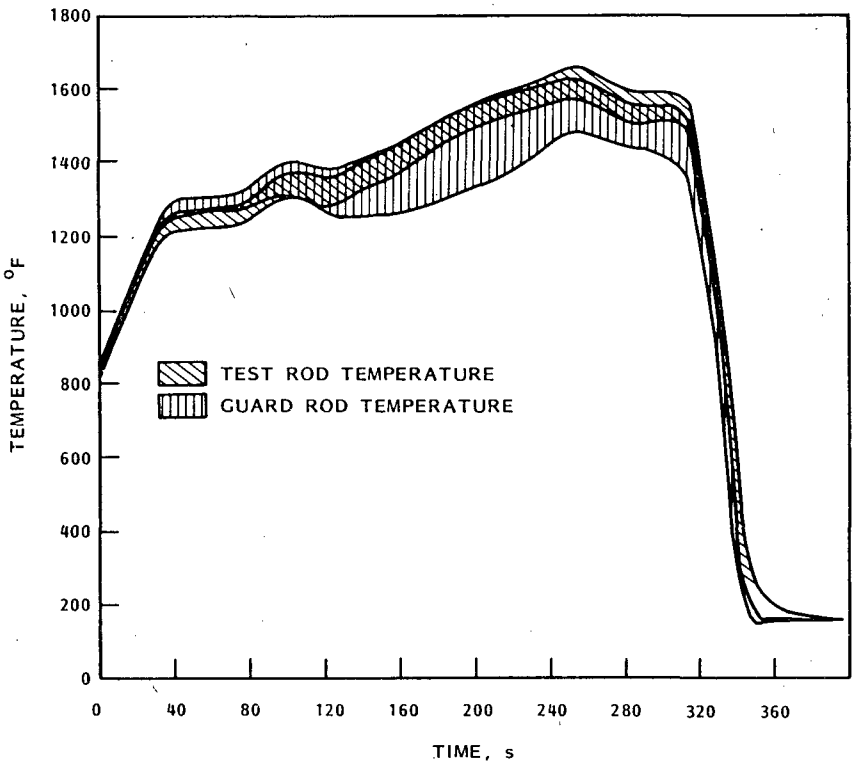

FIGURE 41. Comparison of Test Rod and Guard Rod Average Temperatures (±1 standard deviation) for Level 17 During TH-2.14

REFERENCES

1. Hann, C. R. 1979. Program Plan for LOCA Simulation in the National Research Universal (NRU) Reactor. PNL-3056, Pacific Northwest Laboratory, Richland, Washington.

2. Mohr, C. L., et al. 1981. Prototypic Thermal-Hydraulic Experiments in NRU to Simulate Loss-of-Coolant Accidents. NUREG/CR-1882, PNL-3681, Pacific Northwest Laboratory, Richland, Washington.

3. Russcher, G. E., et al. 1981. Materials Test-1 LOCA Simulation in the NRU Reactor. NUREG/CR-2152 Vol. 1, PNL-3835, Pacific Northwest Laboratory, Richland, Washington.

4. Mohr, C. L., et al. Materials Test-2 LOCA Simulation in the NRU Reactor. NUREG/CR-2509, PNL-4155, Pacific Northwest Laboratory, Richland, Washington. March 1982.

5. Lilly, G. P., et al. 1977. PWR FLECHT Cosine Low Flooding Rate Test Series Evaluation Report. WCAP-8838, Westinghouse Electric Corporation, Pittsburgh, Pennsylvania.

6. Edwards, A. L. September 1972. TRUMP: A Computer Program for Transient and Steady-State Temperature Distributions in Multidimensional Systems. UCRL-14754, Rev. 3, TID-4500, Lawrence Livermore Laboratory, University of California, Livermore, California.

APPENDIX A

PRECONDITIONING TEST ASSEMBLY TEMPERATURES

APPENDIX A

PRECONDITIONING TEST ASSEMBLY TEMPERATURES

Data from the second thermal-hydraulic experiment (TH-2) were recorded during the power ascension and during the full-power, steady-state preconditioning phase of National Research Universal (NRU) reactor operation. This appendix contains plots showing the test assembly environment at the third and final rise to full power. U-2 loop water at 16.3 kg/s (129,400 lbm/h) and 827 MPa (1200 psig) was used to cool the cracking fuel.

The average axial temperature profile for the test assembly shroud is shown in Figure A.1, and the individual corner channel axial temperature profiles are presented in Figure A.2. Modest (<12K) coolant temperature gradients (in water) across the test assembly are evident from this comparison of individual corner channel temperatures. The inlet piping temperature at -27.43 m (-1080 in.) upstream from the test assembly and the outlet region coolant (Level 20) and shroud temperatures are illustrated in Figure A.3. Intervening data (Levels 1 through 18) represent average shroud temperatures in the test assembly. These temperatures are very comparable to temperatures measured in MT-1[3] and MT-2.[4] Axial and radial coolant channel temperatures are provided by steam probe thermocouples (TCs) (see Figures A.4 and A.5, respectively).

Average fuel rod cladding temperatures during preconditioning are shown in Figure A.6. TCs located on both the interior and exterior of the cladding provided axial temperature distributions. Coolant temperatures determined by steam probes at four elevations are also included on Figure A.6 for comparison. Temperatures for exterior TCs for three fuel rods at three levels are shown in Figure A.7 to illustrate the negligible effect of radial power gradients. The average of the interior cladding temperatures is shown in Figure A.8 along with plots of average exterior cladding temperatures and the average fuel centerline temperature for Level 17.

The remainder of this appendix consists of the following graphical data:

Figure A.1. Average Temperature Profile for the Shroud During Preconditioning

Figure A.2. Individual Axial Temperature Profiles for the Shroud During Preconditioning

Figure A.3. Shroud and Test Train Coolant Temperatures During Preconditioning

Figure A.4. Average Steam Probe Temperature Profile (in water) During Preconditioning

Figure A.5. Diagonal Temperature Profiles Across Test Assembly Coolant at Levels 13, 15, and 17 During Preconditioning

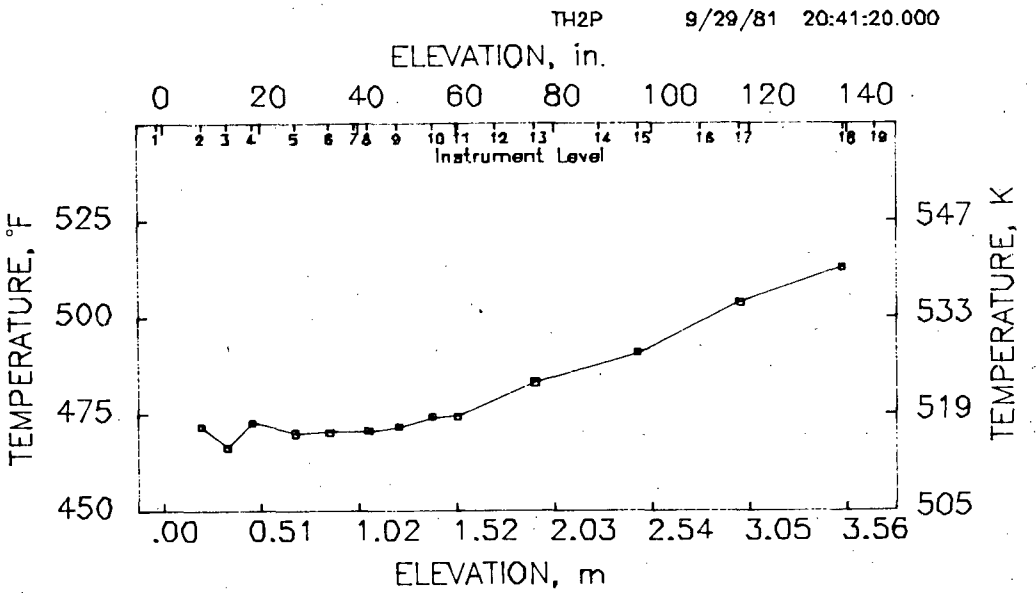

FIGURE A.1. Average Temperature Profile for the Shroud During Preconditioning

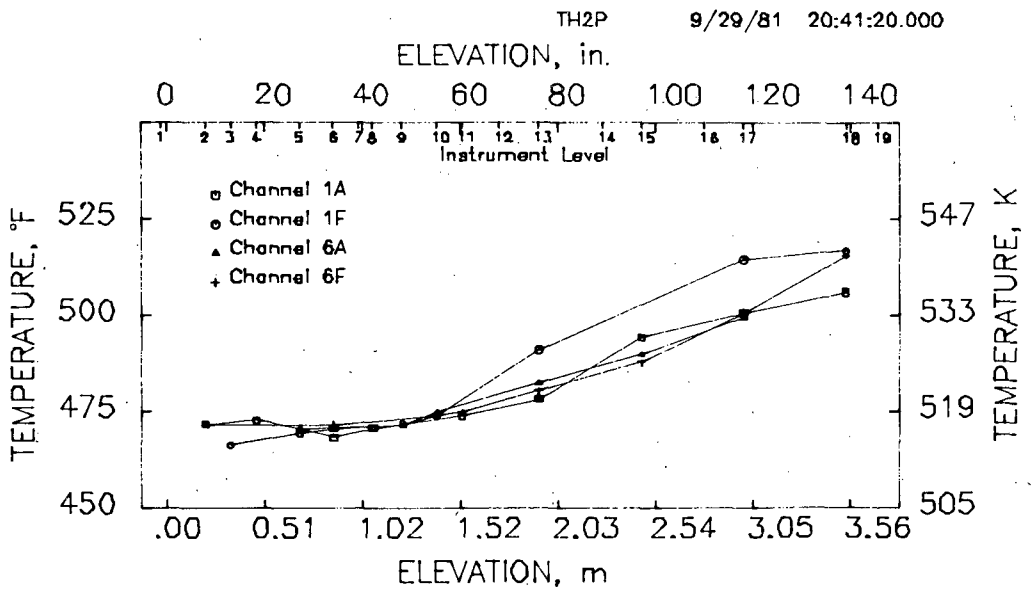

FIGURE A.2. Individual Axial Temperature Profiles for the Shroud During Preconditioning

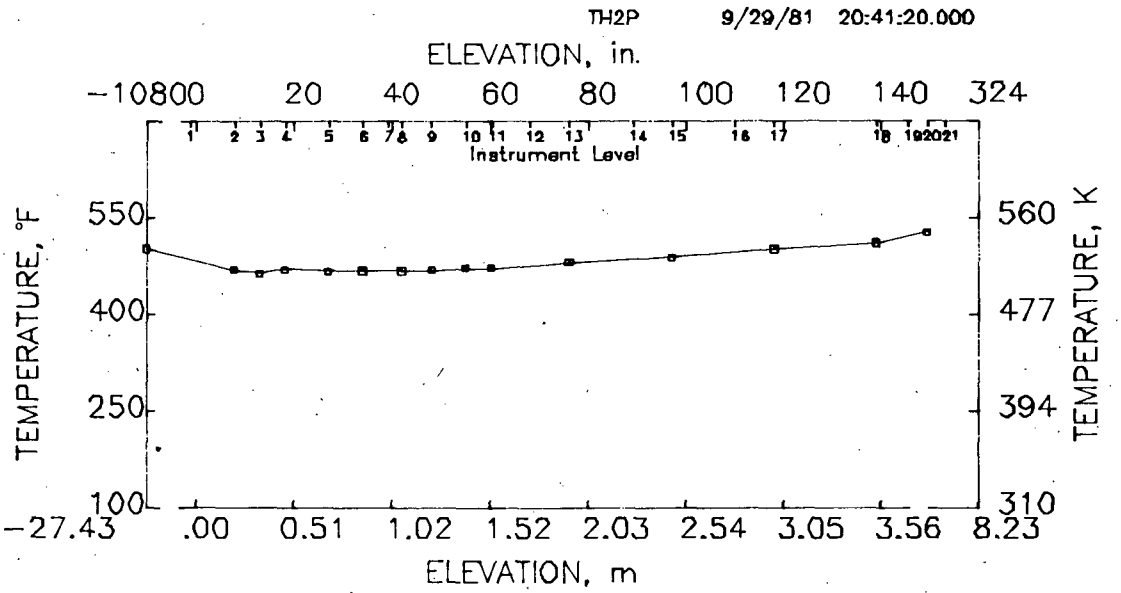

FIGURE A.3. Shroud and Test Train Coolant Temperatures During Preconditioning

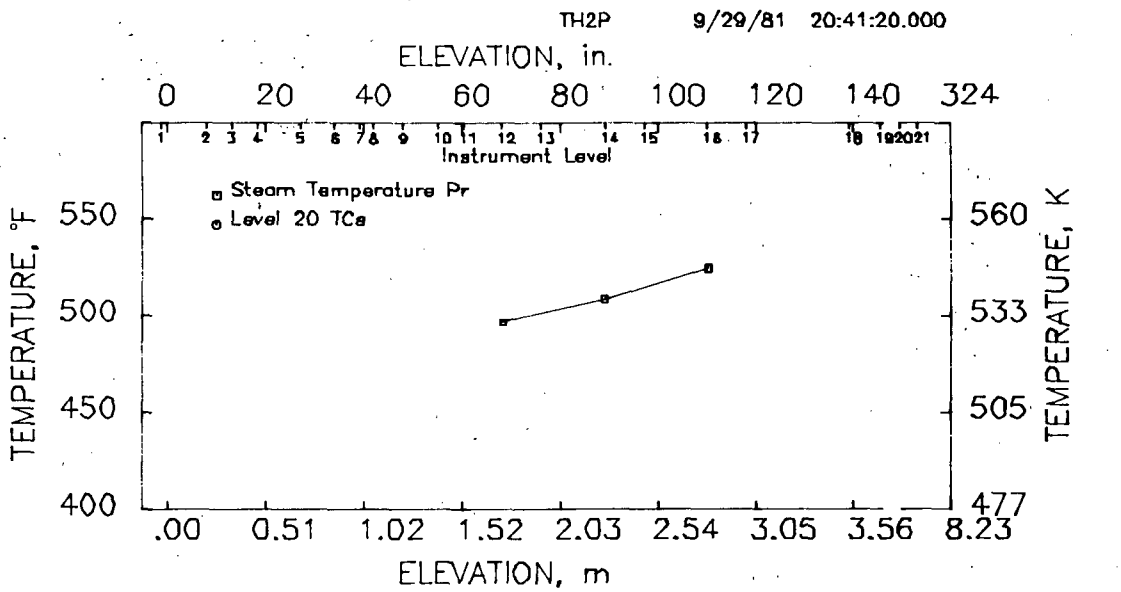

FIGURE A.4. Average Steam Probe Temperature Profile (in water) During Preconditioning

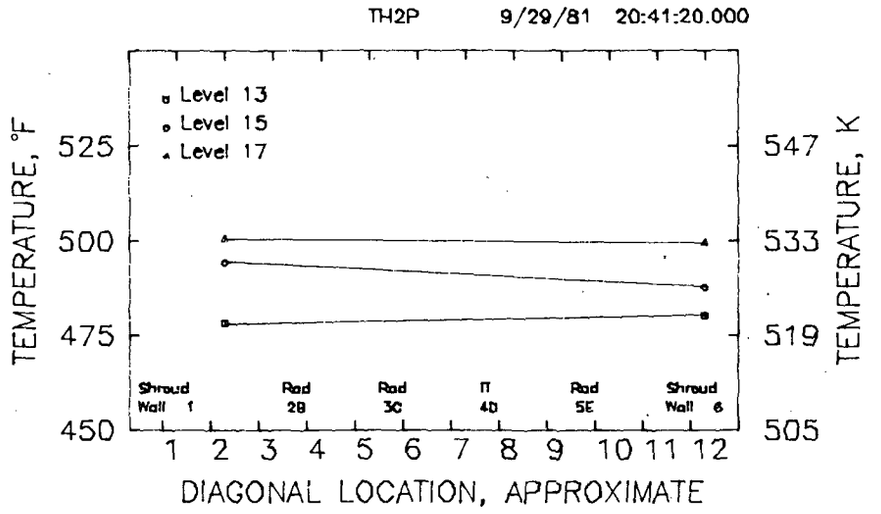

FIGURE A.5. Diagonal Temperature Profiles Across Test Assembly Coolant at Levels 13, 15, and 17 During Preconditioning

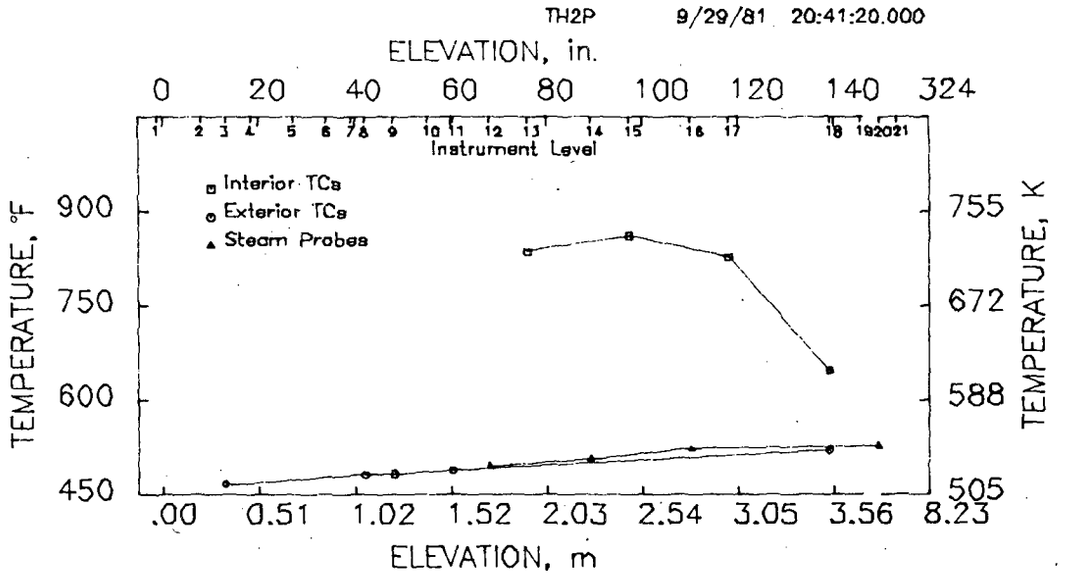

FIGURE A.6. Average Fuel Rod Cladding Temperature Profiles for Interior and Exterior TCs During Preconditioning

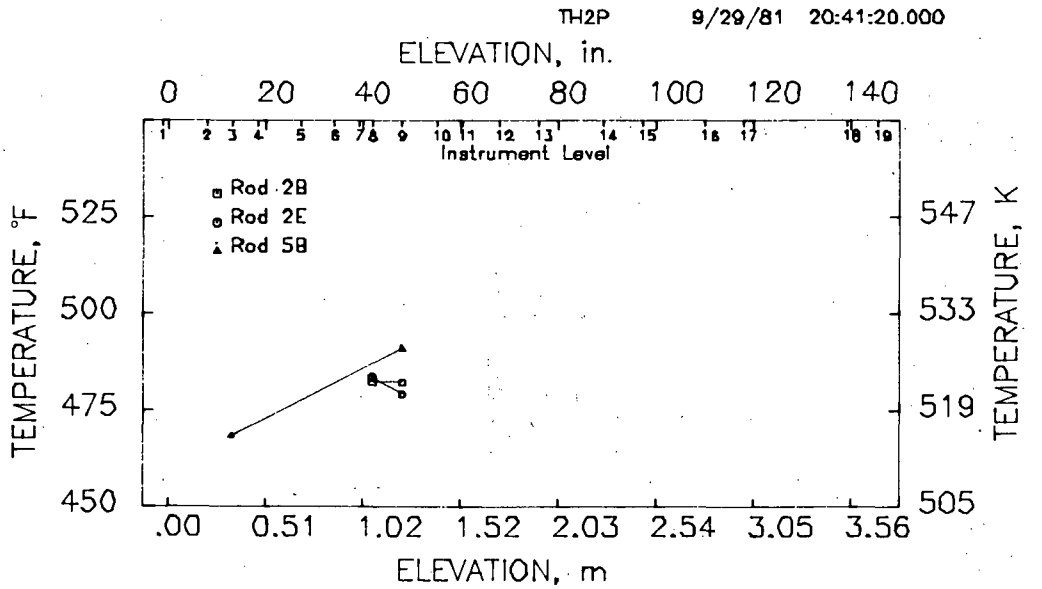

FIGURE A.7. Individual Guard Rod Cladding Exterior Temperature Profiles During Preconditioning

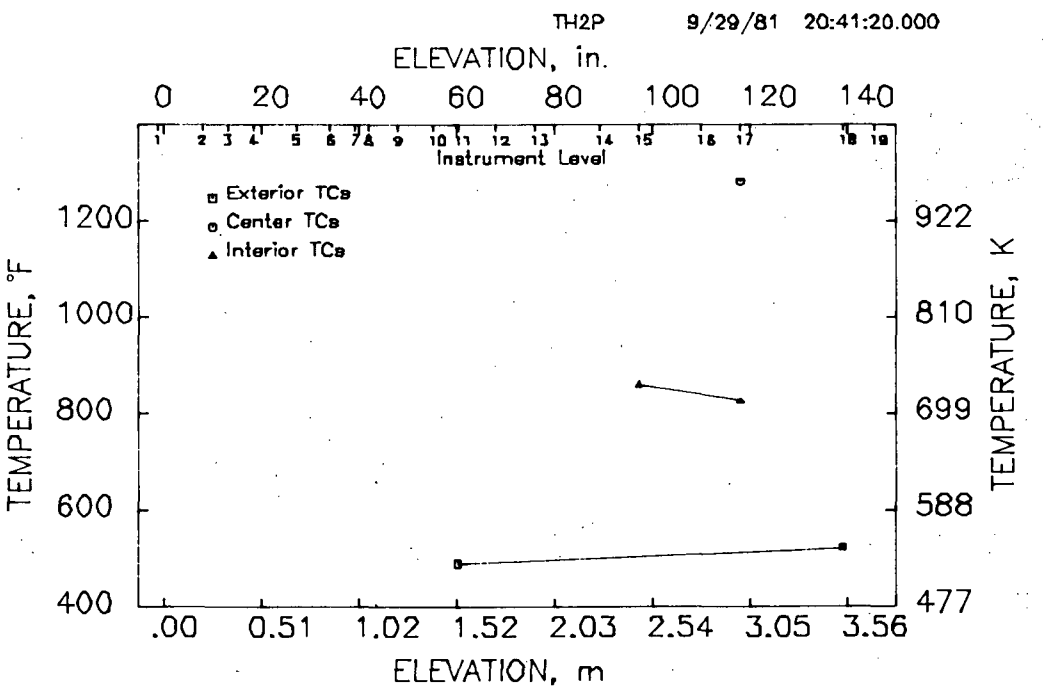

FIGURE A.8. Average Fuel Rod Cladding Temperature Profiles for Exterior, Interior, and Center TCs During Preconditioning

APPENDIX B

PRETRANSIENT TEST ASSEMBLY TEMPERATURES

APPENDIX B

PRETRANSIENT TEST ASSEMBLY TEMPERATURES

Pretransient temperature data summaries are presented in this appendix. Steam at 0.378 kg/s (3000 lbm/h) was used to cool the test assembly, and test assembly backpressure was maintained at 0.28 MPa (40 psia).

Diagonal temperature profiles from one shroud corner to the opposite shroud corner at Levels 13, 15, and 17 are shown in Figures B.1 through B.4. A set of axial temperature profiles obtained from steam probes, carrier thermocouples (TCs), and shroud TCs (all located in the shroud corners) are shown in Figures B.5 through B.8. Average steam probe axial temperatures are shown in Figures B.9 through B.12.

The remainder of this appendix consists of the following graphical data:

Figure B.1. Diagonal Temperature Profile Across Test Assembly Coolant During Pretransient for TH-2.02

Figure B.2. Diagonal Temperature Profile Across Test Assembly Coolant During Pretransient for TH-2.12

Figure B.3. Diagonal Temperature Profile Across Test Assembly Coolant During Pretransient for TH-2.13

Figure B.4. Diagonal Temperature Profile Across Test Assembly Coolant During Pretransient for TH-2.14

Figure B.5. Axial Temperature Profiles for the Shroud During Pretransient for TH-2.02

Figure B.6. Axial Temperature Profiles for the Shroud During Pretransient for TH-2.12

Figure B.7. Axial Temperature Profiles for the Shroud During Pretransient for TH-2.13

Figure B.8. Axial Temperature Profiles for the Shroud During Pretransient for TH-2.14

Figure B.9. Average Steam Probe Temperature Profile (in steam) During Pretransient for TH-2.02

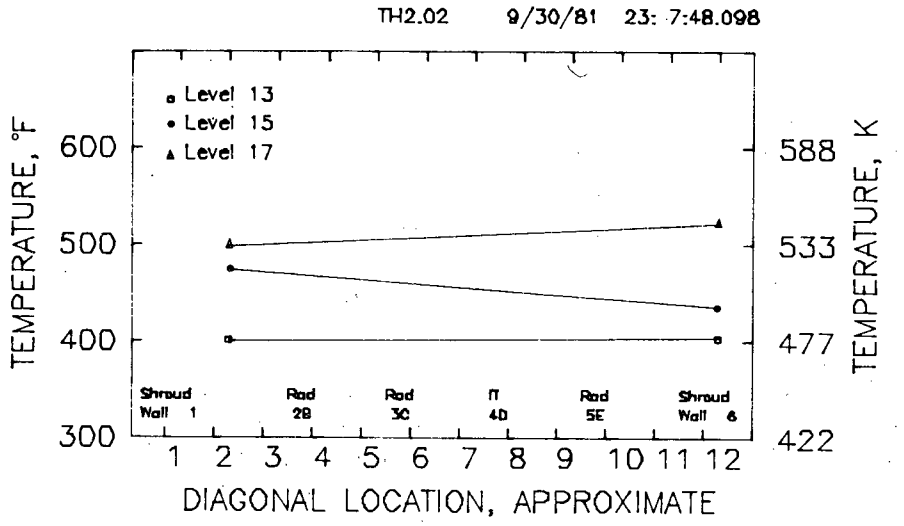

FIGURE B.1. Diagonal Temperature Profile Across Test Assembly Coolant During Pretransient for TH-2.02

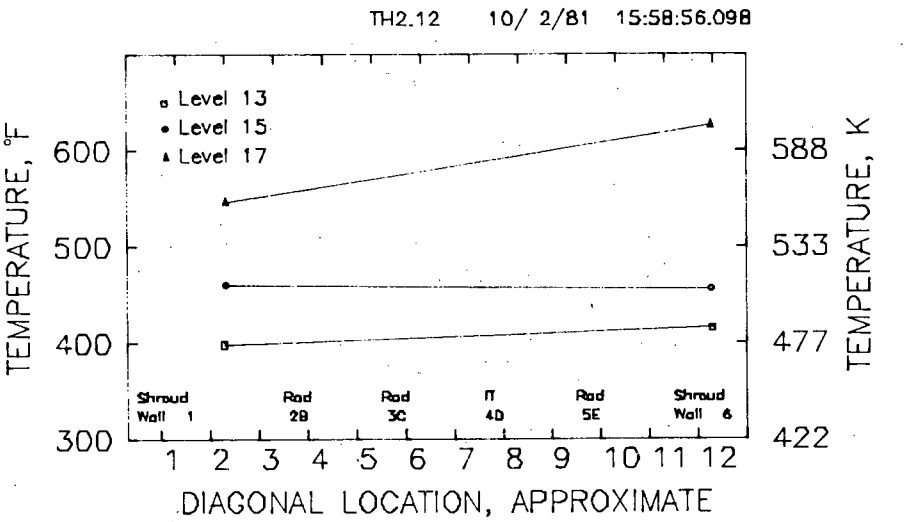

FIGURE B.2. Diagonal Temperature Profile Across Test Assembly Coolant During Pretransient for TH-2.12

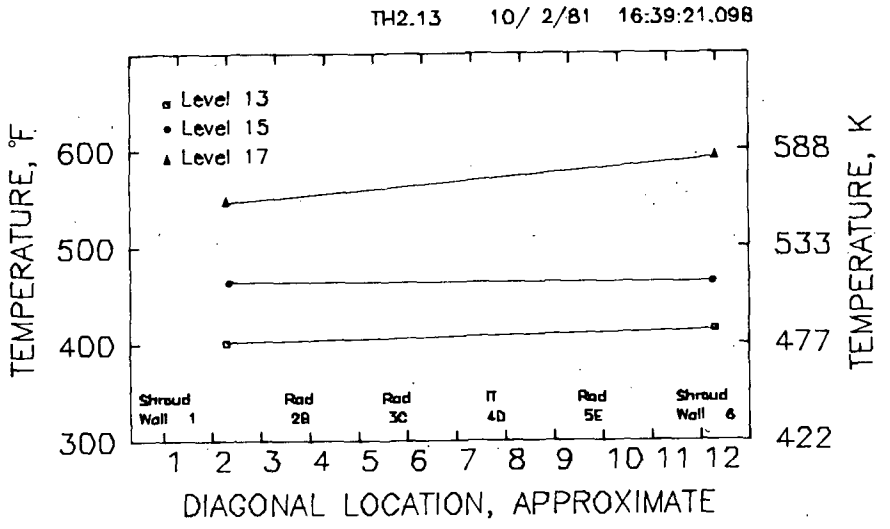

FIGURE B.3. Diagonal Temperature Profile Across Test Assembly Coolant During Pretransient for TH-2.13

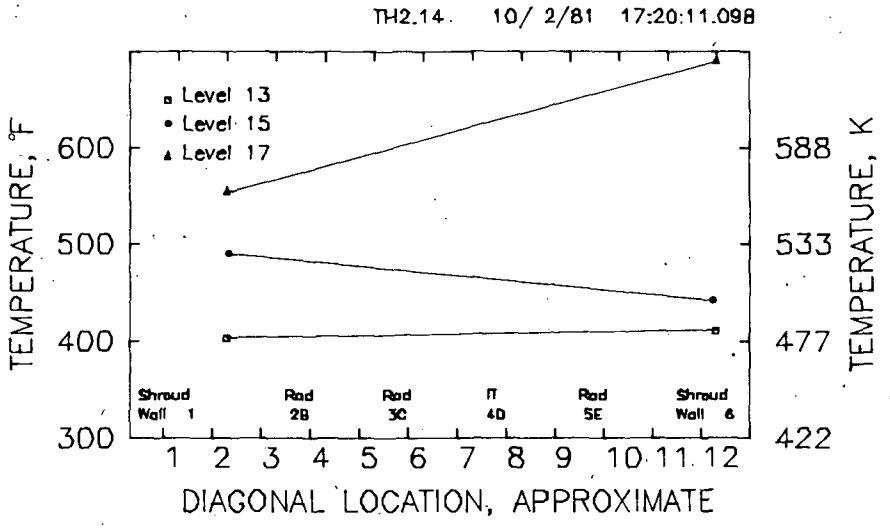

FIGURE B.4. Diagonal Temperature Profile Across Test Assembly Coolant During Pretransient for TH-2.14

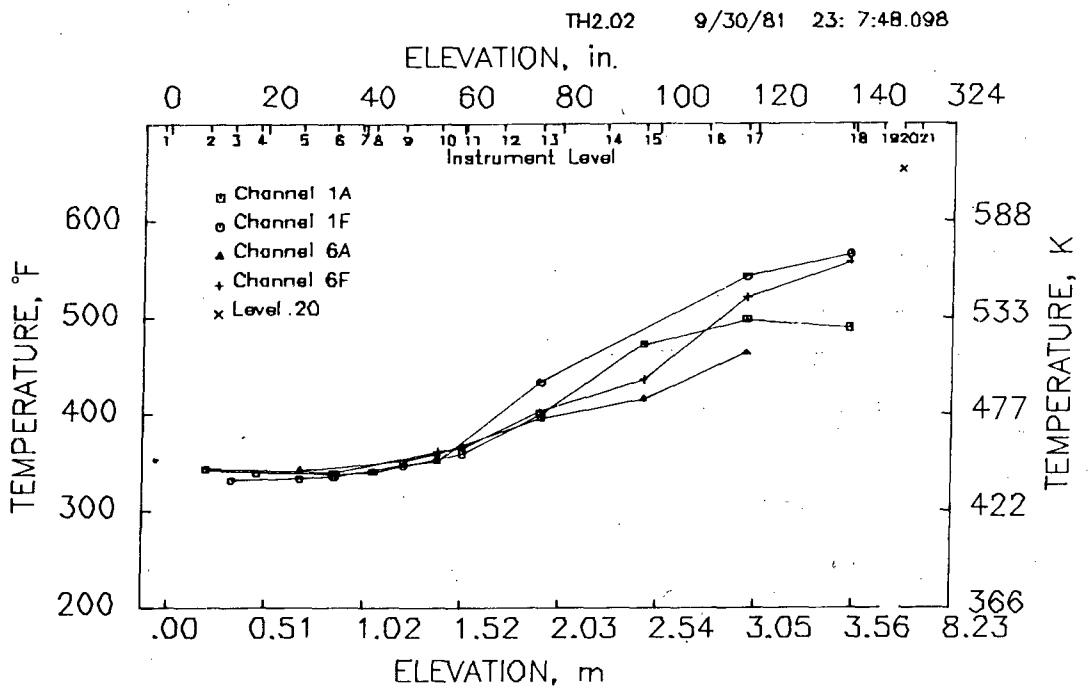

FIGURE B.5. Axial Temperature Profiles for the Shroud During Pretransient for TH-2.02

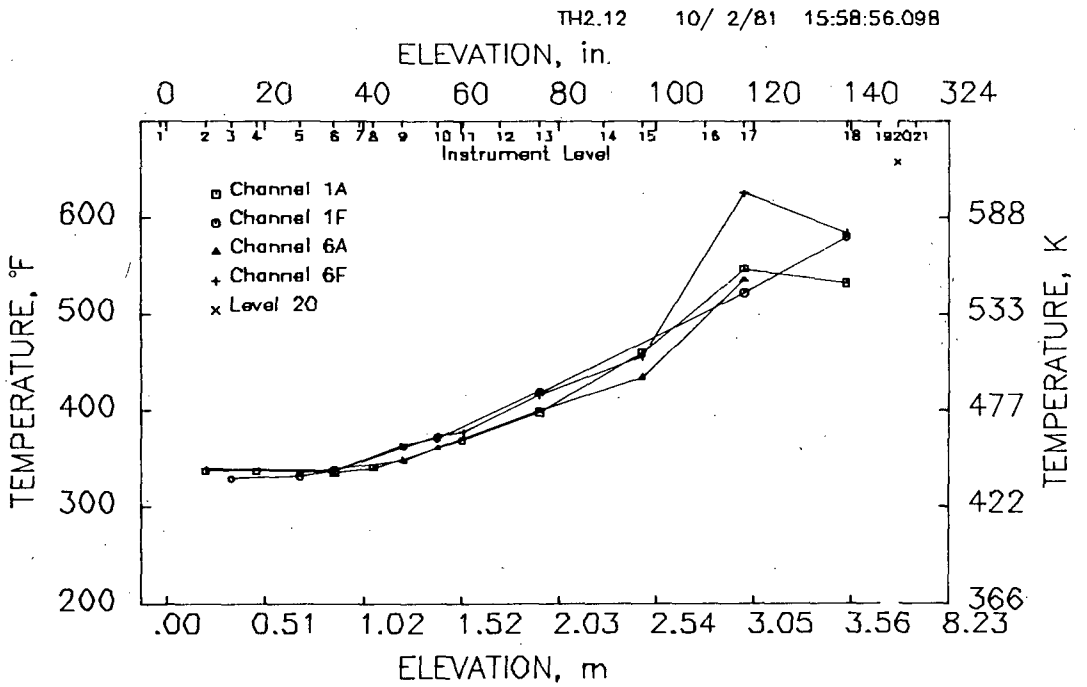

FIGURE B.6. Axial Temperature Profiles for the Shroud During Pretransient for TH-2.12

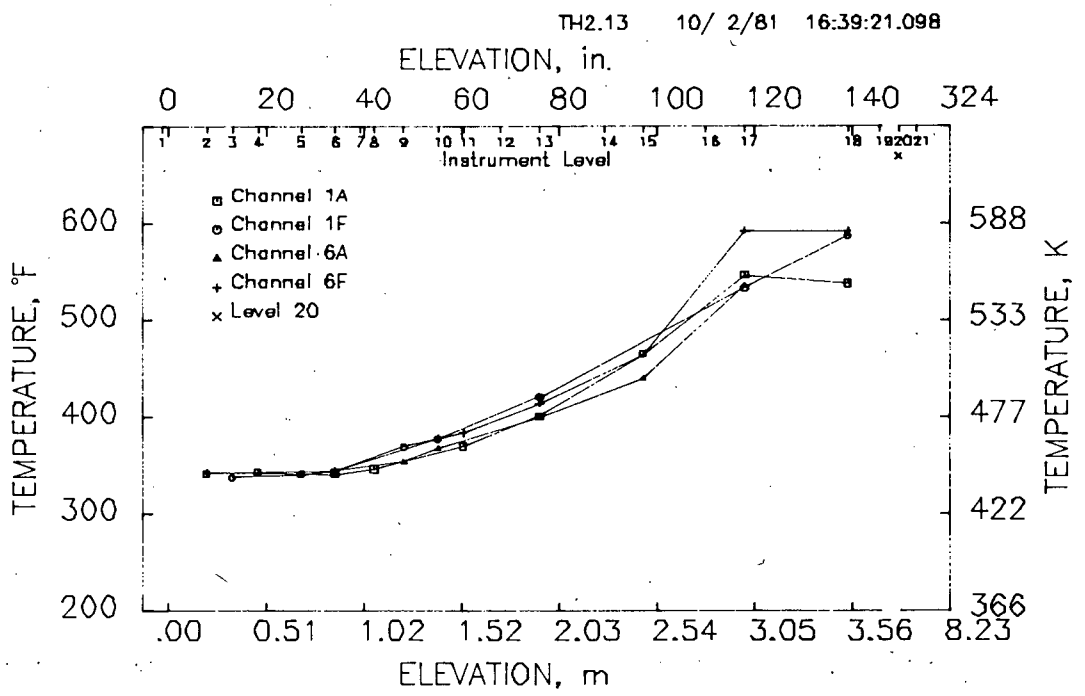

FIGURE B.7. Axial Temperature Profiles for the Shroud During Pretransient for TH-2.13

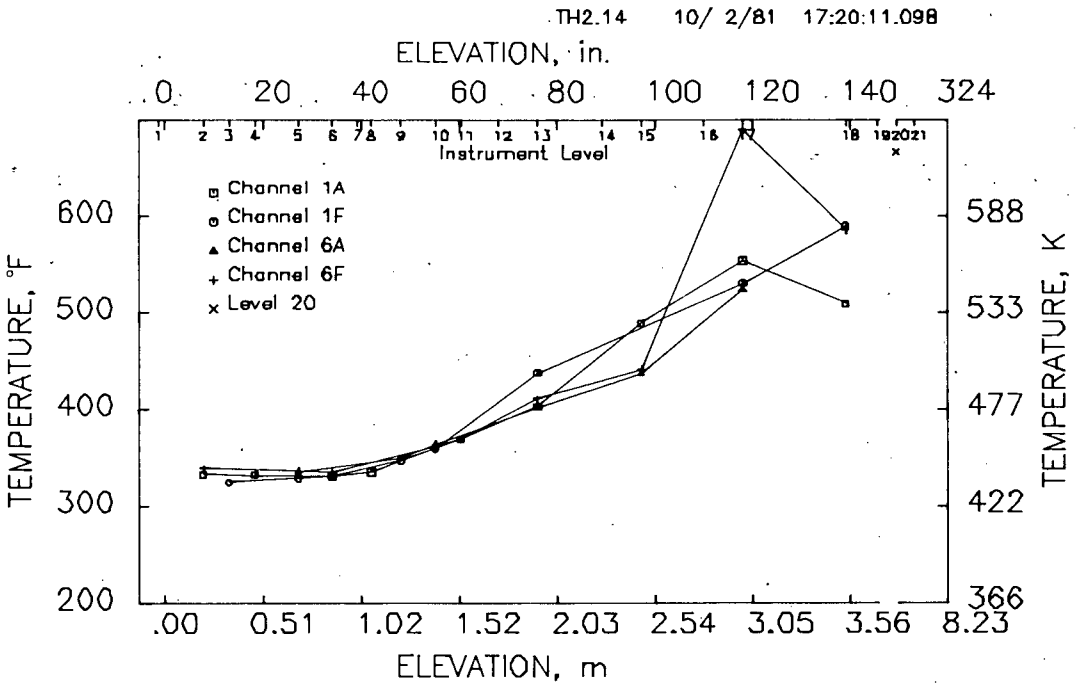

FIGURE B.8. Axial Temperature Profiles for the Shroud During Pretransient for TH-2.14

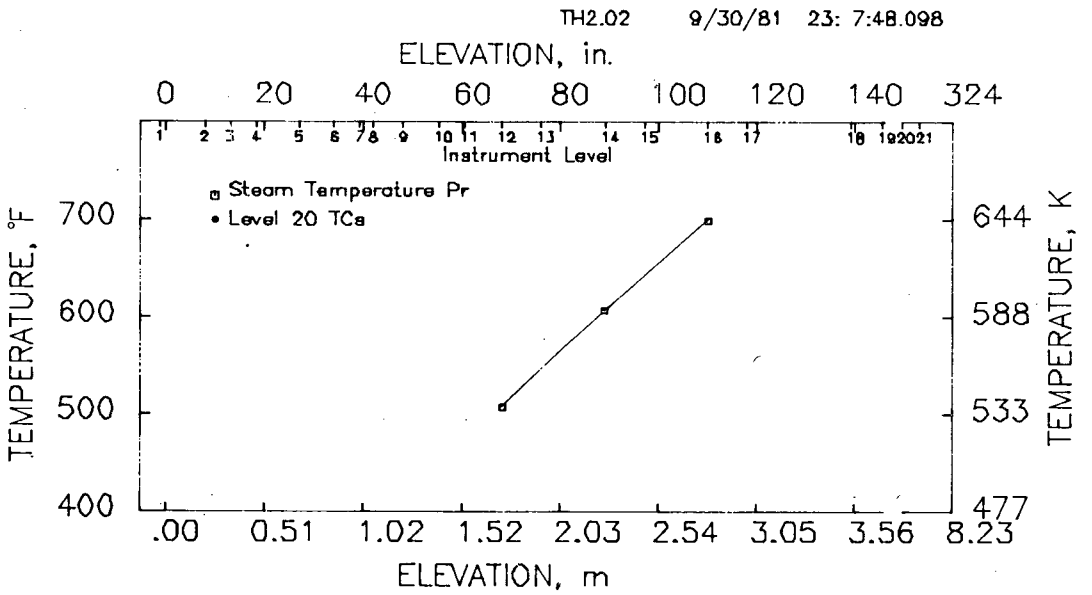

FIGURE B.9. Average Steam Probe Temperature (in steam) During Pretransient for TH-2.02

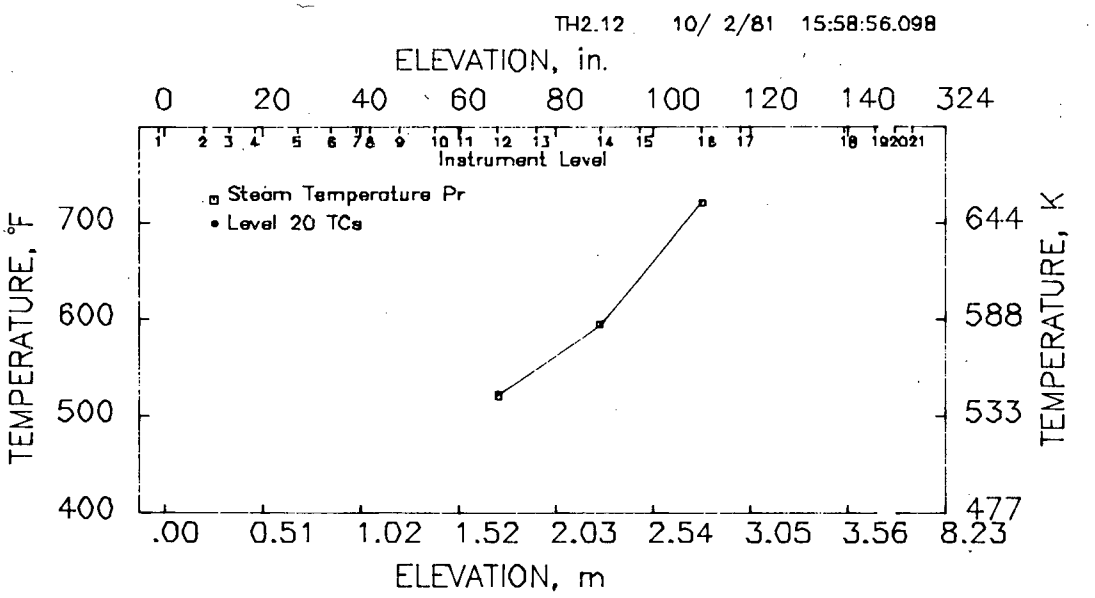

FIGURE B.10. Average Steam Probe Temperature (in steam) During Pretransient for TH-2.12

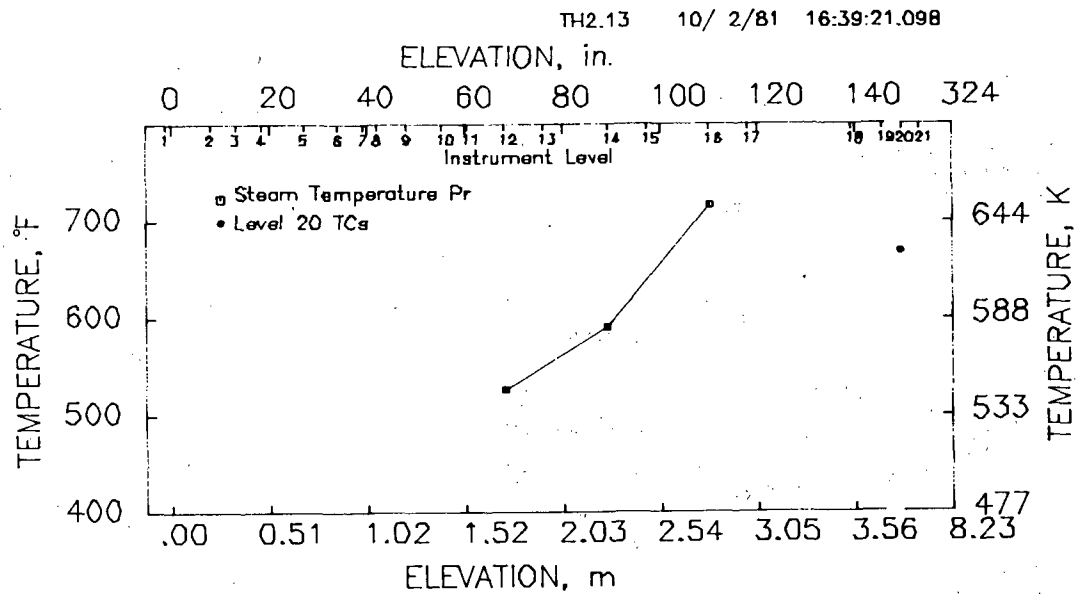

FIGURE B.11. Average Steam Probe Temperature Profile (in steam) During Pretransient for TH-2.13

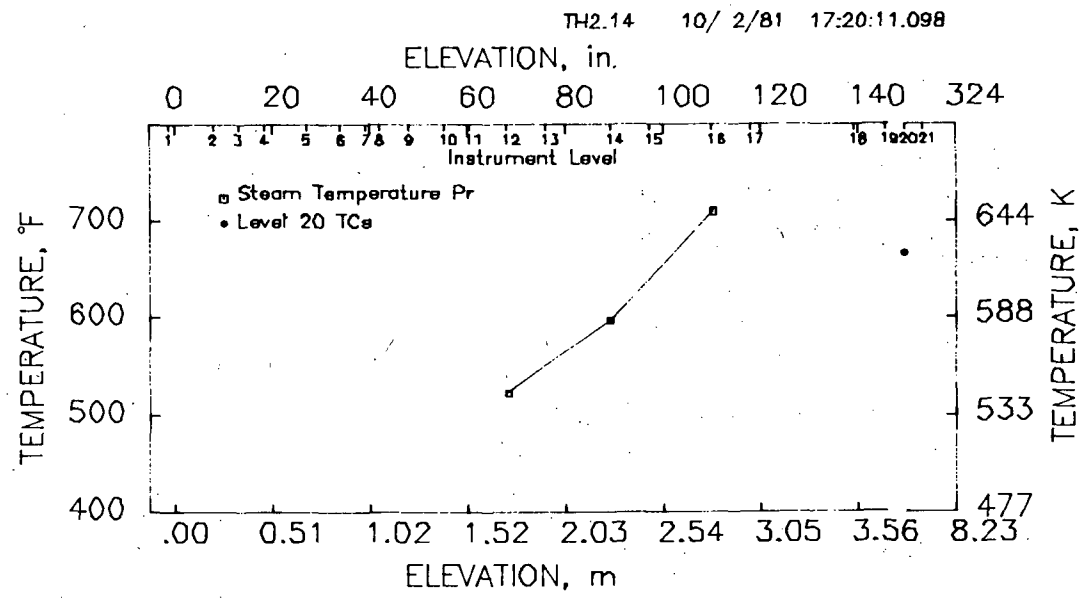

FIGURE B.12. Average Steam Probe Temperature Profile (in steam) During Pretransient for TH-2.14

APPENDIX C

TRANSIENT FUEL AND CLADDING TEMPERATURES

APPENDIX C

TRANSIENT FUEL AND CLADDING TEMPERATURES

Transient fuel and cladding temperatures are presented in this appendix. The test assembly environment during the transient can be steam, water, or both with a changing neutron flux depending partially on control rod position and the changing reactivity of water and steam. The test assembly backpressure was maintained at about 0.28 MPa (40 psia).

Test rod center and interior cladding temperatures are shown in Figures C.1 through C.12 at Levels 13, 15, and 17 for selected tests. Axial temperature profiles for the shroud and test train (Figures C.13 through C.15) show the effects of reflooding and the axial power profile on temperature distributions throughout the transient.

Two adiabatic tests--TH-2.01 and TH-2.13--were performed to determine radial and axial fuel power and to provide a check on the pretransient calorimetric (see Figures C.16 and C.17). Test rod power is indicated by the heatup rates at Levels 13, 15, and 17; the amount of heat loss to the shroud, by shroud temperatures at Levels 13, 15, and 17.

The ability of the loop control system (LCS) to maintain a constant cladding temperature above 1033K (1400°F) using preprogrammed reflood flow is shown in Figure C.18. Figures C.19 and C.20 illustrate the ability of the data acquisition and control system (DACS) with cladding temperature feedback to repeatedly maintain cladding temperatures above 1033K.

Average fuel temperatures for guard and test rods at Levels 13, 15, and 17 for test TH-2.14 are shown in Figures C.21 through C.23. These figures demonstrate the resultant average guard and test fuel temperatures when using hot spot sensor feedback control.

The remainder of this appendix consists of the following graphical data:

Figure C.1. Test Rod Interior Cladding Temperature History at Level 13 During Transient for TH-2.02

Figure C.2. Test Rod Interior Cladding Temperature History at Level 13 During Transient for TH-2.12

Figure C.3. Test Rod Interior Cladding Temperature History at Level 13 During Transient for TH-2.13

Figure C.4. Test Rod Interior Cladding Temperature History at Level 13 During Transient for TH-2.14

Figure C.22. Average Guard and Test Rod Interior Cladding Temperatures at Level 15 for TH-2.14

Figure C.23. Average Guard and Test Rod Interior Cladding Temperatures at Level 17 for TH-2.14

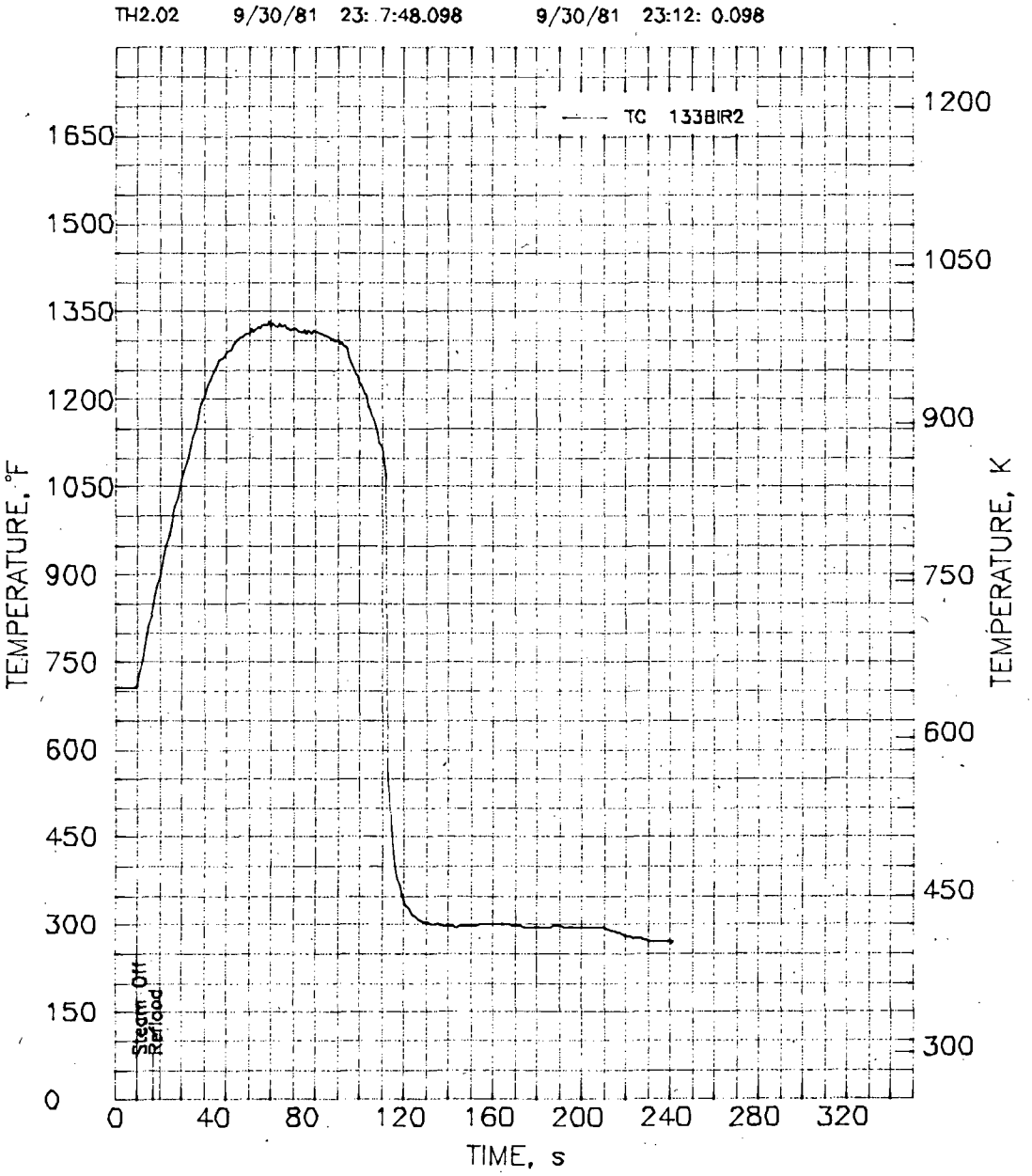

FIGURE C.1. Test Rod Interior Cladding Temperature History at Level 13 During Transient for TH-2.02

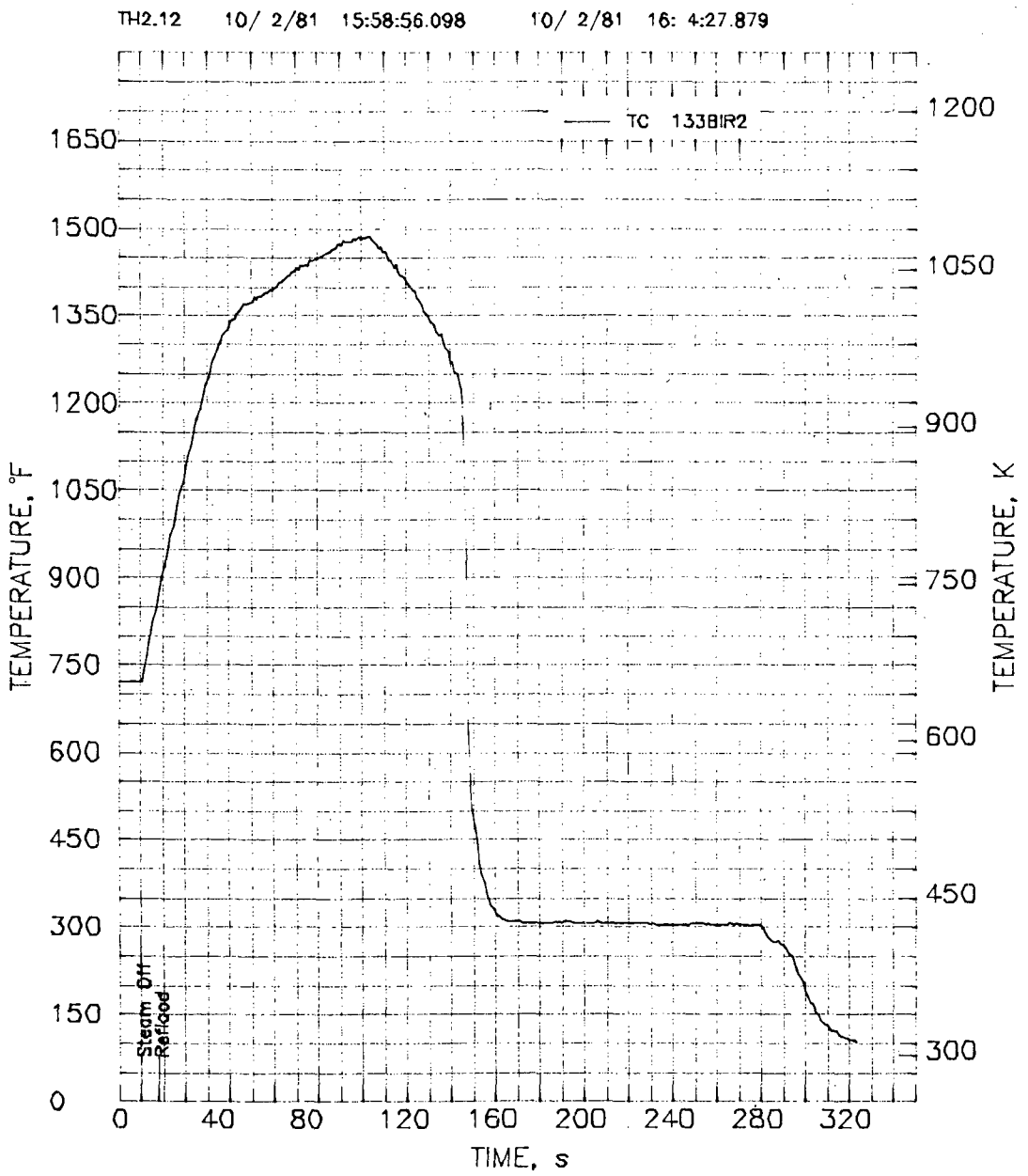

FIGURE C.2. Test Rod Interior Cladding Temperature History at Level 13 During Transient for TH-2.12

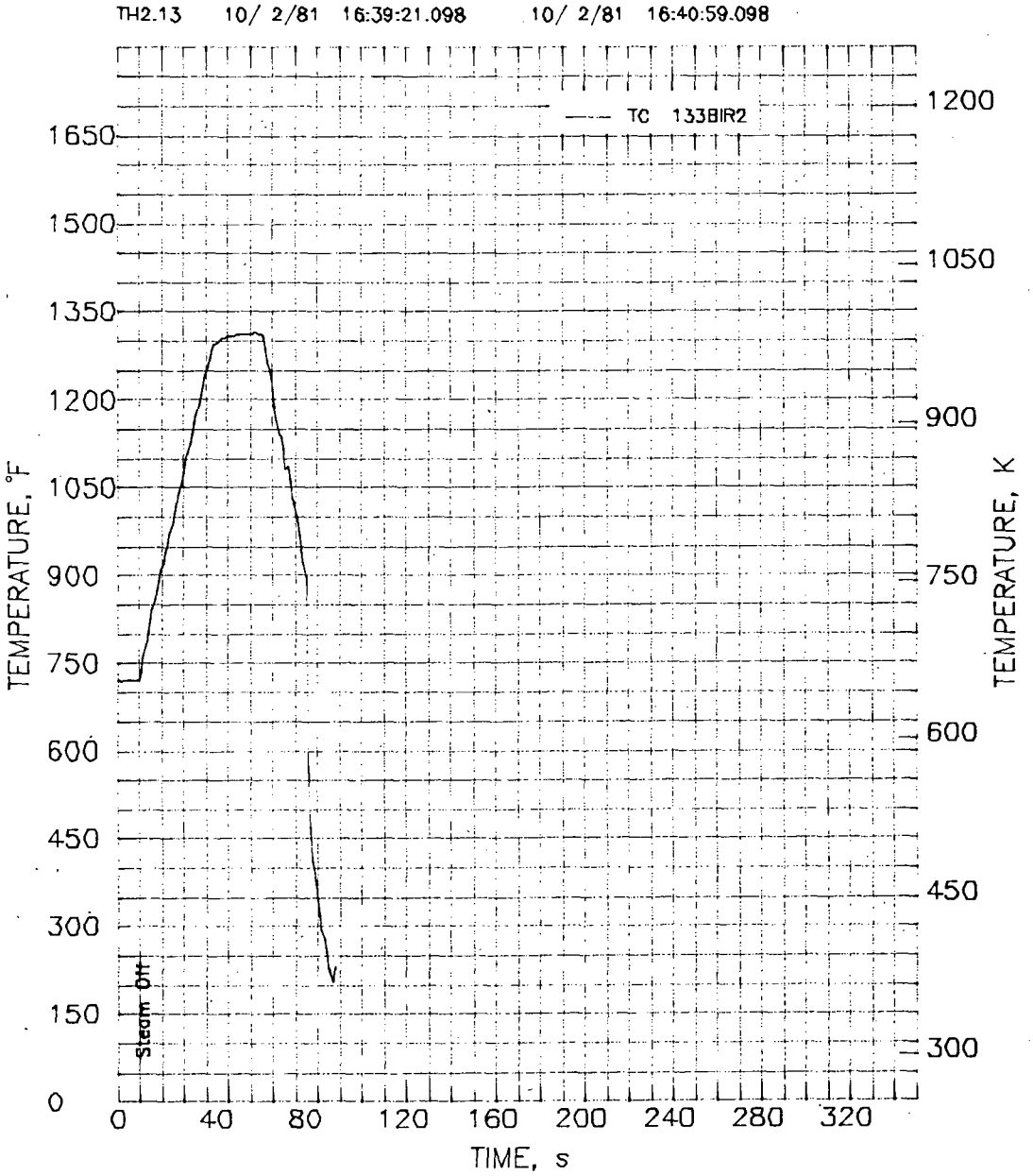

FIGURE C.3. Test Rod Interior Cladding Temperature History at Level 13 During Transient for TH-2.13

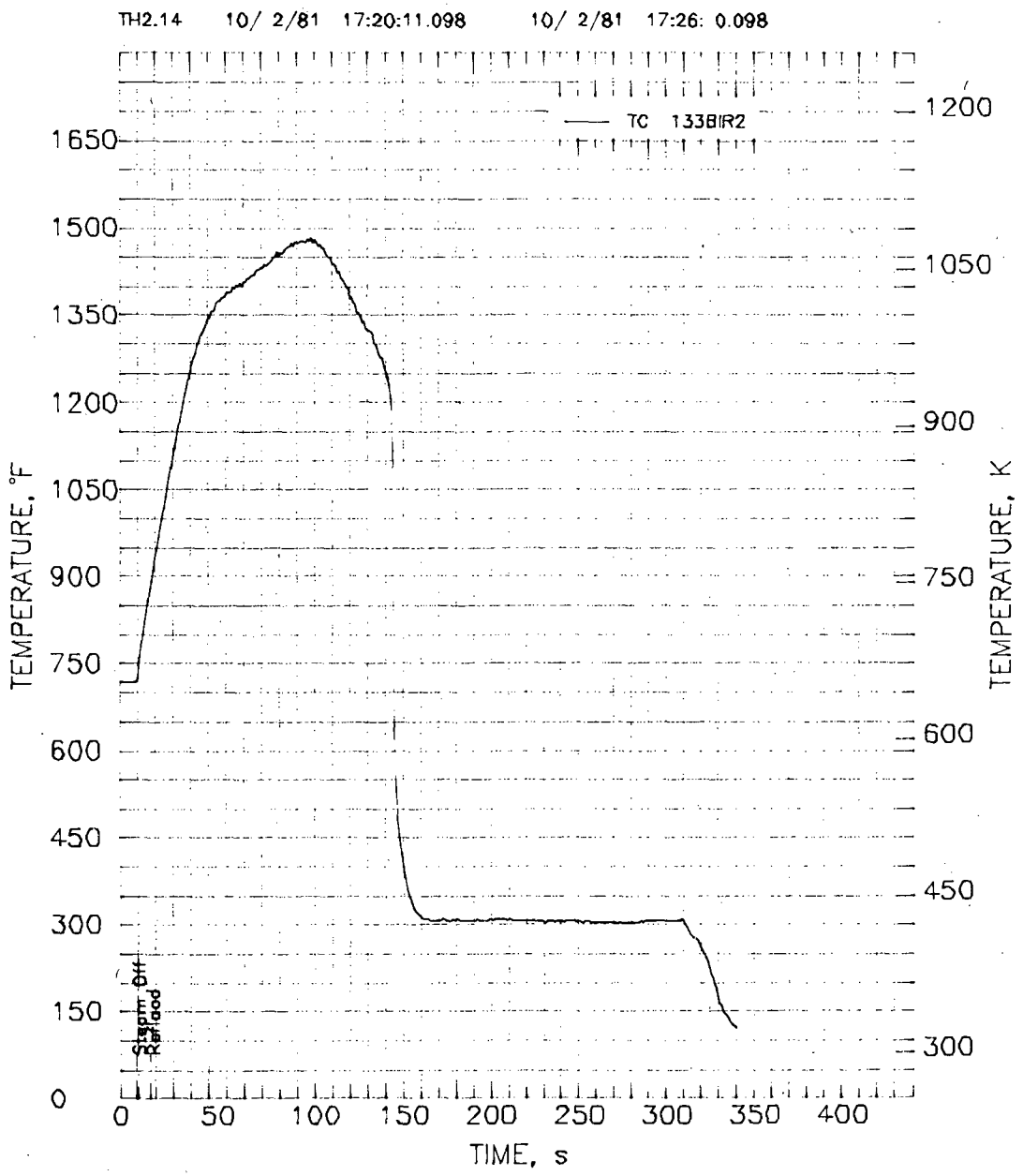

FIGURE C.4. Test Rod Interior Cladding Temperature History at Level 13 During Transient for TH-2.14

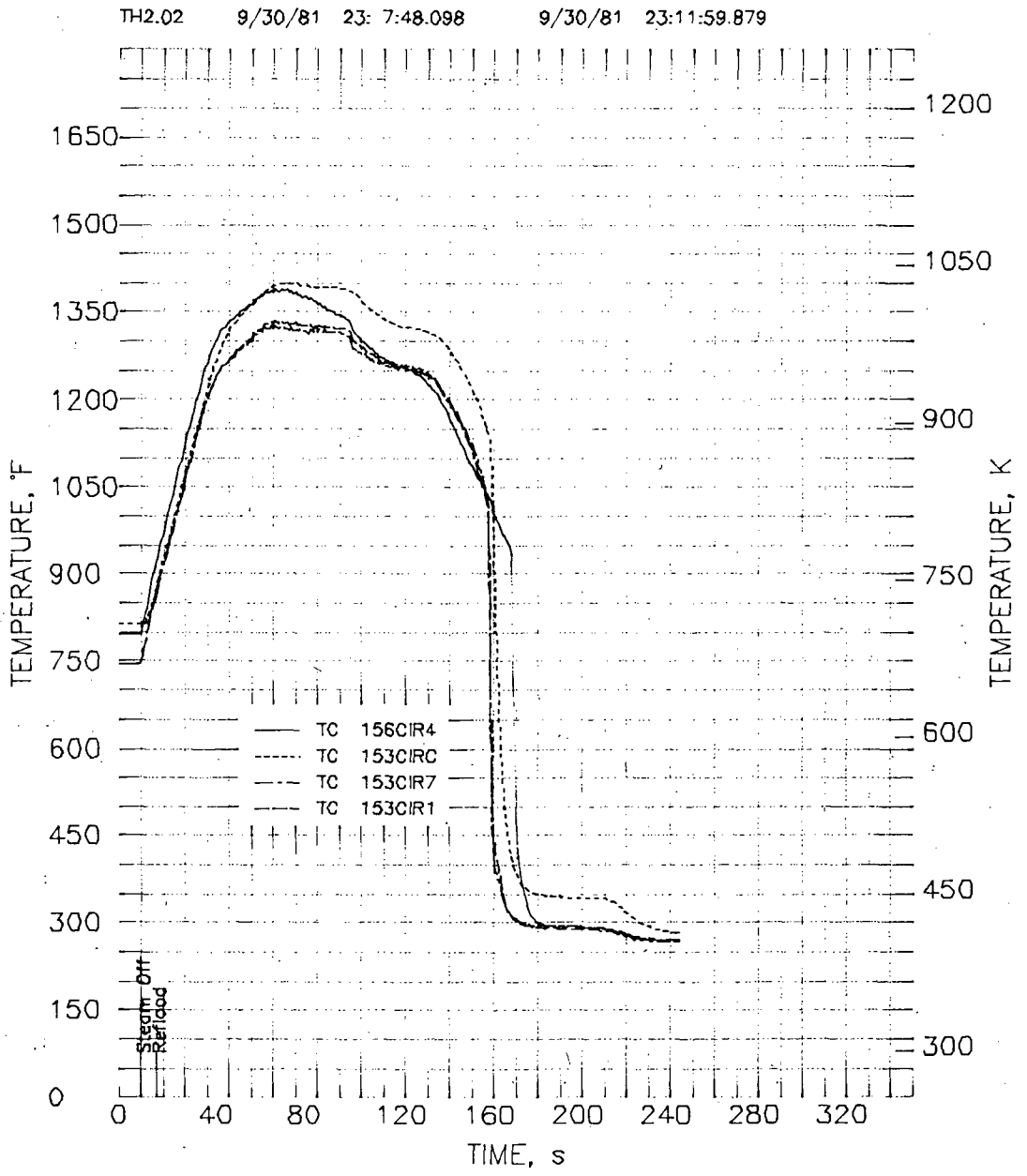

FIGURE C.5. Test Rod Center and Interior Cladding Temperature Histories at Level 15 During Transient for TH-2.02

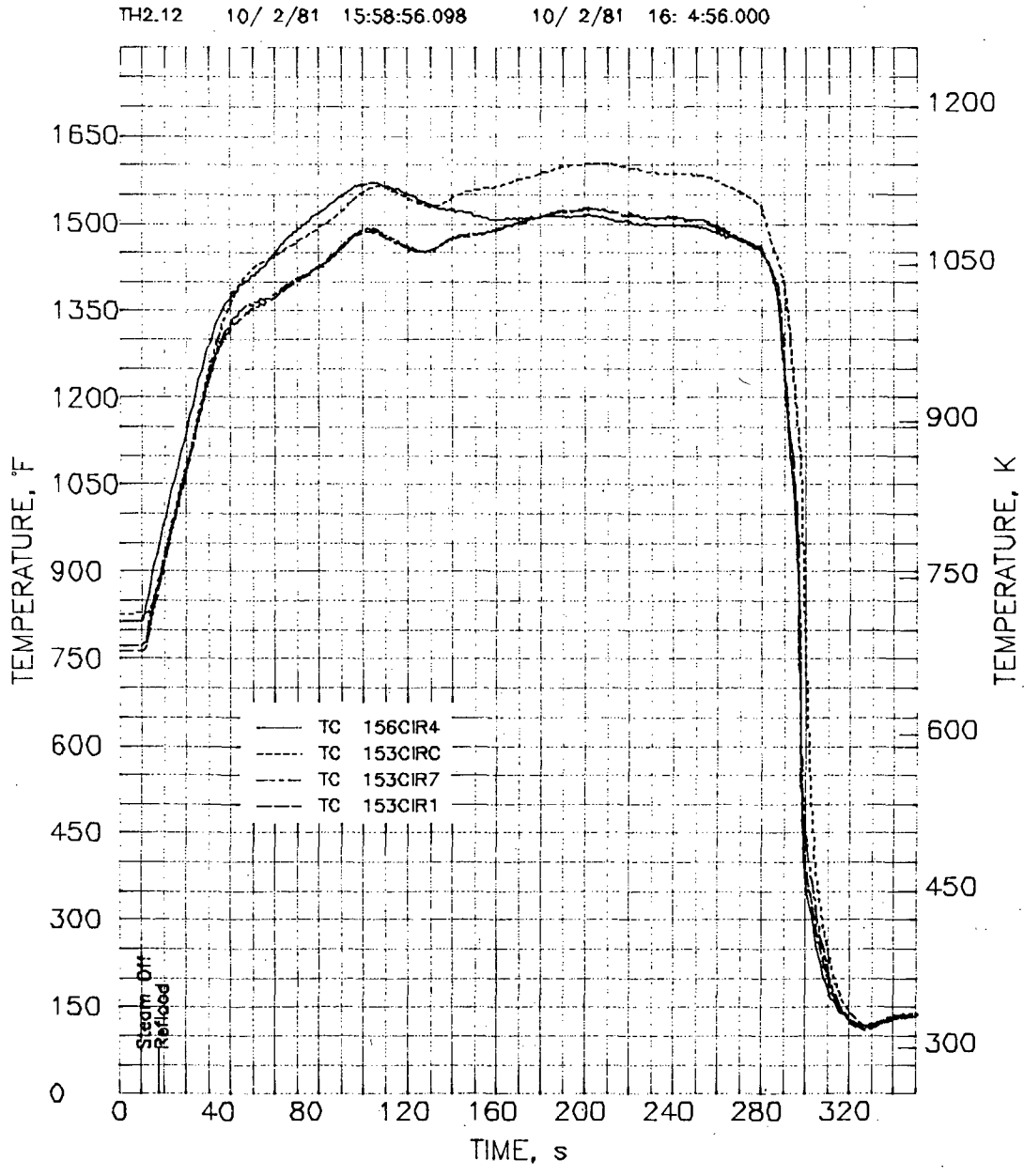

FIGURE C.6. Test Rod Center and Interior Cladding Temperature Histories at Level 15 During Transient for TH-2.12

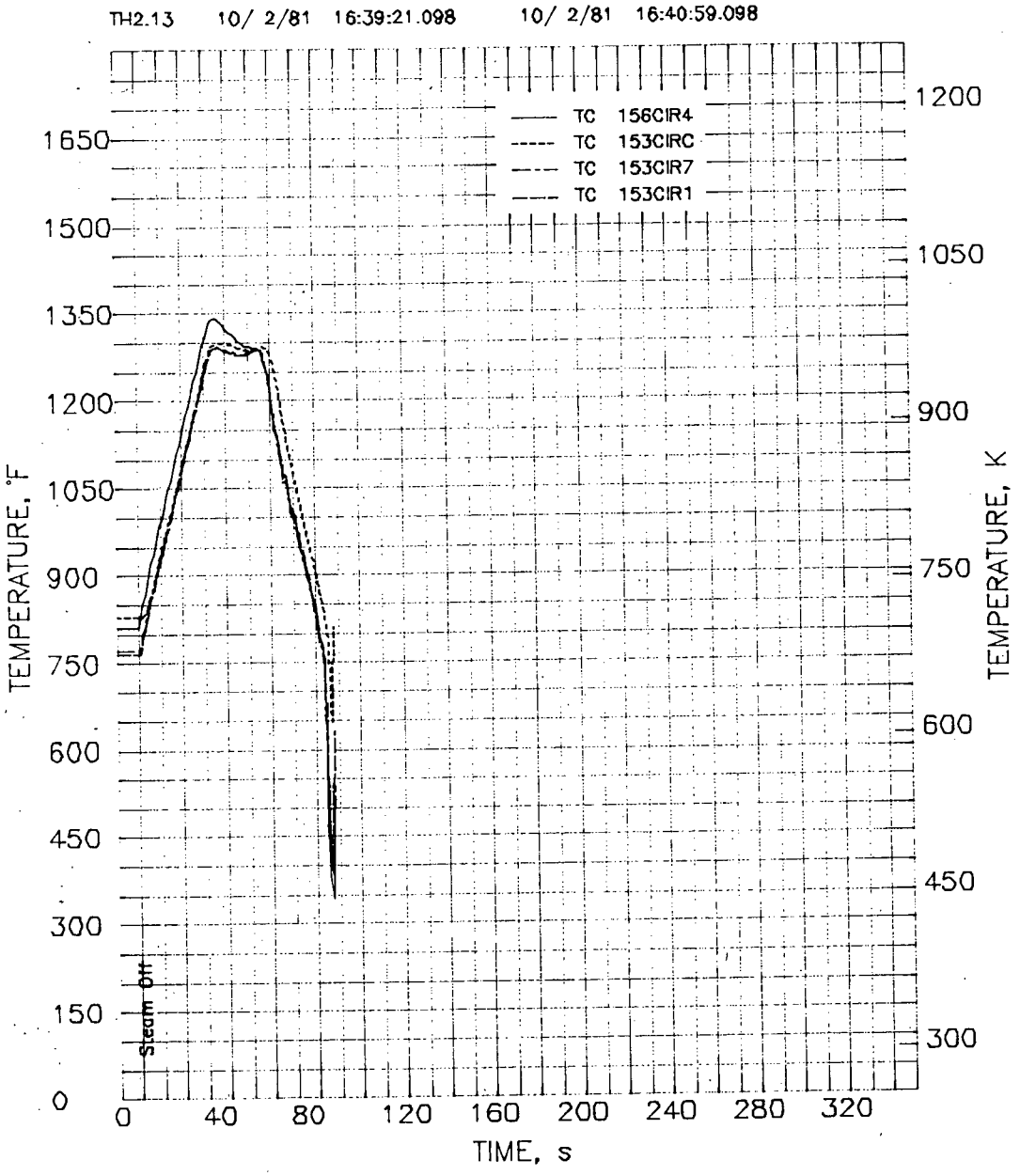

FIGURE C.7. Test Rod Center and Interior Cladding Temperature Histories at Level 15 During Transient for TH-2.13

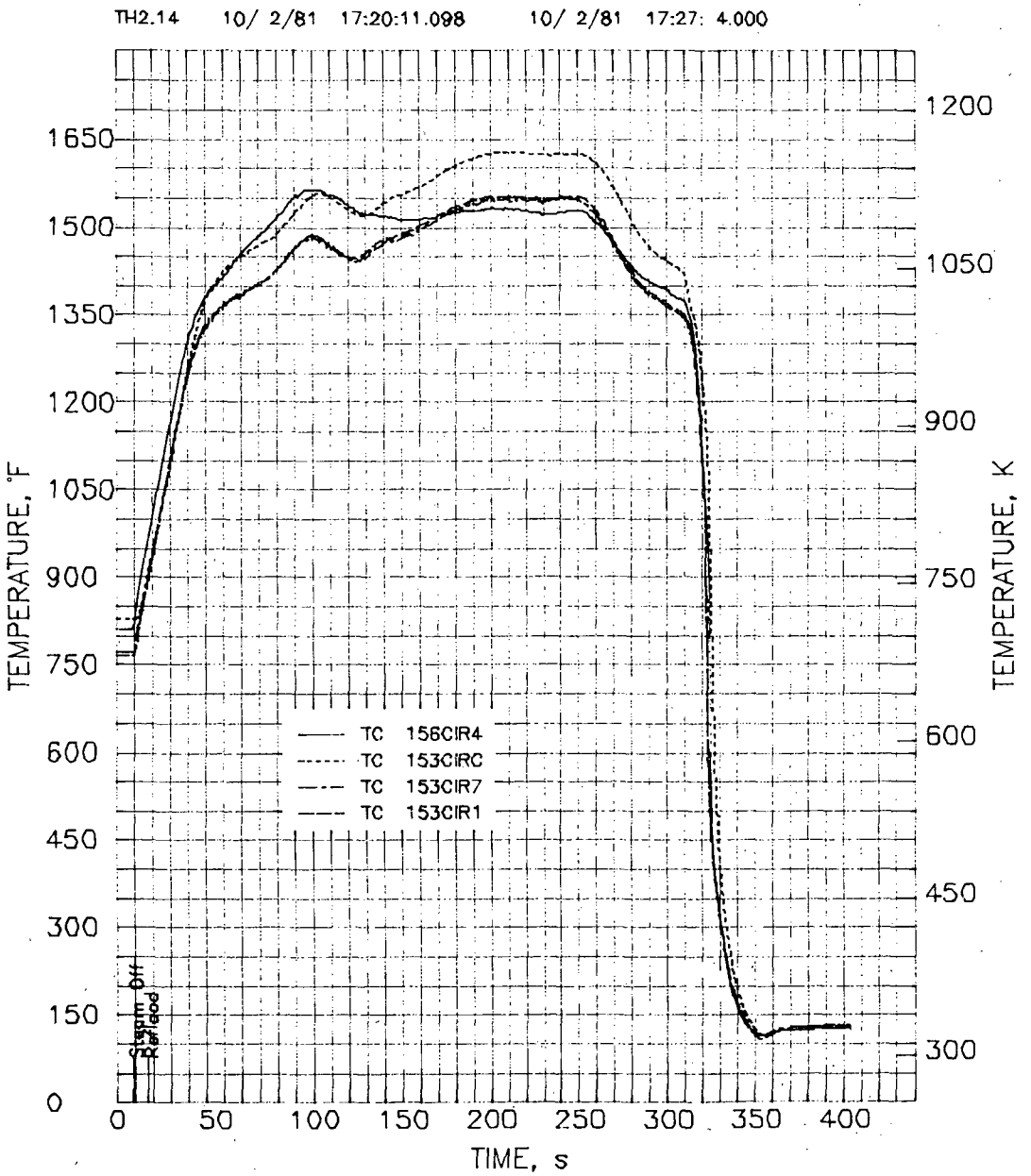

FIGURE C.8. Test Rod Center and Interior Cladding Temperature Histories at Level 15 During Transient for TH-2.14

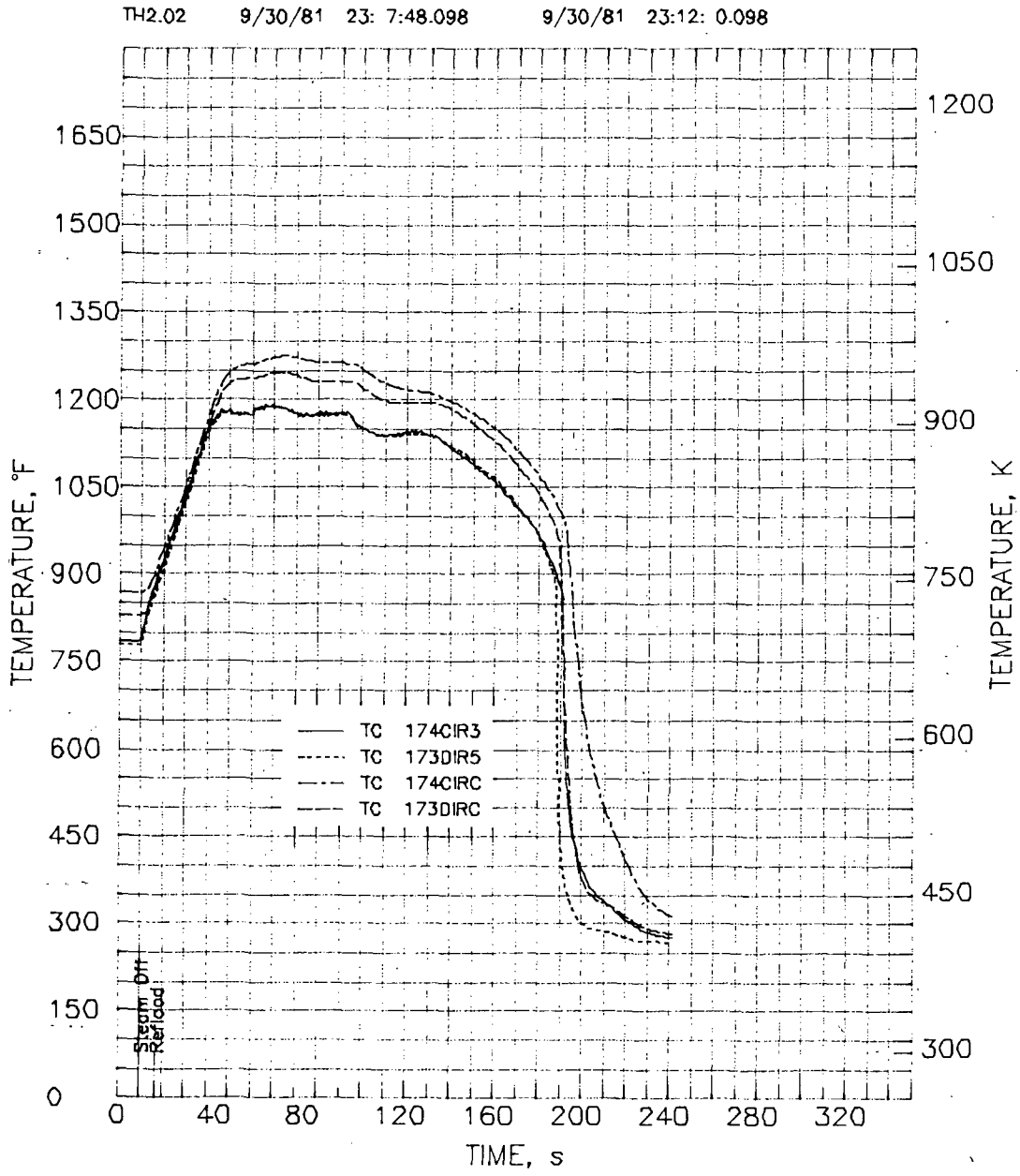

FIGURE C.9. Test Rod Center and Interior Cladding Temperature Histories at Level 17 During Transient for TH-2.02

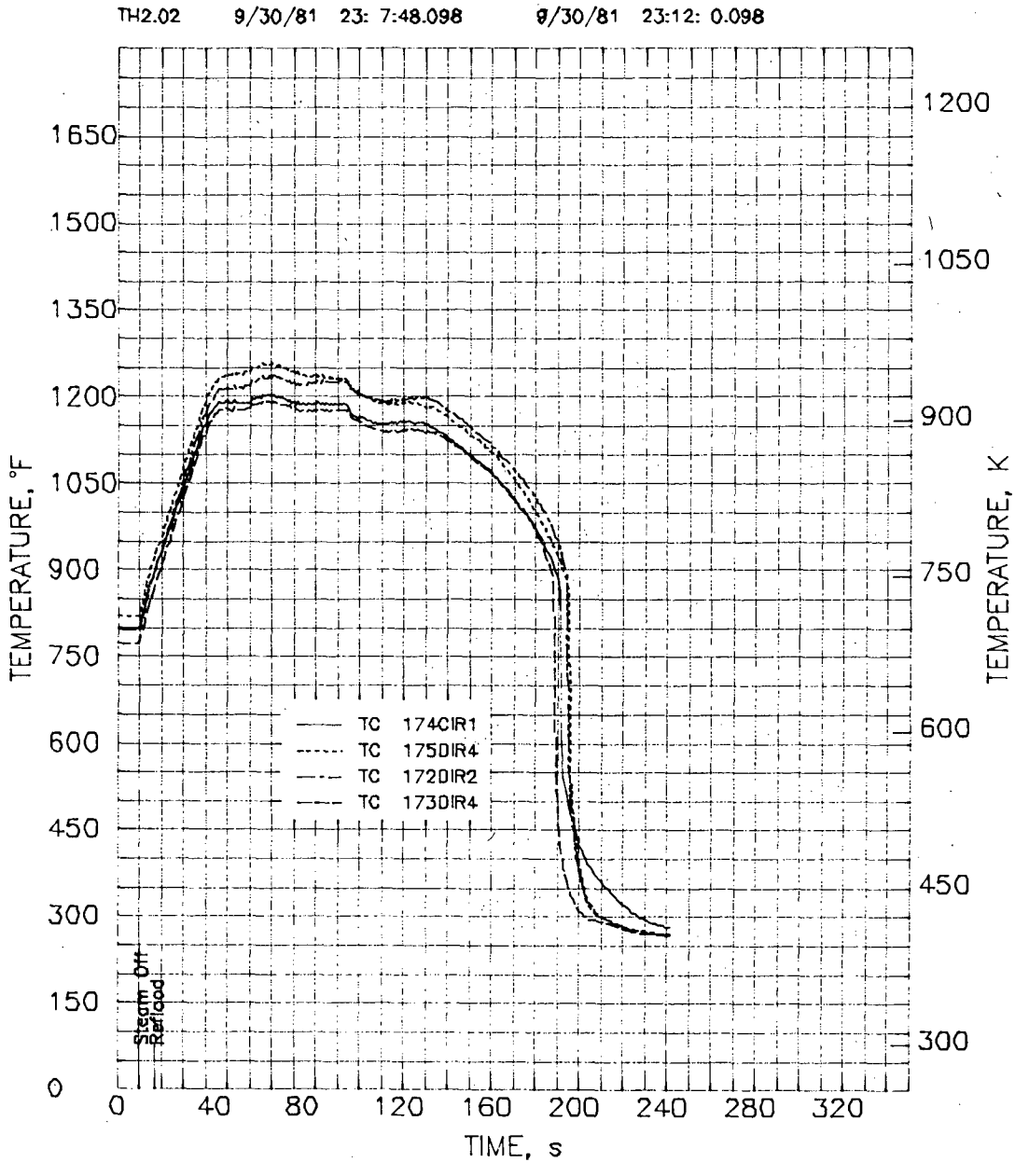

FIGURE C.9. (contd)

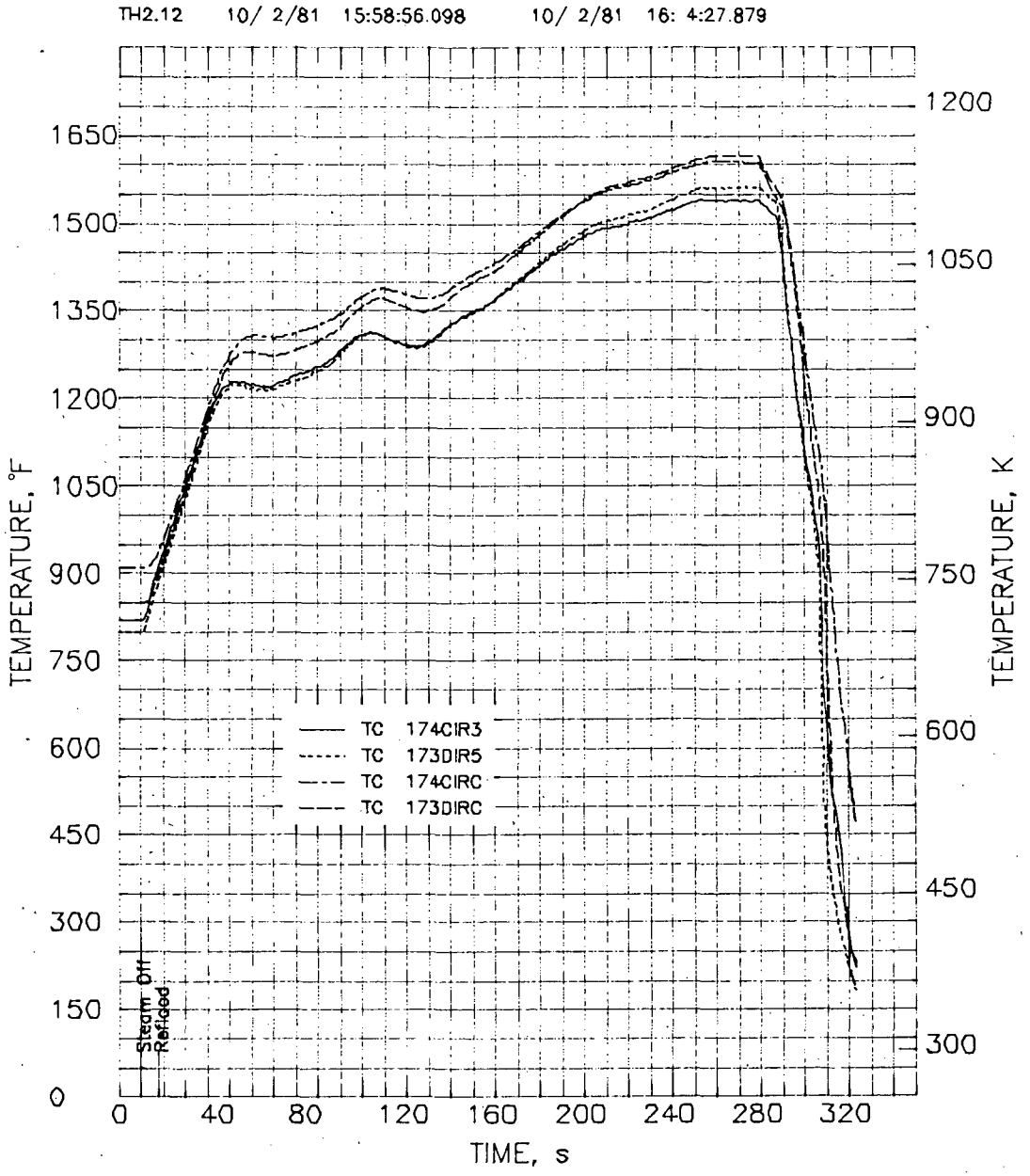

FIGURE C.10. Test Rod Center and Interior Cladding Temperature Histories at Level 17 During Transient for TH-2.12

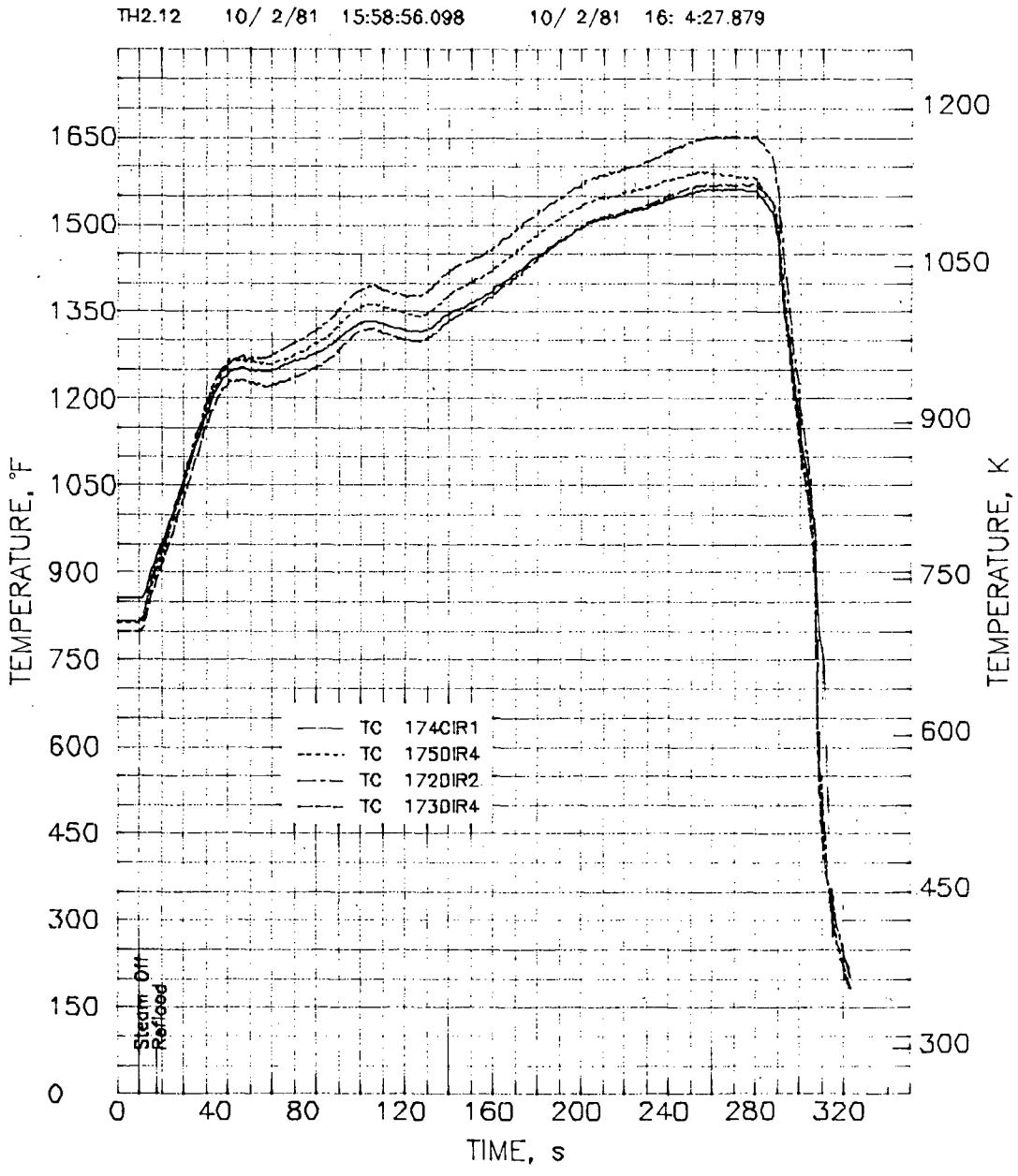

FIGURE C.10. (contd)

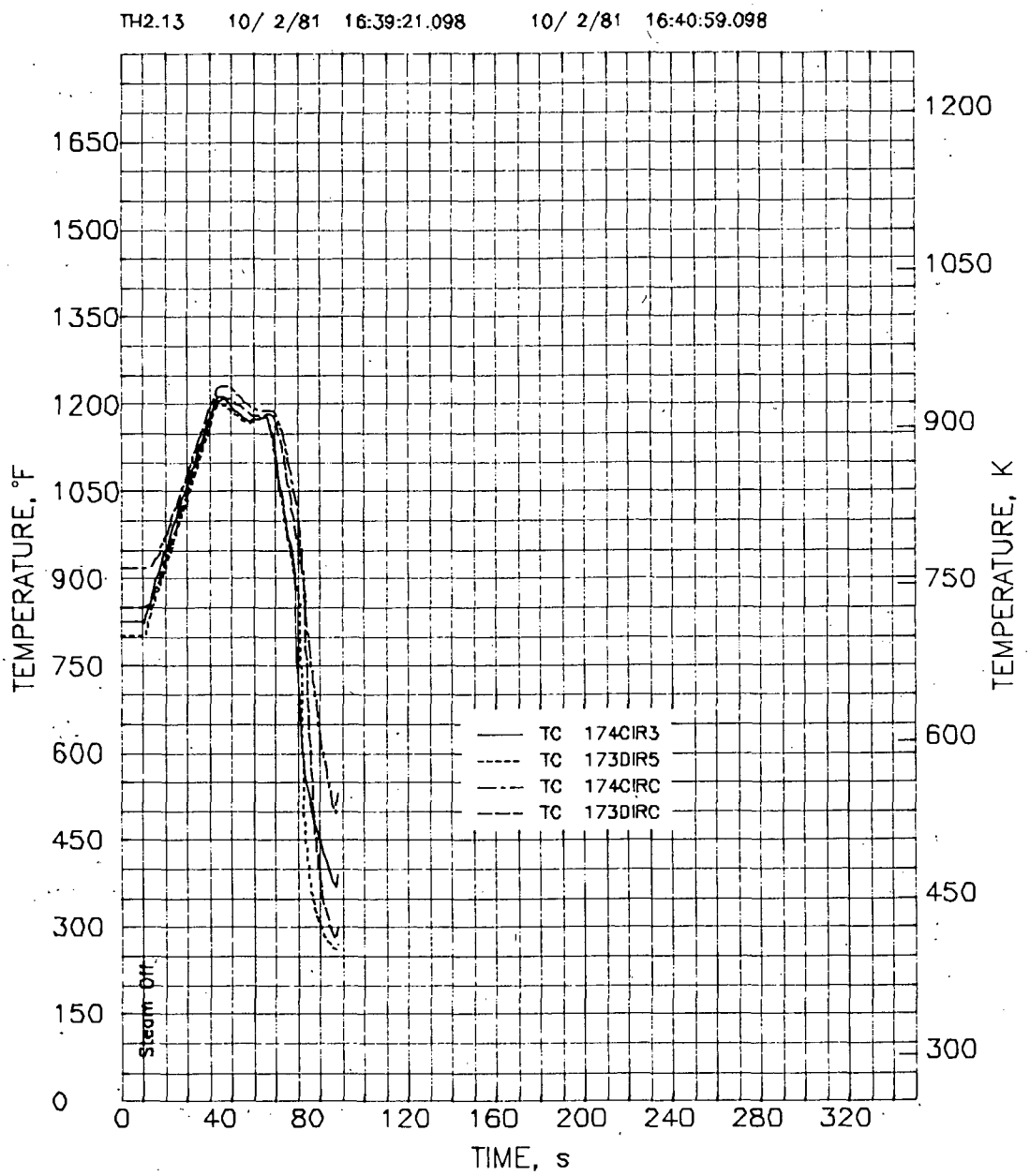

FIGURE C.11. Test Rod Center and Interior Cladding Temperature Histories at Level 17 During Transient for TH-2.13

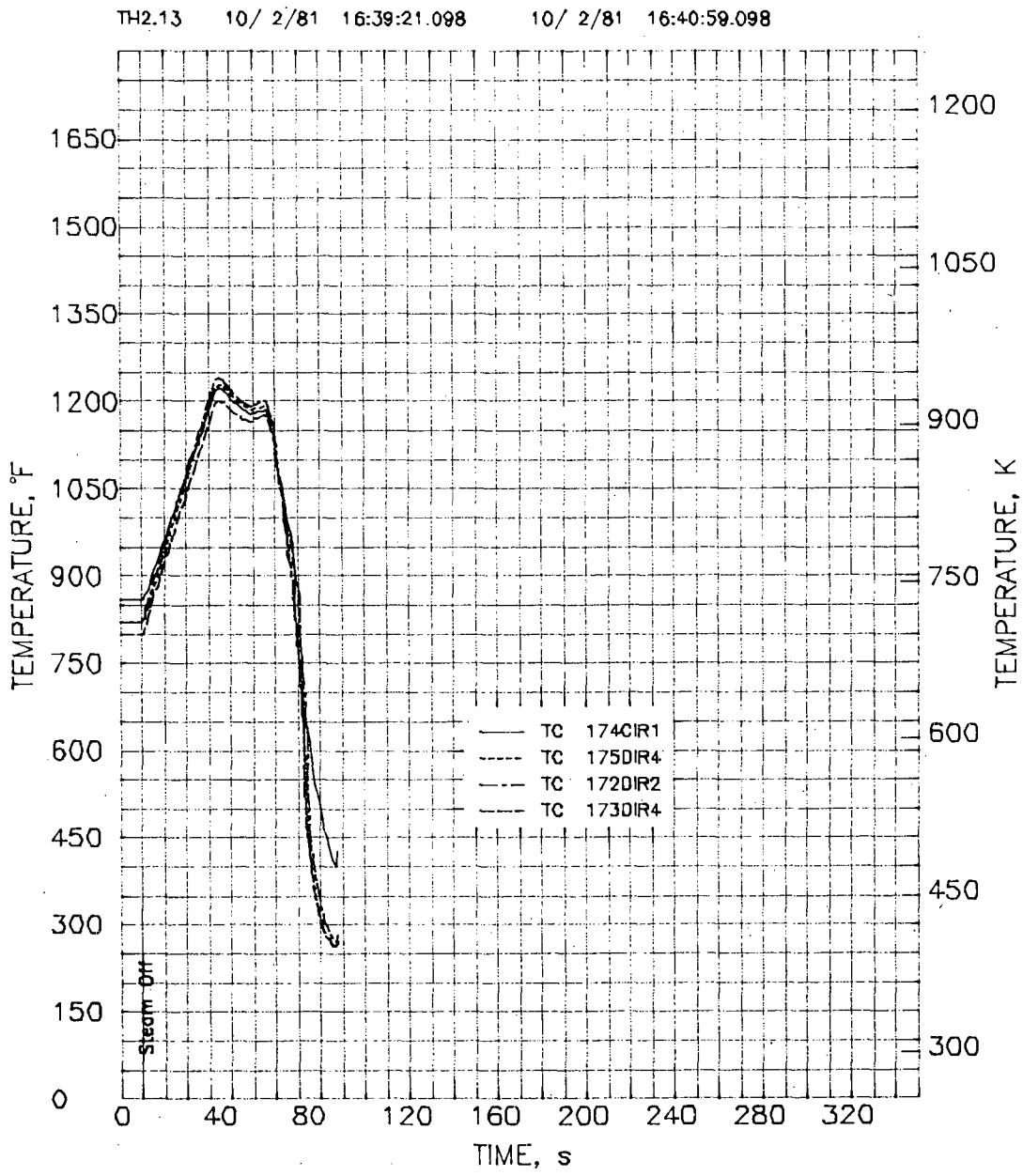

FIGURE C.11. (contd)

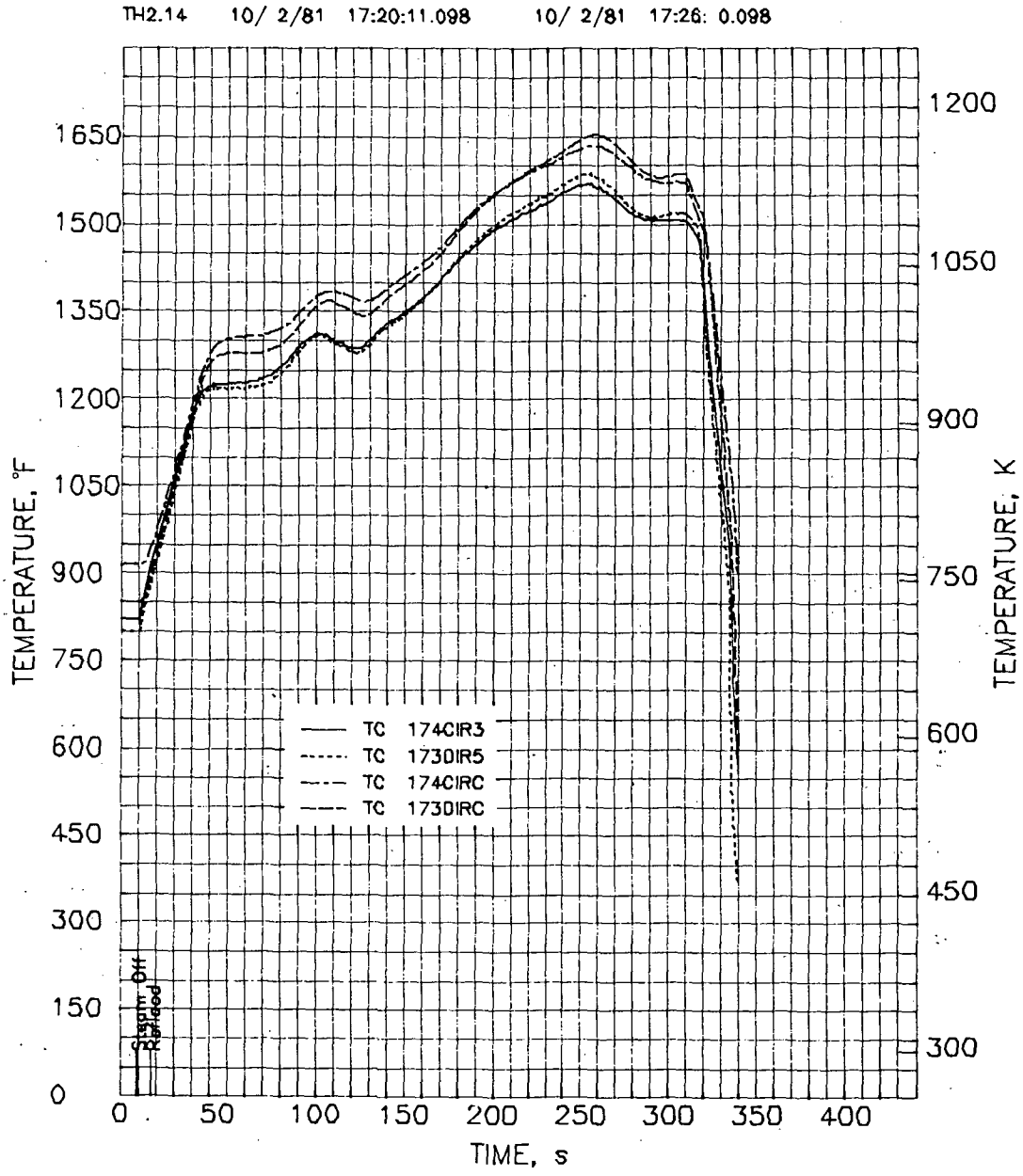

FIGURE C.12. Test Rod Center and Interior Cladding Temperature Histories at Level 17 During Transient for TH-2.14

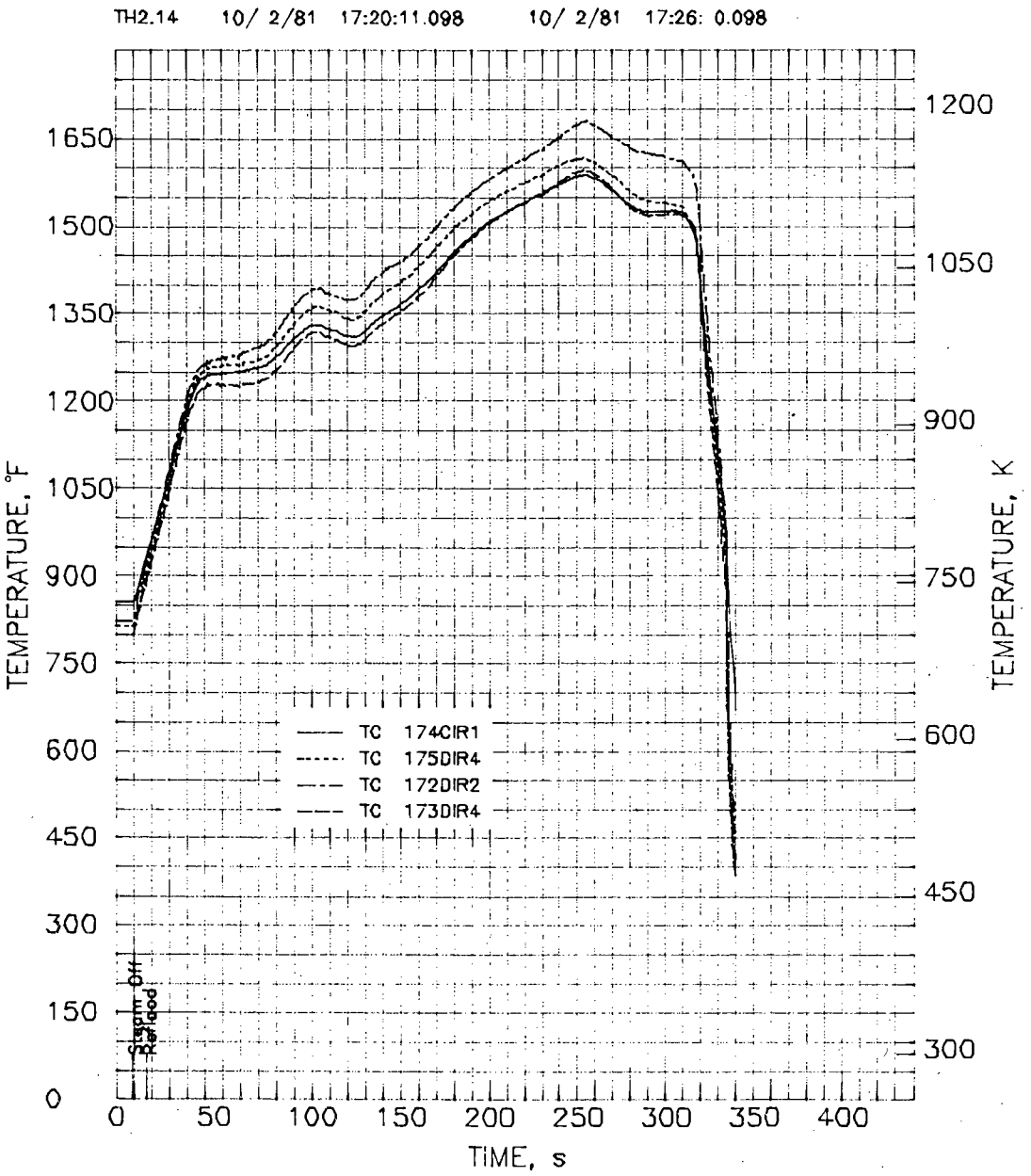

FIGURE C.12. (contd)

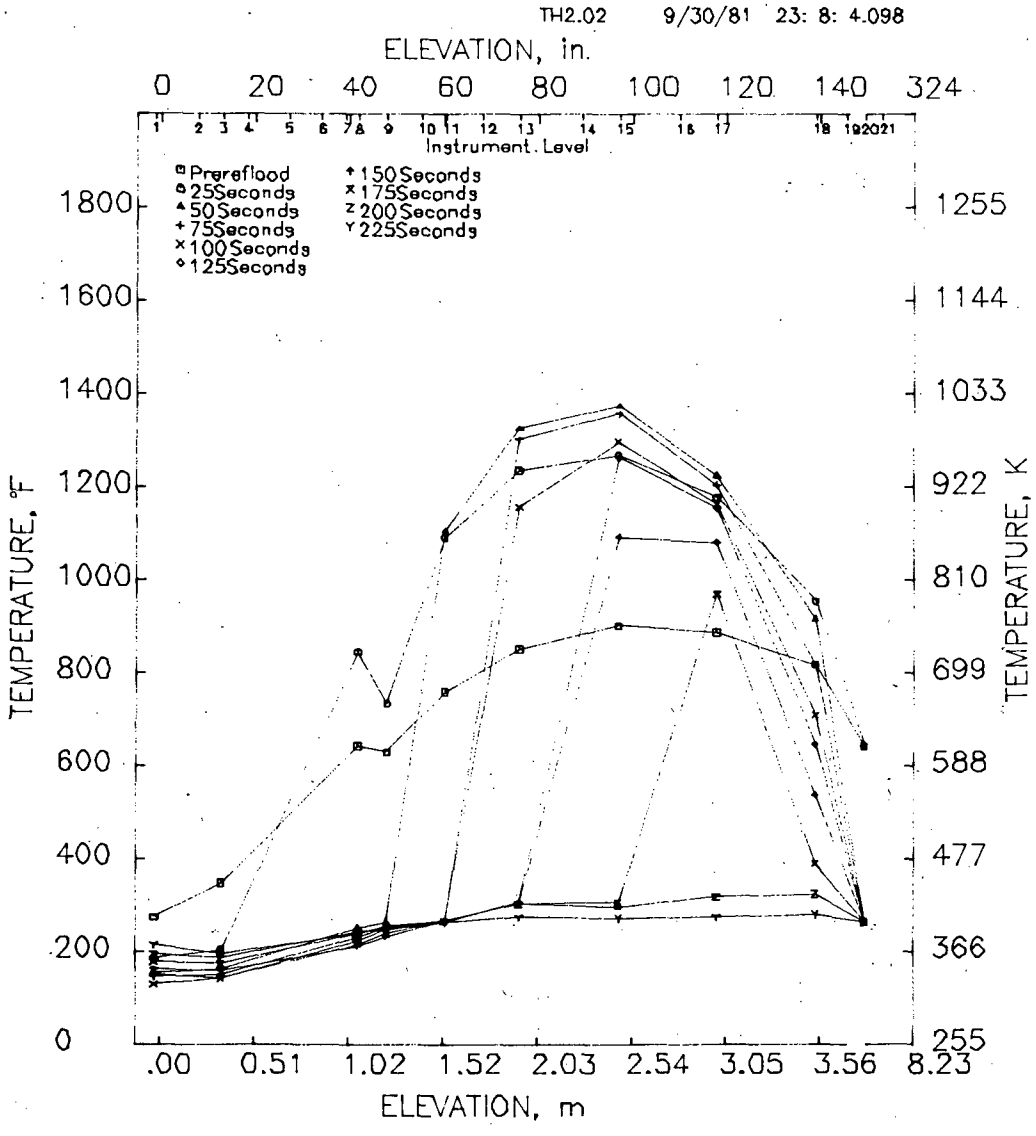

FIGURE C.13. Shroud and Test Train Temperature Profiles During Reflood at 25-s Intervals During Transient for TH-2.02

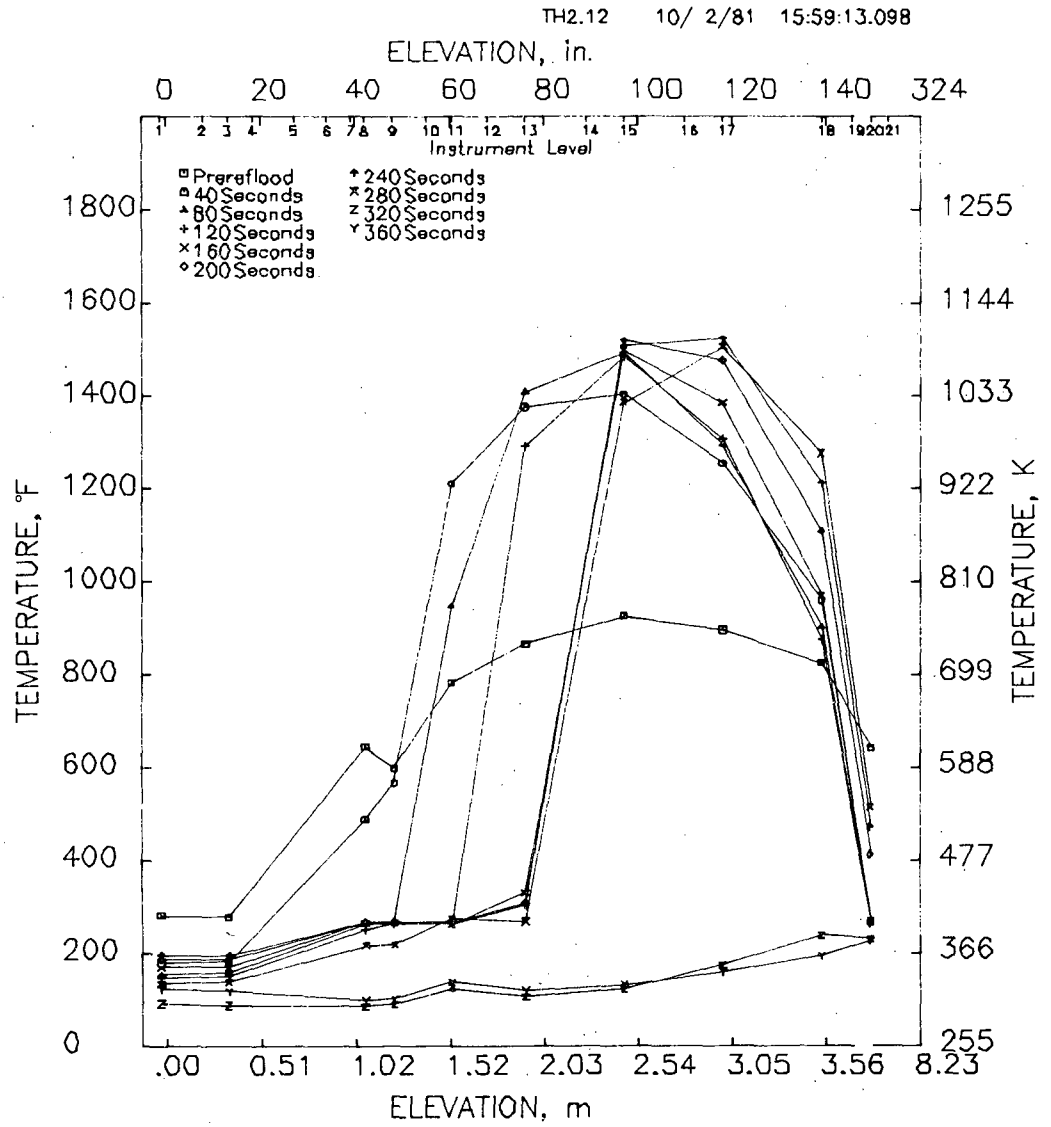

FIGURE C.14. Shroud and Test Train Temperature Profiles During Reflood at 40-s Intervals During Transient for TH-2.12

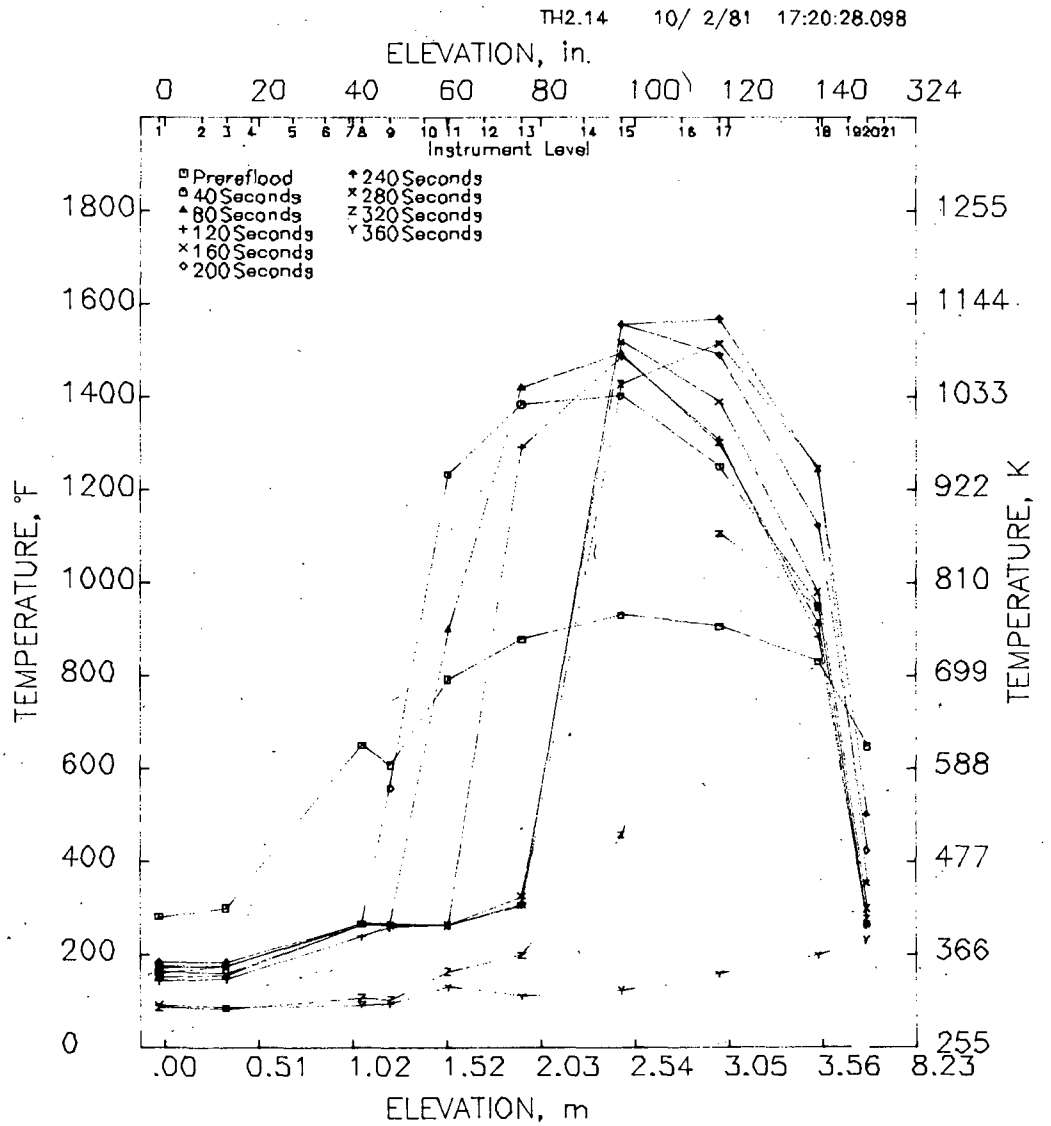

FIGURE C.15. Shroud and Test Train Temperature Profiles During Reflood at 40-s Intervals During Transient for TH-2.14

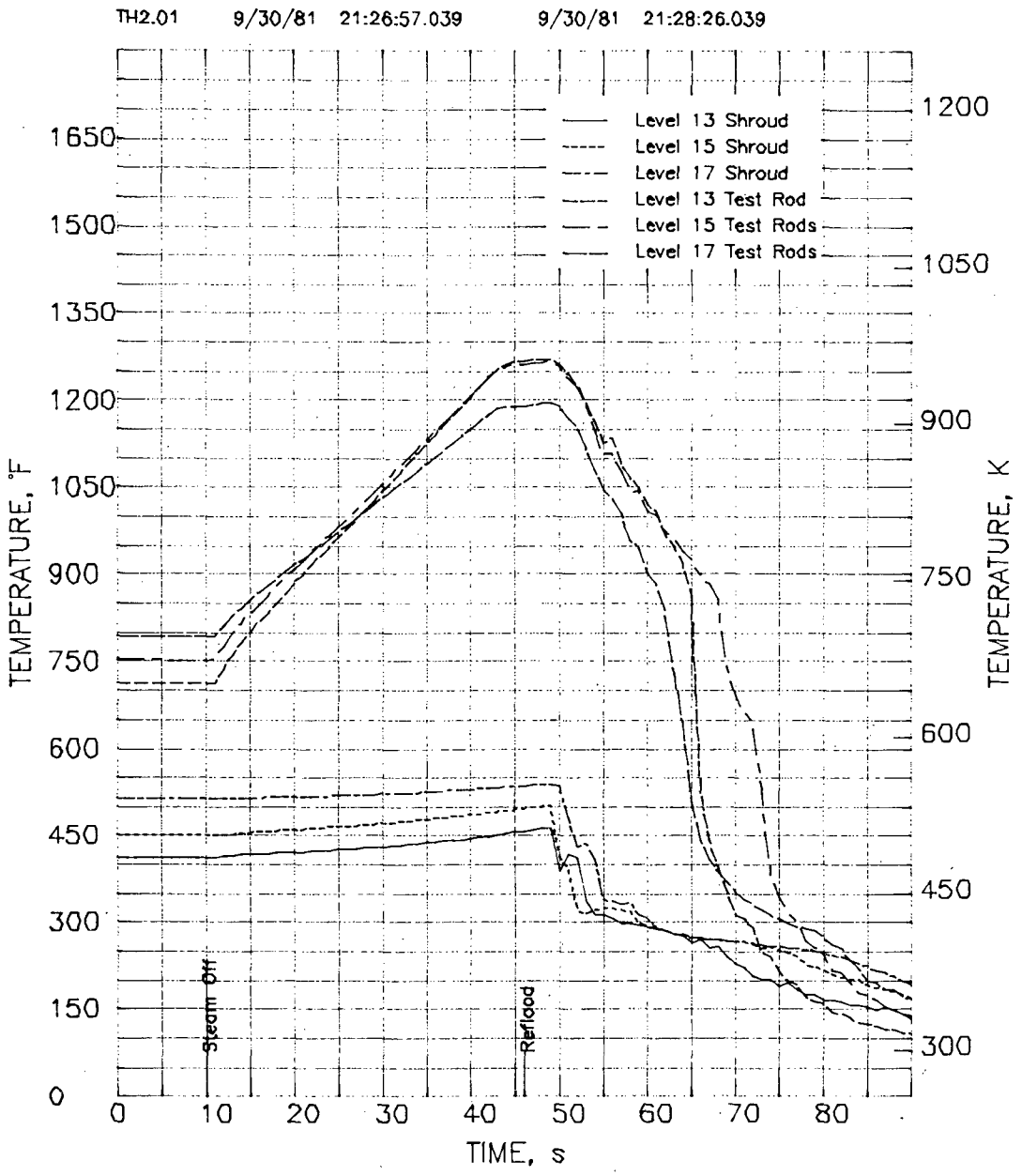

FIGURE C.16. Adiabatic Heatup for TH-2.01

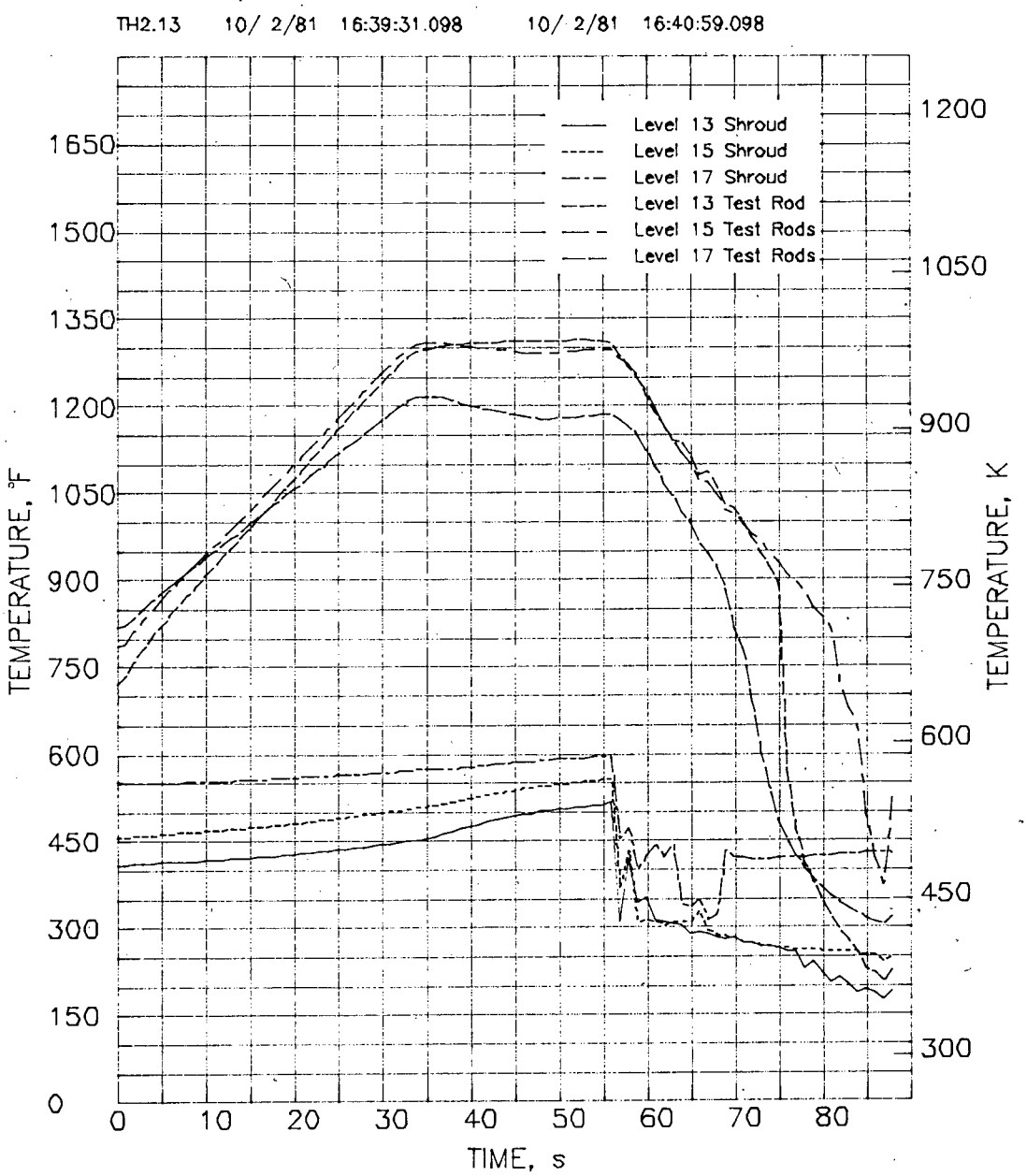

FIGURE C.17. Adiabatic Heatup for TH-2.13

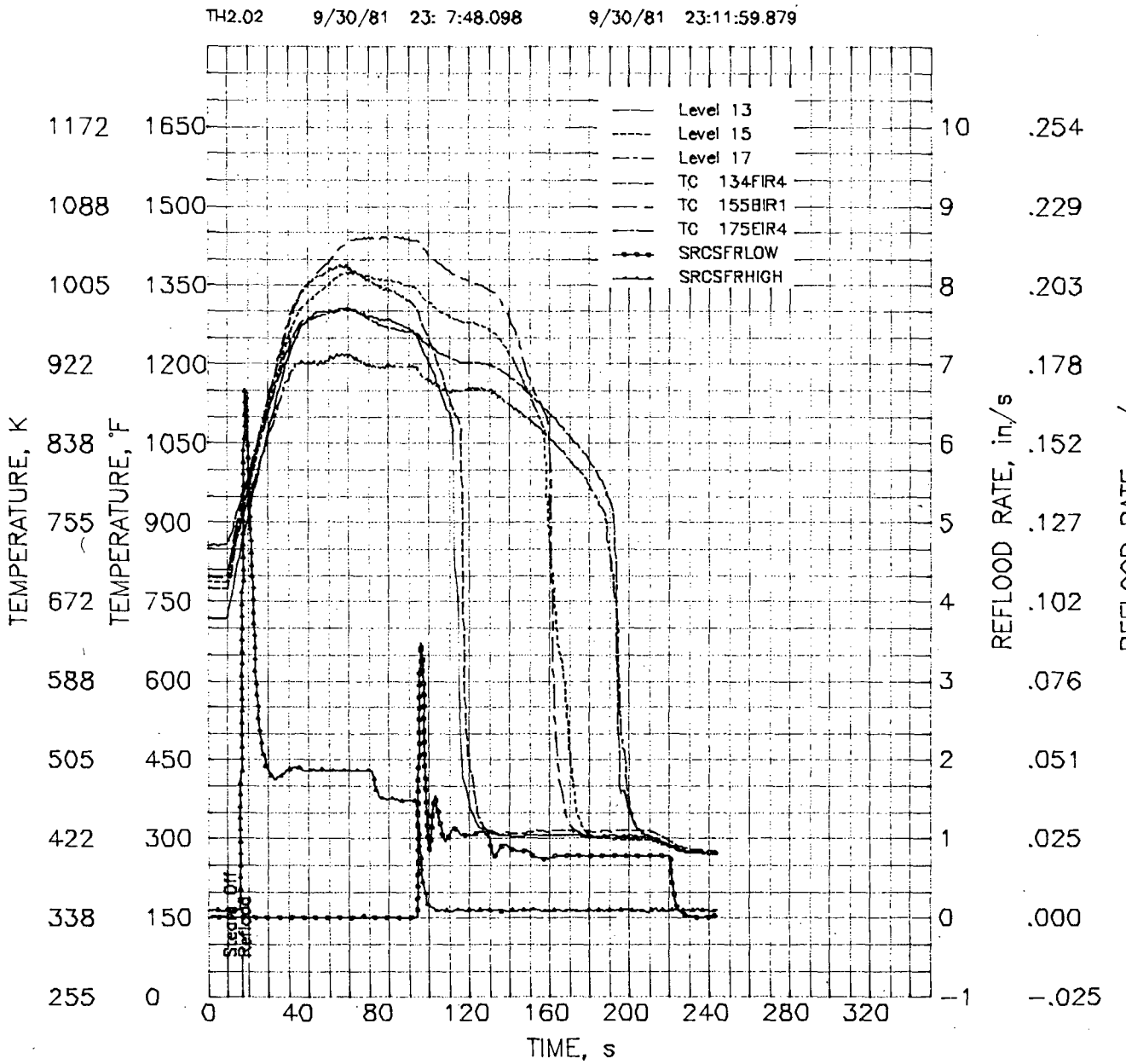

FIGURE C.18. Hot Spot Sensor Averages, Hottest Senors, and Reflood Flow Rates for TH-2.02 Using LCS Preprogrammed Control

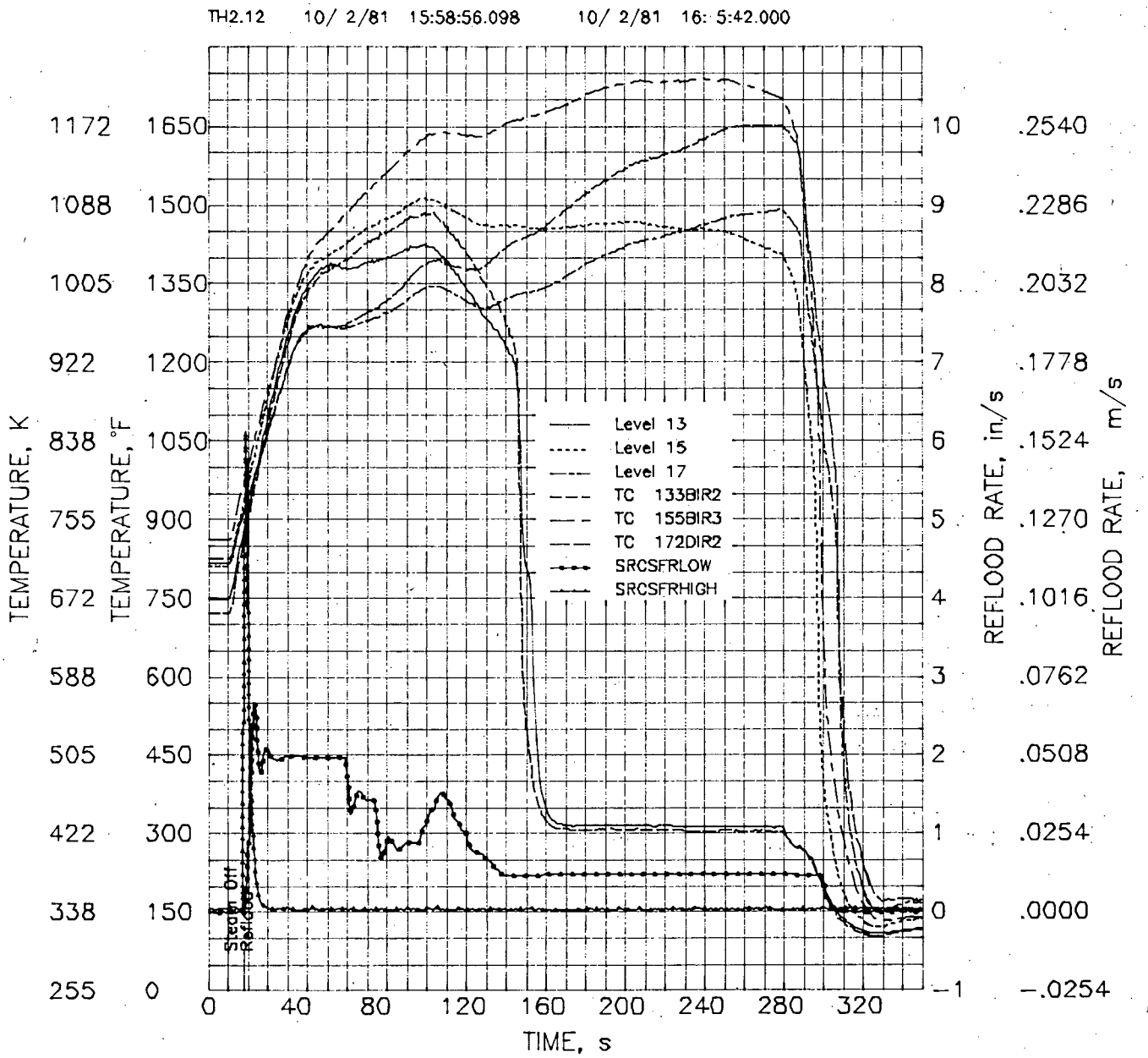

FIGURE C.19. Hot Spot Sensor Averages, Hottest Sensors, and Reflood Flow Rates for TH-2.12 Using DACS Control

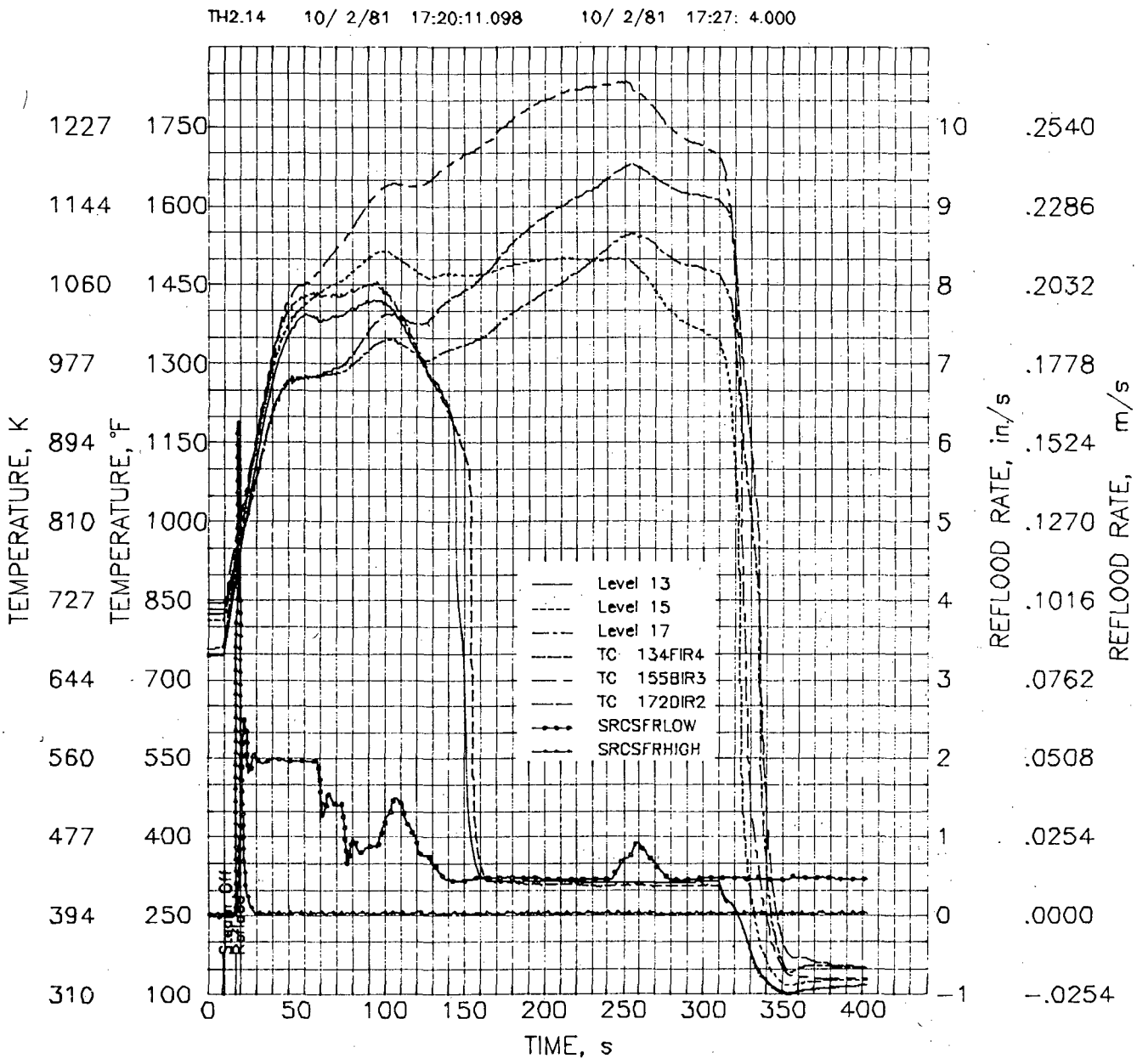

FIGURE C.20. Hot Spot Sensor Averages, Hottest Sensors, and Reflood Flow Rates for TH-2.14 Using DACS Control

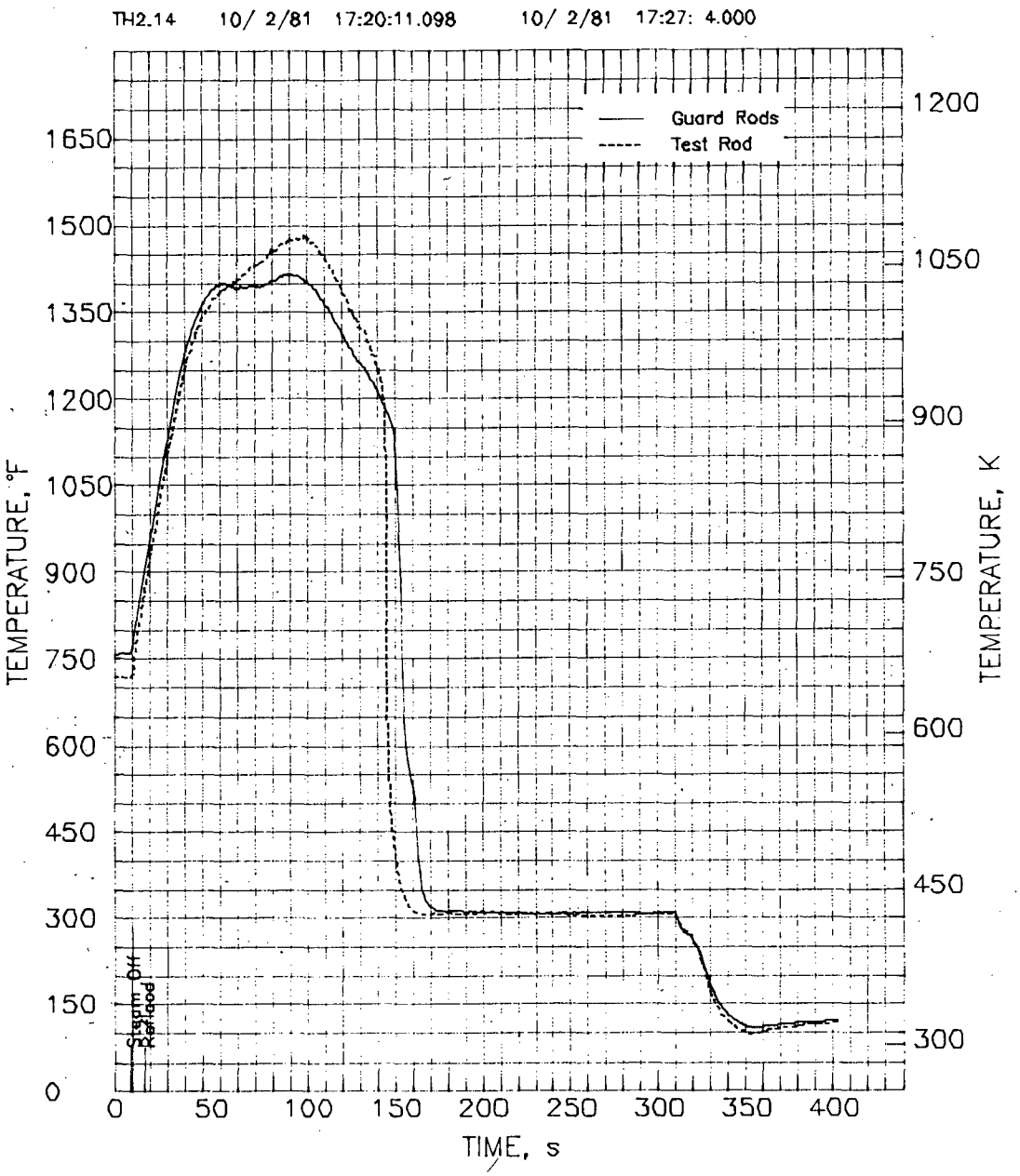

FIGURE C.21. Average Guard and Test Rod Interior Cladding Temperatures at Level 13 for TH-2.14

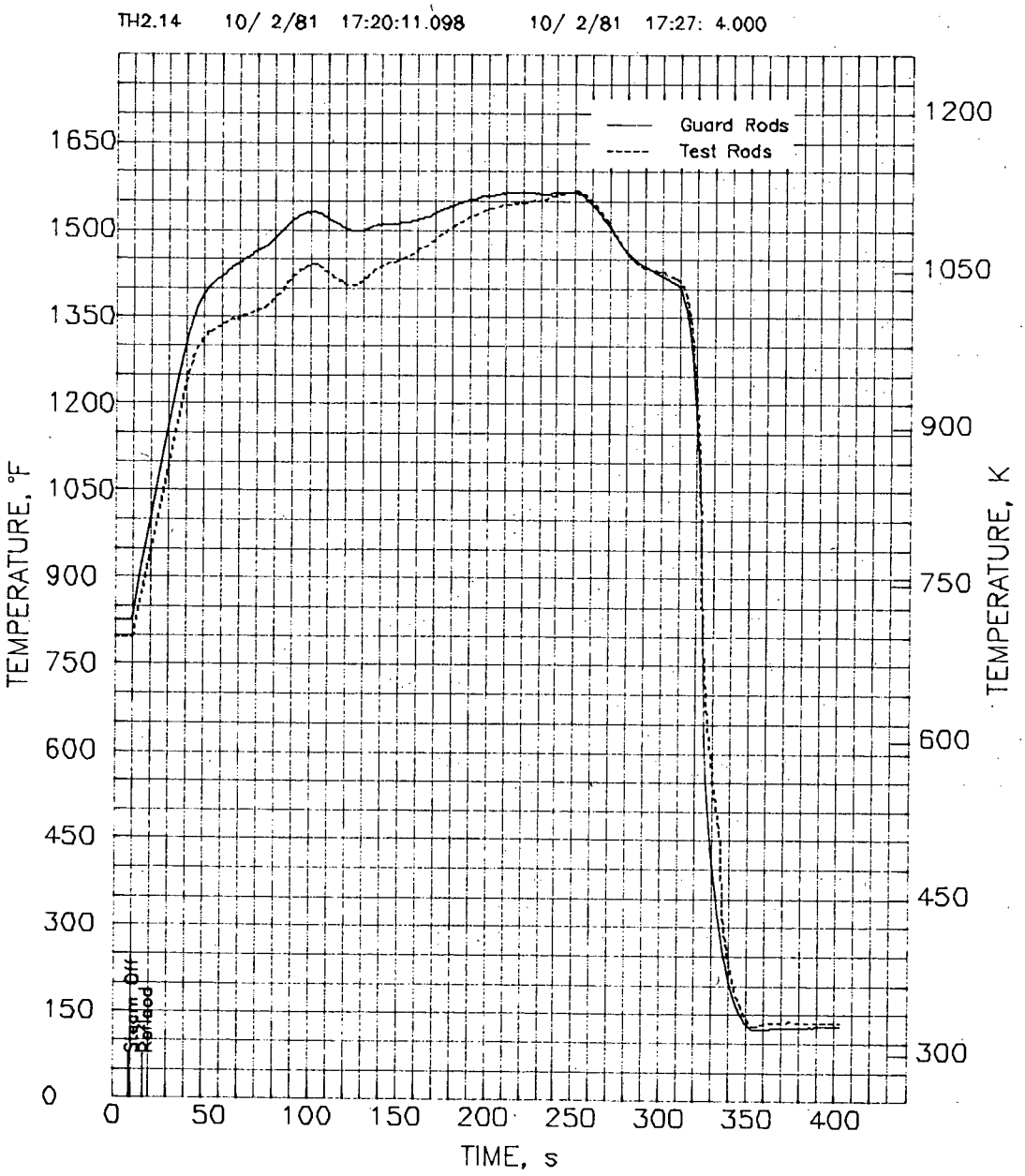

FIGURE C.22. Average Guard and Test Rod Interior Cladding Temperatures at Level 15 for TH-2.14

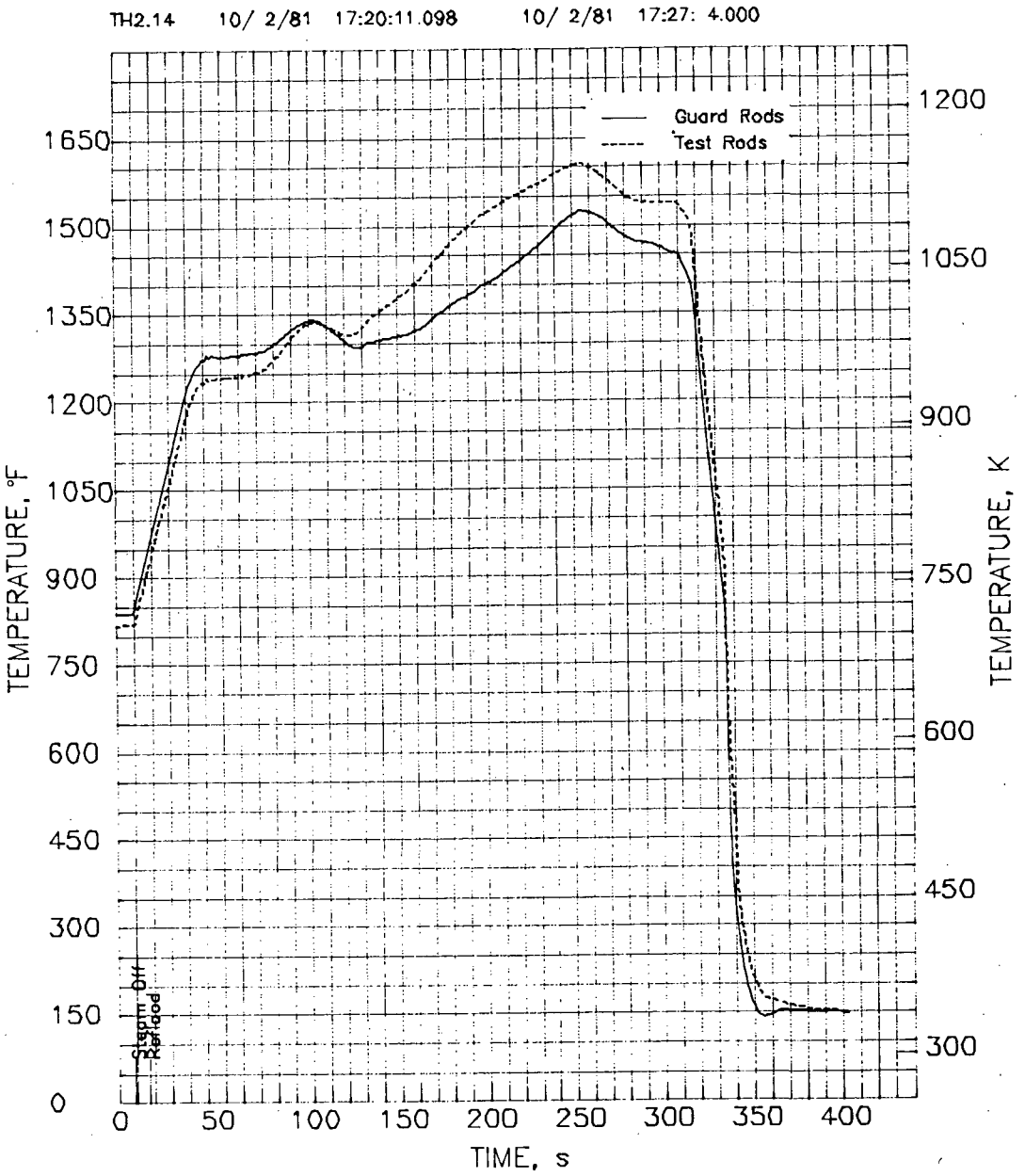

FIGURE C.23. Average Guard and Test Rod Interior Cladding Temperatures at Level 17 for TH-2.14

APPENDIX D

TEST COOLANT AND SHROUD TEMPERATURES

APPENDIX D

TEST COOLANT AND SHROUD TEMPERATURES

It is difficult to measure the temperature of the coolant once reflooding occurs because much of the time the coolant is in two phases: liquid and entrained liquid with steam. Thermocouple (TC) readings of coolant flow are thus a rough indication of the steam and water temperature with the additional effects of the response time and the in situ environment. Test assembly inlet, outlet, and steam probe TCs at Levels 12, 14, and 16 are shown in Figures D.1 through D.4

Shroud temperatures at Levels 10, 13, 15, and 17 are shown in Figures D.5 through D.20. The shroud temperature should be known to insure that the shroud does not overheat; if it did, it could warp and thereby delay removal of the test assembly from the test site.

Shroud temperatures tended to be lower than coolant temperatures, which may be an indication that the heat was transferred radially outward, allowing the shroud TCs to quench before the coolant TCs. There may be a tendency for upper level shroud and coolant TCs to be hotter, which might be caused by less quenching by entrained liquid at the higher levels.

The remainder of this appendix consists of the following graphical data:

Figure D.1. Temperature Histories for Inlet TCs (Level 1), Outlet TCs (Level 20), and Steam Probe TCs at Levels 12, 14, and 16 During Transient for TH-2.02

Figure D.2. Temperature Histories for Inlet TCs (Level 1), Outlet TCs (Level 20), and Steam Probe TCs at Levels 12, 14, and 16 During Transient for TH-2.12

Figure D.3. Temperature Histories for Inlet TCs (Level 1), Outlet TCs (Level 20), and Steam Probe TCs at Levels 12, 14, and 16 During Transient for TH-2.13

Figure D.4. Temperature Histories for Inlet TCs (Level 1), Outlet TCs (Level 20), and Steam Probe TCs at Levels 12, 14, and 16 During Transient for TH-2.14

Figure D.5. Shroud Temperature Histories at Level 10 During Transient for TH-2.02

Figure D.6. Shroud Temperature Histories at Level 10 During Transient for TH-2.12

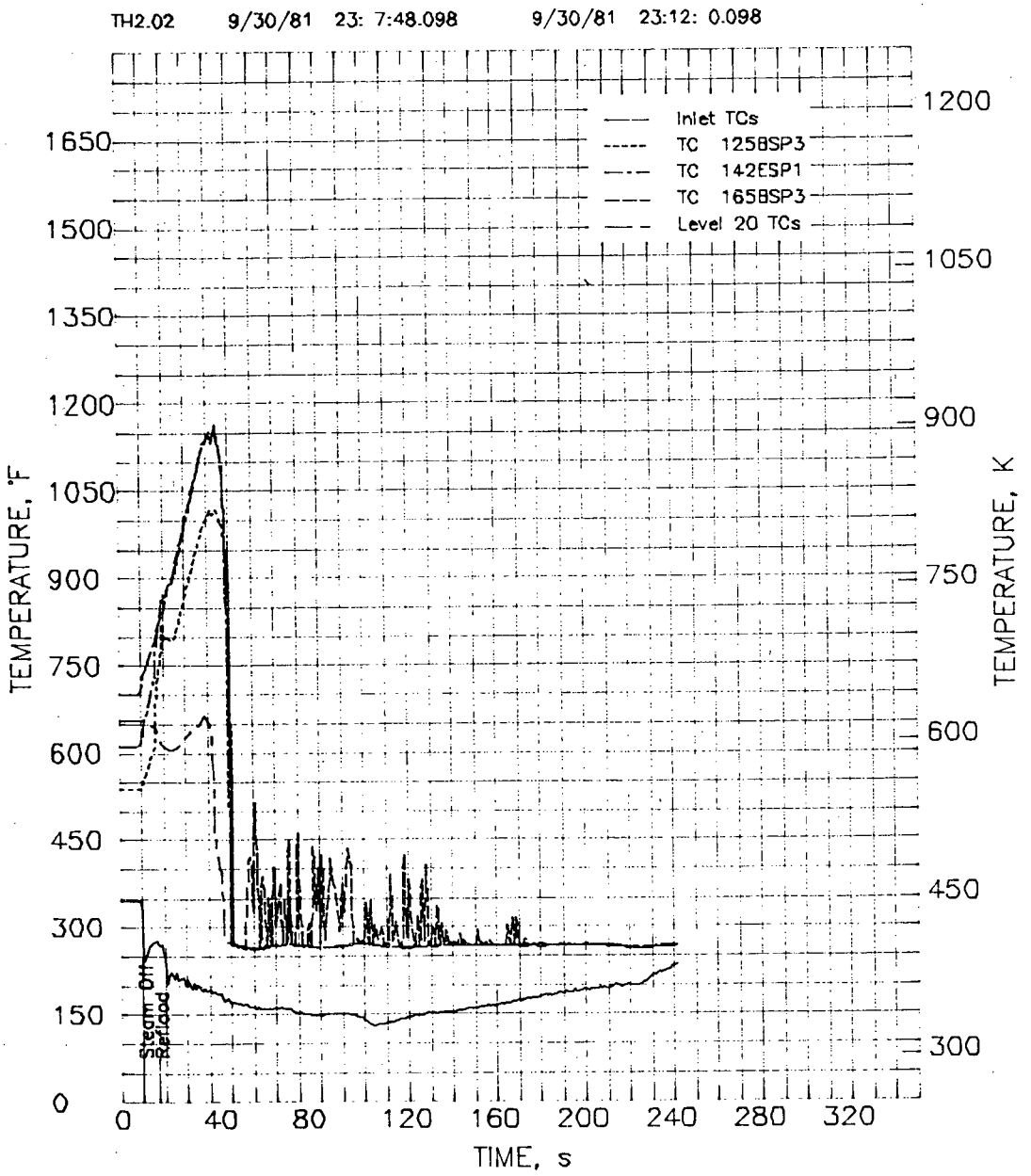

FIGURE D.1. Temperature Histories for Inlet TCs (Level 1), Outlet TCs (Level 20), and Steam Probe TCs at Levels 12, 14, and 16 During Transient for TH-2.02

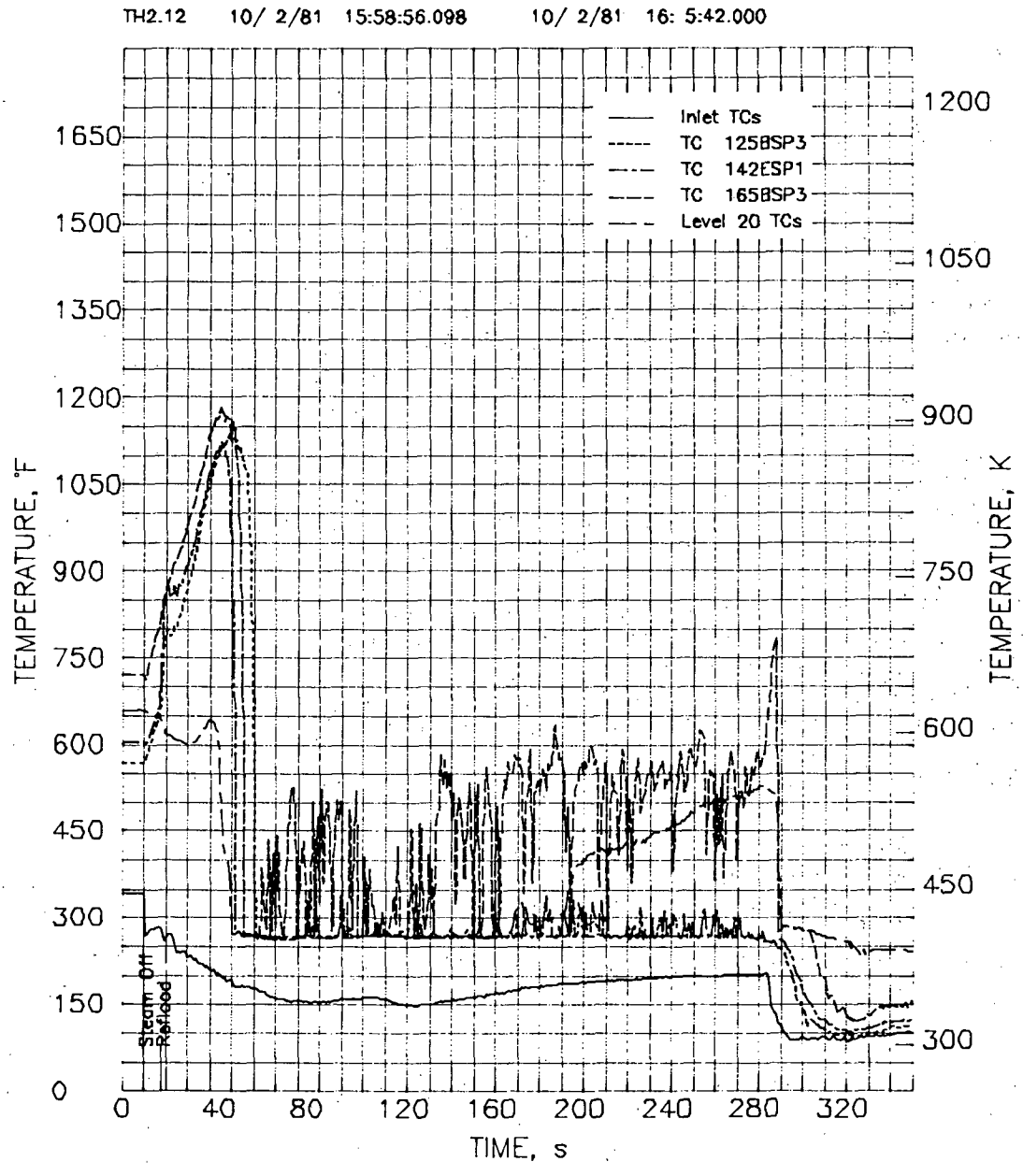

FIGURE D.2. Temperature Histories for Inlet TCs (Level 1), Outlet TCs (Level 20), and Steam Probe TCs at Levels 12, 14, and 16 During Transient for TH-2.12

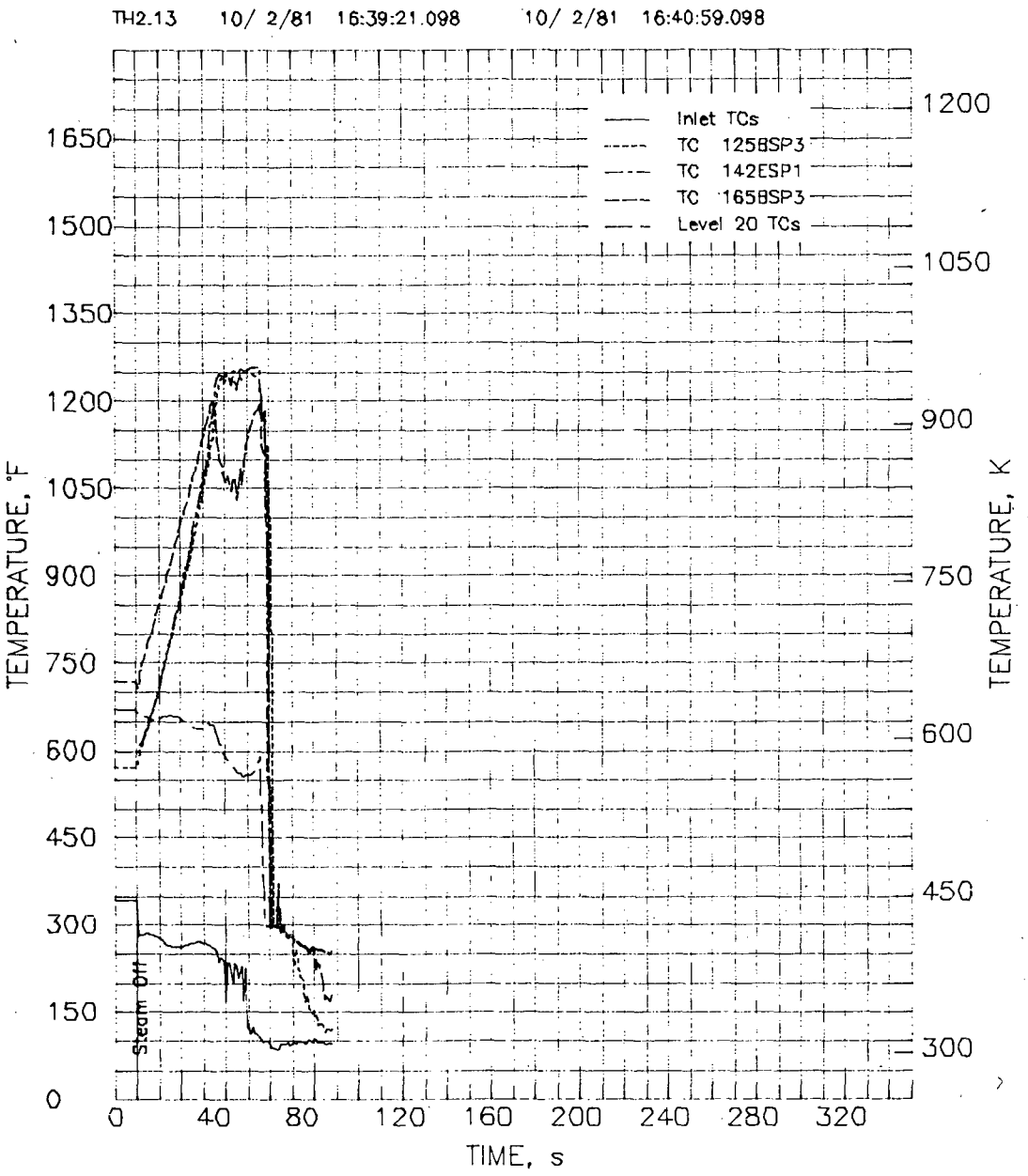

FIGURE D.3. Temperature Histories for Inlet TCs (Level 1), Outlet TCs (Level 20), and Steam Probe TCs at Levels 12, 14, and 16 During Transient for TH-2.13

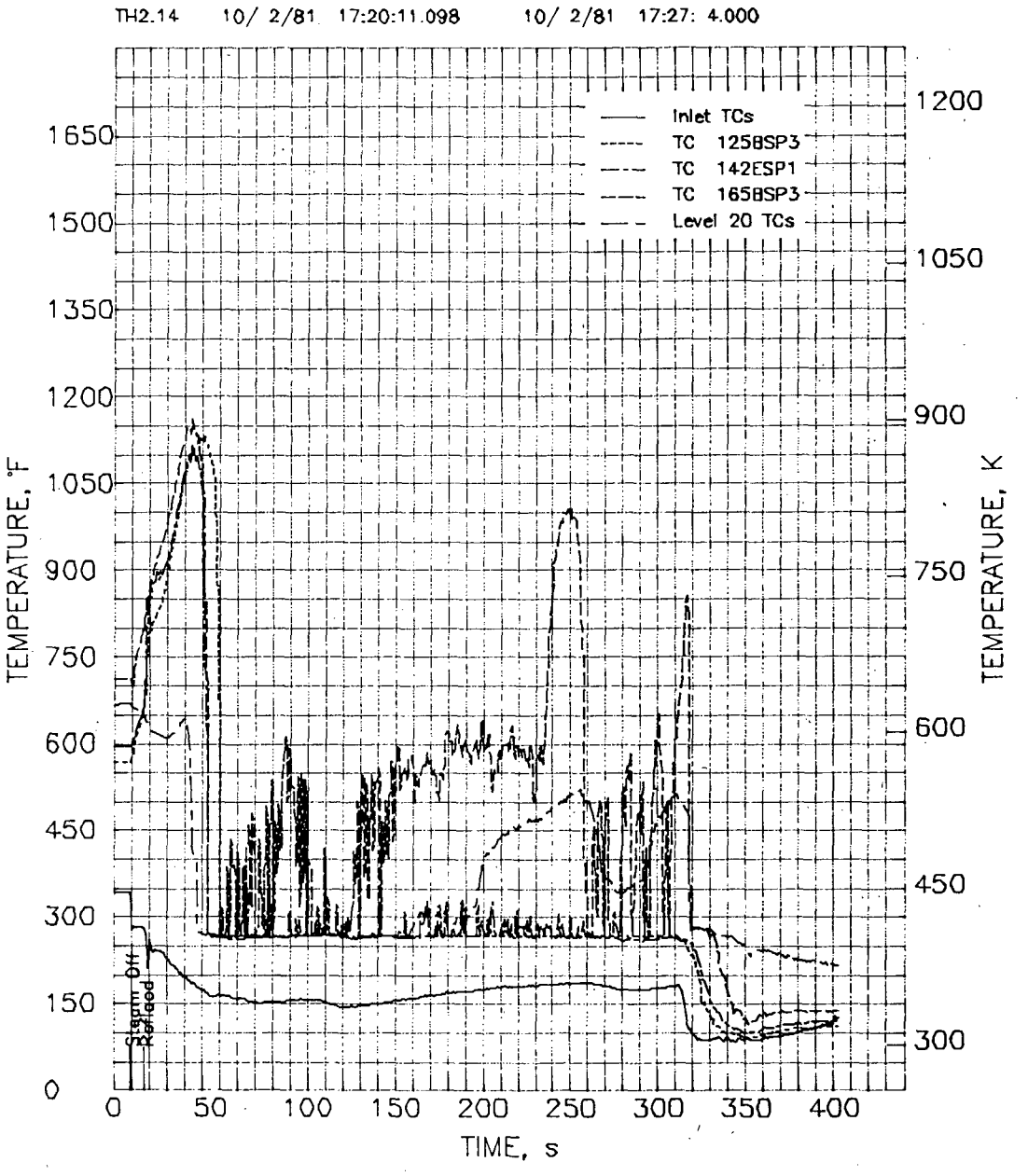

FIGURE D.4. Temperature Histories for Inlet TCs (Level 1), Outlet TCs (Level 20), and Steam Probe TCs at Levels 12, 14, and 16 During Transient for TH-2.14

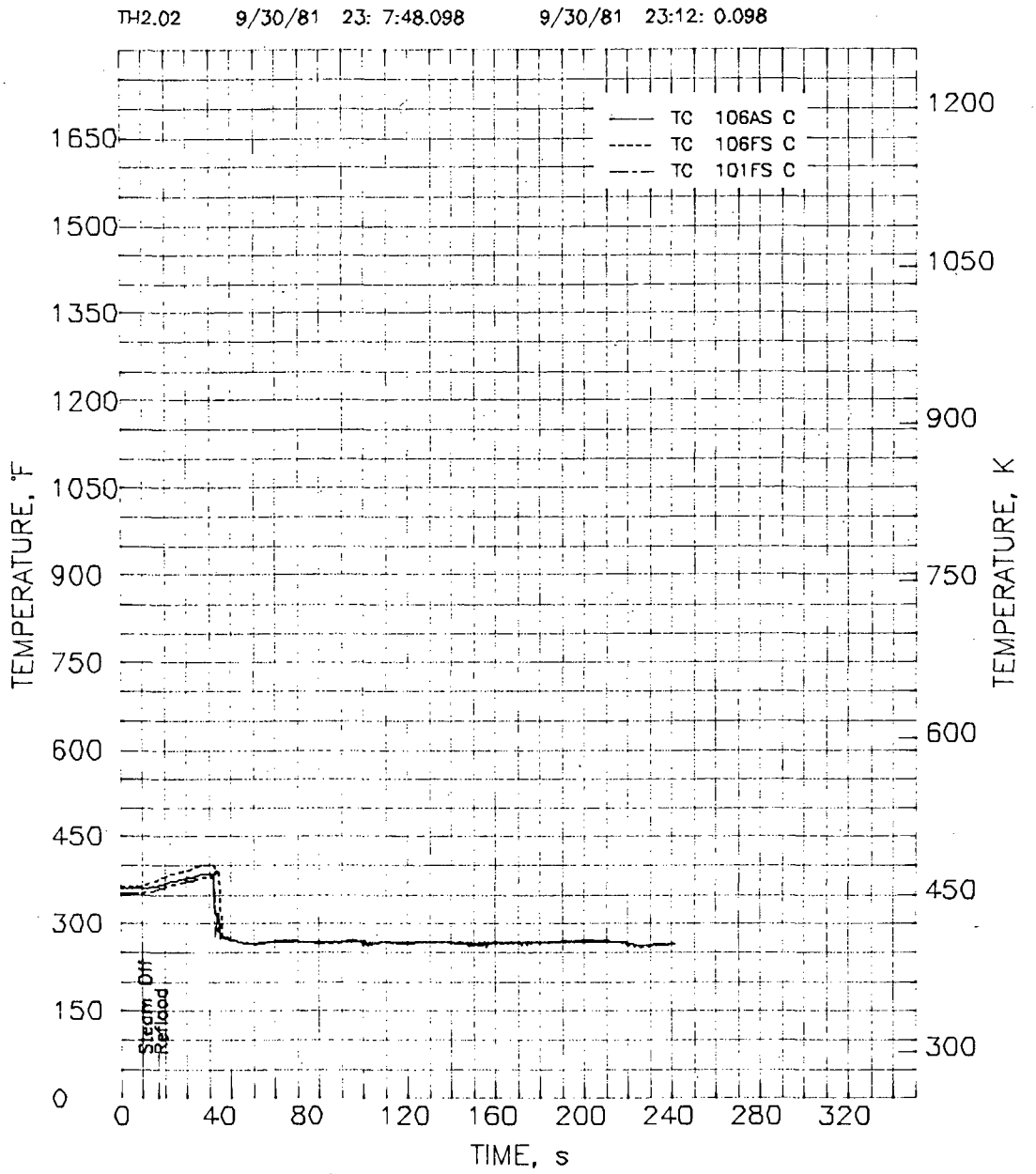

FIGURE D.5. Shroud Temperature Histories at Level 10 During Transient for TH-2.02

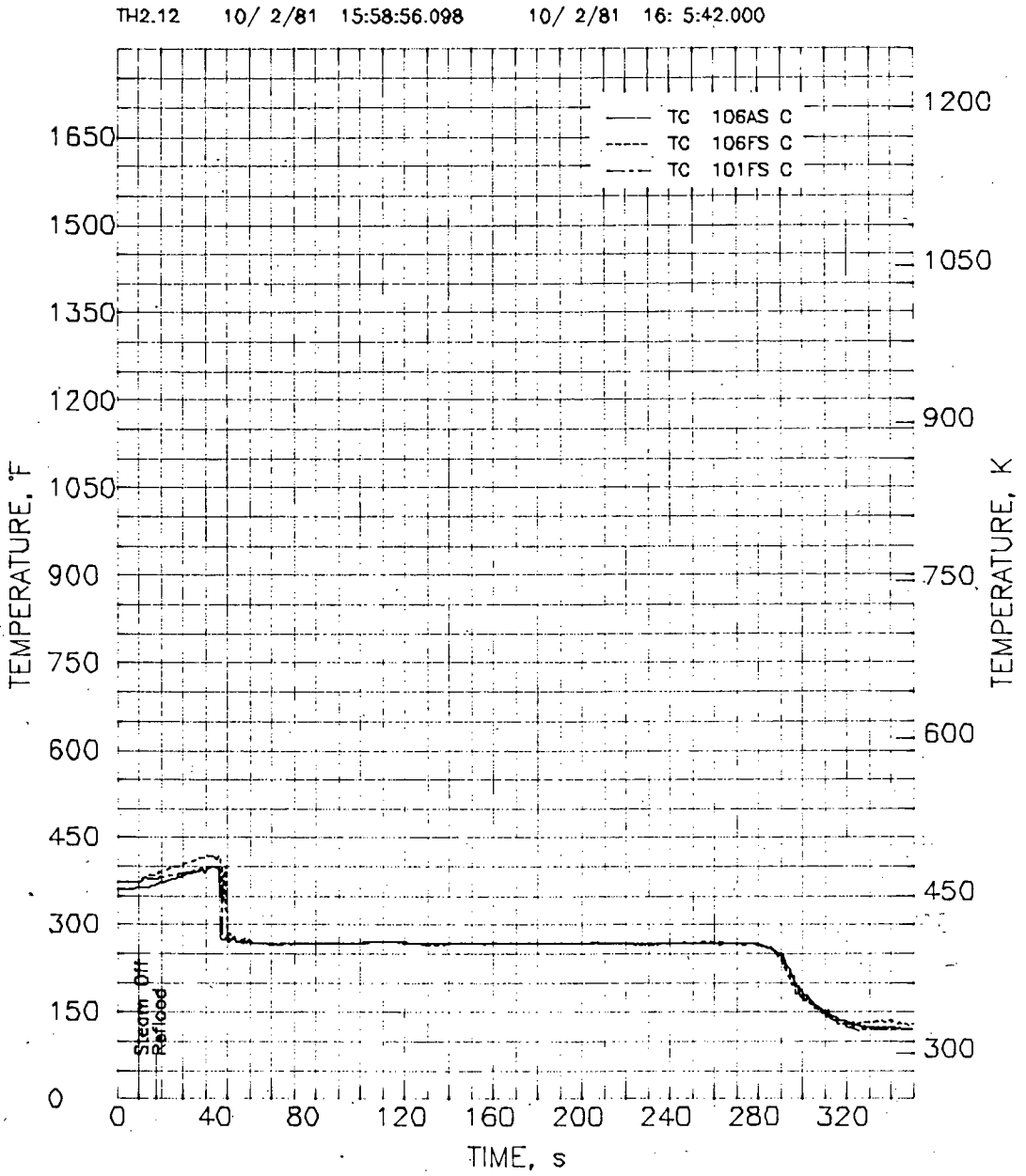

FIGURE D.6. Shroud Temperature Histories at Level 10 During Transient for TH-2.12

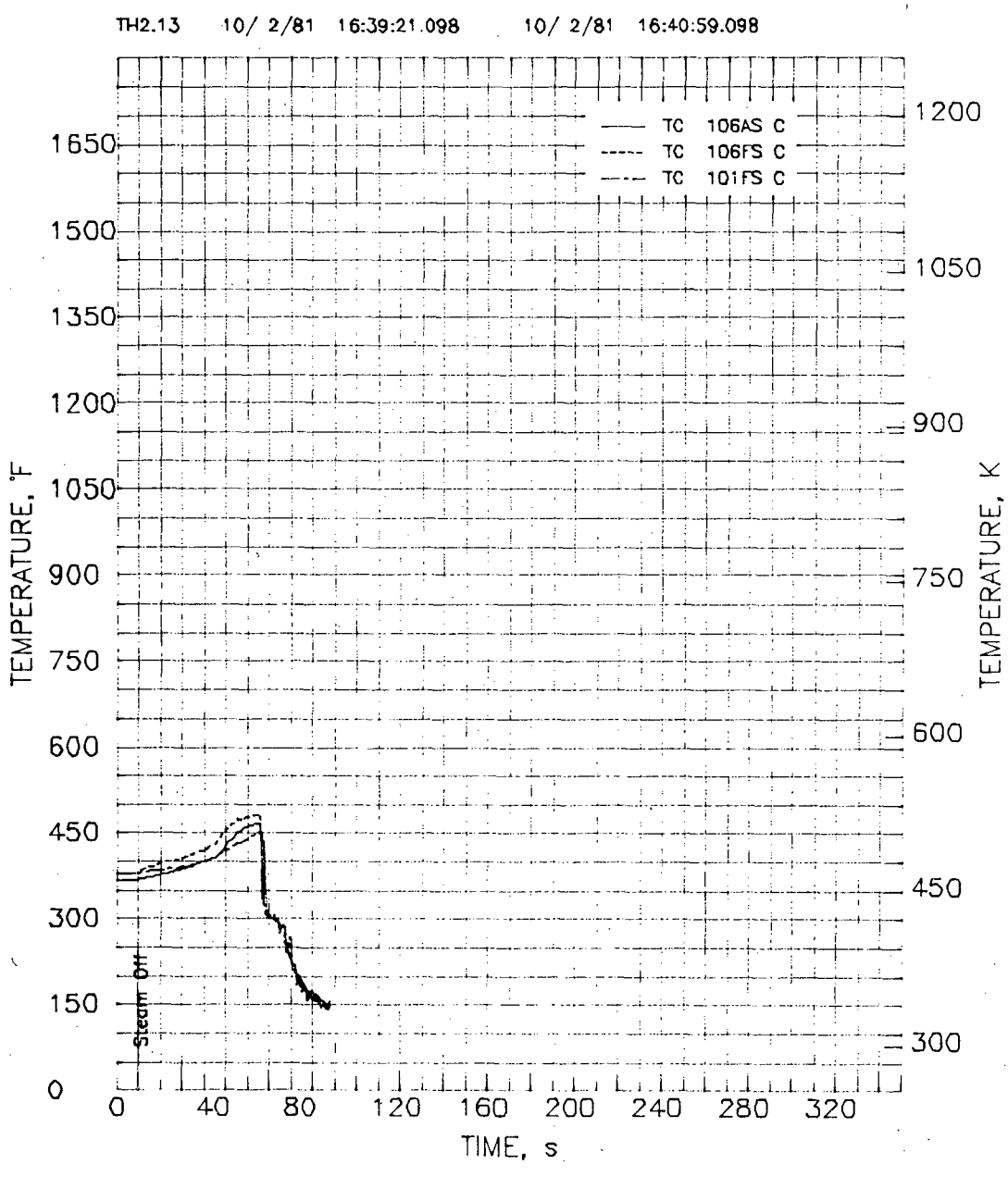

FIGURE D.7. Shroud Temperature Histories at Level 10 During Transient for TH-2.13

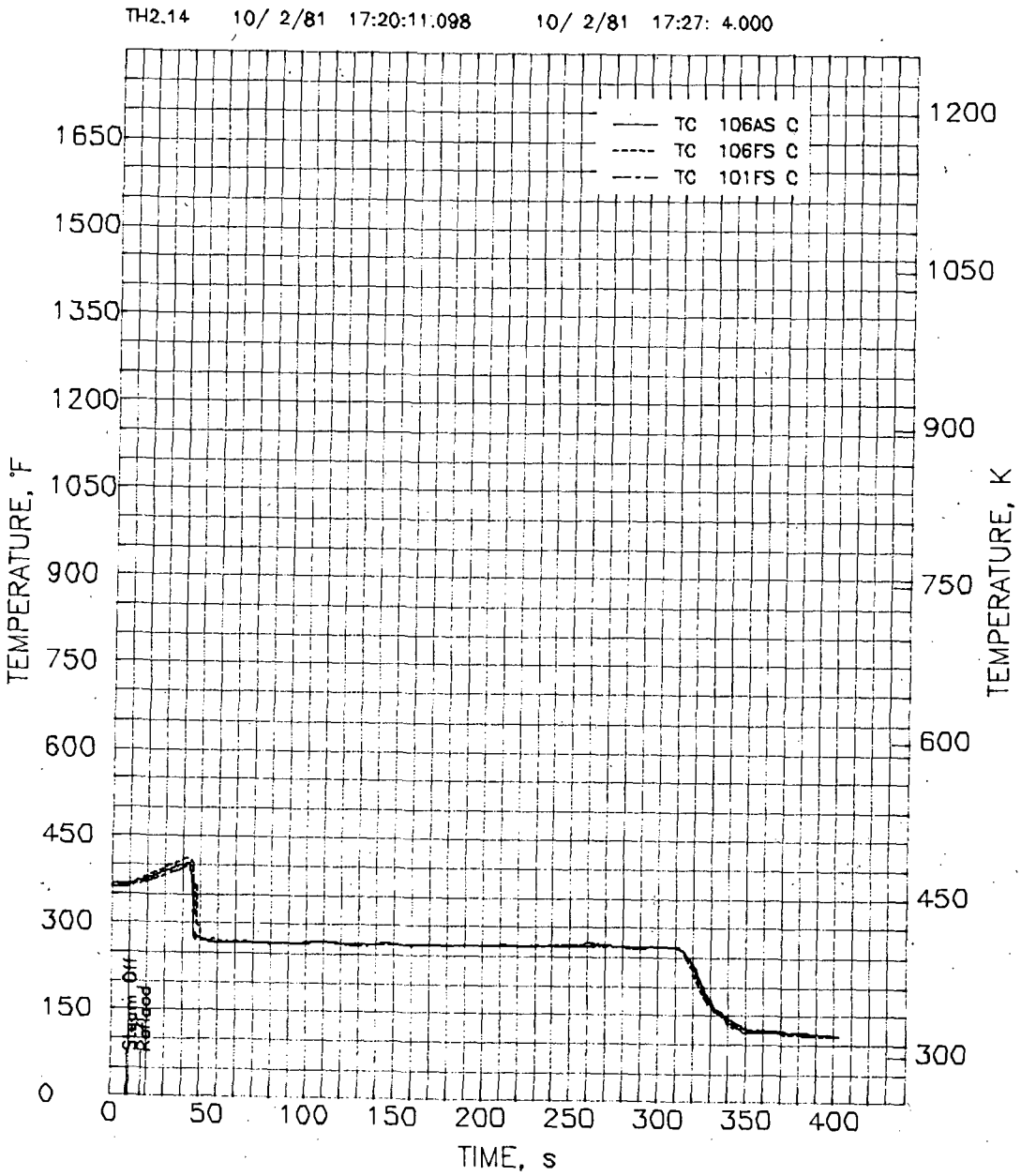

FIGURE D.8. Shroud Temperature Histories at Level 10 During Transient for TH-2.14

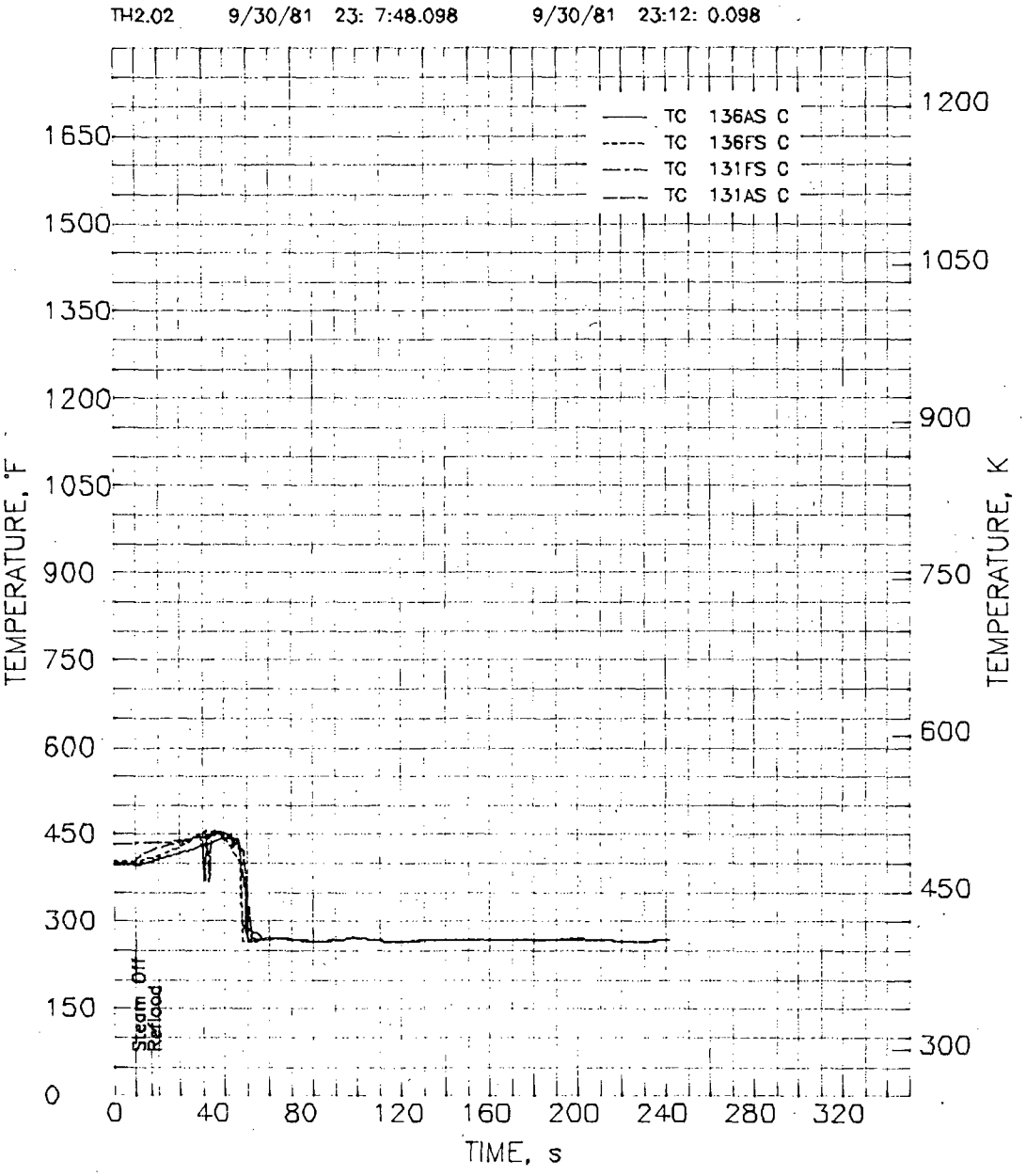

FIGURE D.9. Shroud Temperature Histories at Level 13 During Transient for TH-2.02

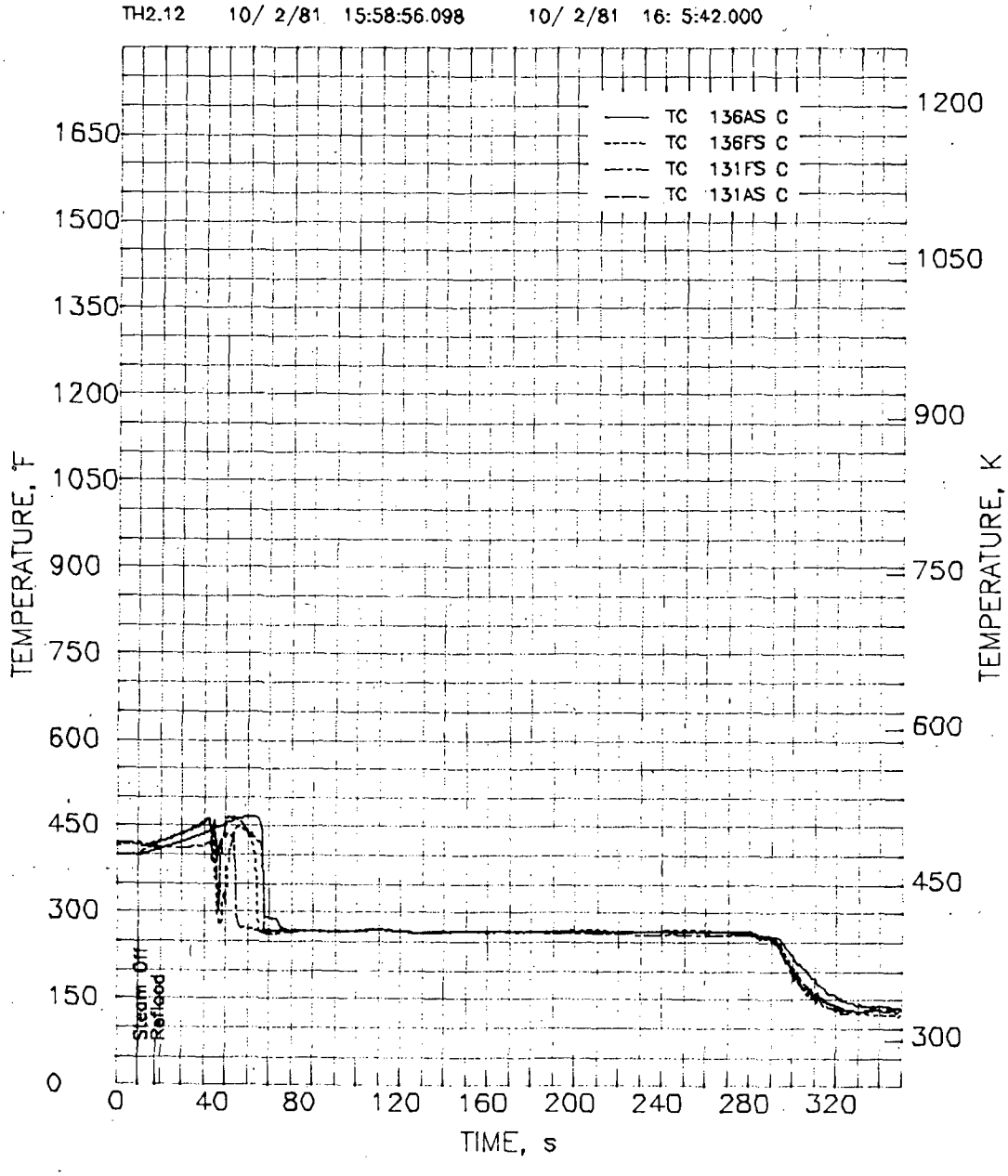

FIGURE D.10. Shroud Temperature Histories at Level 13 During Transient for TH-2.12

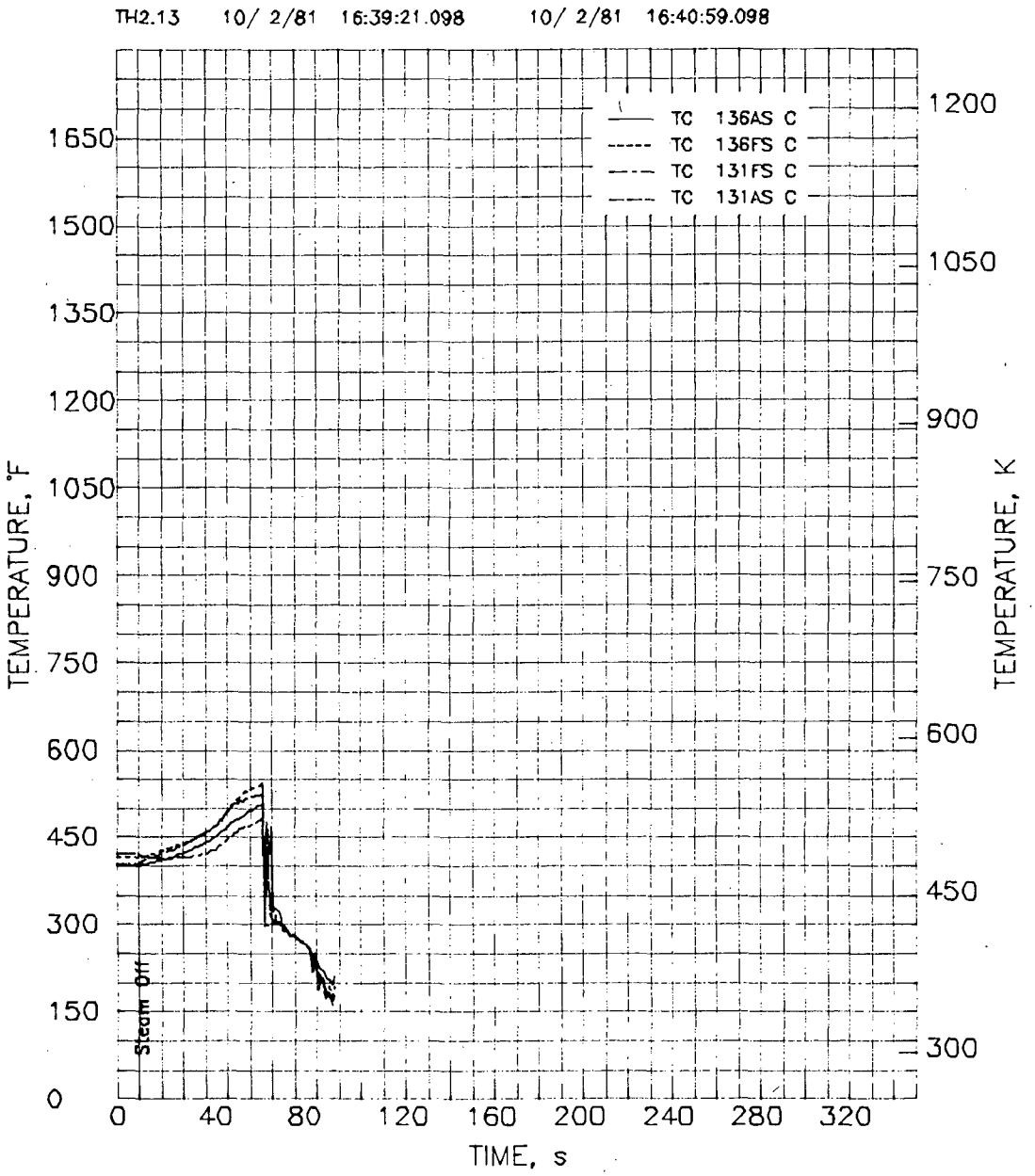

FIGURE D.11. Shroud Temperature Histories at Level 13 During Transient for TH-2.13

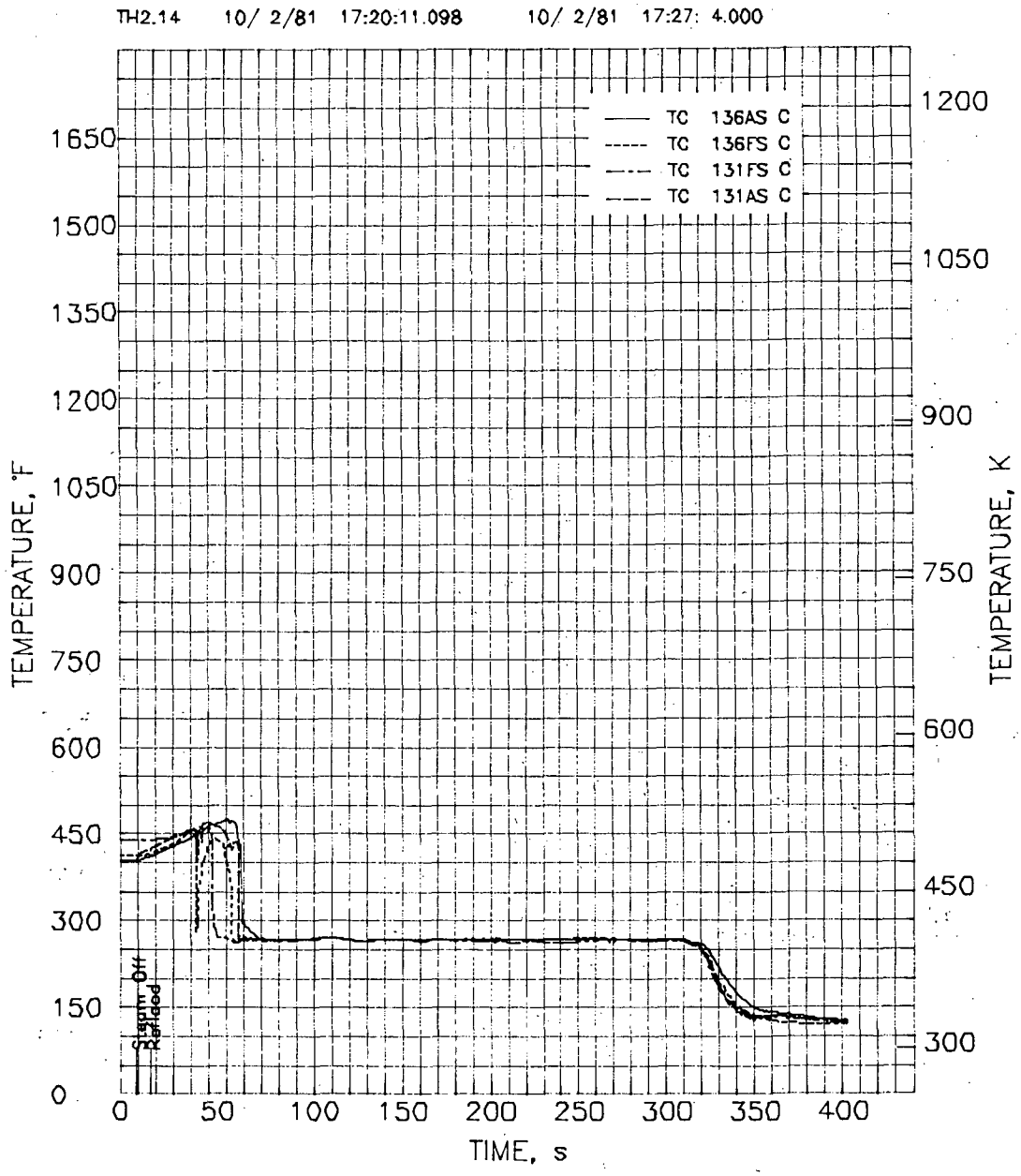

FIGURE D.12. Shroud Temperature Histories at Level 13 During Transient for TH-2.14

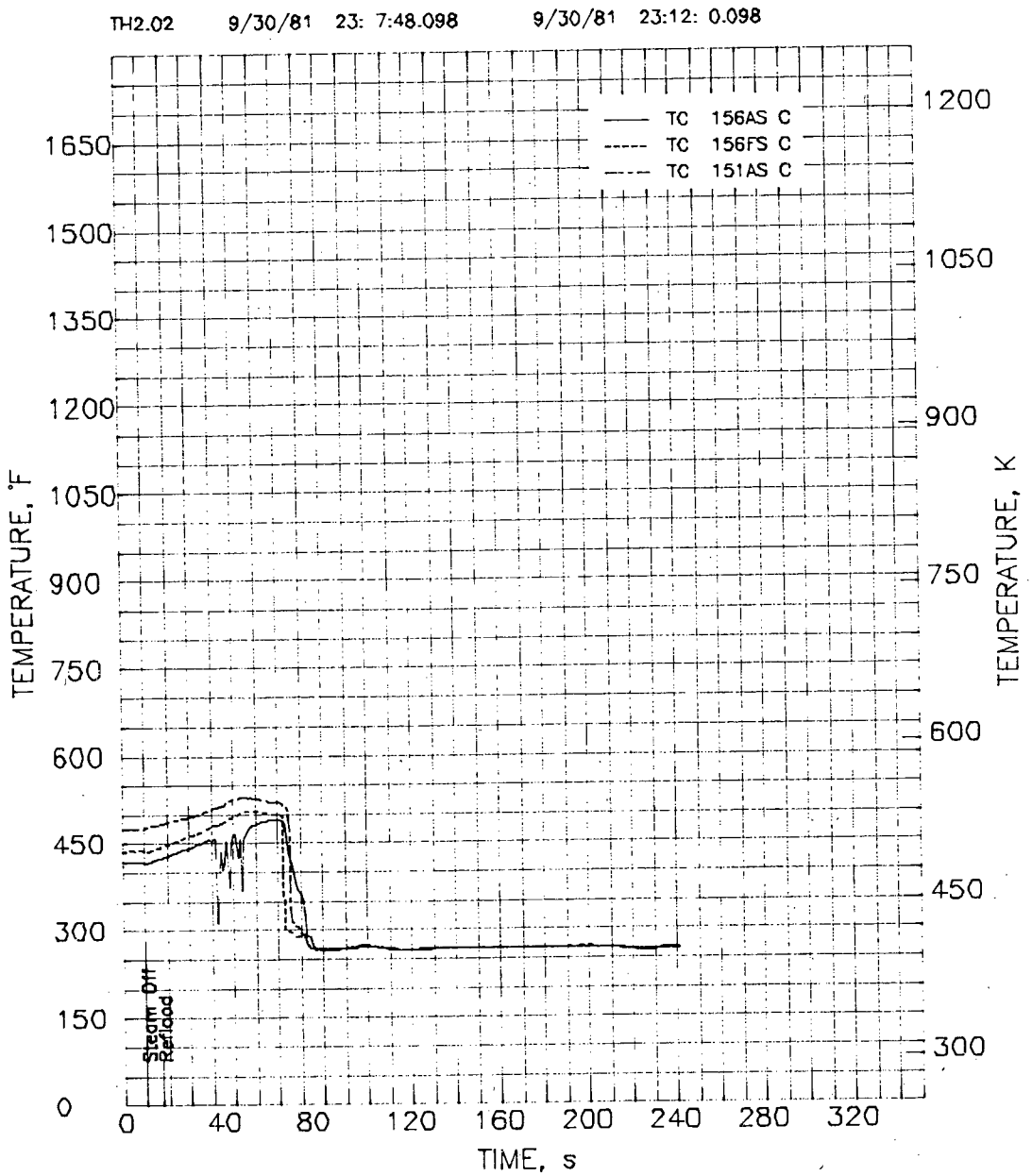

FIGURE D.13. Shroud Temperature Histories at Level 15 During Transient for TH-2.02

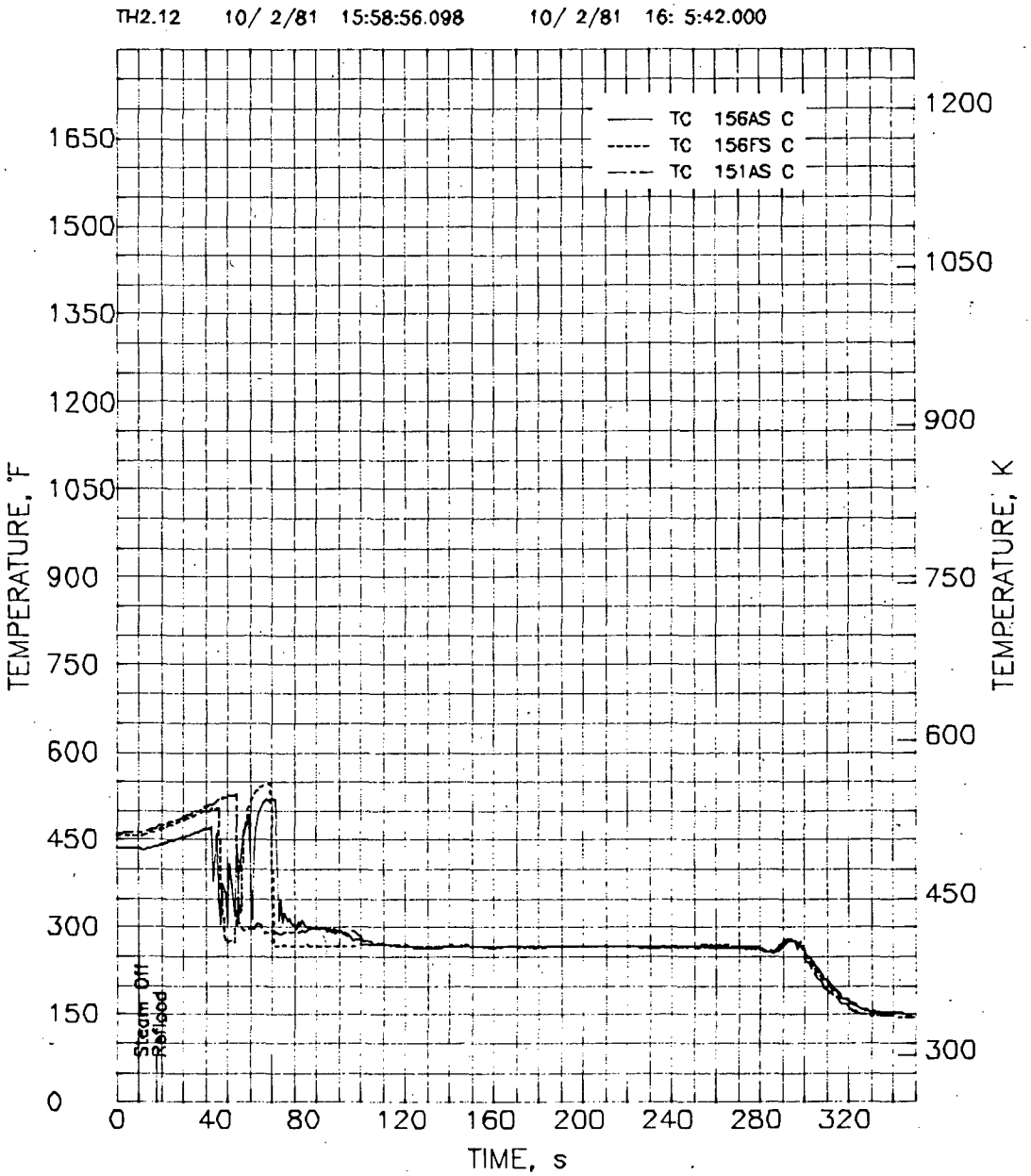

FIGURE D.14. Shroud Temperature Histories at Level 15 During Transient for TH-2.12

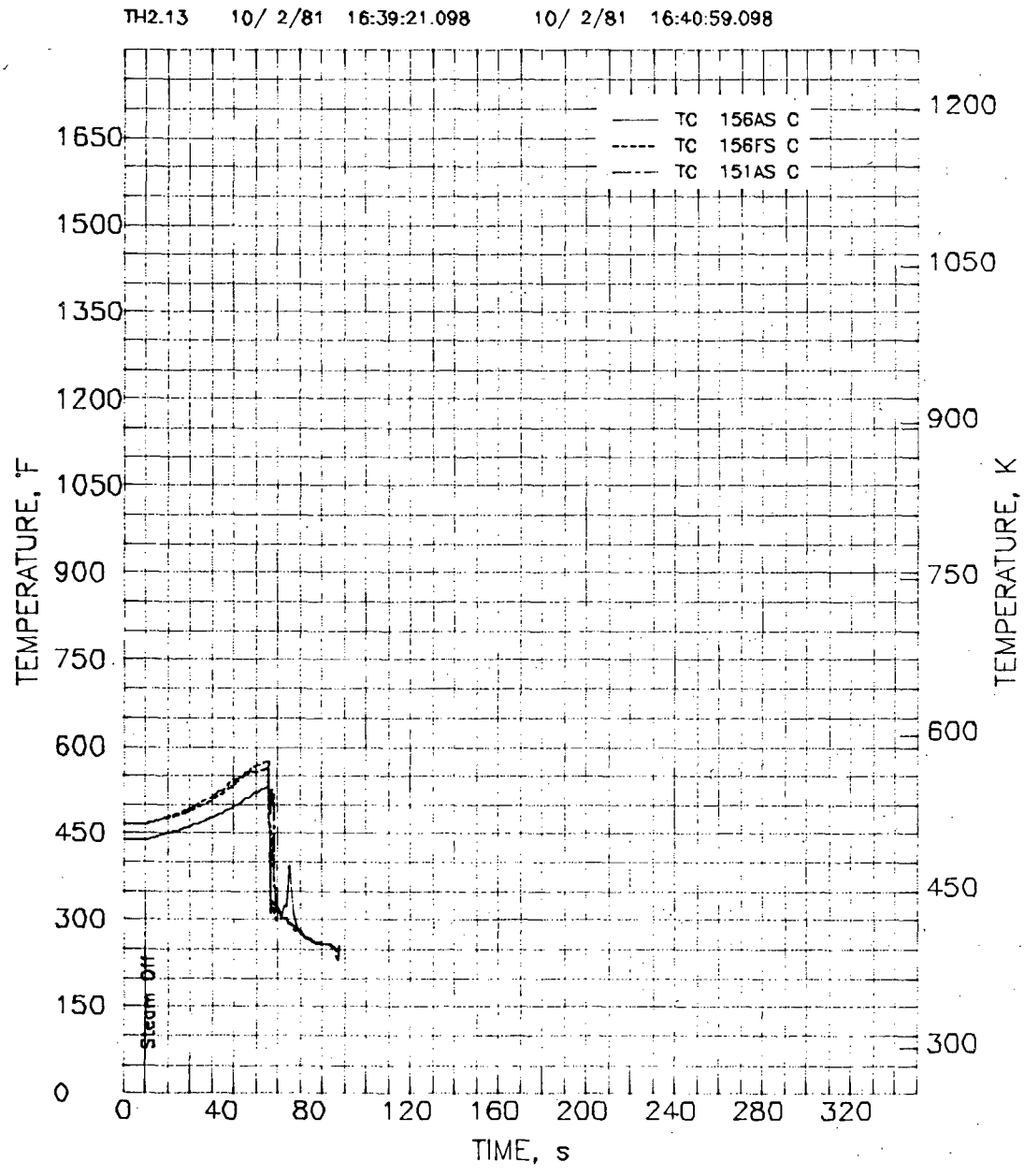

FIGURE D.15. Shroud Temperature Histories at Level 15 During Transient for TH-2.13

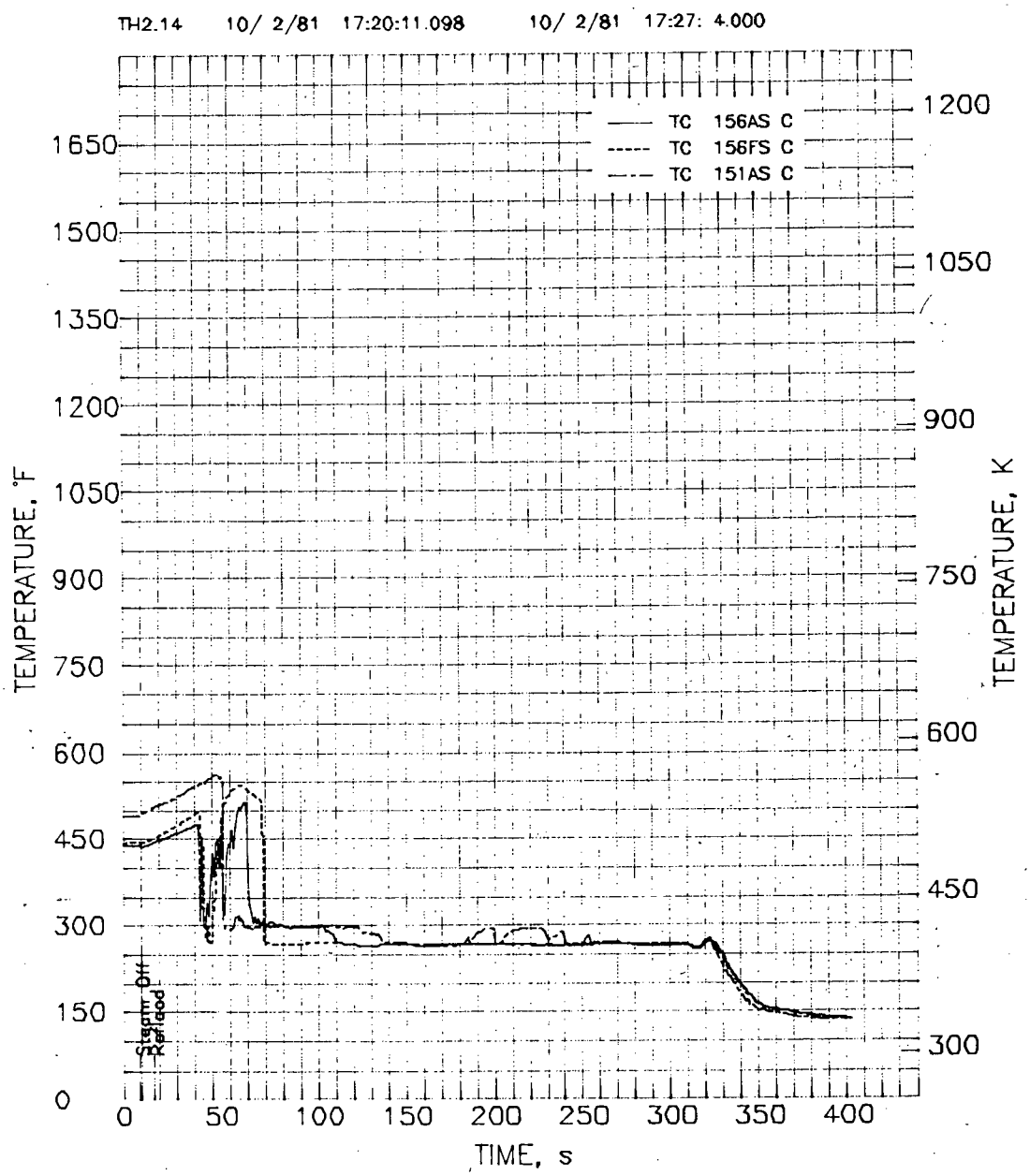

FIGURE D.16. Shroud Temperature Histories at Level 15 During Transient for TH-2.14

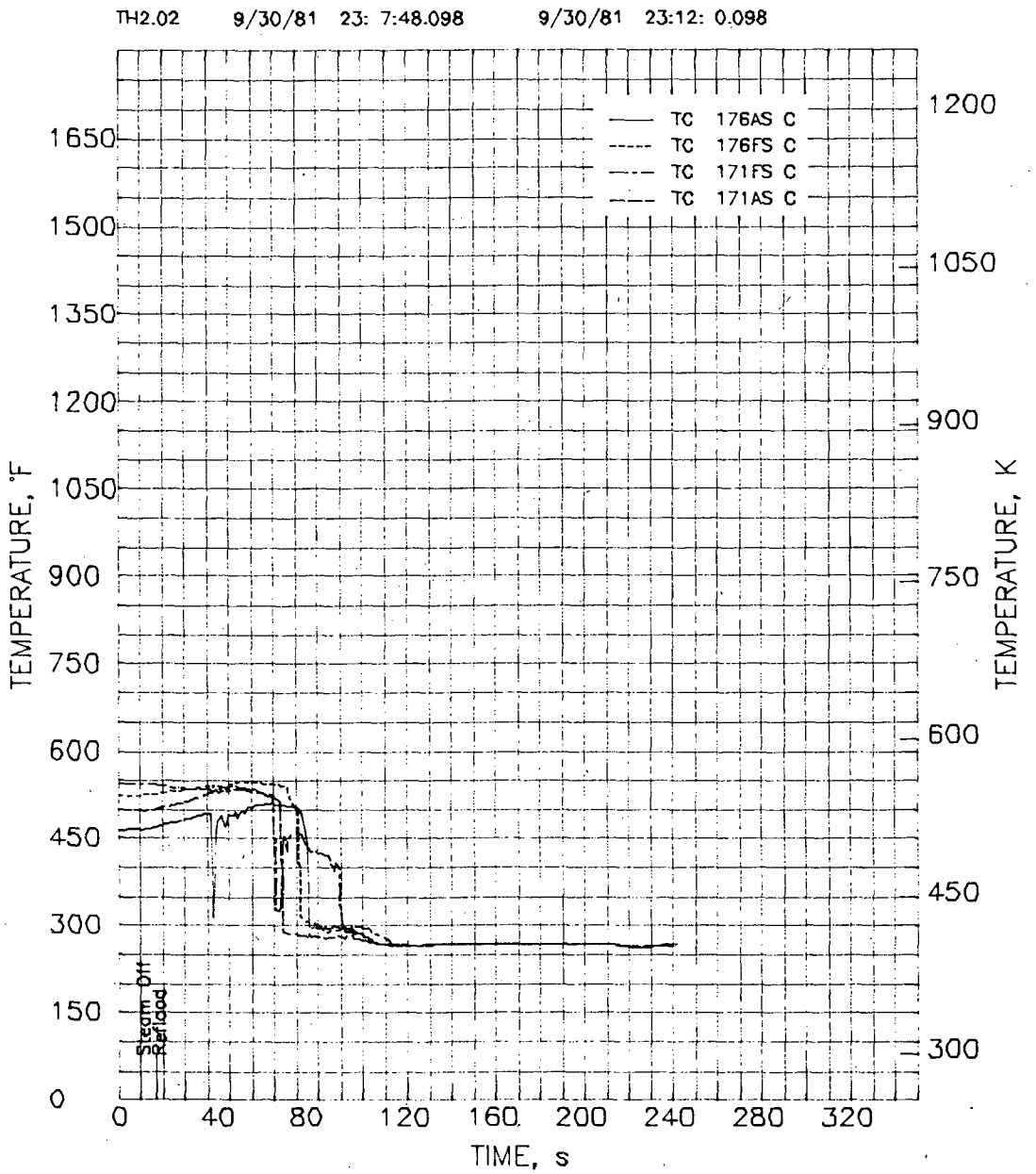

FIGURE D.17. Shroud Temperature Histories at Level 17 During Transient for TH-2.02

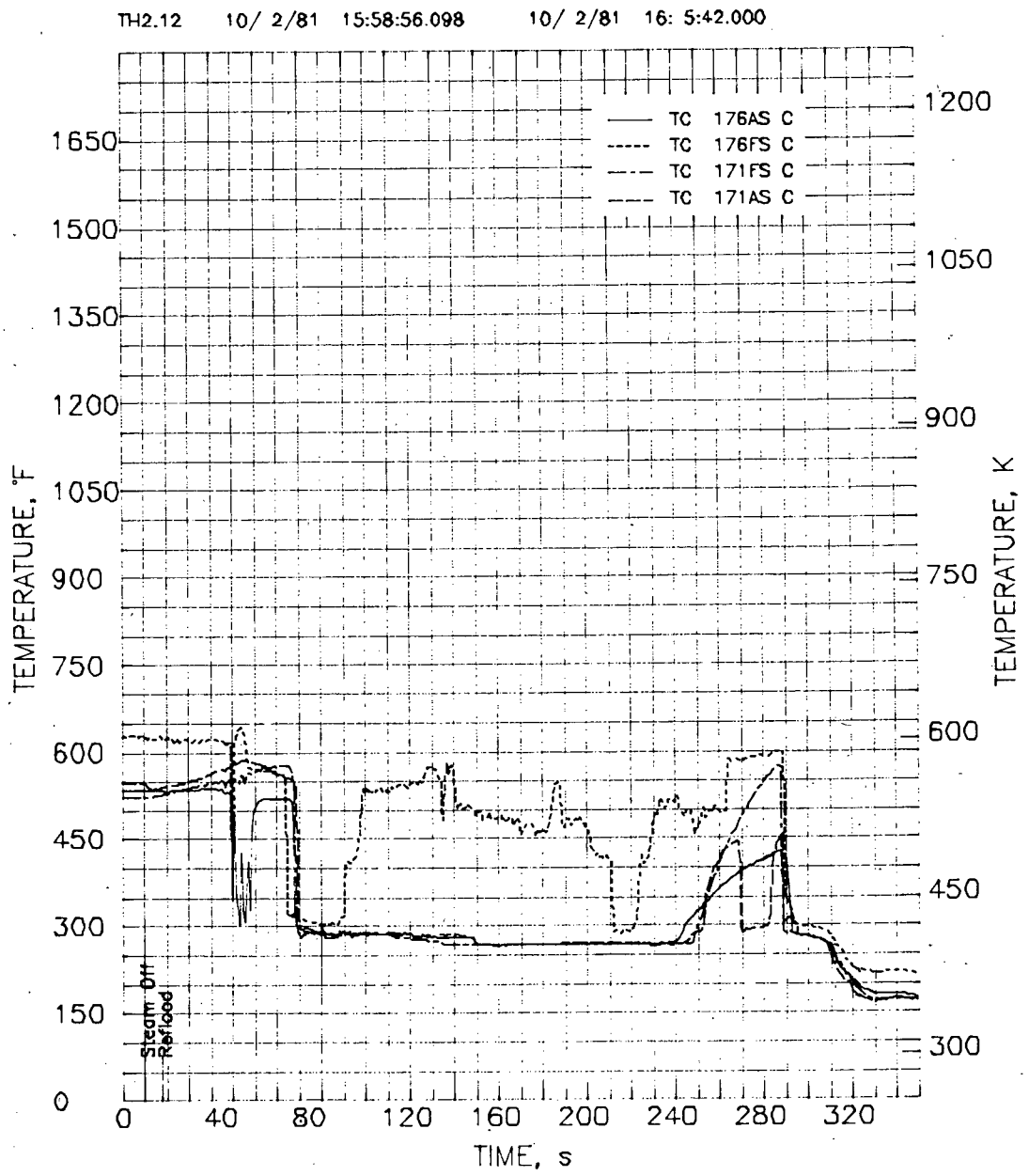

FIGURE D.18. Shroud Temperature Histories at Level 17 During Transient for TH-2.12

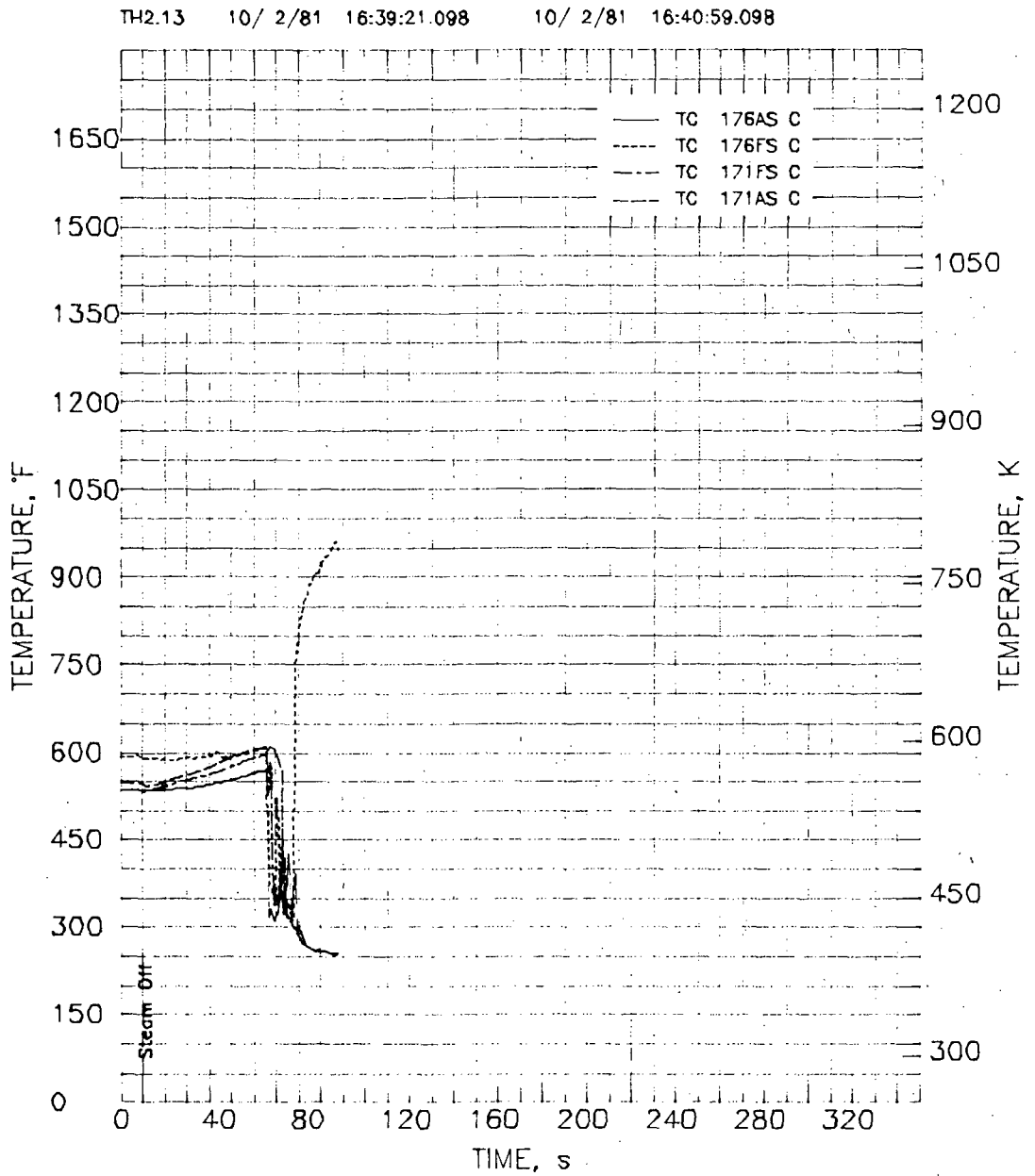

FIGURE D.19. Shroud Temperature Histories at Level 17 During Transient for TH-2.13

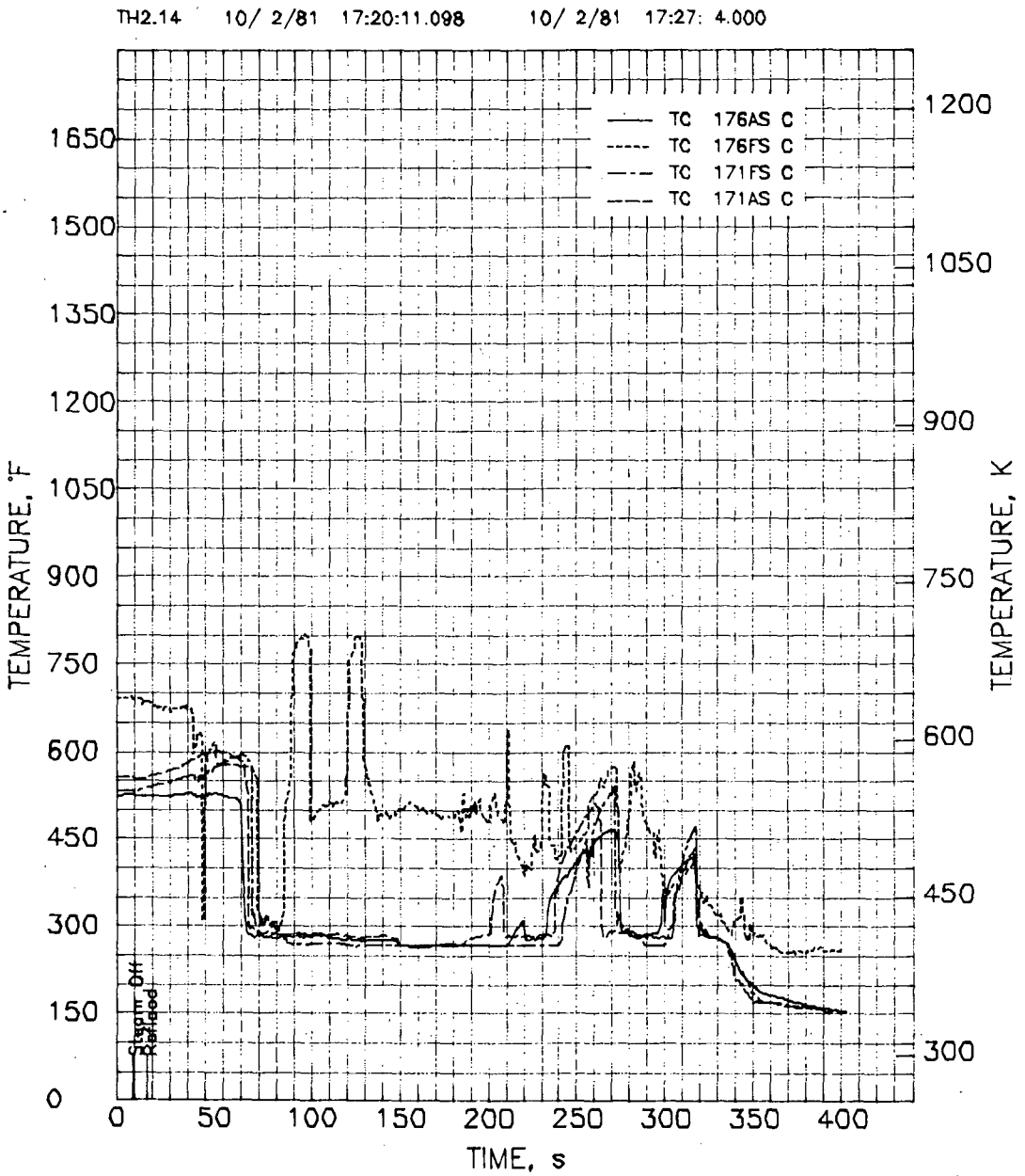

FIGURE D.20. Shroud Temperature Histories at Level 17 During Transient for TH-2.14

APPENDIX E

NEUTRON FLUX

APPENDIX E

NEUTRON FLUX

This appendix discusses the neutron flux that was measured during the preconditioning, pretransient, and transient phases of the second thermal-hydraulics experiment (TH-2).

PRECONDITIONING AND PRETRANSIENT NEUTRON FLUX

Neutron flux was measured inside the test assembly on the wall of the shroud and elsewhere in the National Research Universal (NRU) reactor. The internal flux was measured by self-powered neutron detectors (SPNDs) in opposite corners of the stainless steel (SS) shroud and at several elevations, ranging from 0.337 to 3.538 m (13.3 to 139.3 in.) above the bottom of the fuel column. The SPNDs provided both a measure of the radial neutron flux gradient and the neutron flux distribution over the vertical axis of the test assembly. Because neutron flux was measured in opposite corners of the test assembly, radial neutron flux gradients are evident. Figure E.1 presents the axial distribution of neutron flux measured in each corner; the maximum radial neutron flux gradient--(maximum-minimum/nominal)--was less than 22%. The neutron flux gradient for the preconditioning operation was 19%. Similar measurements made during the MT-2 experiment were 20% and 33%, respectively, for preconditioning and pretransient operations.[4]

Flux detector rods in the NRU reactor provided an independent measure of the neutron flux axial distribution at two other locations. In Figure E.2, neutron flux measured inside and outside the test assembly is compared. The magnitude of the difference is predominately due to the addition of structural material (SS) and absorber material (light water) in a heavy-water-moderated reactor. However, the normalized neutron flux distributions are quite comparable, especially when platinum flux detector rods are corrected for burnup.

The only obvious difference among these flux distributions is the location of the peak flux measured inside the test assembly--fuel rods 3.66 m (144 in.) long--compared with the peak measured in the NRU reactor--fuel rods 2.74 m (108 in.) long. The core midplanes are offset by 0.305 m (12 in.).

TRANSIENT NEUTRON FLUX

To investigate the possibility of changing neutron flux during a simulated loss-of-coolant accident (LOCA) (while the NRU reactor power is held constant), neutron flux histories are presented with time histories of control rod movement. During the course of the transient, light water is injected to reflood the test train. In a heavy-water-moderated reactor, this injection acts as a mild absorber; consequently, the dynamic control rod is withdrawn. Control

rod positioning is displayed in Figure E.3 as is the average neutron flux time history measured at Level 15. It is evident that there is no direct correlation between the two for any of the transients (see, for example, Figure E.4).

It has been proposed that the measured neutron flux is affected by the changing temperature of test assembly SPNDs and their instrument leads. The effect is primarily due to dielectrical resistivity changes in the leads due to a high-temperature, ionizing environment. High-temperature calibration of these sensors can be further compensated by SPND characteristics measured in high-temperature transients of the initial thermal-hydraulic experiment. However, because the temperature of the SPNDs and their instrument leads (attached to the shroud) remained cool throughout the experiment, temperature compensation of these data is not appropriate. The temperatures remained well within the SPND calibration temperature range.

The calculated neutron flux distribution is shown in Figure E.5 and is compared to SPND data and adiabatic heatup rate data. These data represent the SPND neutron flux and power generated during the adiabatic heatup portion of the transient--the same time when transient thermal data provided the thermal-hydraulic basis for power estimates. The two power estimates compare well; Figure E.5 shows their axial distribution during the heatup transient.

The remainder of this appendix consists of the following graphical data:

Figure E.1. Axial Distribution of Pretransient Neutron Flux for TH-2.14

Figure E.2. Normalized Axial Distribution of Pretransient Neutron Flux for TH-2.14

Figure E.3. Changing Control Rod 15 Position and Neutron Flux During TH-2.12

Figure E.4. Changing Control Rod 15 Position and Neutron Flux During TH-2.14

Figure E.5. Comparison of TH-2.13 SPND Data and TH-2.13 Heatup Rate Based on Calculated Axial Power Profiles for the NRU Test Assembly

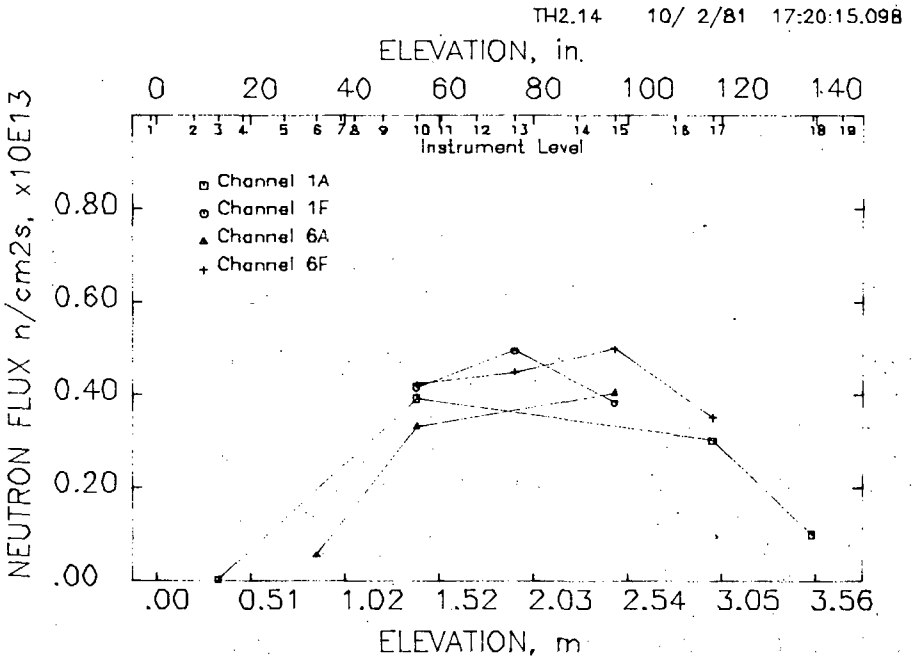

FIGURE E.1. Axial Distribution of Pretransient Neutron Flux for TH-2.14

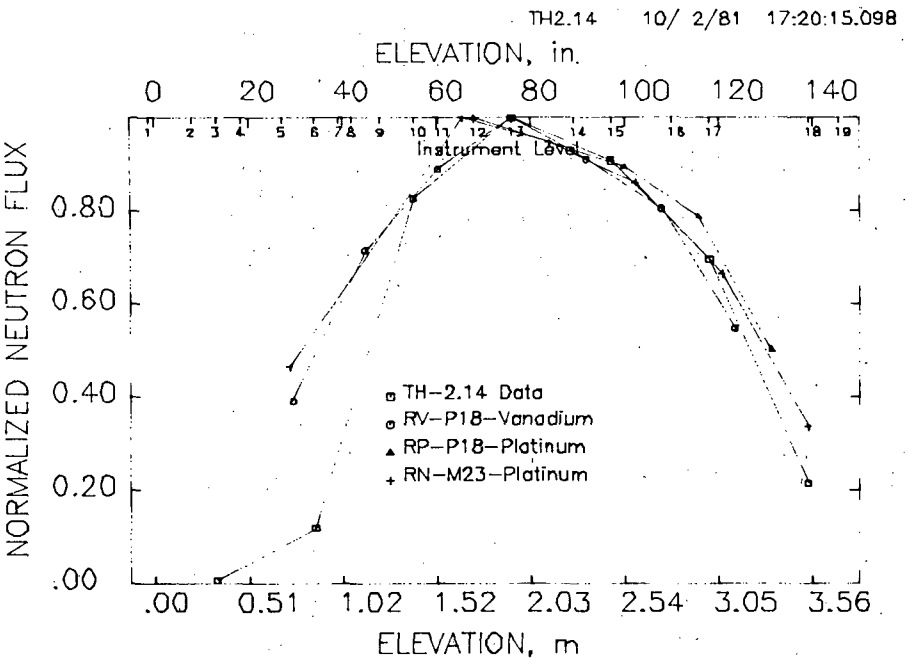

FIGURE E.2. Normalized Axial Distribution of Pretransient Neutron Flux for TH-2.14

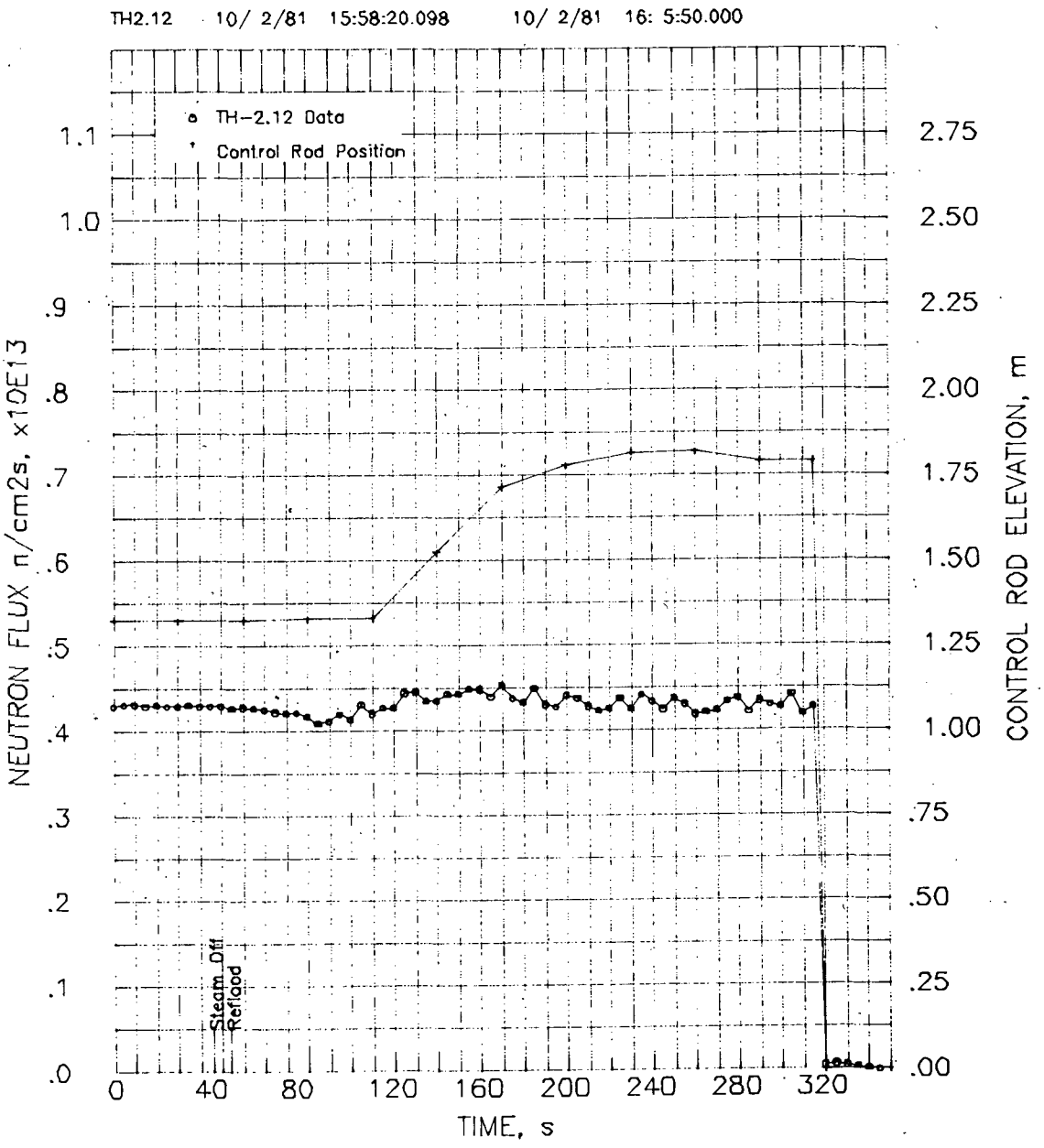

FIGURE E.3. Changing Control Rod 15 Position and Neutron Flux During TH-2.12

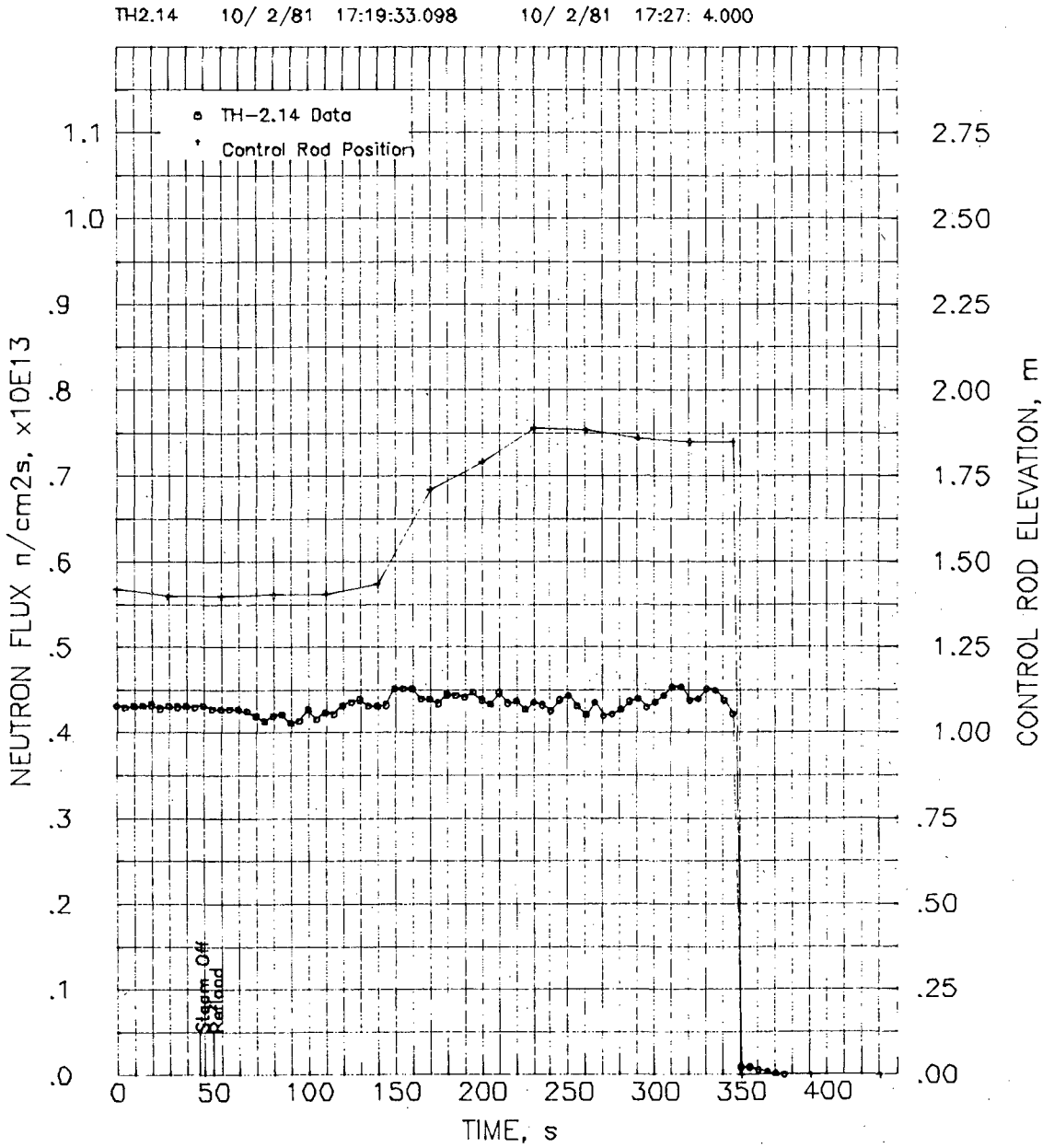

FIGURE E.4. Changing Control Rod 15 Position and Neutron Flux During TH-2.14

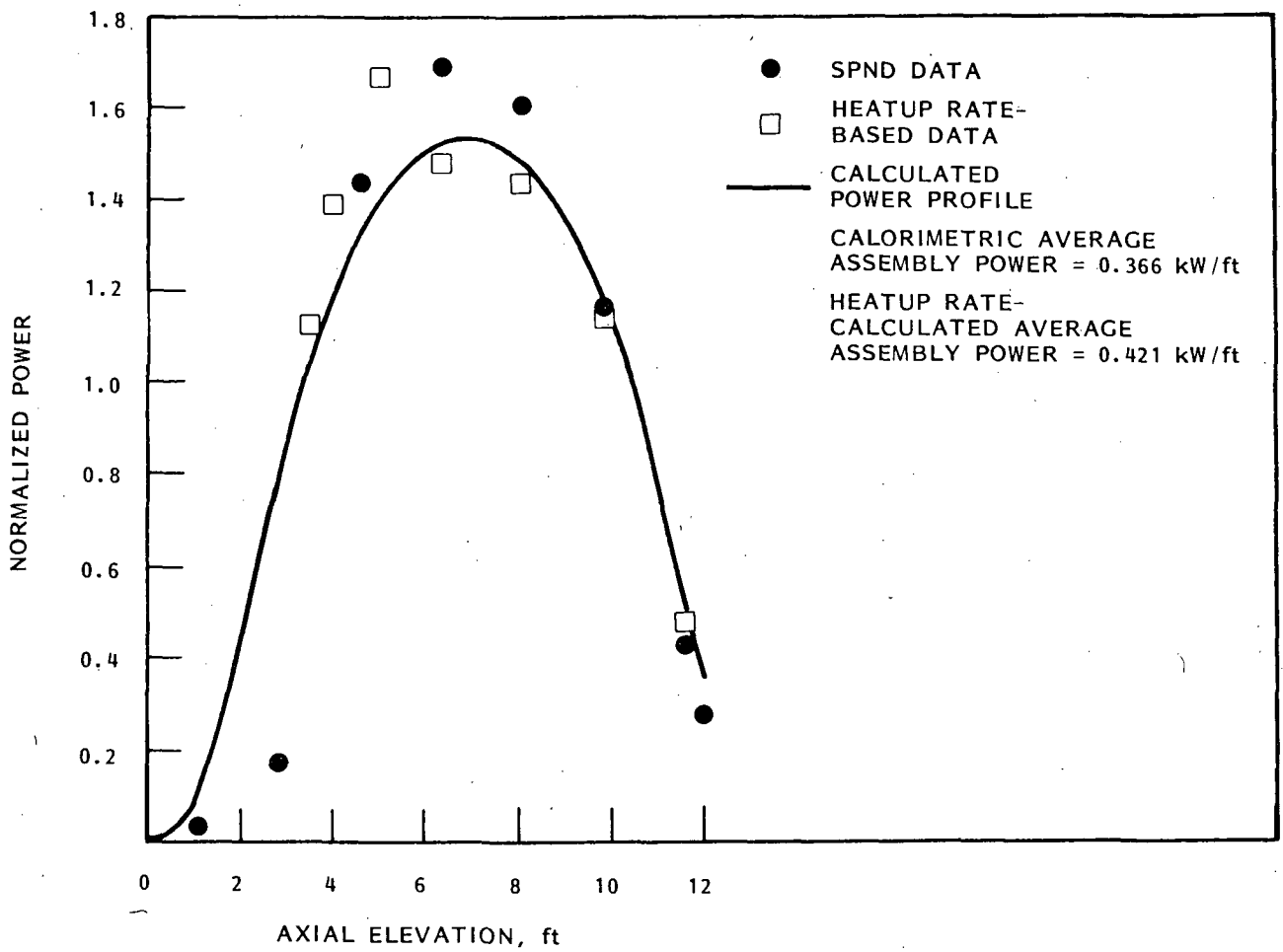

FIGURE E.5. Comparison of TH-2.13 SPND Data and TH-2.13 Heatup Rate Based on Calculated Axial Power Profiles for the NRU Test Assembly

APPENDIX F

REFLOOD FLOW MEASUREMENTS

APPENDIX F

REFLOOD FLOW MEASUREMENTS

The reflood flow system included a Fisher-Porter turbine flowmeter in the high flow rate line and series-connected Barton and Fisher-Porter turbine flowmeters in a parallel low flow rate line. A parallel standby reflood line was also provided to supply emergency reflood coolant, but it was not used during the TH-2 experiment.

The reflood control system was calibrated before the first transient using steam probe data to monitor the water/steam interface during reflood operation. Prior to the pretransient test phase, three reflood flow tests were performed at 0.0508, 0.0254, and 0.0508 m/s (2.0, 1.0, and 2.0 in./s) to calibrate the reflood loop (see Figures F.1 through F.3 for the flow rate recordings).

Steam probe temperature histories provided independent measurements of the reflood coolant level (and reflood flow rate) in the test assembly. Figures F.4 through F.6 provided the data for the pretest reflood rate calibrations by showing the time required between subsequent level quenches.

Transient test starting times and reflood delay times are dependent on the flow conditions at the bottom of the active fuel. These flow conditions are related to the temperature response of TCs located at Level 1, which is 0.013 m (0.5 in.) below the active fuel. The transients start when steam coolant is shut off, as determined from a quick drop in temperature at Level 1. The reflood initiation times occur when the reflood water quenches thermocouples (TCs) at Level 1, as indicated by a second quick drop in temperature.

At the start of each transient test, a fast reflood rate was used to bring the reflood coolant level up to the bottom of the fuel rods (Level 1). After that, the loop control system (LCS) used preset reflood rates. For transient TH-2.02, the reflood rate was controlled by the LCS throughout the test (see Figure F.7). For tests TH-2.03 through TH-2.05, the data acquisition and control system (DACS) computer controlled the reflood flow rate after 85 s. For tests TH-2.06 through TH-2.14 (excluding adiabatic test TH-2.13), the DACS controlled the reflood rate 95 s after initiation of the transient. The reflood rates for TH-2.12 and TH-2.14 best represent DACS-controlled reflood flow (see Figures F.8 and F.9).

The remainder of this appendix consists of the following graphical data:

Figure F.1. Pretest Reflood Flow Rate for Calibration Test 1

Figure F.2. Pretest Reflood Flow Rate for Calibration Test 2

Figure F.3. Pretest Reflood Flow Rate for Calibration Test 3

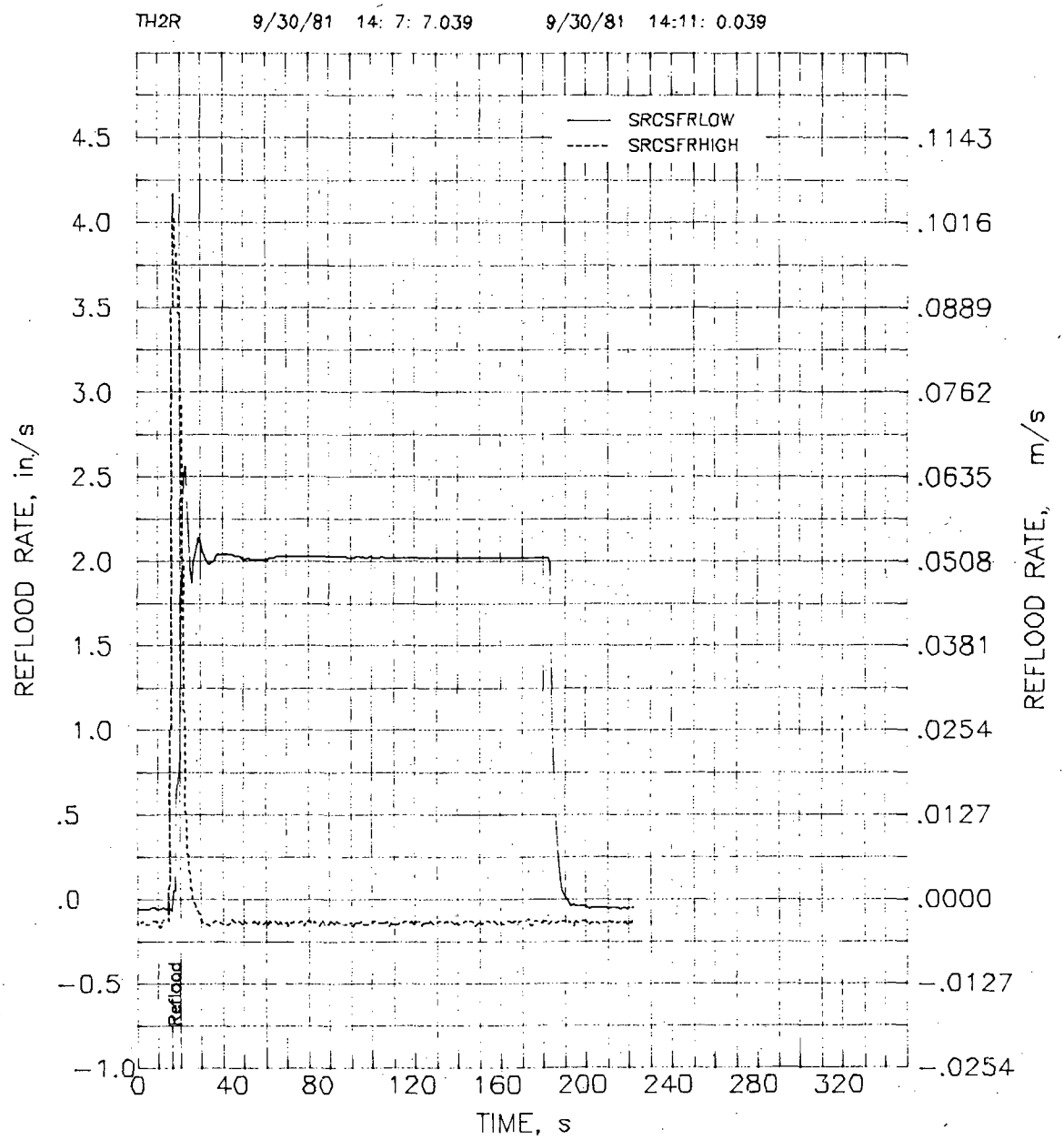

FIGURE F.1. Pretest Reflood Flow Rate for Calibration Test 1

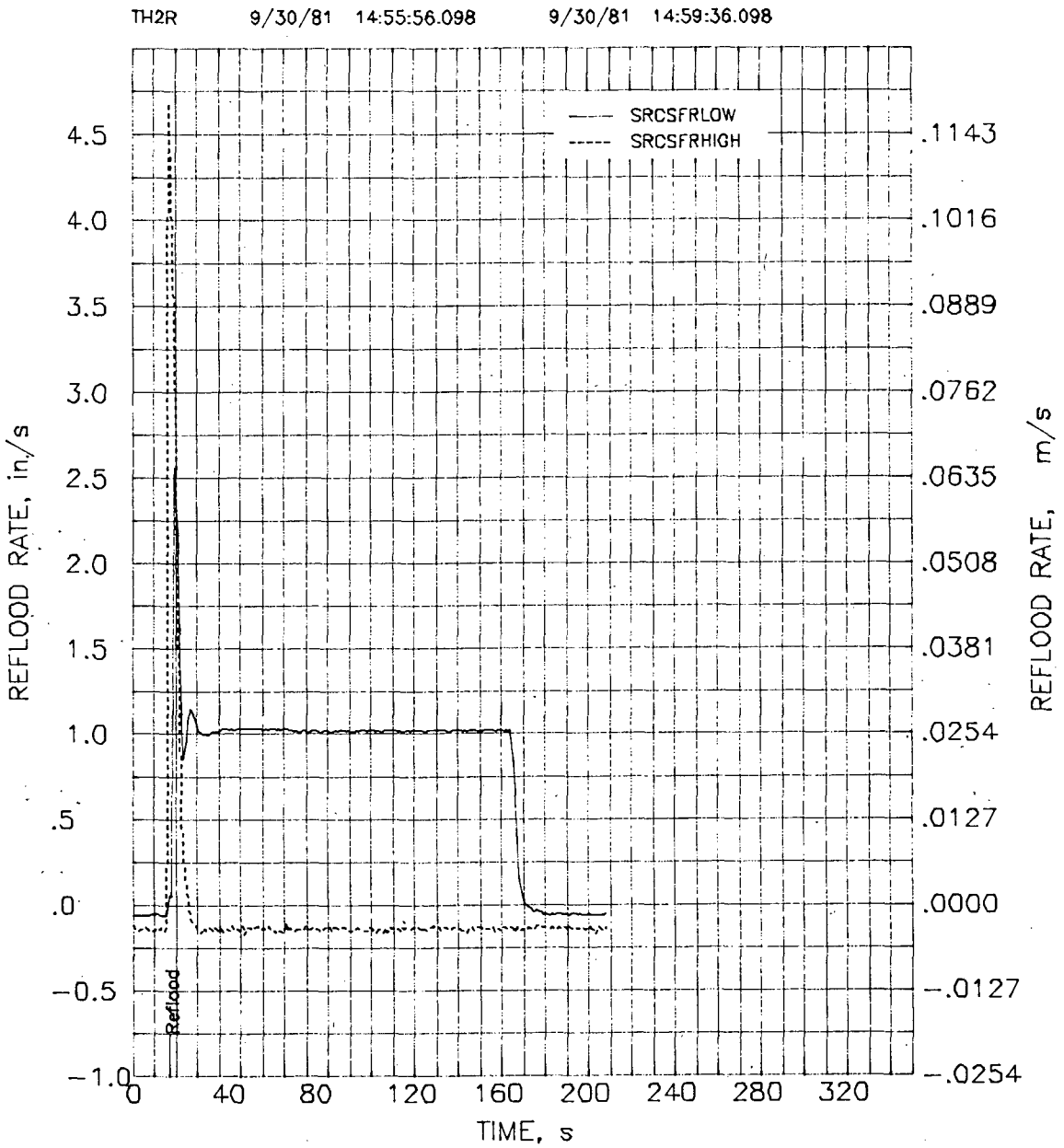

FIGURE F.2. Pretest Reflood Flow Rate for Calibration Test 2

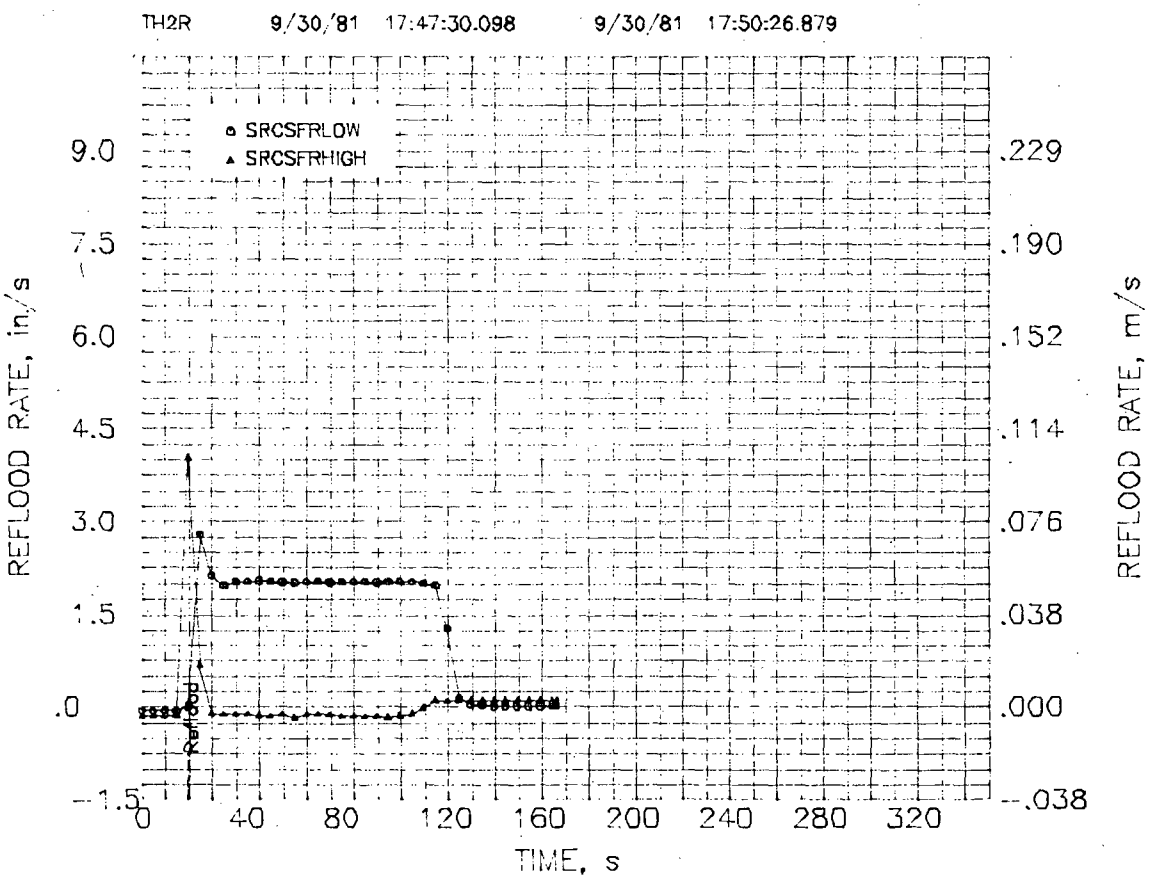

FIGURE F.3. Pretest Reflood Flow Rate for Calibration Test 3

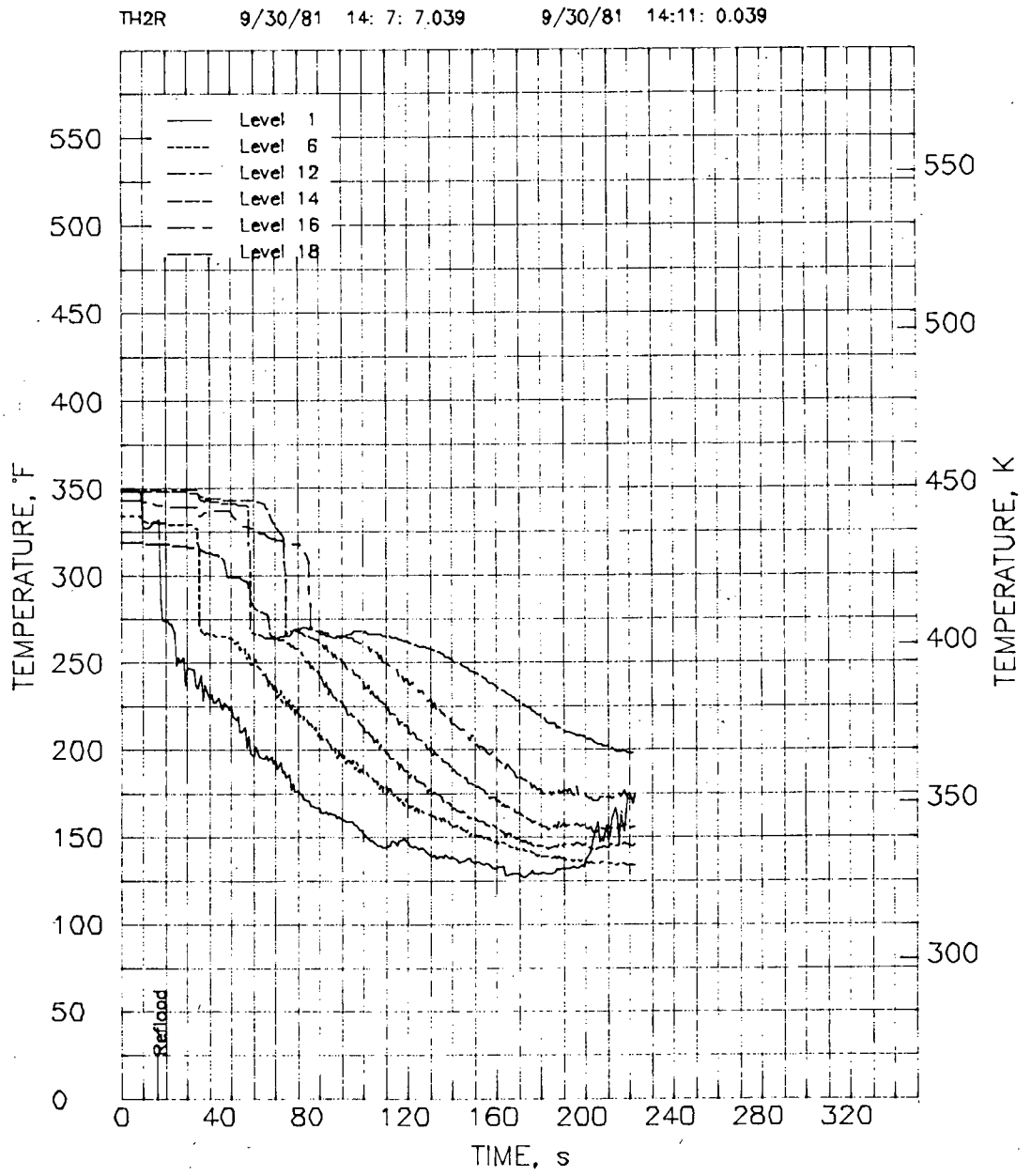

FIGURE F.4. Steam Probe and Shroud Temperatures for Reflood Calibration Test 1

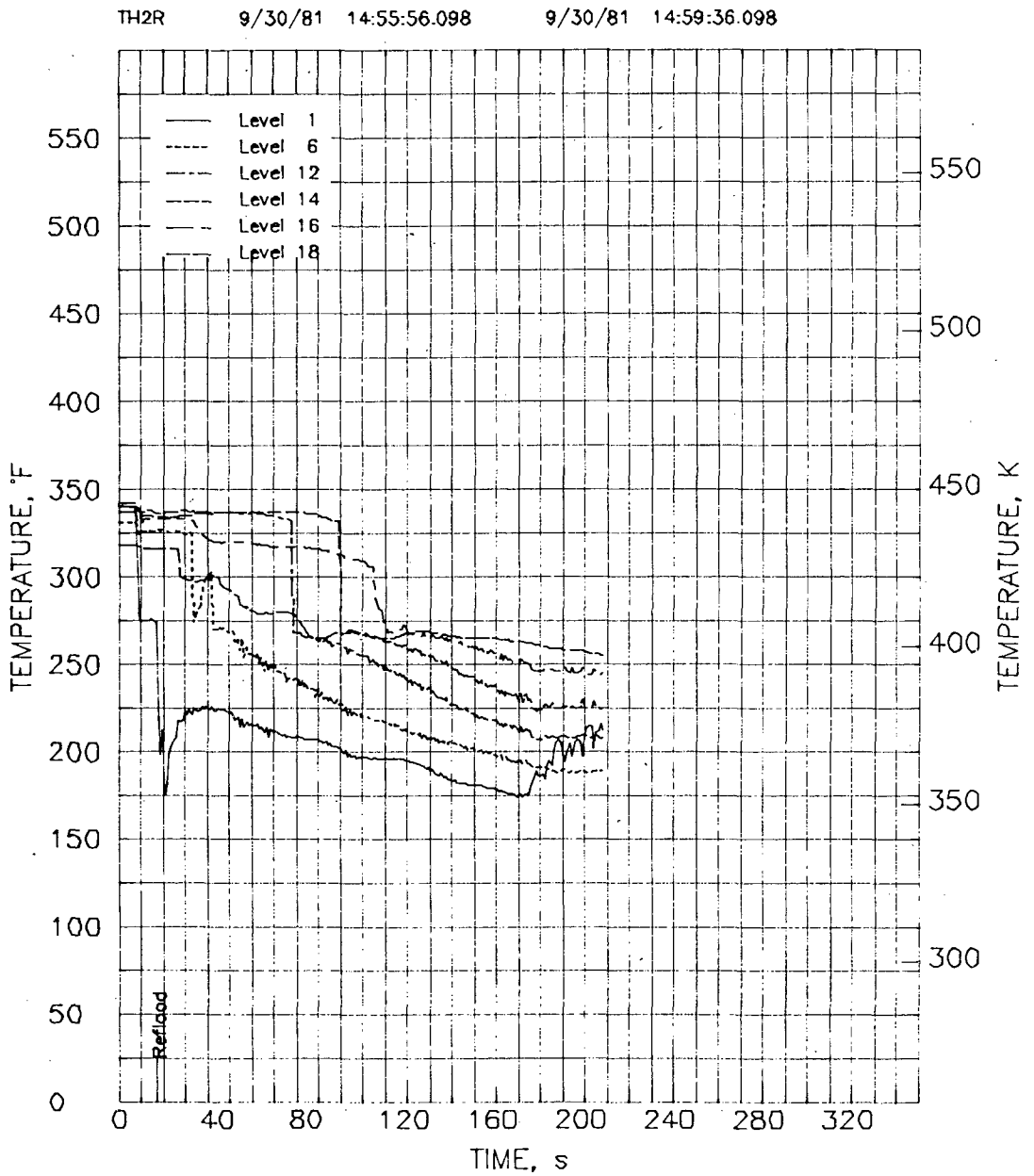

FIGURE F.5. Steam Probe and Shroud Temperatures for Reflood Calibration Test 2

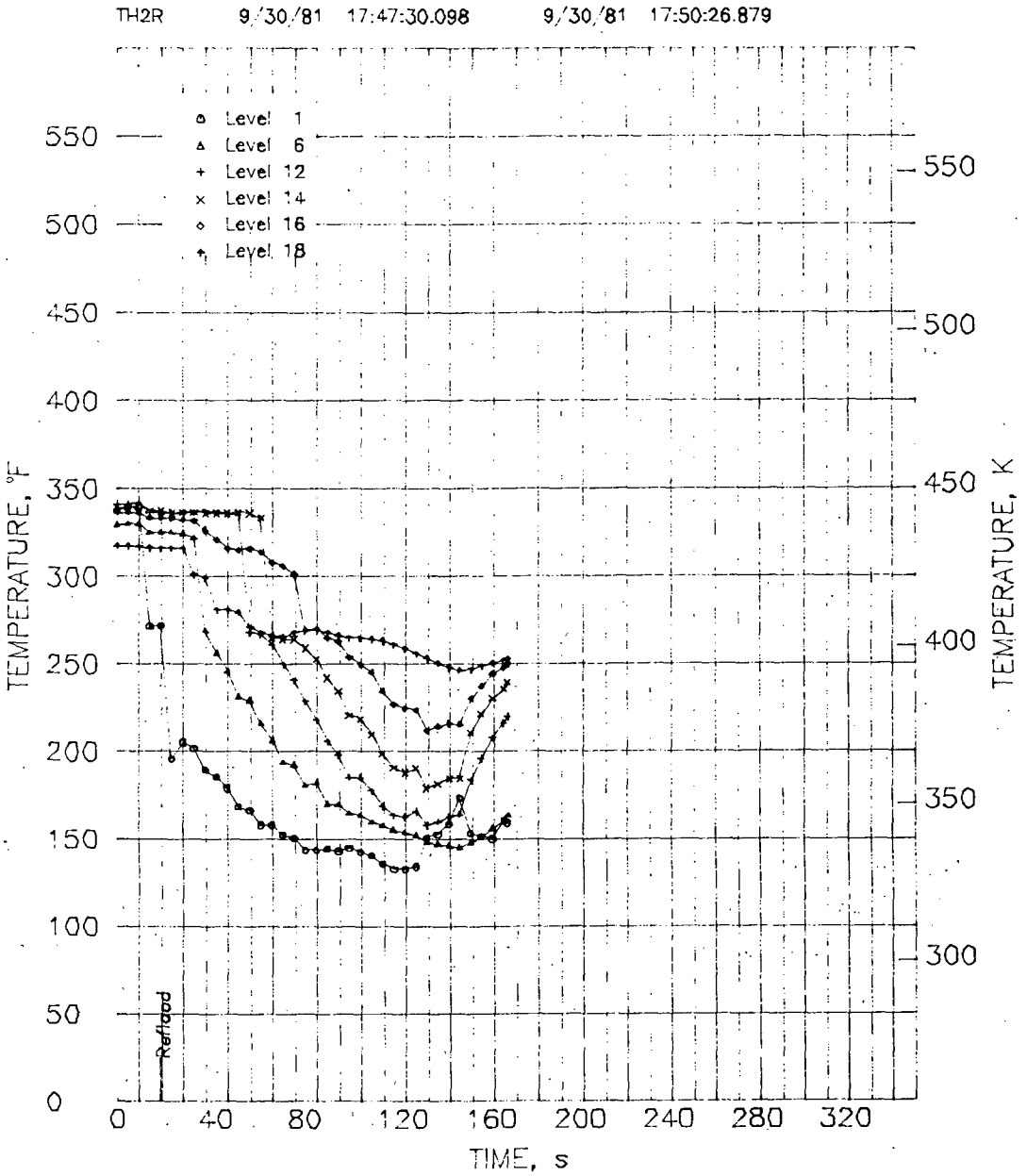

FIGURE F.6. Steam Probe and Shroud Temperatures for Reflood Calibration Test 3

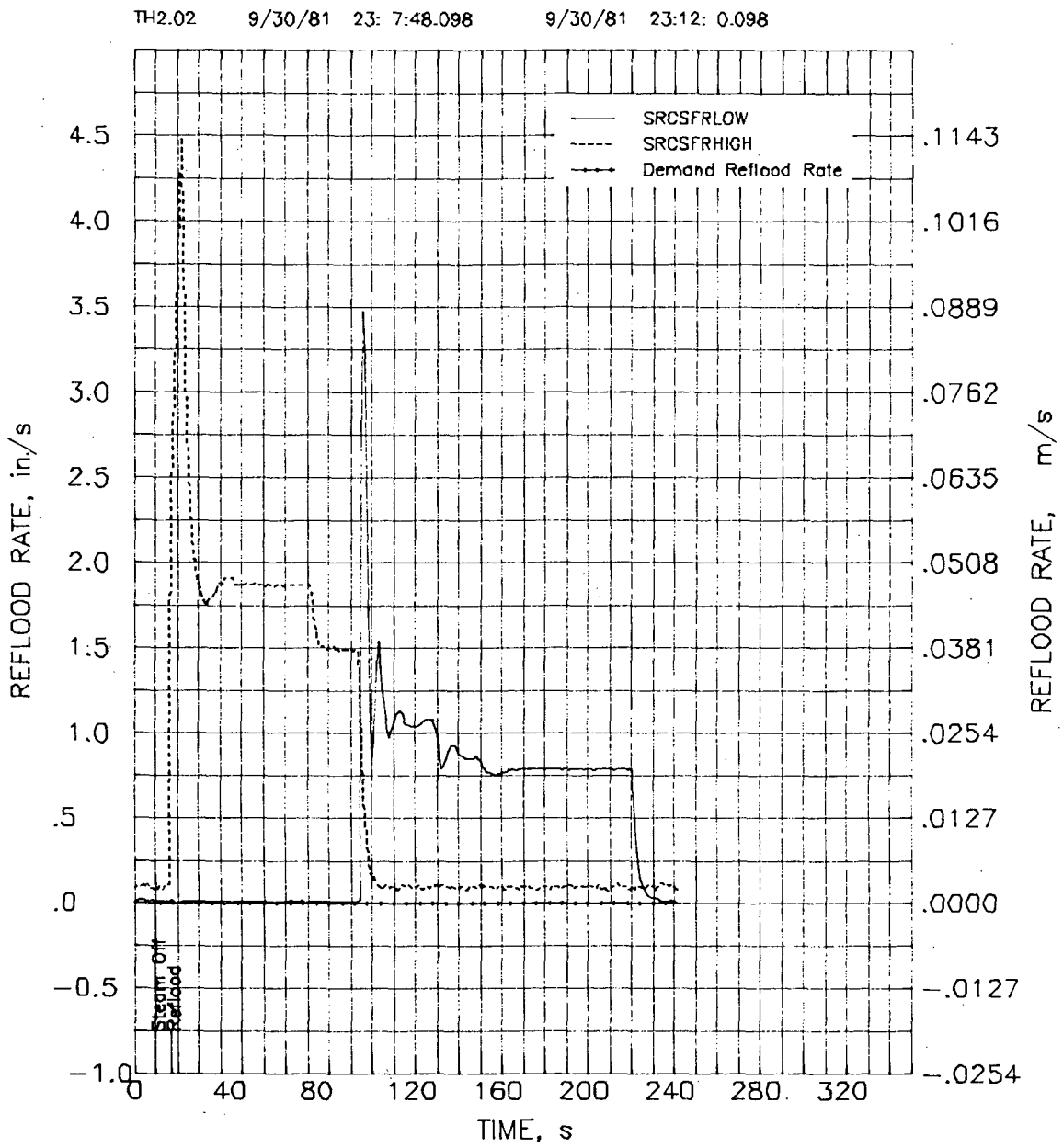

FIGURE F.7. Turbine Flowmeter Data for TH-2.02

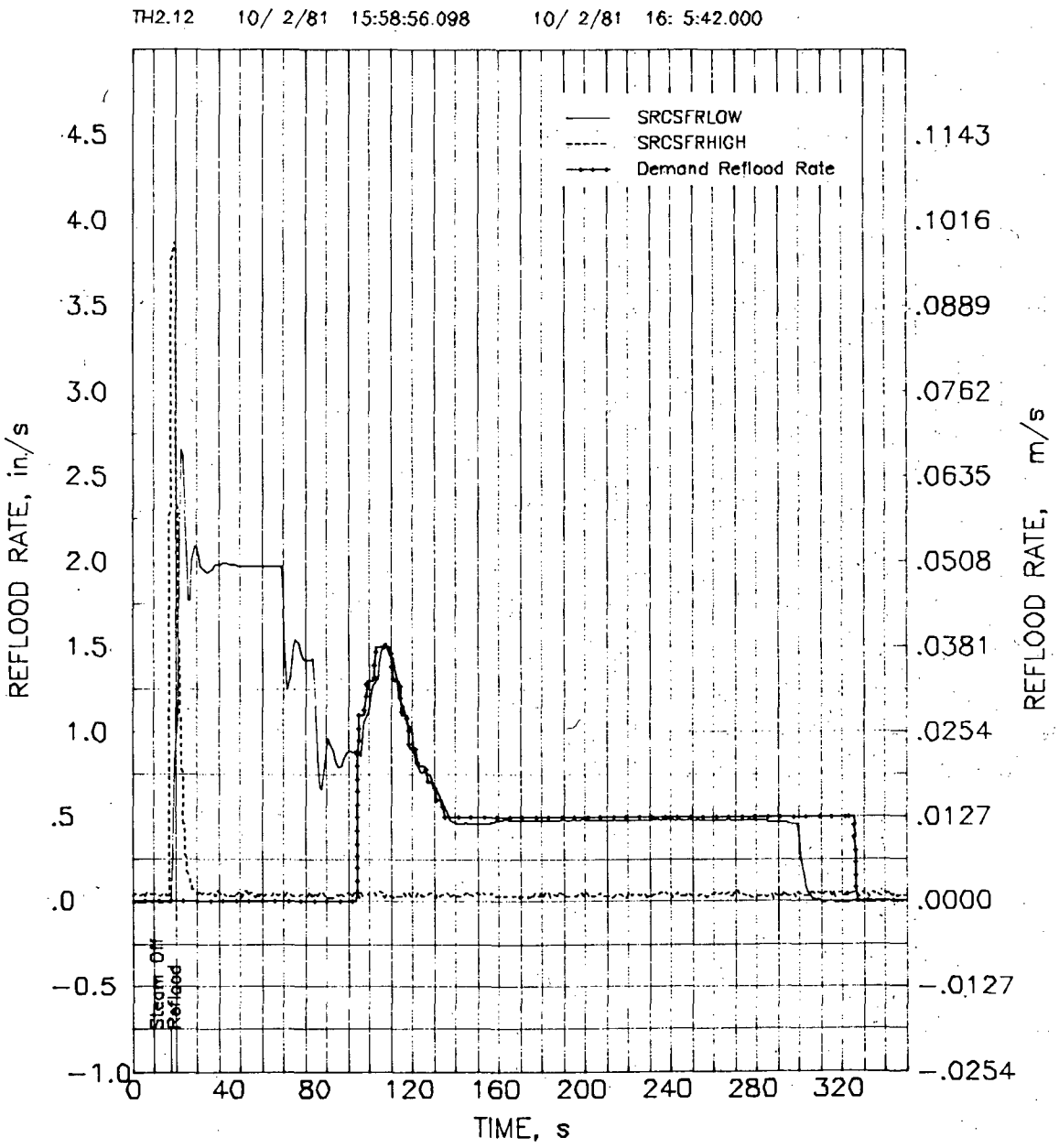

FIGURE F.8. Turbine Flowmeter Data for TH-2.12

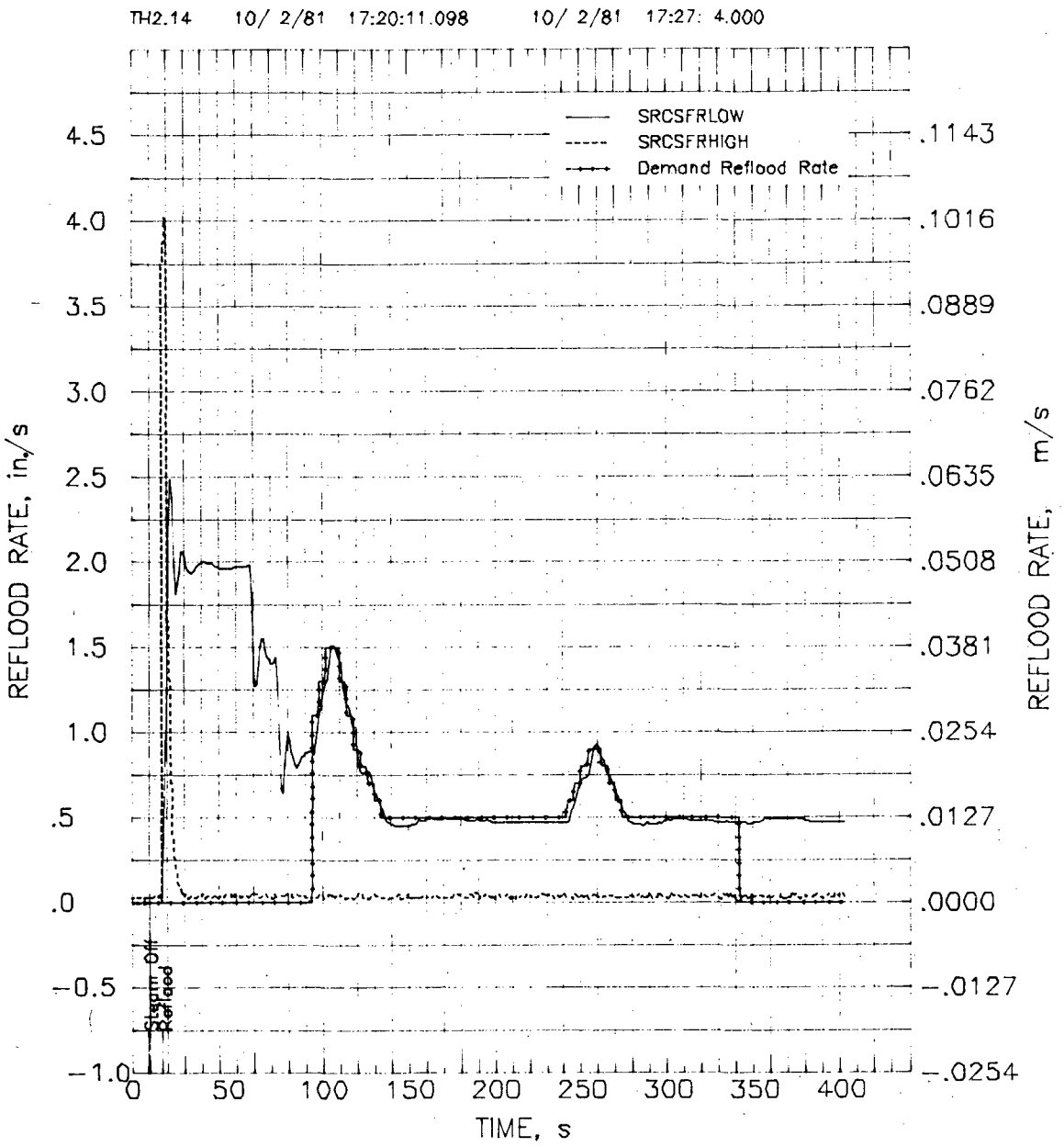

FIGURE F.9. Turbine Flowmeter Data for TH-2.14

DISTRIBUTION

No. of Copies

OFFSITE

U.S. Nuclear Regulatory Commission
Division of Technical Information
and Document Control
7920 Norfolk Avenue
Bethesda, MD 20014

DOE Technical Information Center

W. Hodges
U.S. Nuclear Regulatory Commission
M/S P-1132
Washington, DC 20555

A. Hon
U.S. Nuclear Regulatory Commission
M/S 1130-SS
Washington, DC 20555

Y. Hsu
U.S. Nuclear Regulatory Commission
M/S 1130-SS
Washington, DC 20555

N. Lauben
U.S. Nuclear Regulatory Commission
M/S P-1132
Washington, DC 20555

G. Marino
U.S. Nuclear Regulatory Commission
M/S 1130-SS
Washington, DC 20555

No. of Copies

G. McPherson
U.S. Nuclear Regulatory Commission
M/S 1130-SS
Washington, DC 20555

R. Meyer
U.S. Nuclear Regulatory Commission
M/S P-1114
Washington, DC 20555

J. Norberg
U.S. Nuclear Regulatory Commission
M/S NL-5650
Washington, DC 20555

M. Picklesimer
U.S. Nuclear Regulatory Commission
M/S 1130-SS
Washington, DC 20555

L. Phillips
U.S. Nuclear Regulatory Commission
M/S P-1114
Washington, DC 20555

D. Power
U.S. Nuclear Regulatory Commission
M/S P-1114
Washington, DC 20555

L. Shotkin
U.S. Nuclear Regulatory Commission
M/S 1130-SS
Washington, DC 20555

No. of Copies

M. Silberberg
U.S. Nuclear Regulatory Commission
M/S P-1114
Washington, DC 20555

L. Tong
U.S. Nuclear Regulatory Commission
M/S 1130-SS
Washington, DC 20555

3 R. Van Houten
U.S. Nuclear Regulatory Commission
M/S 1130-SS
Washington, DC 20555

Z. Zuber
U.S. Nuclear Regulatory Commission
M/S 1130-SS
Washington, DC 20555

P. Boehnert
U.S. Nuclear Regulatory Commission
Advisory Committee on Reactor Safeguards
M/S H-1016
Washington, DC 20555

D. Okrent
U.S. Nuclear Regulatory Commission
Advisory Committee on Reactor Safeguards
M/S H-1016
Washington, DC 20555

P. Shewmon
U.S. Nuclear Regulatory Commission
Advisory Committee on Reactor Safeguards
M/S H-1016
Washington, DC 20555

B. Bingham
Babcock and Wilcox Co.
P.O. Box 1200
Lynchburg, VA 24505

No. of Copies

C. Morgan
Babcock and Wilcox Co.
P.O. Box 1200
Lynchburg, VA 24505

R. Duncan
Combustion Engineering
1000 Prospect Hill Road
P.O. Box 500
Windsor, CT 06095

S. Ritterbush
Combustion Engineering
1000 Prospect Hill Road
P.O. Box 500
Windsor, CT 06095

2 L. P. Leach
EG&G Idaho, Inc.
P.O. Box 1625
Idaho Falls, ID 83401

D. Ogden
EG&G Idaho, Inc.
P.O. Box 1625
Idaho Falls, ID 83401

P. Davis (ITI)
Electric Power Research Institute
3412 Hillview Avenue
Palo Alto, CA 94022

R. Duffey
Electric Power Research Institute
3412 Hillview Avenue
Palo Alto, CA 94022

R. Oehlberg
Electric Power Research Institute
3412 Hillview Avenue
Palo Alto, CA 94022

No. of
Copies

W. Sun
Electric Power Research
Institute
3412 Hillview Avenue
Palo Alto, CA 94022

G. Thomas
Electric Power Research
Institute
3412 Hillview Avenue
Palo Alto, CA 94022

L. Thompson
Electric Power Research
Institute
3412 Hillview Avenue
Palo Alto, CA 94022

S. Armijo
General Electric Company
175 Curtner Avenue
San Jose, CA 95114

L. Noble
General Electric Company
175 Curtner Avenue
San Jose, CA 95114

N. Shirley
General Electric Company
175 Curtner Avenue
San Jose, CA 95114

G. Sozzi
General Electric Company
175 Curtner Avenue
San Jose, CA 95114

R. Williams
General Electric Company
175 Curtner Avenue
San Jose, CA 95114

W. Kirchner
Los Alamos Scientific Laboratory
P.O. Box 1663
Los Alamos, NM 87544

No. of
Copies

D. M. Chapin
MPR Associates, Inc.
1140 Connecticut Avenue, NW
Washington, DC 20036

P. Griffith
Massachusetts Institute of
Technology
Department of Nuclear Engineering
Cambridge, MA 02139

J. Davis
Nuclear Engineering Department
Potomac Electric Avenue, NW
Washington, DC 20068

2 R. Chapman
Oak Ridge National Laboratory
P.O. Box X
Oak Ridge, TN 37830

F. Mynatt
Oak Ridge National Laboratory
P.O. Box X
Oak Ridge, TN 37830

D. Burman
Westinghouse Electric Corporation
P.O. Box 355
Pittsburgh, PA 15230

L. Hochreiter
Westinghouse Electric Corporation
P.O. Box 355
Pittsburgh, PA 15230

R. Rosal
Westinghouse Electric Corporation
P.O. Box 355
Pittsburgh, PA 15230

FOREIGN

D. J. Axford
Chalk River Nuclear Laboratories
Atomic Energy of Canada Ltd.
Chalk River, Ontario, Canada
KOJ 1JO

No. of Copies

6 D. T. Nishimura
Chalk River Nuclear Laboratories
Atomic Energy of Canada Ltd.
Chalk River, Ontario, Canada
KOJ 1JO

I. D. Ross
Chalk River Nuclear Laboratories
Atomic Energy of Canada Ltd.
Chalk River, Ontario, Canada
KOJ 1JO

A. Smith
Chalk River Nuclear Laboratories
Atomic Energy of Canada Ltd.
Chalk River, Ontario, Canada
KOJ 1JO

2 T. Healey
Central Electricity Generating Board
Berkeley Nuclear Laboratories
Berkeley, Gloucestershire GL13 9PB
England

4 M. Ishikawa, Chief
Reactivity Accident Laboratory
Japan Atomic Energy Research Institute
Tokai Research Establishment
Tokai-Mura, Naka-Gun
Ibaraki-Ken
Japan

T. Doyle
JRC-ISPRA, EURATOM
CCR ESSOR Division
21020 Cento Euratom Di Ispra (Varese)
Italy

H. Holtbecker
JRC-ISPRA, EURATOM
CCR ESSOR Division
21020 Cento Euratom Di Ispra (Varese)
Italy

No. of Copies

R. Klersy
JRC-ISPRA, EURATOM
CCR ESSOR Division
21020 Cento Euratom Di Ispra (Varese)
Italy

J. Randles
JRC-ISPRA, EURATOM
CCR ESSOR Division
21020 Cento Euratom Di Ispra (Varese)
Italy

J. Upton
JRC-ISPRA, EURATOM
CCR ESSOR Division
21020 Cento Euratom Di Ispra (Varese)
Italy

F. Erbacher
Kernforschungzentrum Karlsruhe
Weberstrasse 5
75 Karlsruhe 1
Federal Republic of Germany

A. Fiege
Kernforschungzentrum Karlsruhe
Weberstrasse 5
75 Karlsruhe 1
Federal Republic of Germany

2 H. Rininslandd
Kernforschungzentrum Karlsruhe
Weberstrasse 5
75 Karlsruhe 1
Federal Republic of Germany

No. of
Copies

J. Gittus
Springfields Nuclear Power
Development Laboratory
United Kingdom Atomic Energy
Authority
Springfields, Salwick
Preston PR 4 ORR
England

5 C. A. Mann
Springfields Nuclear Power
Development Laboratory
United Kingdom Atomic Energy
Authority
Springfields, Salwick
Preston PR 4 ORR
England

ONSITE

4 Exxon Nuclear Company Inc.

T. Doyle
W. Kayser
J. Morgan
W. Nechodom

No. of
Copies

50 Pacific Northwest Laboratory

J. O. Barner
L. W. Cannon
S. K. Edler
M. D. Freshley
R. L. Goodman
C. R. Hann
G. M. Hesson (3)
L. L. King
R. K. Marshall
P. N. McDuffie (3)
C. L. Mohr (8)
F. E. Panisko
L. J. Parchen (5)
J. P. Pilger
W. N. Rausch
G. E. Russcher (5)
B. J. Webb
N. J. Wildung
C. L. Wilson (5)
M. C. Wismer
Publishing Coordination (2)
Technical Publication (5)

NRC FORM 335 (11-81)

U.S. NUCLEAR REGULATORY COMMISSION

BIBLIOGRAPHIC DATA SHEET

1. REPORT NUMBER *(Assigned by DDC)*
NUREG/CR-2526
PNL-4164

4. TITLE AND SUBTITLE *(Add Volume No., if appropriate)*
LOCA SIMULATION IN NRU PROGRAM DATA REPORT FOR THERMAL-HYDRAULIC EXPERIMENT 2 (TH-2)

2. *(Leave blank)*

3. RECIPIENT'S ACCESSION NO.

7. AUTHOR(S) MOHR, HESSON, KING, MARSHALL, PARCHEN, PILGER, RUSSCHER, WEBB, WILDUNG, WILSON, WISMER

5. DATE REPORT COMPLETED
MONTH October YEAR 1982

9. PERFORMING ORGANIZATION NAME AND MAILING ADDRESS *(Include Zip Code)*
Pacific Northwest Laboratory
P O Box 999
Richland, Washington 99352

DATE REPORT ISSUED
MONTH November YEAR 1982

6. *(Leave blank)*

8. *(Leave blank)*

12. SPONSORING ORGANIZATION NAME AND MAILING ADDRESS *(Include Zip Code)*
U S Nuclear Regulatory Commission
Division of Accident Evaluation
Washington, DC 20555

10. PROJECT/TASK/WORK UNIT NO.

11. FIN NO.
B 2277

13. TYPE OF REPORT
Topical

PERIOD COVERED *(Inclusive dates)*

15. SUPPLEMENTARY NOTES

14. *(Leave blank)*

16. ABSTRACT *(200 words or less)*

A series of thermal-hydraulic and cladding material experiments are being conducted using LWR fuel as part of the PNL LOCA Simulation Program. Experimental data and initial results from the fourth experiment in the program--thermal-hydraulic experiment 2 (TH-2)--are presented in this report. The program is being conducted in the NRU reactor, Chalk River, Canada. A full-length test bundle containing 12 test rods and 20 guard rods (all nonpressurized) was used to develop reflood control parameters and procedures that will produce a reduced heatup rate or a "flat top" transient for extended periods of time. Variable reflood rates were used, and experimentally determined control system logic parameters were developed. Using these concepts, cladding temperatures from 1033 to 1274 K were produced for 283 seconds.

17. KEY WORDS AND DOCUMENT ANALYSIS

17a. DESCRIPTORS

National Research Universal (NRU) reactor
Light Water Reactor (LWR) fuel rods
Thermal-hydraulic experiment
Loss of Coolant Accident (LOCA) simulation
Zircaloy cladding
Temperature transient

17b. IDENTIFIERS/OPEN-ENDED TERMS

18. AVAILABILITY STATEMENT
Unlimited

19. SECURITY CLASS *(This report)*
Unclassified

21. NO. OF PAGES

20. SECURITY CLASS *(This page)*
Unclassified

22. PRICE
S

UNITED STATES
NUCLEAR REGULATORY COMMISSION
WASHINGTON, D.C. 20555

120555003908 1 ANR3
US NRC
ASLBP
CHAIRMAN
EW439
WASHINGTON DC 20555